London's Global University

Design Optimisation towards Lower Embodied Carbon Emissions in Prefabricated Constructions in China: A Micro-level Parametric Approach

Yiming Xiang
BArch, MArch

Supervised by:
Dr Abdul-Majeed Mahamadu
Dr Laura Florez-Perez

A thesis submitted in fulfilment of the requirements for the degree of
Doctor of Philosophy

The Bartlett School of Sustainable Construction
University College London (UCL)

2021-2024

Declaration

I, Yiming Xiang, confirm that the work presented in my thesis is my own. Where information has been derived from other sources, I confirm that this has been indicated in the thesis.

Abstract

Prefabricated construction, especially precast concrete structure, is widely acknowledged for its potential in reducing embodied carbon emissions (CE) in the Chinese construction industry. Although efforts have been made to enhance sustainability through optimised prefabrication design, their practical implementation often falls short due to a lack of real-world considerations during the design stage. Therefore, this research aims to address these issues by developing a novel design optimisation model aimed at minimizing embodied CE in prefabricated construction, considering practical constraints such as architectural design, manufacturing, transportation, and assembly.

Using a parametric approach, the proposed model generates geometric design alternatives based on the original architectural design. The finite element analysis and structure design are subsequently employed to determine the detailed design of building elements. The manufacturing CE is calculated by summing emissions from building materials and casting formwork. Next, the transportation CE is estimated by simulating the transportation status of building elements using a bin-packing algorithm and calculating transportation emissions with a modal analysis model. A genetic algorithm (GA) is then used to identify the feasible solution with the lowest emissions from manufacturing and transportation.

The model was implemented and tested in a real-world project case in China, achieving significant reductions in embodied CE: 11.09% in materials, 0.13% in formwork, and 30.82% in transportation, leading to an overall 10.06% reduction. A survey of 134 Chinese designers further confirmed the model's practicality and effectiveness, with most participants expressing willingness to adopt it in their design processes.

These findings underscore the model’s ability to aid designers and contractors in reducing embodied CE in prefabricated projects. Introducing micro-level variables enhances the application of conventional design principles and reveals novel carbon reduction strategies. Although validated in China, this micro-level approach can be adapted in regions with similar regulatory and construction frameworks, offering a path toward a more sustainable built environment. Scholars, designers, and policymakers can employ these insights to for greater sustainability in project delivery.

Keywords: Embodied carbon emissions; Prefabricated construction; Design optimisation; Micro-level analysis.

Impact statement

This study evaluates existing sustainable design optimisation strategies, providing a comprehensive overview of their advantages, application, and limitations. It critically assesses the strategies' practicality and effectiveness via estimating the theoretical assumptions against real-word conditions. Scholars are provided a practical perspective on current carbon reduction strategies, highlighting their potential variance from reality.

Unlike the conventional macro-level analysis model, which factors entire building material consumption, average energy usage, and general emission factors, this study performs a micro-level analysis of the design and embodied CE in precast projects. This micro-level analysis focuses on the specific impacts of detailed element design, construction operations, and transportation plan. The approach introduces detailed variables including building element features, connection method, vehicle characteristic, and transportation routines. As a result, a practical perspective on existing estimation and optimisation models is provided.

Results from micro-level analysis reveals that the uncertainty in micro-level design decisions may offset the expected carbon reductions from broad design principles. Thus, the significance of micro-level analysis in the design and construction process is underscored. Scholars and designers are offered with a more practical interpretation of existing macro-level design principles. They can use these novel interpretations as general guidelines for sustainable precast project design.

Introducing micro-level variables links detailed project design and embodied CE during element manufacturing, construction, and transportation. This approach offers scholars a novel and comprehensive understanding of design impact. Novel carbon reduction strategies concerning optimising formwork design, element manufacturing, assembly, and transportation are unveiled. These strategies can complement existing carbon reduction methods, enabling researchers and designers to reduce the environmental impact of precast projects.

Additionally, this study includes a questionnaire survey with Chinese designers to investigate the engineering information formats (EIF) used in design practice. In addition to offering an in-depth analysis of EIF utilisations, the survey results establish a relationship between design activities and EIF. Scholars can leverage these findings to identify specific EIF for various design tasks, paving the way for future studies on sustainable design tools developments and

promotions. Designers and contractors can also use the data to identify the most suitable EIF in their projects, improving the design and communication efficiency.

The proposed optimisation model can be directly applied to current design optimisation efforts. It equips architects and civil engineers with specific design details and transportation plans. This data could guide the design and construction processes towards lower CE, preventing potential CE increases from inappropriate decisions in project delivery. It, therefore, facilitates the implementation of early-stage design decisions and addresses gaps left by previous early-stage tools. Additionally, the model considers formwork design and the prefabricated element transportation. Manufactures and constructors are provided with detailed formwork blueprints and transportation plans. They can use these data to produce efficient formwork pieces and arrange efficient element transportation, reducing emissions and construction cost. Although this research is based in Chinese context, the proposed optimisation model can be promoted to other regions having the similar construction method and delivery process.

Acknowledgements

I would like to express my deepest gratitude to those who supported and guided me throughout my doctoral journey.

First and foremost, I am immensely thankful to my supervisor, Dr Abdul-Majeed Mahamadu and Dr Laura Florez-Perez, for their unwavering guidance, insightful feedback, and constant encouragement. In July 2022, I faced immense frustration after my manuscript was rejected by several journals. During this challenging time, my supervisors offered me the kindest advice and strongest support, helping me to emerge from the shadows of failure. Their inspiring insights reshaped how I approached my interdisciplinary research, laying a solid foundation for my subsequent work on reducing embodied carbon emissions. Dr Mahamadu often responded to my emails almost instantly, even late at night, providing the most reassuring support during the periods of great anxiety.

I would also like to extend my sincere thanks to Professor Stephen Emmitt and Dr. Wei Wang, for their valuable suggestions, thoughtful guidance, and generous time in reviewing my first paper. Their insights and expertise have significantly contributed to the refinement of my academic writing and the success of my publication. Additionally, I am deeply grateful to Professor Alex Opoku, my first supervisor, for giving me the opportunity to pursue my PhD research at UCL. Although our collaboration lasted only one year, his invaluable advice helped shape the foundational design of my project.

I am thankful to the mentors, colleagues, and friends who have supported my research journey, including Professor Hong Zhang, Mr. Yanhua Wu, Dr Tan Tan, Dr Jiachen Bu, Dr Yusong Zhu, Dr Ke Zhu, Dr Kehan Ma, Dr Yifan Zhang, Dr Pengju Zhang, Mr. Min Zhang. Their wisdom, camaraderie, and accomplishments have consistently inspired me throughout this challenging journey.

Finally, I would like to express my heartfelt appreciation to my family for their unwavering support in my pursuit of the doctoral degree overseas. It brings me great pride to share the achievement and joy of completing this PhD with them.

UCL Research Paper Declaration Form: referencing the doctoral candidate's own published work(s)

1. **For a research manuscript that has already been published** (if not yet published, please skip to section 2)**:**
   (a) What is the title of the manuscript?
   (1) Carbon Emissions Optimisation in Prefabrication Construction: A Review of Current Design Integrated Approaches
   (2) Design Optimisation towards Lower Embodied Carbon of Prefabricated Buildings: Balancing Standardisation and Customisation
   (3) Embodied Carbon Determination in the Transportation Stage of Prefabricated Constructions: A Micro-level Model Using the Bin-packing Algorithm and Modal Analysis Model
   (4) Engineering Information Format Utilisation Across Building Design Stages: An Exploration of BIM Applicability in China
   (5) Reconsidering adaptive industrialized construction in Chinese rural areas: responding to the challenge of COVID-19
   (b) Please include a link to or doi for the work:
   (1) https://discovery.ucl.ac.uk/id/eprint/10137756/
   (2) https://doi.org/https://doi.org/10.1016/j.dibe.2024.100413
   (3) https://doi.org/10.1016/j.enbuild.2022.112640
   (4) https://doi.org/10.1016/j.jobe.2024.110030
   (5) https://doi.org/10.1080/09613218.2022.2081119
   (c) Where was the work published?
   (1) Proceedings of the 37th Annual ARCOM Conference
   (2) Developments in the Built Environment
   (3) Energy and Buildings
   (4) Journal of Building Engineering
   (5) Building Research and Information
   (d) Who published the work?
   (1) Association of Researchers in Construction Management
   (2) Elsevier Ltd
   (3) Elsevier Ltd

(4) Elsevier Ltd

(5) Taylor & Francis Group

(e) When was the work published?

(1) 2021.09

(2) 2024.03

(3) 2022.11

(4) 2024.06

(5) 2022.05

(f) List the manuscript's authors in the order they appear on the publication:

(1) **Xiang, Y.***, Opoku, A., Florez-Perez, L.

(2) **Xiang, Y.***, Mahamadu, A.-M., Florez-Perez, L., & Wu, Y.

(3) **Xiang, Y.***, Ma, K., Mahamadu, A.-M., Florez-Perez, L., Zhu, K., & Wu, Y.

(4) **Xiang, Y.***, Mahamadu, A.-M., & Florez-Perez, L.

(5) **Xiang, Y.**, Bu, J., Zhu, K., Ma, K., Opoku, A., Florez-Perez, L., Zhang, H.*, & Wu, Y.

(g) Was the work peer reviewd?

(1) Yes

(2) Yes

(3) Yes

(4) Yes

(5) Yes

(h) Have you retained the copyright?

(1) No

(2) No

(3) No

(4) No

(5) No

(i) Was an earlier form of the manuscript uploaded to a preprint server (e.g. medRxiv)?

If 'Yes', please give a link or doi

If 'No', please seek permission from the relevant publisher and check the box next to the below statement:

√ I acknowledge permission of the publisher named under 1d to include in this thesis portions of the publication named as included in 1c.

2. **For a research manuscript prepared for publication but that has not yet been published** (if already published, please skip to section 3)**:**
   (a) What is the current title of the manuscript?
   (b) Has the manuscript been uploaded to a preprint server, e.g. medRxiv'?
   If 'Yes', please give a link or doi:
   (c) Where is the work intended to be published?
   (d) List the manuscript's authors in the intended authorship order:
   (e) Stage of publication:
3. **For multi-authored work, please give a statement of contribution covering all authors** (if single-author, please skip to section 4)**:**
   (1) **Yiming Xiang:** Conceptualization, Methodology, Investigation, Programming, Validation, Data Collection, Writing - original draft. **Alex Opoku:** Supervision, Writing - review & editing. **Laura Florez Perez:** Supervision, Writing - review & editing.
   (2) **Yiming Xiang:** Writing – original draft, Visualization, Validation, Software, Methodology, Investigation, Formal analysis, Data curation, Conceptualization. **Abdul-Majeed Mahamadu:** Writing – review & editing, Supervision. **Laura Florez-Perez:** Writing – review & editing, Supervision. **Yanhua Wu:** Validation, Methodology, Investigation, Funding acquisition.
   (3) **Yiming Xiang:** Conceptualization, Methodology, Investigation, Programming, Validation, Data Collection, Writing - original draft. **Kehan Ma:** Writing - original draft. **Abdul-Majeed Mahamadu:** Supervision, Writing - review & editing. **Laura Florez Perez:** Supervision, Writing - review & editing. **Ke Zhu:** Data Processing. **Yanhua Wu:** Engineering design.
   (4) **Yiming Xiang**: Writing – original draft, Visualization, Validation, Software, Methodology, Investigation, Formal analysis, Data curation, Conceptualization. **Abdul-Majeed Mahamadu**: Writing – review & editing, Supervision. **Laura Florez-Perez**: Writing – review & editing, Supervision.
   (5) **Yiming Xiang:** Conceptualization, Methodology, Investigation, Programming, Validation, Data Collection, Writing - original draft. **Jiachen Bu:** Methodology, Investigation, Validation, Data Collection, Writing - original draft. **Ke Zhu:** Data

Processing, Writing - original draft. **Kehan Ma:** Writing - original draft. **Alex Opoku:** Supervision, Writing - review & editing. **Laura Florez Perez:** Supervision, Writing - review & editing. **Hong Zhang:** Supervision, Funding acquisition. **Yanhua Wu:** Engineering design.

4. **In which chapter(s) of your thesis can this material be found?**
   (1) In chapters 1, 2
   (2) In chapters 1, 2, 4, 7, 8, 9
   (3) In chapters 1, 2, 5, 7, 8, 9
   (4) In chapters 1, 2, 6, 7, 8, 9
   (5) In chapters 1, 2

e-Signatures confirming that the information above is accurate (this form should be co-signed by the supervisor/ senior author unless this is not appropriate, e.g. if the paper was a single-author work):

Candidate:

Date: 25/08/2024

Supervisor/Senior Author signature (where appropriate):

Date:14/10/2024

Contents

Table of contents

Table of figures

Table of tables

Abbreviation	
3D-RSO	Three-dimensional residual-space optimised algorithm
ANOVA	Analysis of variance
BIM	Building information modelling
BP	Bin packing
CE	Carbon emissions
EIF	Engineering information format
GA	Generic algorithm
LCA	Life cycle analysis
MCA	Multiple-correspondence analysis
STP	Scaled tractive power

Nomenclature	
ADG_{f-i-j}	The distance between the j-th adjusted walls in the i-th grid on the f-th floor and the node of corresponding grid of the design alternative (m)
$adjusted\_wall\_list$	The list of walls after scaling
A_{n-f}	The area of the $(n-f)$-th floor (m^2)
$A_{open_{i-j}}$	The area of the j-th opening on the i-th piece of formwork (m^2)
$area$	The windward area of the vehicle (m^2)
$AWC_{f-i-j-0}$	The coordinate of the start point of the j-th wall in the i-th grid on the f-th floor in the design alternative
$AWC_{f-i-j-1}$	The coordinate of the end point of the j-th wall in the i-th grid on the f-th floor in the design alternative
AWL_{f-i-j}	The length of the j-th wall in the i-th grid on the f-th floor of the design alternative
B	The set of boxes
B'	The set of residual boxes (boxes that are not placed)
b_i	The i-th box in set B
b_i'	A parameter set that defines each box b_i in the box set B
BD_i	The designed depth of the i-th beam (m)
bot_rebar_num	The number of tensioned bars on the bottom
bot_rebar_size	The diameter of tensioned bar on the bottom (m)
box_num_i	The selected sequence number of box in set B'
BRD_i	The reinforcement design of the i-th beam
BW_i	The designed width of the i-th beam (m)
C	The set of containers
C_{i-j}	The j-th container of the i-the vehicle
CBT_{f-d-i}	The top reinforcement design of the continuous beams on i-th axis in d direction on the f-th floor
CCD	The concrete cover depth (m)
CCS	The axial compressive strength of column concrete (kN/m^2)
$CDIW_{f-i-j}$	The coordinates of the j-th re-allocated wall in the i-th grid on the f-th floor

CE	The embodied carbon emissions of the target project
CE_{3D-RSO}	The CE of 3D-RSO algorithm (kg CO_2e)
$CE_{benchmark}$	The benchmarked CE value (kg CO_2e)
CE_{ELE-i}	The CE of the i-th element (kg CO_2e)
$CE_{elements}$	The carbon emissions generated by moving only prefabricated elements to the construction site (kg CO_2e)
CE_{FW-i}	The CE of each piece of formwork (kg CO_2e)
CE_{GA}	The CE of GA-based algorithm (kg CO_2e)
$CE_{vehicles}$	The carbon emissions generated by moving vehicles without freight to the construction site (kg CO_2e)
$CE(F)$	The CE of fleet F (kg CO_2e)
CED_{i-j-k}	The k-th feasible design of the element $CELE_{i-j}$
CED^*_{i-j-k}	The element design containing $top\_rebar\_size^*_{i-j-k}$
$CEDL_{i-j}$	The list of all feasible designs of the continual element $CELE_{i-1}$ or $CELE_{i-2}$
$CEDL^*_{i-j}$	The list of coordinated design for continual beams or sub-beams $CELE_{i-1}$ or $CELE_{i-2}$
CEL_i	Two continually connected beams or sub-beams ($CELE_{i-1}$ and $CELE_{i-2}$) at the node i
$CELE_{i-1}/CELE_{i-2}$	Continual connected element at the node i
Coe_{CON}	The CE coefficient of the concrete (kg CO_2e/m^3)
Coe_{FW-i}	The CE coefficient of material of the i-th piece of formwork (kg CO_2e/m^2)
Coe_i	The CE coefficient of the transport method [kg CO_2e/(ton·km)]
Coe_{RE}	The CE coefficient of the reinforcement (kg CO_2e/kg)
Coe_{RE-COU}	The CE coefficient of the rebar coupler (kg CO_2e/kg)
$COIW_{f-i-j}$	The coordinates of the j-th original wall in the i-th grid on the f-th floor
$column\_num_f$	The number of columns on the f-th floor
CON_{beam}	The grade of concrete used in beams
CON_{column}	The grade of concrete used in columns
$CON_{floor-slab}$	The grade of concrete used in floor slabs
$CON_{secondary-beam}$	The grade of concrete used in secondary beams
con_rebar_num	The number of constructional rebar on each side
$con\_rebar\_num\_0$	The number of constructional rebar at node 0 on the top
$con\_rebar\_num\_1$	The number of constructional rebar at node 1 on the top
$con\_rebar\_num\_mid$	The number of constructional rebar in the middle of top side
$con\_rebar\_num\_web$	The number of constructional rebar of web
con_rebar_size	The diameter of constructional rebar (m)
CRD_i	The reinforcement design of the i-th column
$CSBT_i$	The top reinforcement design of the i-th group of continuous secondary beams

$CTRS_{i-j}$	The list of all feasible top rebar size of the element $CELE_{i-1}$ or $CELE_{i-2}$
CW_f	The width of columns on the f-th floor (m)
$cycle_l$	The required cycle times of the l-th piece of formwork
D_{f-i}	The adjusted lateral stiffness of the i-th column on the f-th floor (kN/m)
Dis_i	The transport distance (km)
DIW_{f-i-j}	The distance between the j-th original and corresponding re-allocated walls in the i-th grid on the f-th floor (m)
DFH_i	The designed floor-to-floor height of the i-th floor (m)
DSL_{d-i}	The span length of the i-th column grid in d direction (m)
EFW_{i-j}	The formwork required to manufacture a specific precast element
EL_f	The estimated vertical load on the columns of f-th floor (kN)
F	The set of vehicles
F_{Ek}	The standard value of horizontal seismic action on the entire structure (kN)
F_f	the standard value of horizontal seismic action on the f-th floor (kN)
f_j	The CE rate of operating mode j (ton/h)
f_{scale}	The fixed mass of the vehicle (ton)
F_n'	The standard value of horizontal seismic action on the top floor (kN)
f_0	The emission rate of the vehicle operating with the STP value of 0 (kg CO_2e/h)
Fac_i	The CE factor of the transport method i (kg CO_2e/km)
FD_i	The designed depth of the i-th floor slab (m)
FL	The length of floor slab (m)
FRD_i	The reinforcement design of the i-th floor slab
FW	The width of floor slab (m)
G	A set of discrete variables that determines the selection between two space generation method in each placing
g	The acceleration due to gravity (9.8 m/s^2)
G_{eq}	The equivalent gravity load of the whole structure (kN)
G_f	The equivalent gravity loads of structure elements on the f-th floor (kN)
G_{f-1}	The equivalent gravity loads of structure elements on the $(f-1)$-th floor (kN)
G_i	The selection of place generation method in the i-th time box placing
H_f	The heights of f-th floor (m)
H_{f-1}	The heights of $(f-1)$-th floor (m)
h_{f-i}	The height of the i-th column on the f-th floor (m)

H_i	The height of S_i (m)
H_{i-j}	The height of C_{i-j} (m)
h_i	The height of b_i (m)
h_{i-1}	The extension length of the rebar on one of the height sides (m)
h_{i-2}	The height of precast concrete (m)
h_{i-3}	The extension length of the rebar on the other height side (m)
h_{i-4}	The interval between adjacent elements in the height dimension (m)
$hooping\_num$	The number of hooping limbs
$hooping\_size$	The diameter of hooping (m)
k_f	The coefficient factor of STP and emission rate (1000·kg^2 CO_2e/kWh)
L_i	The length of S_i (m)
L_{i-j}	The length of C_{i-j} (m)
l_i	The length of b_i (m)
l_{i-1}	The extension length of the rebar on one of the length sides (m)
l_{i-2}	The length of precast concrete (m)
l_{i-3}	The extension length of the rebar on the other length side (m)
l_{i-4}	The interval between adjacent elements in the length dimension (m)
$Layer_i$	The layer number of S_i
LE_i	The i-th linear element
$length_{i-j}$	The length of the j-th surface of the i-th elements to which the formwork is attached (m)
$length_l$	The length of $MEFW_l$ (m)
$length(B')$	The number of items in set B'
$length(S')$	The number of items in set S'
$Load_{average}$	The average load capacity (ton)
$Load_i$	The load capacity of S_i (ton)
$Load_{i-j}$	The load capacity of C_{i-j} (ton)
$Load\_rate_i$	The average loading rate
m	Number of boxes in set F
m_{3D-RSO}	The number of vehicles of 3D-RSO algorithm
m_{GA}	The number of vehicles of GA-based algorithm
M_i	A discrete variable that represents the box placing method when S_i is used to place a box
M_{i-j}	The j-th member of the i-th linear element
Mal_i	The material quantity that transported by method i (ton)
m_num_l	The number of the l-th piece of formwork requires to be produced
$mass$	The total mass of individual vehicle (ton)
max_BDWR	The maximum depth-width ratios of beams

max_BSDR	The maximum span-depth ratios of beams
max_FW	The maximum widths of floor slabs (m)
max_reuse_cycle	The maximum reuse cycles of the formwork piece
max_SBDWR	The maximum depth-width ratios of secondary beams
max_SBSDR	The maximum span-depth ratios of secondary beams
max_TFH_i	The upper boundary of the tolerance for the floor-to-floor height of the i-th floor (m)
max_TSL_{d-i}	The upper boundary of the tolerance for the i-th span in d direction (m)
max_TTH	The upper boundary of the tolerance of the overall height of structure (m)
max_TTL_d	The upper boundary of the tolerance of the overall dimension of structure in d direction (m)
MC_{i-j-0}	The coordinates of the vertex 0 of the member M_{i-j}
MC_{i-j-1}	The coordinates of the vertex 1 of the member M_{i-j}
$MEFW_l$	The l-th piece of formwork that is going to be manufactured
min_BDWR	The minimum depth-width ratios of beams
min_BSDR	The minimum span-depth ratios of beams
min_FW	The minimum widths of floor slabs (m)
min_SBDWR	The minimum depth-width ratios of secondary beams
min_SBSDR	The minimum span-depth ratios of secondary beams
min_TFH_i	The lower boundary of the tolerance for the floor-to-floor height of the i-th floor (m)
min_TSL_{d-i}	The lower boundary of the tolerance for the i-th span in d direction (m)
min_TTH	The lower boundary of the tolerance of the overall height of structure (m)
min_TTL_d	The lower boundary of the tolerance of the overall dimension of structure in d direction (m)
N	A set of float-type variables that determines the order of boxes O
n	Number of boxes in set B
num_{f-i}	The number of beams connected to the i-th column on the f-th floor
O	The order of boxes to be packed
ODG_{f-i-j}	The distance between the j-th adjusted walls in the i-th grid on the f-th floor and the node of corresponding grid of the original design (m)
OFH_i	The original floor-to-floor height of the i-th floor (m)
OMF_{i-j}	The fraction of time that V_i spent in the operating mode j
$open_{i-j-k}$	The size of the k-th opening on the piece of formwork EFW_{i-j}
$open_{l-k}$	The size of the k-th opening on the piece of formwork $MEFW_l$
$original\_height\_list$	The list of original floor-to-floor heights

$original\_span\_list_d$	The list of original span length in the d direction
$original\_wall\_list$	The list of original walls
OSL_{d-i}	The original length of the i-th span in the d direction (m)
$OWC_{f-i-j-0}$	The coordinates of the start point of the j-th wall in the i-th grid on the f-th floor
$OWC_{f-i-j-1}$	The coordinates of the end point of the j-th wall in the i-th grid on the f-th floor
OWL_{f-i-j}	The length of the j-th walls in the i-th grid on the f-th floor of the original design (m)
P	A set of float-type variables that determines the selection of a specific space in set S' in each placing
p	The number of containers in V_i
P_i	A float-type variable that determine the selection of a specific space in set S'
$Para$	Design parameters of design alternatives
PE_i	The i-th plane element
PEC_{i-n}	The coordinates of vertices of the member PE_i
$position_{i-j-k}$	The position of the k-th opening on j-th surface of the i-th elements to which the formwork is attached
$position_{l-k}$	The position of the k-th opening on $MEFW_l$
Q_{CON-i}	The quantity of concrete consumed by the i-th element (m^3)
q_{n-f}	The estimated load coefficient of the $(n-f)$-th floor (kN/m^2)
$Q_{RE-COU-i}$	The quantity of rebar coupler consumed by the i-th element (kg)
Q_{RE-i}	The quantity of reinforcement consumed by the i-th element (kg)
r_{i-H}	The binary variable that determines whether b_i can rotate around the height (Z) axis. The value equals to 1 if the box can and 0 otherwise.
r_{i-L}	The binary variable that determines whether b_i can rotate around the length (X) axis. The value equals to 1 if the box can and 0 otherwise.
r_{i-W}	The binary variable that determines whether b_i can rotate around the width (Y) axis. The value equals to 1 if the box can and 0 otherwise.
R	The range of design paramters
RE_{beam}	The grade of tensioned bars used in beams
$RE_{beam-hop}$	The grade of hooping used in beams
RE_{column}	The grade of tensioned bars used in columns
$RE_{column-hop}$	The grade of hooping used in columns
$RE_{floor-slab}$	The grade of reinforcement used in floor slabs
$RE_{secondary-beam}$	The grade of tensioned bars used in secondary beams
$RE_{secondary-beam-hop}$	The grade of hooping used in secondary beams
$rebar\_num\_0$	The number of tensioned bars at node 0 on the top

$rebar\_num\_1$	The number of tensioned bars at node 1 on the top
$rebar\_num\_mid$	The number of tensioned bars in the middle of top side
$rebar\_size$	The diameter of tensioned bar (m)
$rebar\_spacing$	The spacing of tensioned bars (m)
$REFW_l$	The l-th list of formwork pieces share the similar characteristics
res_{aero}	The aerodynamic drag coefficient (kW·sec^3/m^3)
res_{roll}	The rolling resistance coefficient (kW·sec/m)
res_{rotate}	The rotational resistance coefficient (kW·sec^2/m^2)
S	A sequence of parameter sets that defines each space in set of containers C
S'	The set of available space to place box b_i
S_i	The i-th space in the space set S
SBD_i	The designed depth of the i-th secondary beam (m)
SBN_{f-i}	The number of secondary beams in the i-th column grid on the f-th floor
SBO_{f-i}	The orientation of secondary beams in the i-th column grid on the f-th floor
$SBRD_i$	The reinforcement design of the i-th secondary beam
SBW_i	The designed width of the i-th secondary beam (m)
SL_i	The span length of the i-th beam or secondary beam (m)
$space\_num_i$	the selected sequence number of space in set S'
stf_{f-i}	The original linear stiffness of the i-th column on the f-th floor (kN·m)
stf_{f-i-k}	The linear stiffness of the k-th beam connected to the i-th column on the f-th floor(kN·m)
$STP_{elements}$	The STP to move only prefabricated elements to the construction site (kW/ton)
STP_j	The STP of operating mode j (kW/ton)
STP_t	The STP at time t (kW/ton)
$STP_{vehicles}$	The STP to move vehicles without freight to the construction site (kW/ton)
T	A set of discrete variables that determines the selection among different vehicle types once a new vehicle is added
T_i	The type of i-th vehicle in the fleet F
$Time_i$	The operating hours of the i-th vehicle (V_i) in the fleet F (h)
top_rebar_size	The diameter of tensioned bar on the top (m)
$top\_rebar\_size^*_{i-j-k}$	The intersection of top_rebar_size for $CTRS_{i-1}$ and $CTRS_{i-2}$
$top\_rebar\_size\_x$	The diameter of tensioned bar in the x direction on the top (m)
$top\_rebar\_size\_y$	The diameter of tensioned bar in the y direction on the top (m)
$total\_DIW_{f-i}$	The sum of distances between original and corresponding re-allocated walls in the i-th grid on the f-th floor (m)
$type\_num$	The total number of available vehicle types

V_{fj}	The shear force caused by seismic load on the i-th column on the f-th floor (kN)
V_i	The i-th vehicle in set F
v_t	The instantaneous vehicle velocity at time t (m/s)
v_num_i	The number of vehicles in which b_i is placed
W_i	The width of S_i (m)
w_i	The width of b_i (m)
w_{i-1}	The extension length of the rebar on one of the width sides (m)
w_{i-2}	The width of precast concrete (m)
w_{i-3}	The extension length of the rebar on the other width side (m)
w_{i-4}	The interval between adjacent elements in the width dimension (m)
W_{i-j}	The width of C_{i-j} (m)
$weight_i$	The weight of b_i (ton)
$width_{i-j}$	The width of the j-th surface of the i-th elements to which the formwork is attached (m)
$width_l$	The width of the $MEFW_l$ (m)
x_i	The X coordinate of the box b_i's bottom-left corner
y_i	The Y coordinate of the box b_i's bottom-left corner
z_i	The Z coordinate of the box b_i's bottom-left corner
α_1	The horizontal earthquake influence coefficient
α_d	The correction factor of stiffness
α_t	The instantaneous vehicle acceleration (m/s^2)
ε_{column}	The estimated coefficient of compression zone of columns
δ_n	The additional seismic action coefficient of the top floor
θ_t	The road grade at time t
μ_{aero}	The aero drag coefficient of the vehicle
$\mu_{rolling}$	The rolling resistance coefficient of the vehicle (N/kN)
ρ_{aero}	The density of the air (1.29 kg/m^3)
$\rho_{material}$	The density of element material (ton/m^3)

1 Introduction

1.1 Background

In 2020, global carbon emissions (CE) reached 32 billion tons (BP, 2021). The construction industry, as the primary contributor, accounts for 36% of global energy consumption and 37% of energy-related emissions (United Nations Environment Programme, 2022). Besides generating operational emissions from air conditioning, heating, lighting, and operations of building equipment, buildings also emit a considerable amount of embodied carbon during initial construction, life-cycle maintenance, and final demolition (Dixit, 2019). The decarbonisation of energy supply systems and advancement in building energy efficiency have shifted operational emissions from its previous dominant position in life-cycle emissions (Arslan et al., 2023; E. Marsh et al., 2021). Nevertheless, this change does not necessarily imply a net reduction in CE, but a decline in operational emissions offset by an increase in embodied emissions (Battisti et al., 2019; Copiello, 2017). The decrease in operational CE and increase in embodied CE are expected to raise the latter's share to 60% in the near future (Dixit, 2017). Therefore, the opportunity for embodied CE reduction should not be overlooked (Cabeza et al., 2014; Jayasinghe et al., 2021).

In response, China is increasingly adopting prefabrication to mitigate environmental effects because the modern method has the potential to reduce 15% of initial embodied CE compared to conventional constructions (Hao et al., 2020). *Prefabrication* involves assembling buildings from prefabricated elements (Yuan et al., 2018). Its construction process includes off-site manufacturing, transportation from factory to site, and on-site installation of prefabricated elements (H. Zhu et al., 2018). By manufacturing elements in a specialised facility, prefabrication reduces material consumption and waste (Z. Li et al., 2014), contributing to lower embodied CE.

Throughout the lifecycle stages of prefabricated projects, design significantly influences the environmental performance of prefabricated projects (C. Z. Li et al., 2020). Variance in design decisions can lead to a 137–460% difference in building emissions (Cavalliere et al., 2019) and a 400-500% difference in emissions from individual building element (such as beam) (X. Zhang & Wang, 2022). This variance points out the potential of carbon reduction via project

design, attracting significant academic interest in sustainable design optimisation (Jusselme et al., 2020).

In this process, data uncertainty at the design stage, notably the lack of necessary information for sustainability estimation and optimisation like material selection and quantity, is identified as a crucial challenge (R. Marsh, 2016). On the one hand, data uncertainty contributes to the variance in project CE, forming the foundation for sustainable design optimisation. On the other, data uncertainty may lead to the consequence that early-stage design decisions based on predictions of low environmental impact may result in unsustainable outcomes if actual settings differ from initial analyses (J. P. Basbagill et al., 2014; Muthumanickam et al., 2023). Therefore, the primary task of design optimisation is to comprehensively predict and compare the performance of design alternatives determined by varying decisions.

To achieve this goal, the parametric approach has been introduced (Roberts et al., 2020). This method is built upon the concept of feature-controlled composition (Battisti et al., 2019). The parametric approach describes design features using mathematical variables, allowing for the automatic creation of alternatives by adjusting these variables (Hollberg & Ruth, 2016). This feature underpins optimisation, an iterative process of generating, evaluating, and comparing design alternatives (Basic et al., 2019; Muthumanickam et al., 2023). Studies have applied the method to assess design sustainability (Basic et al., 2019; Hollberg & Ruth, 2016), optimise CE of projects (Al-Obaidy et al., 2022; Jayasinghe et al., 2021; Teng & Pan, 2020), and perform multi-objective (usually cost and sustainability) construction optimisation (J. P. Basbagill et al., 2014; Gauch et al., 2022; Kanyilmaz et al., 2022; X. Zhang & Zhang, 2021), indicating the parametric approach as a promising tool for performance optimisation at the design stage.

Given the influence of design parameters, carbon reduction strategies are heavily dependent on uncertain design variables employed in CE estimation (Xiang, Mahamadu, Florez-Perez, et al., 2024). For instance, Alotaibi et al. (2022) estimated construction emissions of projects by factoring building material quantities and corresponding emission factors, leading to carbon reduction strategies like optimising material utilisation for less material consumption and using less carbon-intensive materials for smaller emission factors. Dong et al. (2015) analysed transportation emissions during prefabrication delivery based on material quantity, transportation distance, and transportation emission factors per weight of load per kilometre, leading to potential reduction strategy of selecting suitable suppliers for shorter transportation distance.

However, most studies (like Xu et al. (2022) and Hao et al. (2020)) and emission estimation standards (like Calculation standard of building carbon emissions GB/T 51366-2019 (2014)) fail to provide specific estimation methods for prefabricated projects. Additionally, the design of prefabricated projects shows minor differences to conventional projects in the original design files (Polat, 2008). Therefore, the unique characteristics of prefabrication are often ignored in sustainability studies, leading to biased emission results and carbon reduction strategies (Xiang et al., 2022).

1.2 Problem statement

1.2.1 Disadvantages of existing carbon reduction strategies

Buildings generate over 80% of their embodied CE in the manufacturing stage by consuming building materials (Teng & Pan, 2020). The reinforced concrete structure, as a prevalent structure form(Cabeza et al., 2021), is a significant producer of building embodied CE (X. Zhang & Zhang, 2021). The main materials it consumes, steel and cement, are emissions-intensive and have proven difficult to decarbonize (Nidheesh & Kumar, 2019). Hence, scholars have concentrated on reducing embodied CE by optimising the consumption of emission-intensive materials(Arehart et al., 2022).

Considering that material quantity and material emission factors have the most mitigation potential of embodied CE (C. Zhu et al., 2022), there are generally two strategies to embodied CE reduction: using less-carbon-intensive materials and structure design optimisation. Approaches of the former strategy include structure material substitution (e.g., replacing reinforced concrete with timber), recycled material utilisation, and by-production integration (e.g., substitute cement by fly ash), through which scholars claim that 15-70% embodied carbon can be saved (Minunno et al., 2021).

However, implementing these approaches in practice remains challenging (Giesekam et al., 2016). For instance, it is claimed that replacing 35-75% of cement in concrete with supplementary cementing materials (e.g., fly ash and ground-granulated slag) can reduce embodied energy by 10-20% (Gan et al., 2017). Yet, the limited global availability of these materials (which is only 16% of global Portland cement production and is likely to decrease due to decarbonisation of energy and steel (Moncaster et al., 2022)) impedes their widespread adoption. Moreover, the use of recycled building materials (e.g., recycled concrete aggregates)

has uncertain impacts on decreasing the embodied CE due to the additional treatment process (which consumes extra energy and might compromise CE savings) (S. Chen et al., 2023).

An alternative promising strategy for mitigating embodied CE lies in reducing building material consumption through design optimisation (Jayasinghe et al., 2021, 2022). This strategy, which targets absolute reduction in total material quantity rather than substituting emissions-intensive materials (e.g., steel and concrete) with sustainable alternatives (e.g., timber), is material-independent and thus applicable in most situations. Additionally, reducing material consumption also causes cost savings, which aligns with the objective of conventional design optimisation (Trinh et al., 2021; X. Zhang & Wang, 2022), making the approach economically attractive to contractors.

Despite this, material inefficiency remains a prevalent issue in design practice, leading to an average of 50% material waste (Orr et al., 2019). Given that sustainability is seldom prioritised in projects, constraints from more overarching requirements (e.g., cost limitations, real-world construction conditions, aesthetics requirements, and the preferences of clients and designers (Chan et al., 2022; Nawarathna et al., 2021)) limit the available design alternatives to a narrow range (Gauch et al., 2023). Additionally, owing to the complexity of building design (which involves a huge number of variables (Gauch et al., 2023)), it is impractical for designers to evaluate all possible solutions and determine the most sustainable solutions among them (Kanyilmaz et al., 2022). As a result, designers often resort to feasible design alternatives based on their experience or common practices (Y. Zhou et al., 2023), potentially causing carbon-intensive outcomes due to the inability to precisely predict the environment impacts of each design decision (W. Wang et al., 2005).

1.2.2 Side-effects of prefabrication in embodied carbon emissions

Despite reducing material usage and waste via controlled factory production is widely believed to significantly contribute toward sustainability in prefabrication (Iacovidou et al., 2021), Teng et al. (2018) challenged the assertion that prefabrication can necessarily lead to reduced CE, particularly when excluding material reusability. Sebaibi and Boutouil (2020) reinforced this argument, finding that precast elements have a higher environmental impact than cast-in-situ elements. They attributed the increased CE to thermal treatment processes in factory production. Hong et al. (2016) compared CE calculation methods in prefabrication and claimed that the CE result of the input-output hybrid model is 50% higher than that of either the pure input-output

model or process-based model. Their findings indicate that conventional analysis may neglect additional emissions from intensive transportation tasks and complex manufacturing and construction processes (Xiang et al., 2022).

Regarding transportation, many studies indicate it contributes to only 1%-8% of the life-cycle CE (Chau et al., 2015). Researchers often estimate transportation CE using average or assumed data without practical analysis (Abd Rashid & Yusoff, 2015), reporting a minimal and same-as-cast-in-situ transportation contribution (Du et al., 2019; Hao et al., 2020). However, a significant side effect of prefabrication is the decrease in transportation and hanging efficiency (Anvari et al., 2016; Fenner et al., 2017), which leads to higher CE. Specifically, prefabricated elements occupy more space than raw materials, thus requiring more vehicles. Meanwhile, the solid state of elements precludes the use of efficient transportation methods, like pumping. Dong et al. (2015) observed an increase in the transportation CE share from 12% to 18% with the shift from cast-in-situ to prefabrication. The increase in transportation CE (4% of the total CE) was attributed to the transportation of prefabricated elements from precast yards to construction sites. Considering prefabrication waste reduction reduces approximately 3% of the total CE (Dong et al., 2015; Mao et al., 2013), the extra emissions caused by inefficient element transportation will, without effective management, offset or conceal environmental advantages during the manufacturing process.

Furthermore, overlooking details in manufacturing and construction may overvalue the benefit of existing optimisation strategies. One of the cases is the principle of standardisation, which has been a longstanding strategy for prefabrication design (Bo, 2018; Yuan et al., 2018). Although using standardised precast elements contribute to CE reduction of precast constructions, primarily by facilitating the reuse and recycling of formwork—since it decreases the diversity and volume of concrete formwork (Dong et al., 2015; Wong & Tang, 2012)—there are side effects as well. The dimensions of structural elements have significant impacts on the material consumption and embodied CE (Gascón Alvarez et al., 2022; Ismail & Mueller, 2021; X. Zhang & Zhang, 2021). Consequently, using standardised elements (e.g., columns) may inadvertently lead to an escalation in structural material use and associated CE (Hart et al., 2021). The trade-off between the consumption of structure material and formwork in optimising structure CE has been highlighted (Guilherme Fleith de Medeiros & Moacir Kripka, 2014) while seldom considered in current sustainability analysis (X. Zhang & Wang, 2022), potentially leading to errors.

1.2.3 Summary

According to the previous analysis, existing carbon reduction strategies are theoretically effective but fail to account for real-world conditions, making their application in design practice challenging. Likewise, sustainability assessments of prefabrication neglect detailed project delivery considerations, overlooking emissions from complex construction processes and intensive transportation demands. Consequently, accurately estimating embodied CE in prefabricated projects and effectively reducing these emissions through design optimisation remain significant challenges in sustainable prefabrication design.

These issues are more obvious in Chinese construction industry, which provide service across the area of 9.6 million km^2. Although Chinese government establish the code, Calculation standard of building carbon emissions GB/T 51366-2019 (2014), to guide the life-cycle emission estimation of projects, it only provides average emission factors across various project type and areas, leading to variance in emissions estimation. On the one hand, the average emission factors neglect variance from prefabrication and conventional construction methods, as mentioned before. On the other hand, the emission factors, especially the energy emission factors significantly vary across regions in China (W. Li et al., 2021; LÜ et al., 2021). Utilising national-wide average emission factors and statistic-based emission estimation methods lead to errors in project-specific emission estimation. Therefore, refining existing emission estimation and optimisation methods by consider real-world project delivery conditions is significant for providing effective and practical carbon reduction strategies in Chinese construction industry.

1.3 Research questions and hypothesis

1.3.1 Research questions

To address these issues, the following key questions are posed:

1) How can embodied CE from prefabricated constructions be calculated more accurately using current estimation methods and accessible data?
2) What is the practical approach of predicting and optimising embodied CE of prefabricated projects in the design stage?
3) To what extent can design optimisation be applied and what is the most appropriate way of implementing optimisation as a guidance to designers in prefabricated design?

1.3.2 Research hypothesis

This research is based on the following hypothesis:

1) Design decisions (represented by difference in design parameters) lead to variations in project embodied CE.
2) The original design does not have the lowest CE, thus there remains potential for optimisation of prefabricated design
3) At least one parameter in the parameter set of design decisions is variable, allowing for modifications to the original design and its embodied CE. This enables to generate design alternatives.
4) Each parameter in the parameter set has a specific range, indicating a finite set of design alternatives and a predictable lower boundary for embodied CE.
5) Optimising micro-level design variables enables further reductions in embodied CE of prefabricated construction than conventional methods.
6) Design content influence the selection of engineering information format (EIF) used in design.
7) The design and its optimisation are implemented in Chinese construction industry.

1.4 Aims and objectives

This research aims to develop a novel micro-level optimisation model for identifying the most sustainable design with minimal embodied CE in prefabricated construction in China.

Unlike the conventional macro-level optimisation models, which simply reduce CE by reducing material consumption and utilising less carbon-intensive materials, this micro-level optimisation model enables carbon reduction through optimising element design, construction management, and transportation plan. Besides conventional variables like material type and building dimensions, this micro-level model can introduce detailed variables including building element features, connection method, vehicle characteristic, and transportation routines.

To address the aim, the following objectives are undertaken:

1) Identify the stages, impact variables, calculation methods, and available database for calculating embodied CE of prefabricated constructions.

These elements establish a foundational understanding of construction CE calculation, defining the scope of research. The research focus then shifts to optimising elements within this defined range.

2) Analyse embodied CE of prefabricated construction using micro-level design variables.

   This research will integrate variables used in conventional embodied CE methods and in current design practices. The proposed analysis method aims to establish a direct and accurate relationship between design decisions and their corresponding sustainability performance.

3) Generate design alternatives and compare their CE to identify the most sustainable design.

   This study will employ the parametric design approach to generate alternatives by varying parameter values within specific ranges. Their CE are predicted by the method studied in objective 2. With the single objective of minimising embodied CE values, an optimisation algorithm is going to be employed to identify the alternative with the lowest CE as the feasible solution.

4) Develop a practical method to communicate the optimisation outputs to designers effectively.

   While the parameter set identified in objective 4 is valuable for sustainability analysis, it is not easily applicable in architectural design due to the difficulty architects face in evaluating designs through numbers alone. Thus, the parameter set of the feasible solution is presented into a designer-friendly format to aid decision-making.

For clarity, Table 1-1 gives information on the interrelationship among research questions, objectives, and hypothesis, and identifies the corresponding sections.

Table 1-1: Correspondence among research questions, objectives, hypothesis, and thesis sections.

Research questions	**Research objectives**	**Research hypothesis**	**Sections**
Question 1: How can embodied CE from prefabricated constructions be calculated more accurately using current estimation methods and accessible data?	Objective 1: Identify the stages, impact variables, calculation methods, and available database for calculating embodied CE of prefabricated constructions	Hypothesis 7: The design and its optimisation are implemented in Chinese construction industry	Section 2
	Objective 2: Analyse embodied CE of prefabricated construction using micro-level design variables.	Hypothesis 5: Optimising micro-level design variables enables further reductions in embodied CE of prefabricated construction than conventional methods.	Sections 4, 5
Question 2: What is the practical approach of predicting and optimising embodied CE of prefabricated constructions in the design stage?	Objective 3: Generate design alternatives and compare their CE to identify the most sustainable design.	Hypothesis 1: Design decisions (represented by difference in design parameters) lead to variations in project embodied CE.	Sections 4, 5, 7
		Hypothesis 2: The original design does not have the lowest CE, thus there remains potential for optimisation of prefabricated design	
		Hypothesis 3: At least one parameter in the parameter set of design decisions is variable, allowing for modifications to the original design and its embodied CE. This enables to generate design alternatives.	
		Hypothesis 4: Each parameter in the parameter set has a specific range,	

		indicating a finite set of design alternatives and a predictable lower boundary for embodied CE.	
Question 3: To what extent can design optimisation be applied and what is the most appropriate way of implementing optimisation as a guidance to designers in prefabricated design?	Objective 4: Develop a practical method to communicate the optimisation outputs to designers effectively.	Hypothesis 6: Design content influence the selection of engineering information format (EIF) used in design.	Sections 6, 7

1.5 Expected contributions

This study evaluates existing sustainable design optimisation strategies, providing a comprehensive overview of their advantages, application, and limitations. It critically assesses the strategies' practicality and effectiveness via estimating the theoretical assumptions against real-word conditions. Scholars are provided a practical perspective on current carbon reduction strategies, highlighting their potential variance from reality.

Unlike the conventional macro-level analysis model, which factors entire building material consumption, average energy usage, and general emission factors, this study performs a micro-level analysis of the design and embodied CE in precast projects. This micro-level analysis focuses on the specific impacts of detailed element design, construction operations, and transportation plan. The approach introduces detailed variables including building element features, connection method, vehicle characteristic, and transportation routines. As a result, a practical perspective on existing macro-level model is provided.

Results from micro-level analysis reveals that the uncertainty in micro-level design decisions may offset the expected carbon reductions from broad design principles. Thus, the significance of micro-level analysis in the design and construction process is underscored. Scholars and designers are offered with a more practical interpretation of existing macro-level design principles. They can use these novel interpretations as general guidelines for sustainable precast project design.

Introducing micro-level variables links detailed project design and embodied CE during element manufacturing, construction, and transportation. This approach offers scholars a novel

and comprehensive understanding of design impact. Novel carbon reduction strategies concerning optimising formwork design, element manufacturing, assembly, and transportation are unveiled. These strategies can complement existing carbon reduction methods, enabling researchers and designers to reduce the environmental impact of precast projects.

Additionally, this study includes a questionnaire survey with Chinese designers to investigate the engineering information formats (EIF) used in design practice. In addition to offering an in-depth analysis of EIF utilisations, the survey results establish a relationship between design activities and EIF. Scholars can leverage these findings to identify the most suitable EIF for various design tasks, paving the way for future studies on sustainable design tools developments and promotions. Designers and contractors can also use the data to identify the most suitable EIF in their projects, improving the design and communication efficiency.

The proposed optimisation model can be directly applied to current design optimisation efforts. It equips architects and civil engineers with specific design details and transportation plans. This data could guide the design and construction towards lower CE, preventing potential CE increases from inappropriate decisions in project delivery. It, therefore, facilitates the implementation of early-stage design decisions and addresses gaps left by previous early-stage tools. Additionally, the model considers formwork design and the prefabricated element transportation. Manufactures and constructers are provided with detailed formwork blueprints and transportation plans. They can use these data to produce efficient formwork pieces and arrange efficient element transportation, reducing emissions and construction cost. Although this research is based in Chinese context, the proposed optimisation model can be promoted to other regions having the similar construction method and delivery process.

2 Literature review

2.1 Environmental impact of buildings

The environmental impact of buildings refers to the influence on the natural environment and ecosystems resulting from activities, products, and services in the delivery and use of construction projects (ISO 14001:2015: Environmental management systems — Requirements with guidance for use, 2015). Such impacts include climate change, air pollution, water pollution, and land pollution (EN 15978:2011: Sustainability of construction works - Assessment of environmental performance of buildings. Calculation method, 2011), among which, climate change is considered the most pervasive threat (United Nations, 2021) as it generates significant effects on the ecosystems and human health (Farinha et al., 2021). Given the energy-related greenhouse gas emissions contributes the most to climate change over the past decades (Stocker et al., 2014), indicators like primary energy demand and greenhouse gas emissions are widely used to estimate projects' environmental impacts (EN 15978:2011: Sustainability of construction works - Assessment of environmental performance of buildings. Calculation method, 2011).

Greenhouse gas includes CO_2, CH_4, N_2O, and fluorinated gases like HFCs, PFCs, SF_6, and NF_3, where CO_2 is the most prevalent greenhouse gas, contributing to 79.7% of the amount (EPA, 2023). For estimating emissions with varied greenhouse gas combinations, the unit CO_2 equivalent (CO_2-eq) is introduced. It converts the amounts of other greenhouse gas to the equivalent amount of CO_2 with the same global warming potential (Eurostat, 2023). Simultaneously, scholars use the term 'carbon emissions' synonymously with 'greenhouse gas emissions' to describe the release of climate-altering gases into the atmosphere (Giesekam et al., 2014; C. Guo et al., 2019; Hong et al., 2015; Mao et al., 2013; C. Zhang et al., 2020).

According to the Global Statues Report for Buildings and Construction (United Nations environment programme, 2024), CE from the construction industry reached new highs in 2022, making up 37% of global CE to 10 billion tons. Construction projects generate CE in two categories: namely embodied emissions, and operational emissions (Dixit et al., 2013). Operational emissions are those associated with the operation of built environment. These include activities such as space heating, lighting, and air conditioning (Giesekam et al., 2014). Embodied emissions refer to those generate in life cycle stages other than the operation, including initial construction, life cycle maintenance, and final demolition (Dixit, 2019).

Compared to embodied emissions, operational emissions usually constitute a relatively larger proportion of a building's total life cycle emissions (Dixit et al., 2012). The ratio of operational emissions was around 80% as reported by previous studies (Giesekam et al., 2014; T. K. Lim et al., 2016). However, the dominant contribution of operational emissions is decreasing with the improved building energy efficiency (Arslan et al., 2023; E. Marsh et al., 2021). The ratio of operational emissions reduced from 80-94% in conventional buildings to 67-89% in passive projects, 43-74% in low energy buildings, and 0-26% in nearly zero energy buildings (Chastas et al., 2016). An average ratio of embodied emissions is predicted to be up to 60% in the future (Roberts et al., 2020), underscoring the environmental significance of embodied energy (Dixit et al., 2012).

2.2 Embodied carbon emissions analysis

2.2.1 System boundaries for embodied carbon emissions

System boundary defines the processes and products involved in manufacturing an objective product (Dixit et al., 2013; ISO 14040:2006: Environmental management - Life cycle assessment - Principles and framework, 2006). It identifies the energy and material inputs, as well as waste and emission outputs, involved in the embodied CE analysis of a construction project (Dixit et al., 2013). Typically, five system boundaries are recognised for buildings and their components (Pan et al., 2018):

1) The "cradle to gate" system boundary includes upstream process from the raw material extraction to the end of manufacturing and prefabrication, where the finished product leaves the factory gate.
2) The "cradle to site" system boundary covers the "cradle to gate" process and transportation process of finished construction products to the construction site.
3) The "cradle to end of construction" system boundary further involves the construction and assembly on-site and wastage disposal processes.
4) The "cradle to grave" system boundary considers the use phase with operations, maintenance, renovation, refurbishment and retrofit activities.
5) The "cradle to cradle" system boundary considers the end-of-life phase with processes like building demolition, waste sorting, hauling, and disposal, and material recycling and reuse.

Variance in system boundaries results in an up to 600% discrepancy in project CE analysis (Dixit et al., 2013; Pan et al., 2018). Thus, analysis results using different system boundaries cannot be directly compared or combined (Hong et al., 2016). The system boundaries must be consistently defined across the analysis to align with the objective of the study (ISO 14040:2006: Environmental management - Life cycle assessment - Principles and framework, 2006), varying from a broad perspective emphasizing the general life cycle of a building to a more detailed examination of specific upstream and downstream processes (Dixit et al., 2013).

Embodied carbon emissions are categorised according to the system boundary: 1) into direct and indirect emissions (Dixit et al., 2013) and 2) into initial, recurrent, and demolition emissions (Dixit, 2019). Regarding the first categorisation, direct emissions arise from the main construction process while indirect emissions occur in finite or infinite upstream stages that include input of goods and services (e.g., emissions generated in the manufacturing of construction equipment). Concerning the second categorisation, initial emissions represent those from onsite and offsite construction, transportation, management, and consulting processes; recurrent emissions generate in maintenance, repair, replacement, and renewal activities after the building is complete and occupied; demolition emissions refer to those generated in materials and systems recycle, reuse, and dispose when the building is taken apart.

Given the availability of data, most studies focusing on the analysis of the initial direct embodied emissions of buildings (Dixit, 2019). Lifecycle analysis reveals that prefabricated projects generate most initial direct embodied CE in the manufacturing (82.9%), transportation (9.3%), and on-site construction (7.8%) phases (Teng & Pan, 2020). The emission ratios of each phase can vary based on project characteristics, especially those for transportation and on-site construction (X. juan Li et al., 2022; Tian & Spatari, 2022). For instance, transportation emissions are influenced by the distance between prefabrication factories and construction sites (Dong et al., 2015), while project height affects on-site vertical transportation emissions (Hasan et al., 2013; Wu et al., 2020). Thus, “cradle to gate” (G. Liu et al., 2019), “cradle to site” (Wong & Tang, 2012), and “cradle to end of construction” (G. Liu, Chen, et al., 2020) system boundaries are all observed in exiting studies. Considering the emission contributions and available data, manufacturing and transportation stages are the most potential stages for carbon reduction.

2.2.2 Estimation methods of embodied carbon emissions

Typically, CE evaluation employs three approaches: life cycle analysis (LCA), economic integration analysis, and direct measurement. However, the definitions of these approaches sometimes overlap with those of the CE calculation methods (Zhao et al., 2018) or the LCA method (T. K. Lim et al., 2016), causing confusion. Therefore, terms with minimum cross-references are adopted in Table 2-1 for classification.

Table 2-1: Classification of construction carbon emissions analysis approach

Approach		Method	Application	Input Data
LCA	Process-based LCA	CE factor	Specific Operation	Construction quantity
	Input-output LCA	Mass balance	Material Level	Material Consumption
	Hybrid LCA	Mass balance	Specific Operation	Material Consumption
Economic Analysis		Mass balance	Economies & Industry	Material Consumption
Direct Measurement		Measurement	All	None

LCA evaluates the environmental impacts through the project's life cycle (ISO 14040:2006: Environmental management - Life cycle assessment - Principles and framework, 2006). It is further categorised into three sub-approaches: 1) process-based LCA, 2) input-output LCA, and 3) hybrid LCA (G. Liu et al., 2019). The process-based LCA, ideal for assessing CE from specific construction methods, directly evaluates CE attributable to construction items (e.g., equipment, labour, and material) (T. K. Lim et al., 2016). Fang et al. (2018) employed this approach to determine the CE distribution across construction operations and equipment. Liu et al. (2020) developed a real-time process-based LCA model for construction CE monitoring. Conversely, the input-output LCA is applied broadly to explore CE driving factors in the construction sector (Cui et al., 2019). It is also adopted when material are the primary focus, calculating CE from the bill of material quantities (Cang et al., 2020; Lu et al., 2019). Specific studies have compared CE across materials (C. Zhang et al., 2020) and analysed carbon reduction through material selection and quantity optimisation (J. P. Basbagill et al., 2014; Basic et al., 2019; R. Marsh, 2016). Hybrid LCA, integrating these two methods, transforms the detailed CE of process-based LCA into the bill of material quantities used in input-output LCA (G. Liu et al., 2019). It is considered to offer a more comprehensive analysis than either process-based or input-output LCA along (Hong et al., 2016).

The link between a nation's energy use and its Gross Domestic Product (GDP) forms the foundation of the economic analysis approach (Dixit et al., 2013). Unlike LCA, this approach assesses sustainability on a macro scale, focusing on economies (Han et al., 2020) or industries (Jindao Chen et al., 2019). These studies aim to address suggestions for policy or regulation, differing from this research's objectives, and are therefore excluded. As for direct measurement, Liu et al. (2020) detailed its application in construction CE monitoring. The technologies they mentioned (e.g., GIS, video camera) are primarily adopted for visualization rather than calculation or analysis. However, Christen et al. (2011) proposed using direct eddy-covariance measurements for urban-scale CE calculation. Their model, effective for scales ranging from 100m (size of the construction site) to 10km, highlights the potential for construction applications.

Regarding CE calculation, the CE factor method, mass balance method, and actual measurement method are three prevalent methods (Zhao et al., 2018). There is an apparent consistency between the selection of analysis approaches and calculation methods. The CE factor method, multiplying the product of item quantities and emission factors, is exclusive to process-based LCA due to the demand of detailed construction quantities (Abey & Anand, 2019; Karlsson et al., 2020; D. Li et al., 2016). The mass balance method, assessing CE by the material difference entering and exiting a process, is used in input-output LCA, hybrid LCA, and economic analysis (Hong et al., 2016; G. Liu, Chen, et al., 2020). Finally, although actual measurement can estimate CE in all the aforementioned approaches, its practical application in construction is currently limited (G. Liu et al., 2019). The method has only been observed in studies utilising a direct measurement approach (Christen et al., 2011).

In China, the hybrid LCA and mass balance method are widely used in estimating embodied CE. Calculation standard of building carbon emissions GB/T 51366-2019 (2014) offers process-based hybrid LCA estimation methods and equations across manufacturing, transportation, construction, operation, maintenance, and demolition phases of construction projects. It offers national-wide average emission factors for building materials and energy consumption. Besides, *China Products Carbon Footprint Factors Database* (CCG, 2022) provides more detailed and up-to-data emission factors for building products in China. These two tools have been widely used in estimating manufacturing (W. Chen et al., 2022; Xiang, Mahamadu, Florez-Perez, et al., 2024), transportation (H. Wang et al., 2023; Xiang et al., 2022),

and lifecycle emissions (Y. Wang et al., 2022; X. Yang et al., 2021), suggesting them reliable and suitable for project-level CE estimation.

2.3 Prefabricated construction

2.3.1 Application of prefabricated construction in China

Prefabricated construction refers to the construction process involving producing construction element in a manufacturing factory, transporting complete element or semi-elements to construction sites, and assembling the component to create buildings (Hong et al., 2018). It is regarded as the first level of building industrialisation, which is followed by mechanisation, automation, robotics, and reproduction (Richard, 2005). Prefabricated construction has been referred to as prefabrication, off-site construction, industrialised construction, and modern methods of construction (MMC) etc (Z. Li et al., 2014).

Generally, prefabricated construction is categorised into four levels according to the degree of prefabrication implemented on the product: 1) element manufacturing and subassembly that are always done in a factory and not considered for onsite production, 2) non-volumetric pre-assembly that refers to pre-assembled elements not enclosing usable space, such as timber roof trusses, 3) volumetric pre-assembly that refers to pre-assembled elements enclosing usable space and usually being manufactured inside factories but do not from a part of building structure, such as modular toilet and bathroom, and 4) entire buildings that refer to pre-assembled volumetric elements forming the actual structure and fabric of building, such as modular residence (Gibb, 1999).

Prefabricated construction serves an effective alternative to the traditional construction methods due to the inherent technology superiority, including reducing construction waste, noise, dust, operation time, construction cost, labour demand, and resource depletion, and improving quality control, health and safety (Z. Li et al., 2014). Such advantages improved the performance of the entire construction industry and attracts the favour of developed and developing countries like China, the US, the UK, Japan, and Singapore (Hong et al., 2018).

The Chinese government has promoted this modern construction method since 1999 (Yue Gao & Tian, 2020). With the introduction of prefabrication standards (e.g., GB/T 51231-2016) and promotion polices (e.g., Opinions on Further Strengthening the Management of Urban Planning and Construction), prefabrication experienced a significant growth in China from

2016 (Luo et al., 2021; Yuna Wang et al., 2020). According to the reports of the Ministry of Housing and Urban-Rural Development, in 2020, the new-built prefabricated projects achieved 740 million m^2, representing 24.5% of the year's total construction area (MOHURD, 2022).

Generally, prefabrication technologies adopted in China can be classified into three types according to the structure material: prefabricated concrete, steel, and timber structure (Ji et al., 2017). Among these three types, prefabricated concrete structure is predominant in Chinese construction industry (L. Li et al., 2020; G. Zhou et al., 2018). In 2021, this type of structure accounted for 67.7% of the new-built prefabricated projects in China (MOHURD, 2022), making it a primary focus of prefabrication studies (L. Li et al., 2020; Yuan et al., 2018; G. Zhou et al., 2018).

The implementation of prefabrication technologies includes preliminary studies and primary project design (Hollberg & Ruth, 2016), prefabricated elements production and transportation, and onsite construction (G. Liu, Chen, et al., 2020). These parts are usually separately divided and undertook by independent companies (Xiang, 2020). Specifically, design institute is responsible for preliminary studies and primary project design. They provide the subsequent links with determined geometry features, determined the design details, and technical specifications. (Hollberg & Ruth, 2016). After that, design files are handed over to industrial experts for a deeper technical design, which details the design files into manufacture-oriented drawings concerning the data of each single prefabricated element (S. Gao et al., 2019). Then, the manufacture factory and project contractor are responsible for the manufacture and assembly of prefabricated elements based on these design files, respectively (Yuan et al., 2018).

2.3.2 Design of prefabricated elements

The design process generally consists of three steps: concept design, developed design, and technical design (RIBA, 2020). Specifically, concept design determines the number of stories, building orientation, and building massing; developed design settles the final geometry and the primary construction material; and the technical design addresses design details and technical specifications (Hollberg & Ruth, 2016). Within this framework, the design of prefabricated elements follows these steps: 1) architects and civil engineers initially select the primary shape and form of structures during conceptual design; 2) Following the developed design stage (when the architecture functional plan is determined), civil engineers are responsible for detailed structural design, including sizing and detailing of structural elements (Anwar &

Najam, 2017); 3) Finally, engineers from manufacture industry or civil engineers divide the prefabricated parts into prefabricated elements and refine the elements design to meet the requirements of manufacturability and buildability (S. Gao et al., 2019; Yuan et al., 2018).

The design and structure analysis of precast elements is not much different from that of conventional structure elements (Polat, 2008). The process typically involves three interdependent steps: 1) select the primary shape and form of structure as well as gravity and lateral load-resisting systems, 2) analysis the expected response of structure elements under all kinds of loadings, and 3) detail the design of elements based on analysis results (Anwar & Najam, 2017). A manual trail-and-error method, i.e., repeated cycles of identify, test, evaluate, and modify the proposed element design until achieving optimal performance and safety, is normally employed in this procedure (Trinh et al., 2021).

Building codes establish rules and guidelines, specifying the minimum standards for both modelling and analysis, to ensure design quality and safety (Anwar & Najam, 2017). In China, the design of prefabricated elements must fulfil the general requirements of the corresponding structure system, like *GB 55006-2021* for the steel structure and *GB 55008-2021* for the concrete structure, as well as the specifications for prefabrications like *JGJ1-2014* for precast concrete structures. These specifications set additional test criteria and technical requirements for element design to ensure the prefabricated structures achieve comparable performance to conventional structures under equivalent conditions.

In addition to the conventional requirements, like safety (Anwar & Najam, 2017), economy (Alkhadashi et al., 2022), material-efficiency (Orr et al., 2019), and sustainablility (Jayasinghe et al., 2021), the design of prefabricated elements emphasises standardisation (Bo, 2018), which is essential to the application of prefabrication technology. Standardisation origins from the design for manufacture (O'driscoll, 2002), aims to minimise the variety and quantity of prefabricated elements, thereby enhancing the efficiency of both off-site manufacture and on-site assembly (Gerth et al., 2013; Kremer, 2018). It is commonly implemented in the design by adopting standardised building products (Polat, 2008).

Considering that building elements with standardised dimensions and connections have a higher capability of reuse, employing the principle of standardisation advances the decarbonisation of prefabricated projects (Anastasiades et al., 2021). However, due to the lack of necessary engineering knowledge and experience (Bröchner et al., 2002), the sake of

employment is normally converted to employing uniform cross-section dimensions and minimising the number of prefabricated elements (Xiang, Mahamadu, Florez-Perez, et al., 2024), leading to potential material waste as descripted in section 1.2.1.

2.3.3 Manufacture of prefabricated elements

Currently, there are two methods of prefabricated element manufacture in China: static production and linear production (G. Liu et al., 2019). Specifically, static production involves manufacturing prefabricated elements in a fixed position. Materials, equipment, services, and labourers are brought to the manufacturing position. After production, the element is lifted out by crane, forklift, or other equipment. It is then either stored temporarily or transported dir(Hough & Lawson, 2019)ion site (Hough & Lawson, 2019).

Linear production refers to the manufacturing process conducted in multiple stages at varied positions. The prefabricated element is manufactured on wheels, trolleys, or production lines and moved between stations by electrical vehicles, motorised trolleys, roller tracks, or conveyor belts. Correspondingly, the materials, facilities, and labourers are prepared in batches around each manufacturing position (Hough & Lawson, 2019).

According to the lifecycle analysis on the manufacturing process, building materials are the main source of manufacturing CE, accounting for 96.2%. The emissions from equipment usage and labourers are 3.65% and 0.16%, respectively. The result highlights the significance of optimising the design to reduce material input for lowering the embodied CE from manufacturing process.

2.3.4 Transportation of prefabricated projects

Transportation is essential in building delivery and generates non-negligible effects on the environmental impact of buildings. Excluding or ignoring transportation energy may cause a variation equal to 5%-7% of the total life-cycle embodied energy (Dixit, 2017). This ratio may increase to more than 10% when the prefabrication is adopted (Dong et al., 2015; Yu; Gao et al., 2018). Mao et al. (2013) identified the transportation phases in prefabrication construction as 1) transporting building materials from a distribution centre to the off-site prefabrication factory and from a distribution centre to the project site, 2) transporting prefabricated elements from off-site prefabrication factory to the project site, 3) transporting construction waste and soil from off-site prefabrication factory to landfill, or from project site to landfill, and 4)

transporting construction equipment and workers. Among these four phases, phases 3 and 4 contribute to a limited percentage of the total life-cycle energy (both less than 1%) (Chastas et al., 2016). Most research attention is thus drawn to the other two phases (Chau et al., 2015), especially the transportation of prefabricated elements that crucially affects the environmental benefits of prefabrication (Mao et al., 2013).

From the literature reviewed, there are two assumptions that impact the calculation and analysis on transportation CE: freight status and vehicle operation mode.

2.3.4.1 Freight status

In construction transportation analysis, freights have traditionally been considered as non-solid substances without fixed shapes. All vehicles are also assumed to reach an identical loading status and generate an average emissions value. Therefore, it is the material weight rather than size that dominates the transportation quantity in traditional transportation estimation. This assumption is widely used in the transportation CE calculation of cast-in-situ construction. For instance, D. Li et al. (2016) calculated the transportation CE of a cast-in-situ residential building. The researchers considered the material weight, transport distance, and vehicle type (i.e., diesel-powered truck, electric locomotive) as variables and reported a 2% total CE contribution of transportation. Similar calculation formulas were seen in the research of Jafary Nasab et al. (2020), who analysed the carbon footprint in the construction phase of high-rise construction in Tehran.

Abey & Anand (2019) adopted the above assumption in their prefabrication transportation CE calculations and reported a similar transportation CE contribution between prefabrication and cast-in-situ construction (3%-5%). Hao et al. (2020) employed the same assumption and claimed that only 1% CE is generated in the transportation stage of either prefabrication or cast-in-situ construction.

However, (H. Wang et al., 2021) claimed that the assumption (i.e., all vehicles achieve an identical loading rate) could not be directly applied to the CE calculation of prefabrication transportation because the actual loading rates of prefabricated elements vary based on the size limit, stacking layer limit, and installation sequence. For instance, prefabrication design codes set different maximum stacking layers for different prefabricated element types (China Institute of Building Standard Design & Research, 2015). Real-world constraints conflict with

calculation assumptions and challenge the results of previous studies, especially at the project level.

G. Liu, Chen, et al. (2020) and G. Liu, Yang, et al. (2020) managed to overcome this defect using micro-level CE calculations. Both sets of researchers divided prefabricated elements into several branches according to the actual transportation plan. CE was calculated based on vehicles concerning specific load, distance, and transport approach. However, their system realises CE monitoring rather than prediction. Detailed results are also provided during or after the construction process. Meanwhile, the emission factors the researchers used were cited from Y. Chen & Zhu (2010), which is out-of-date and does not vary for different vehicle types and loading statuses.

2.3.4.2 Vehicle operation mode

In the studies mentioned in section 2.3.4.1, vehicles were assumed to operate in controlled environments with idealised loading rate, stable speed, and temperate conditions. Therefore, average emission factors from macro-level statistics and laboratory measurements were adopted (H. Wang et al., 2021). Yet these statistical data have significant variances from real-world emissions (Tu et al., 2021) due to the difference in driving cycles, vehicle technology, and emission regulations in different regions (A. Wang et al., 2022).

The modal model (e.g., *EMFAC*, *MOVES3*, and *HBEFA*) allows for calculations considering real-world driving status by providing specific emission factors for different 'operation modes', which are defined by internal observed (e.g., engine parameters) or externally observed (e.g., speed, acceleration, weight) variables (A. Wang et al., 2022). For instance, *MOVES3* provides specific emission rates according to pollutant, emission process, fuel type, regulatory class, operating mode, and vehicle age (EPA, 2020b). Comparative studies between the modal model and statistical model (i.e., calculation using statistical data) show that the modal provides a more accurate emission estimation (Fujita et al., 2012; Vallamsundar & Lin, 2011; Wallace et al., 2012). The modal model is, therefore, preferable in micro-level transportation CE analysis (A. Wang et al., 2022; L. Zhang et al., 2017).

The development and application of the portable emission measurement system (PEMS) provide the emission characteristics of vehicles on actual roads, thus bringing the assumption of vehicle operation closer to reality (Shen et al., 2021). Scholars have used actual measured data to identify the real-world emission characteristics of light-duty vehicles (Chung et al.,

2012), heavy-duty vehicles (Shen et al., 2021; J. Wang et al., 2022), and non-road mobile machines (Desouza et al., 2020; Muresan et al., 2015; Tu et al., 2021). These characteristics allow scholars to verify and adjust the general modal model, as shown in studies conducted by A. Wang et al. (2022) and Seo et al. (2022). However, the sample size of studies using PEMS generally remains limited (1-2), which could be unrepresentative. Such studies also focused on the general situation in the logistic industry rather than practices in the prefabricated construction context.

2.4 Design optimisation for embodied carbon reduction

2.4.1 Stages for design optimisation

Building design is a sequential decision-making process involving various stakeholders (Gauch et al., 2023). It is believed to have a dominant impact on the environmental performance of projects (C. Z. Li et al., 2020), in which, designers, including architects and civil engineers exert the greatest influence over design decisions (Stephan & Stephan, 2016). According to the Royal Institute of British Architects (RIBA) plan of work, the design process typically consists of three steps: concept design, developed design (spatial coordination), and technical design (RIBA, 2020). Specifically, concept design determines the number of stories, building orientation, and building massing; developed design settles the final geometry and the primary construction material; and the technical design addresses design details and technical specifications (Hollberg & Ruth, 2016).

Lotteau *et al.* claimed that design decisions related to the overall building massing (e.g., external dimensions of buildings) have a greater influence on the embodied CE than those related to element details (e.g., the thickness of walls) (Lotteau et al., 2017). It is because these decisions set the fundamental constraints for subsequent ones (Paulson, 1976). From a statistical perspective, each decision made in the design process affects the distribution of CE within a certain range. The more decisions are made, the more design variables are fixed, the narrower the result scale, and the higher the concentration on a specific value (J. Basbagill et al., 2013). As a result, scholars have dedicated considerable effort to optimising design decisions at the early design stage (i.e., the concept design), e.g., the overall shape and dimensions of projects (Alwan & Ilhan Jones, 2022; Bernett et al., 2021; Kreiner et al., 2015).

However, continuous monitoring on the variation of CE distribution across different design stages reveals that design decisions made during the developed stage has enough influence to impact the overall sustainability of projects (J. P. Basbagill et al., 2014; Muthumanickam et al., 2023). It indicates that considerable margins to reduce embodied CE are remained in later stages (Dunant et al., 2018; Moynihan & Allwood, 2014). Moreover, the exclusive adoption of design decisions with low environmental impact predictions at the early stages may still culminate in unsustainable results if subsequent decisions are not made judiciously. Therefore, the optimisation of variables determined at the developed design stage warrants further investigation.

2.4.2 Optimisation methods

The uncertainty in design decisions leads to the variance in the CE of projects and thus forming the foundation for sustainable design optimisation. For instance, Cavalliere *et al.* reported a 137–460% difference between the minimum and maximum emissions of building design alternatives by making different decisions(Cavalliere et al., 2019). Similarly, the difference in variables for a single building element (beam) can cause a 400-500% difference in CE (X. Zhang & Wang, 2022).

Therefore, the primary task of design optimisation is to predict and compare the performance of design alternatives determined by different design decisions (Xiang et al., 2021). Typically, previous studies have addressed the issue of data uncertainty through data refining or model simplification. Data refining refers to use information from the later phase for more accurate CE calculations (Hao et al., 2020; D. Li et al., 2016; Lin et al., 2019) and replacing uncertain data with assumed or empirical values (Dixit, 2019).

Obviously, this data refining method is delayed or inaccurate in these scenarios. Therefore, more studies opt for simplifying and adjusting the model to match data quality. Kanafani et al. (2019) categorised model simplification into horizontal approach (i.e., reducing parameters in analysis) and vertical approach (i.e., reducing data quality and allowing generic data). For instance, using the horizontal approach, Victoria & Perera (2018) suggested to design with emphasis on carbon intensity and focusing on the carbon hotspots (elements contributing over 80% of total CE). Rodrigues et al. (2018) reinforced this approach by predicting a robust environmental performance using less than ten design attributes.

Although the horizontal approach claims to be effective and efficient, it is less applied than the vertical approach, which evaluates more design alternatives for comprehensive results (e.g., Shadram & Mukkavaara (2018) evaluated 14,630,112 alternatives). The vertical approach leverages design uncertainty to form the alternative space by distributing uncertain design parameters. This method generates results through the exploration of optimised parameter sets. For instance, Hester et al. (2018) established a design space by varying parameters such as building geometry, occupant behaviour, and material selection. Their design guidance, an optimised scale of crucial attributes, was derived from quasi-optimum solutions (i.e., alternatives possessed 75% of the maximum potential). A similar idea was adopted but not limited to the research of J. Basbagill et al. (2013) and Feng et al. (2019). These studies suggest the vertical approach a suitable method for addressing data uncertainty and result comprehension in early-stage design optimisation.

2.4.3 Parametric approach

Conventionally, designers incorporate design decisions such as design aspects and dimensions of buildings into geometric elements. Once drawn, an initial model with fixed geometry is generated. Changing design decisions necessitates a redrawing of initial geometry (Hollberg & Ruth, 2016). This process is time-consuming and relies on manual efforts (Eltaweel & SU, 2017), preventing designers from evaluating many design alternatives and achieving a global optimum result (Kanyilmaz et al., 2022).

In contrast, the parametric approach treats all design decisions as parameters, such as location, orientation, shape, solar radiation, etc. (Eltaweel & SU, 2017). It defines a building design using these parameters and the mathematical relationships between them (Monedero, 2000). With algorithms or tools like Grasshopper, any change of parameters leads to an immediate and comprehensive update in design output (Eltaweel & SU, 2017). This allows the automated generation of design alternatives by varying design parameters, forming the foundation for computer-aided design optimisation (Hollberg & Ruth, 2016).

The parametric approach transforms design from a concrete representation of geometry to the abstraction of design parameters and their relationships (Monedero, 2000), shifting the focus from evaluating design alternatives to establishing computational logic of design parameters (Tabadkani et al., 2018). This attempt demands comprehensive knowledge of design and engineering logic across design and construction (Coenders, 2021).

Furthermore, the parametric approach necessitates reconsidering or even abandoning conventional design typology (Brown & Mueller, 2019). Such typology, widely employed in conventional design, tends to analyse and solve the design problems using the designer's habitual and fixed patterns. Utilising such pattern makes design results dependent on specific decisions made during the formulation of design problem (Brown & Mueller, 2019), thus limiting the diversity in design alternative exploration and impairing optimisation efficiency. Previous studies, such as Xiang et al. (2024), indicate that excluding experience-based design strategies during parametric design problem formulation results in better optimisation outcomes and counterintuitive solutions.

Currently, parametric approach has been employed to formulate design problems in architecture design (Nembrini et al., 2014; Shiel et al., 2018), structure design (Jayasinghe et al., 2022; X. Zhang & Wang, 2022), urban planning (Abdollahzadeh & Biloria, 2022; Ibrahim et al., 2021), in-door built environment (Tabadkani et al., 2018; J. Zhang et al., 2021), etc. Regarding sustainable design optimisation, scholars employed the method to assess design sustainability (Basic et al., 2019; Hollberg & Ruth, 2016), optimise CE of projects (Al-Obaidy et al., 2022; Jayasinghe et al., 2021; Teng & Pan, 2020), and perform multi-objective (usually cost and sustainability) construction optimisation (J. P. Basbagill et al., 2014; Gauch et al., 2022; Kanyilmaz et al., 2022; X. Zhang & Zhang, 2021), indicating the parametric approach as a promising tool in design optimisation.

2.5 Communicating of optimisation results

2.5.1 Engineering information formats in building design

The design process necessitates collaboration among multi-disciplinary design teams, with diverse backgrounds, expertise, and perspectives of creativity (Muthumanickam et al., 2023), to balance competing objectives (e.g., safety, reliability, cost, etc.) (Ren et al., 2013). In this collaborative environment, design information is retrieved, revised, and renewed multiple times by multiple individuals and organizations (Y. Liu et al., 2017), making the control of information crucial for optimal project performances (Davidson et al., 1988).

However, the construction sector remains highly fragmented (Giesekam et al., 2016). Information is, therefore, transferred in segments across design phases (Tribelsky & Sacks, 2010), causing inevitable errors and inefficiencies in the design process (Murti & Muslim,

2023). For decades, the primary information medium in the construction sector has remained 2D-drawings (Dadi, Taylor, et al., 2014; Mattern & König, 2017). It allows designers to represent the geometric features and engineering details of projects using various projection planes in paper-based drawings, which can be convenient delivered and reviewed on-site (Sweany et al., 2016). However, this two-dimensional information exchange mode involves frequent message processing (i.e., encoding and decoding) and manipulation of multiple drawing sheets to obtain a comprehensive understanding of building systems (Stephen Emmitt & Christopher A. Gorse, 2003), leading to potential information loss (Antwi-Afari et al., 2018). As a result, design information is often harder for recipients to comprehend than for its original creators (Stephen Emmitt & Christopher A. Gorse, 2003). Misunderstandings can occur even when referencing the original design files (Pauwels et al., 2011).

To address the issue, Building Information Modelling (BIM), as a shared digital representation of the physical and functional characteristics of any construction works, has emerged as a superior format of engineering information (Urbieta et al., 2023). BIM supersedes the conventional information format based on descriptive geometry (Sweany et al., 2016) by both comprehensive geometric and semantic data (Antwi-Afari et al., 2018). Project documents in this format allows professionals from various backgrounds and design phases to create, store, and retrieve information consistently and cohesively (Abanda et al., 2017; Ozturk et al., 2016; Tan et al., 2021). Hence BIM is posited to enhance both the quality of engineering information (Andersson & Lessing, 2017; Urbieta et al., 2023) and the efficiency of information exchange (Charef et al., 2018; H. Liu et al., 2018; Yingnan Yang et al., 2023). A considerable number of studies conduct sustainable design estimation and optimisation based on this modern data format (Cavalliere et al., 2019; El-Diraby et al., 2017; Fonseca Arenas & Shafique, 2023; Shadram et al., 2016; Xu et al., 2022).

Recognising the benefits of BIM, governments have promoted this modern information format worldwide (Yonghong Chen et al., 2023). For instance, the Singapore government mandated that all new architectural plans be submitted in BIM format in 2013 through series of codes from Building and Construction Authority (BCA) (Liao et al., 2021). Similarly, Hong Kong identified mandatory and optional BIM use in construction project via the technical circular "Adoption of Building Information Modelling for Capital Works Projects in Hong Kong" since 2017 (Adoption of Building Information Modelling for Capital Works Projects in Hong Kong, 2021). Despite these efforts, the application of BIM has encountered considerable challenges

(Olanrewaju et al., 2022). Liao et al. reported that BIM adoption in Singapore is often compliance-driven rather than value-driven, sometimes making it a “token” action in project delivery (Liao et al., 2021). The Construction Industry Council of Hong Kong found that 73% of contractors had never engaged in any BIM-assisted projects (Yu Yang et al., 2024).

Such a challenge is even more pronounced in China, where BIM is promoted rather than mandated (Yonghong Chen & Ding, 2023). Although Chinese designers are aware of BIM benefits and basic operations through education and policy promotion (J. Li et al., 2020; Yu Yang et al., 2024), they show significant resistance in adopting BIM during design, especially when there is no client requirement for BIM usage (Wei & Hu, 2014). Approximately half of Chinese designers are at the lowest level of BIM application and more than 75% of enterprises use BIM for less than 50% of their projects, including the “token” use to meet government requirements (Deng et al., 2020).

The evidence suggests that while BIM models are beneficial for information exchange, they may not be feasible or valuable across all stages due to the complexity of projects. BIM does not always meet the expectations set by academia nor necessarily yield benefits in practical applications (Lidelöw et al., 2023) because BIM may not be apt for certain design phases due to its limitation in executing specific tasks (Y. Liu et al., 2017). This is particularly evident in early design stages, e.g., the concept design stage. At this stage, design data are fluid, allowing designers to explore various design alternatives to optimise performance (J. P. Basbagill et al., 2014; Muthumanickam et al., 2023). Designers often use general massing instead of determined building elements to investigate the basic shape, form, and layout of projects, leading to ambiguous element types and relationships. However, the semantic ambiguity from general massing in concept design can cause BIM models to fail (H. Liu et al., 2018), as BIM models demand design certainty and well-defined building elements (Leon & Laing, 2022). Although BIM software provides specific functions, like massing in Revit, for designers, their application in early design stages is limited (Lidelöw et al., 2023).

Moreover, design activities in the concept design phase are often viewed in a “black box”, with undefined processes (Y. Liu et al., 2017). The information exchange among designers often surpasses mere drawing or BIM file exchanges, potentially exceeding the capacity of BIM (Tribelsky & Sacks, 2010). While BIM offers benefits in collision control, visualisation, providing foundation for simulations and drawing generation (Lidelöw et al., 2023), they are not the primary focus in the early design stage. Here, rapid modelling and design alternative

evaluation are paramount, amplifying BIM's disadvantages of complex modelling (H. Liu et al., 2018). In these instances, designers often gravitate towards simpler and familiar tools (e.g., Rhino, SketchUp) (Y. Liu et al., 2017). Consequently, BIM adoption is rarer in initial phases but more prevalent in advanced project stages (Lidelöw et al., 2023). Obviously, this adoption of BIM is conflict with the proposed application scenario of those BIM-based sustainable design optimisation methods, which aim to provide design assistance in the early design stages, leading to a limited practicality. Thus, conventional EIF (e.g., 2D drawings and 3D graphs) should not be excluded from expressing design data.

Studies grounded in experimentation shed light on the efficacy of various EIF in detailed design tasks. The experiments using simplified model suggests that 2D drawings more effectively convey relative positioning than perspective or isometric drawings, while 3D displays offer superior depth and shape comprehension (Dadi, Goodrum, Taylor, & Maloney, 2014). Therefore, for tasks emphasizing the relative positioning of building elements in two dimensions, 2D drawings are favoured, while 3D displays are chosen for shape recognition and multi-dimensional tasks (Dadi, Goodrum, Taylor, & Maloney, 2014). Overall, the efficiency difference between 3D and 2D engineering information format in data cognition is insignificant (Dadi, Goodrum, Taylor, & Carswell, 2014). In practical applications, experts report a notably increased cognitive demand when working with 3D model compared to 2D drawings (Shi, Du, & Worthy, 2020). Hardison et al. (2020) observed no marked difference in hazard recognition performance across different information formats. Therefore, it is challenging to assert that a particular format of engineering information holds overarching advantages or could universally supplant the others, let along claiming that BIM is suitable for all design tasks.

The nature of design tasks dictates the process of receiving, creating, processing, and delivering information. Engineering information formats currently in use have been reasonably selected and verified over time, being specifically tailored to particular design tasks. However, contemporary BIM promotion strategies, which emphasize fundamentally altering existing design practices to adopt standardized BIM formats (Tan et al., 2021), tend to oversimplify the design file as merely an information carrier. This simplification overlooks its role in facilitating the creativity of designers and may lead to a misalignment between the tools provided by BIM and the actual needs of designers. Coupled with BIM's failure to realise benefits in conventional design tasks (Y. Liu et al., 2017), those abrupt promotion approaches encounter significant resistance in the design industry (Ahmed, 2018; Tan et al., 2019). Practitioners are

reluctant to shift from their traditional practices without clear benefits and defined application contexts (Lidelöw et al., 2023).

The definition BIM, the process of generating and managing information about a building during its entire life (Fu, 2018), indicates the difference between applying BIM in design process and using BIM model for project design, suggesting for a flexible BIM application. Given the lessons learned from Singapore and Hong Kong (Liao et al., 2021; Yu Yang et al., 2024), where using BIM sometimes become a compliance-driven operation, integrating BIM and conventional EIF in design is crucial.

2.5.2 Methods for optimisation results communication

Generally, sustainable design optimisations are normally conducted via three approaches (Roberts et al., 2020), as given in Table 2-2:

1) cooperation of design and analysis software (J. P. Basbagill et al., 2014);
2) design integrated plug-in tool (Basic et al., 2019);
3) numeric values and tables (Cang et al., 2020);

Approaches 1 and 2 enable architects to evaluate sustainability performance and aesthetics requirements simultaneously (Hollberg & Ruth, 2016). The outputs of these two methods are conveyed via building models, drawings, and corresponding numeric emission values.

Table 2-2: Engineering information format utilisation in design optimisation tools

Design optimisation tools	Engineering information format
Design & Analysis software	3D/BIM models, 2D graphs, and numeric values
Design integrated plug-in tool	3D/BIM models, 2D graphs, and numeric values
Numeric values and tables	numeric values

In approach 1, the design data are normally transferred across varies EIFs and software environments. For instance, Shadram & Mukkavaara (2018) converted BIM data into numeric parameters for optimisation. The optimisation results from algorithms, in parameter form, are then re-applied in Revit for visualisation. This approach fully utilises existing tools but demands additional EIF transformation process across software environments.

In contrast, approach 2 integrates data processing, sustainability analysis, design optimisation, and results visualisation within a single design software. For example, Basic et al. (2019) implemented real-time CE calculation within Rhino 3D using its embedded programming tool,

Grasshopper. Although approach 2 reduces the need for EIF transformation, its computing and optimisation efficiency is usually constrained by the default settings of design software rather than hardware, making it less efficient than approach 1.

Compared to approaches 1 and 2, approach 3 is weaker in visualisation but is software-independent and easy to implement. For instance, Lu et al. (2019) used Microsoft Excel for CE calculation. However, this approach is less user-friendly for designers, as it is difficult to establish direct relationships between design decisions and numeric emission values, hindering design optimisation for better sustainability. Therefore, scholars have integrated numeric-value- or table-based sustainability certification tools (e.g., LEED (USGBC, 2024) and BREEAM (BRE Global Limited, 2024)) with BIM for improved application (Cascone, 2023; Dubljević et al., 2023). This integration ultimately aligns with the frameworks of approaches 1 and 2.

Beyond the aforementioned EIFs for optimisation results communication, J. P. Basbagill et al. (2014) proposed a novel approach that represents the probability distribution of remaining alternatives after each decision is fixed. This approach directed designers to decisions with the highest potential for carbon reduction, balancing design flexibility and sustainability.

2.6 Summary

The review highlights scholars' extensive efforts to enhance sustainability in the design stages, offering effective strategies for estimating and optimising embodied CE. Figure 2-1 depicts the concepts derived from the literature review, which is organized into three key processes: 1) design alternative generation, 2) CE analysis, and 3) optimised solution output. These processes are represented by the vertical colour-coded blocks on the left side of the figure. Within these processes, previous concepts address five pertinent topics: 1) identifying design tasks in different stages, 2) managing design uncertainties, 3) defining system boundaries, 4) estimating CE, and 5) integrating CE optimisation into design. These topics are detailed in the vertical blocks on the right side. Variables in each topic, concerning design content, design data, delivery stage, measured item, reference data, optimisation tool, and EIF, are presented in individual black blocks. Concepts are defined and differentiated by the set of variables they encompass, as indicated by the color-coded blocks surrounding them.

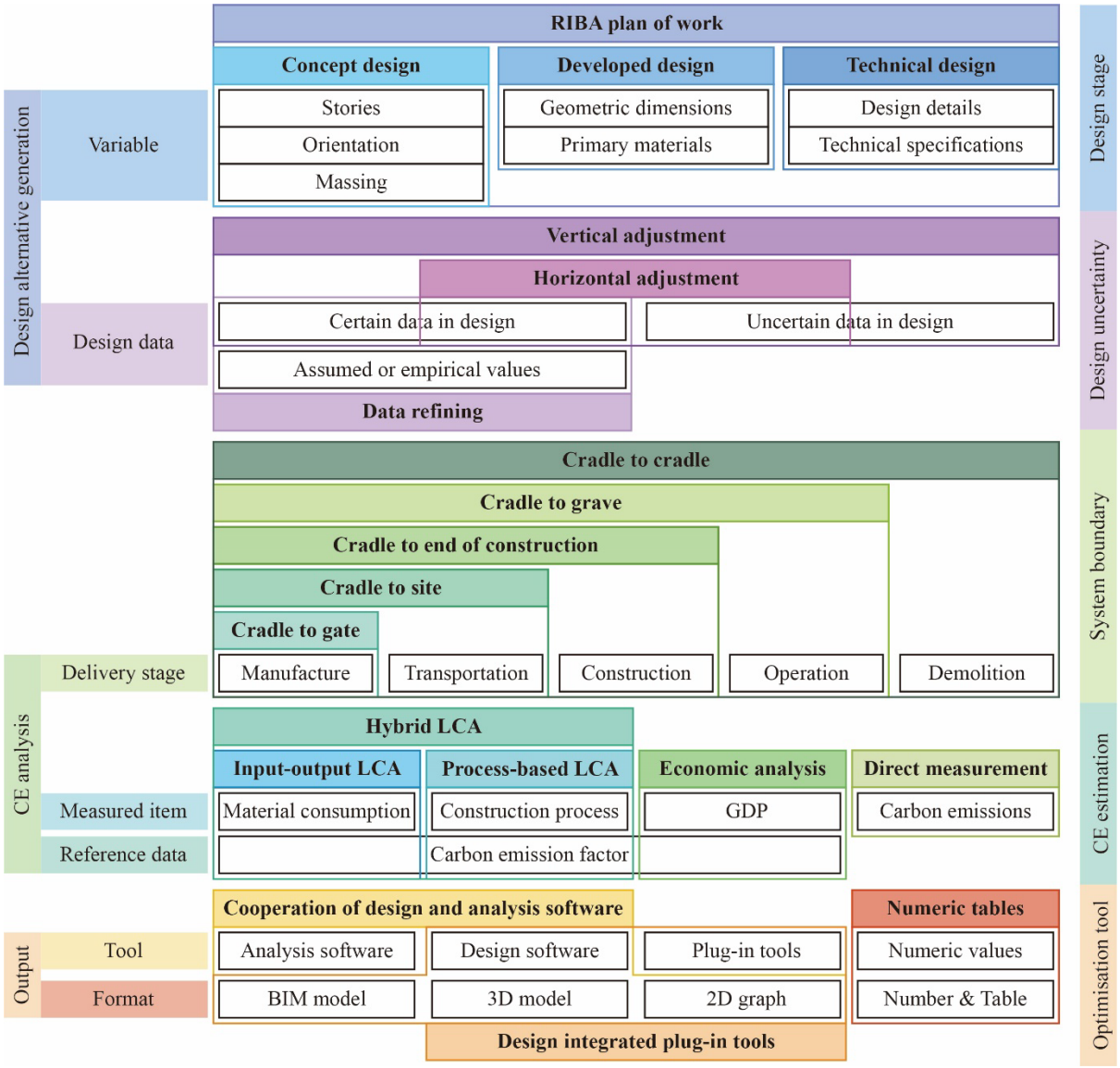

Figure 2-1 Summary of concepts from literature review.

3 Methodology

3.1 Research philosophy and approach

This research adheres to a postpositivist worldview, positing that causes probably determine effects or outcomes. This perspective holds that complicated problems can be tackled through breaking them into smaller, discrete units for testing. Therefore, knowledge development from a postpositivist perspective relies on the observation and measurement of the objective reality in practice. (Creswell & Creswell, 2013).

Adopting a postpositivist worldview, this research design is premised on the following assumptions (Phillips & Burbules, 2000):

1) Knowledge is tentative, and evidence derived in research is inherently imperfect and prone to error. Therefore, research findings do not confirm a hypothesis; rather, they indicate an inability to reject it.
2) Research involves making claims and then refining or discarding them in favour of more substantiated claims. Thus, research usually starts with the test of theories.
3) Knowledge is shaped by data, evidence, and rational considerations. Consequently, the primary method for data collection is through measurement and observations.
4) Research seeks to develop statements that explain concerns or describe causal relationships. As a result, relationships among variables are highlighted through questions or hypotheses.
5) Being objective is an essential aspect of competent inquiry. Research methods and conclusions must be examined for bias.

Given postpositivist philosophy and the abundant studies in sustainable design, this study employs a deductive approach, which relies on facts and previous knowledge (Kyngäs & Kaakinen, 2020). This approach starts with general premises, like existing theories, and aims to draw specific conclusions (Gray & Grove, 2020). Typically, deductive reasoning entails reviewing existing theories, formulating testable hypothesis based on those theories, collecting data for hypothesis test, analysing the data, and concluding whether to reject the hypotheses (Elo & Kyngäs, 2008).

Considering the goal to develop a practical design optimisation model for reducing embodied CE in prefabricated projects, this study's specific application of the deductive method includes:

1) Examining prior research on carbon reduction in prefabricated projects.
2) Identifying potential design variables and strategies for carbon reduction.
3) Assessing the impact of these variables and the effectiveness of proposed strategies.
4) Analysing the test results.
5) Concluding on the effectiveness of the proposed design optimisation model.

3.2 Research strategy

The development of the proposed optimisation model utilises a quantitative research strategy, as illustrated in Figure 3-1. According to hypothesis (1) (section 1.3.2), variables critical to developing the design optimisation model encompass design decisions and embodied CE. Typically, design decisions are predominantly represented as continuous variables, such as dimensions. The rest, like the selection of building materials and products, are considered as categorical variables. These categorical variables can be transformed into quantitative features, such as the compressive strength of concrete. As a result, all design decisions can be quantified as the numerical features of project. Given the quantitative nature of embodied CE, this study establishes quantitative relationships among project design, design features, and project emissions.

Specifically, embodied carbon emissions CE are chosen as the indicator for design estimation (i.e., dependent variable) in this study. Design decisions will be converted into a series of quantitative design parameters (i.e., independent variables) $Para$. The range of each parameter, denoted as set R, is defined according to industrial practise. The goal of the optimisation model can be stated as:

$$\min_{Para \in R} CE(Para) \tag{3-1}$$

The result of equation (3-1) is explored by experimental analysis, which seeks to determine how a change in $Para$ influence CE. The influence of $Para$ on CE is assessed by providing a specific adjustment to $Para$ in one case compare its CE to another without (Creswell & Creswell, 2013).

Hypothesis (6) (section 1.3.2) indicates that the model output form is determined by two variables: design tasks and designers' attitude towards specific EIFs. This study utilises a quantitative survey to measure designer's design tasks and their attitudes towards specific EIFs.

Through analysing the quantitative relationships between these variables, it is possible to predict a specific designer group's preferred EIF based on its population characteristics.

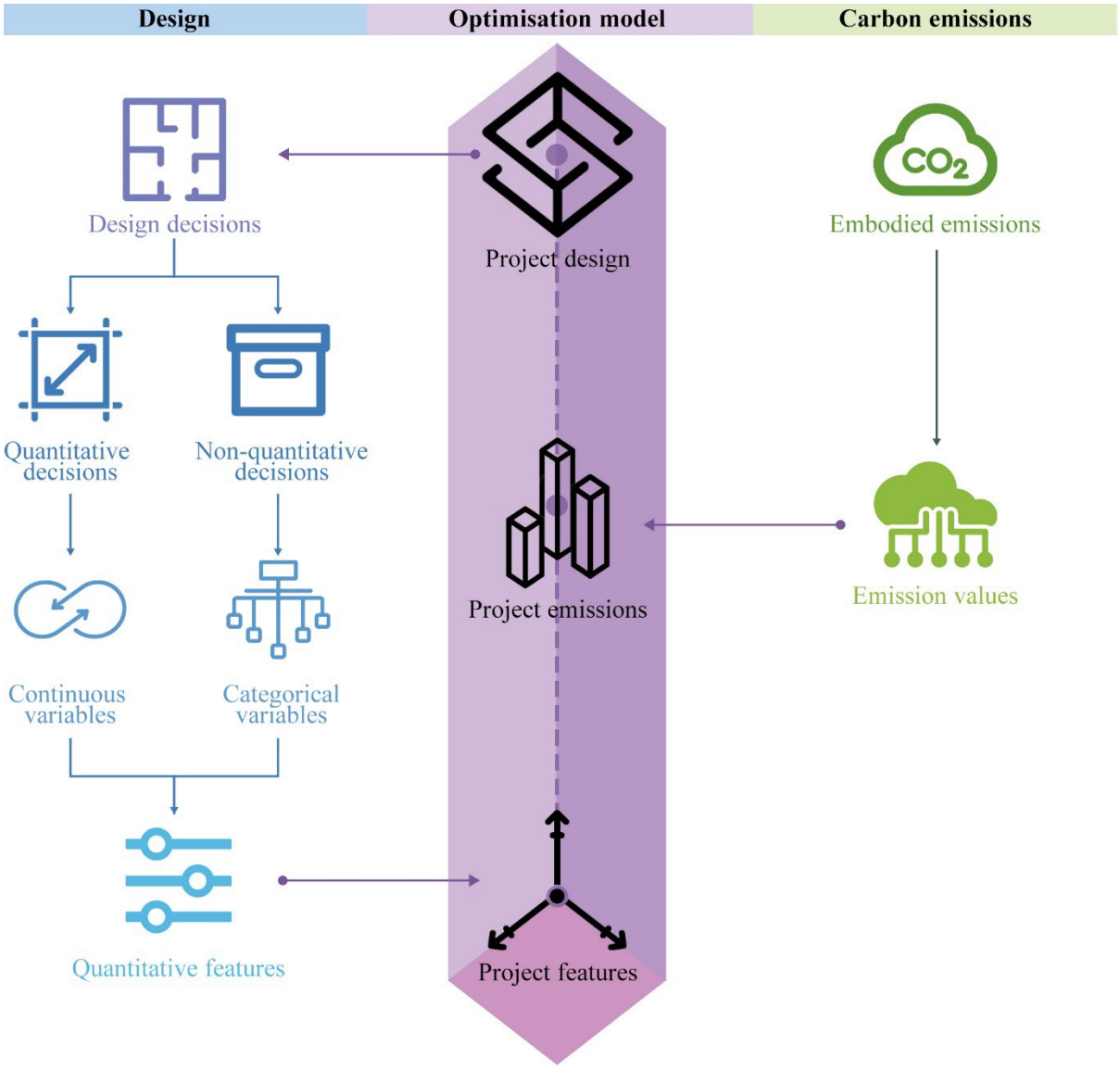

Figure 3-1 Research strategy.

3.3 Research design

3.3.1 Determination of research scope

This study focuses on reducing the embodied CE of prefabricated projects in China. Therefore, the research context is embedded in current Chinese construction industry. The common design process and existing design codes are considered as the foundation and requirement of study design. Considering the variance in technology difference across varied prefabrication methods,

like precast concrete structure, prefabricated steel structure, etc., this study selected the mainstream prefabrication type in China, precast concrete structure, as the prototype.

CE, calculated in CO_2 equivalent (CO_2-eq), serves as the sole indicator for embodied emissions estimation in this study because it represents the projects' primary environmental impacts (Section 2.1). LCA on the construction CE reveals that manufacturing and transportation of building elements present the greatest opportunities for carbon reduction in prefabrication (Teng & Pan, 2020). Restricting the system boundary to these stages could yield the most efficient carbon reduction strategies. Therefore, the system boundary of this study is set to embodied CE from the manufacturing and transportation stages of prefabricated projects. Specifically, it includes the emissions from building materials, formwork, and transportation of prefabricated elements.

Emissions from producing and assembling the prefabricated elements are excluded due to their limited contribution to the overall embodied CE (around 5%), as stated in section 2.2.1. Emissions of project demolition and material reuse and recycling are excluded due to lacking standardised emission data, calculation method, and estimation scenarios (Wen et al., 2024). Additionally, the transportation of building materials is ignored because this process is similar between cast-in-situ construction and prefabricated construction, leading to limited emission reduction potential.

Section 2 indicates that early-stage design decisions have the most carbon reduction potential, while their reliability in reducing CE remains questioned. In contrast, the effect of optimisation in later stages is more reliable but less significant. However, the sporadic results from material optimisation of single structure elements (e.g., beams and floors) demonstrate the potential of reducing embodied CE optimising the size or shape of structures (Xiang, Mahamadu, Florez-Perez, et al., 2024). Considering the balance between effectiveness and reliability, it is valuable to estimate and utilise the carbon reduction potential of design decisions in the developed and technical design stages, i.e., micro-level design variables.

The comparison among process-based LCA, input-output LCA, hybrid LCA, economic analysis, and direct measurement (Section 2.2.2) suggests that hybrid LCA is the optimal method for estimating embodied CE at the project level. The integration of process-based analysis and material-consumption-based CE calculation allows to consider detailed design variables and utilise of existing reliable emission data. This approach is well suited to be

adopted in the micro-level analysis model. Therefore, emission analysis in this study employs the principles and general methods of hybrid LCA. However, introducing micro-level analysis variables differ the estimation process from standard hybrid LCA methods. Furthermore, due to the ongoing confusion about LCA terminology (Section 2.2.2), this study adopts the general term "emission estimation/analysis" for clarity and consistency in subsequent sections.

Regarding the application of sustainable design optimisation, integrating design software and estimation tool is considered the most effective strategy. However, although BIM being the preferred format for sustainable design, its practical effectiveness remains unclear. A comprehensive investigation of design practice is essential to determining the most appropriate method for implementing sustainable design optimisation in the construction industry.

Based on these findings, this study outlines the scope of the optimisation model, as illustrated in Figure 3-2. Specifically, the optimisation model incorporates design variables from both developed and technical design stages, utilising a parametric design approach (a vertical adjustment method) to address design uncertainty. The model employs the Hybrid LCA to estimate and optimise cradle-to-site CE of projects. Through the integration of design and analysis software, the optimised solution is rendered in both 3D models and 2D graphs.

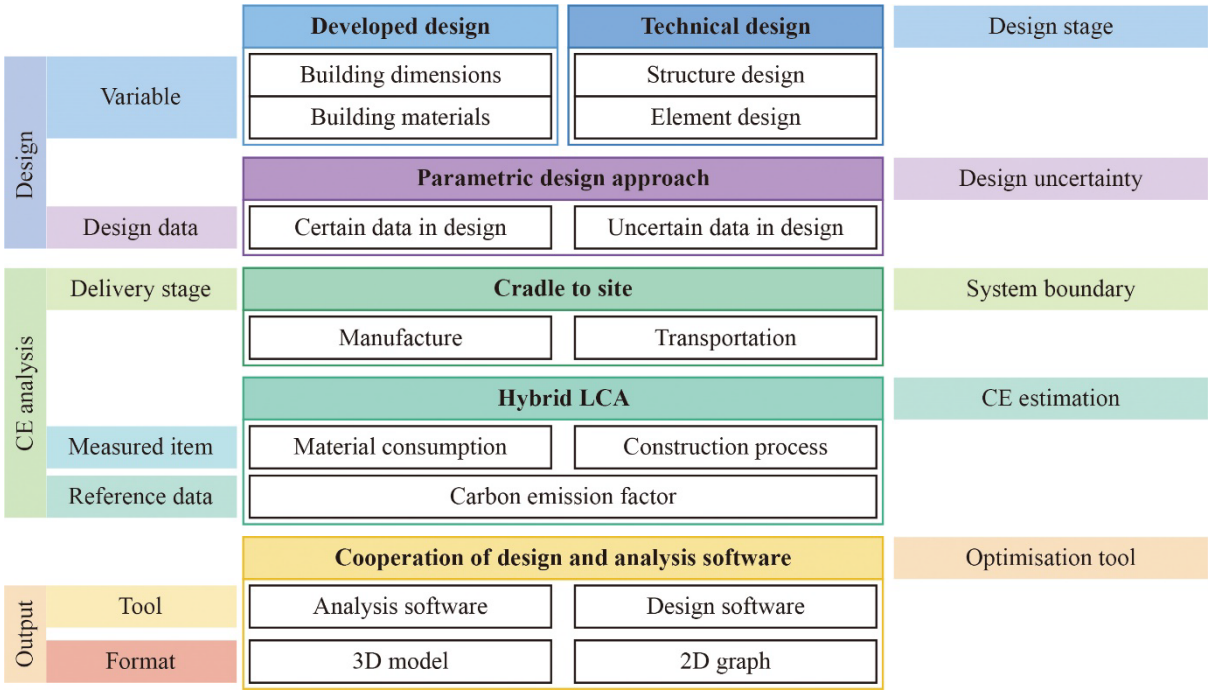

Figure 3-2 The scope of the optimisation model.

3.3.2 Conceptual model

Figure 3-3 depicts the modules and workflow of the design optimisation model. The optimisation comprises four modules: 1) design data extraction, 2) manufacturing CE optimisation, 3) transportation CE optimisation, and 4) feasible solution visualisation.

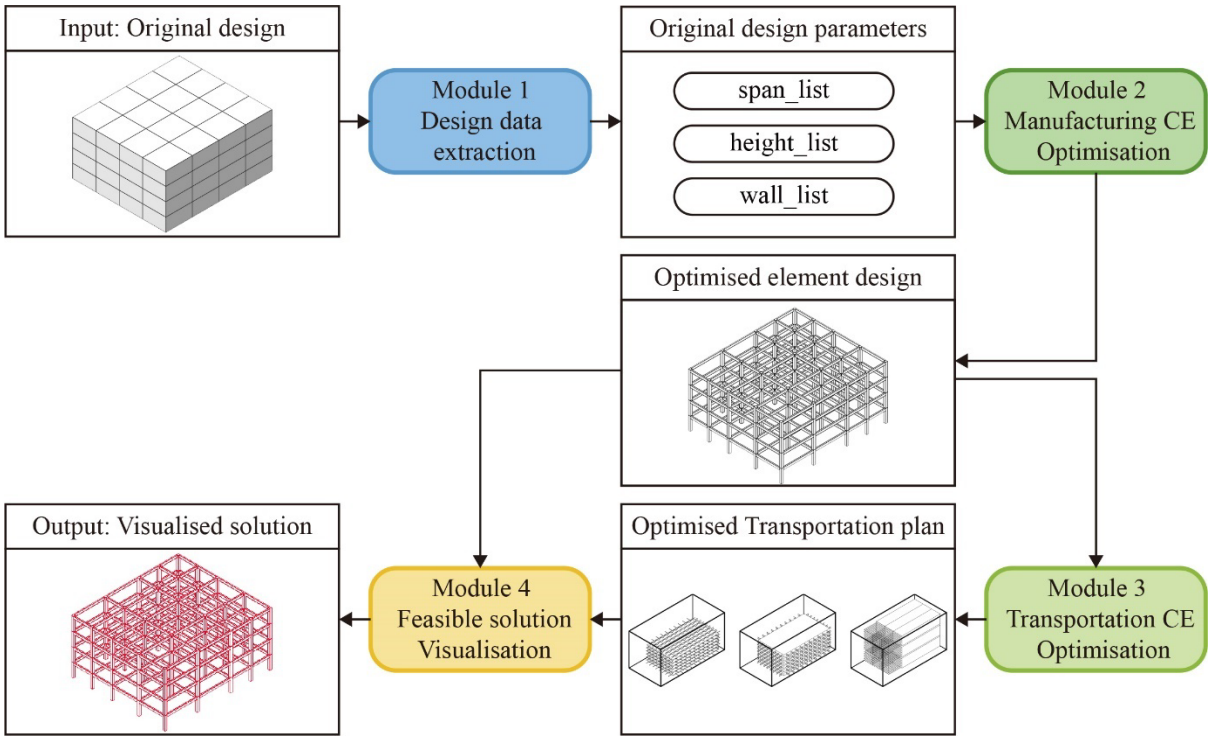

Figure 3-3 The workflow of optimisation model.

The input to the optimisation model is an original architectural design at the LOD 100 to LOD 200 level. Module 1 converts the original design into a set of parameters representing geometric features. Subsequently, module 2 processes these parameters to identify an optimised element design with the lowest manufacturing CE. Module 3 then uses the element data from module 2 to determine an optimised transportation plan with the lowest transportation CE. Finally, module 4 processes results from modules 2 and 3 for visualisation in a designer-friendly format.

Notably, the optimisation model separates the optimisation for manufacturing and transportation CE into two distinct modules instead of integrating them into a single comprehensive module. Results from Xiang et al. (2024) and Xiang et al. (2022) show that optimising CE solely during manufacturing or transportation requires 24-48 hours, nearing the maximum acceptable optimisation period (Jusselme et al., 2020). Integrating both optimisations could lead to an overcomplicated model and reduced optimisation efficiency,

exceeding the acceptable optimisation period. Given that manufacturing contributes to a significantly larger portion of embodied CE than transportation (82.9% vs. 9.3% (Teng & Pan, 2020)), sequential optimisation of manufacturing and transportation CE may offer an efficient and effective carbon reduction.

3.3.3 Research framework

The research design of this study involves six steps: 1) literature review, 2) development of module 2 for manufacturing CE optimisation, 3) development of module 3 for transportation CE optimisation, 4) development of module 1 and 4 for design data processing, 5) case study, and 6) research validation, as illustrated in Figure 3-4 .

The literature review identifies design variables, system boundaries, and emission factors for module 2 and 3, as well as design activities for module 1 and 4, detailed in section 2. Based on a review of current design activities, a questionnaire is created to gather data on design content and EIF utilised in design practices. Statistical analysis of the questionnaire results reveals the quantitative relationship between design tasks and EIF. Estimating design tasks at the developed and technical stages helps identify the most likely EIFs for the original design and visualised solution. Module 1 and 4, which convert the original design into parameters and the feasible solution's parameters into a design model, respectively, are developed based on these EIFs.

The system boundary determined from the literature review sets the scope for modules 2 and 3. Module 2 uses variables identified from the literature review to generate design alternatives based on original design parameters. Emission factors from prior studies are employed to estimate and compare the CE of each design alternative, identifying the feasible one with the lowest manufacturing CE. This feasible alternative is then processed by module 3, which follows a workflow similar to module 2, to determine the feasible transportation plan with the lowest CE. Module 4 processes the feasible design alternative and transportation plan from modules 2 and 3, respectively, to output a visualised solution for designers. A case study is used to test each module of the optimisation model, ensuring its reliability in processing representative project designs.

The effectiveness and practicality of the optimisation are confirmed through internal and external validation, respectively. Internal validation involves comparing the CE between the optimisation model and existing design methods. The optimisation model is deemed effective

if its CE is lower than that of existing methods. External validation involves gathering design variables used in practice and designers' attitude towards the optimisation model. The optimisation model is deemed practical if it satisfies most design practice requirements.

For clarity, this thesis first discusses the development of modules 2 and 3 in sections 4 and 5, respectively. The development of modules 1 and 4 is then detailed in section 6. A case study that testing the entire model is described in section 7.2. Section 7.3 details the validation of the model.

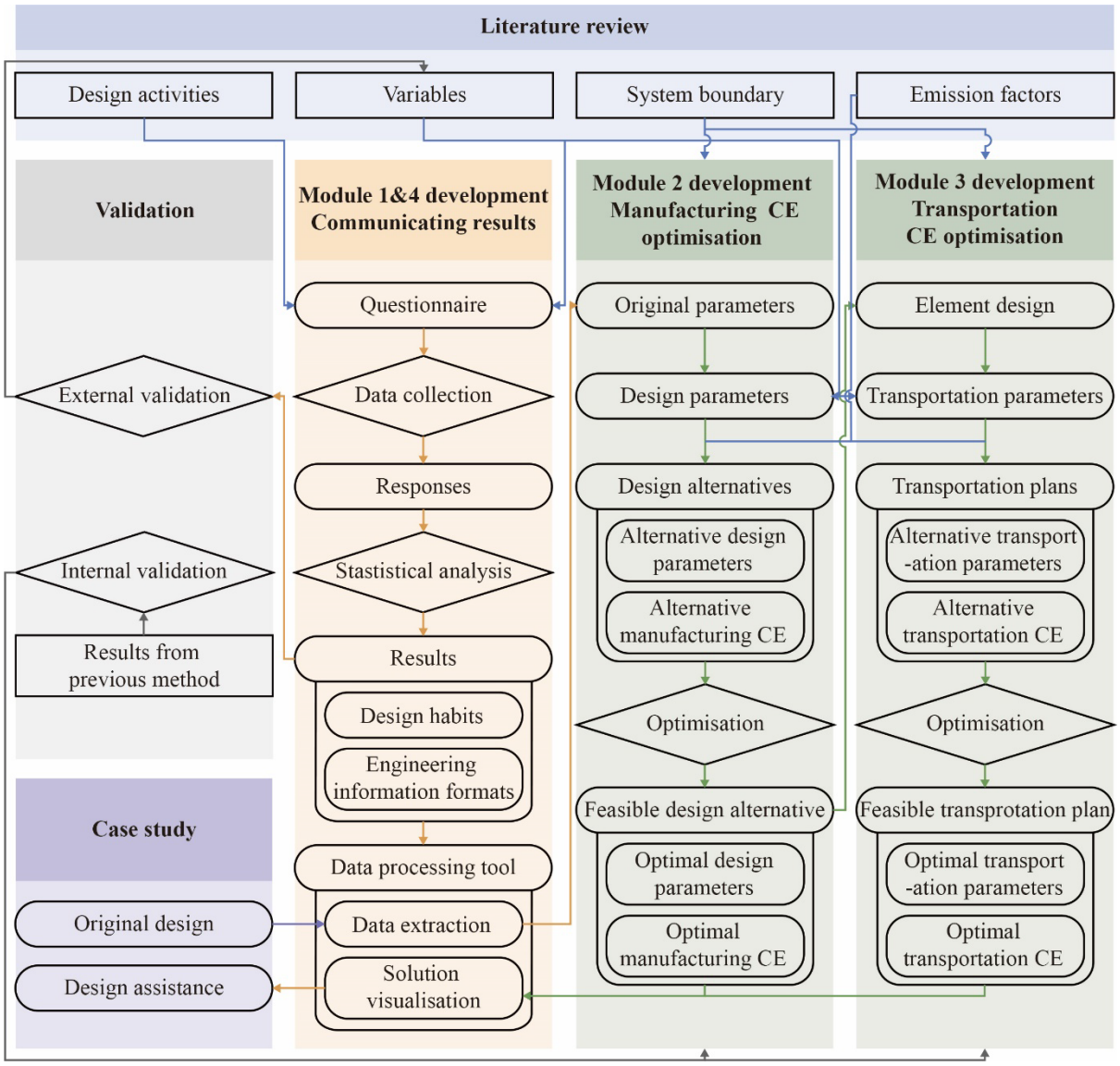

Figure 3-4 The research framework.

4 Optimisation of manufacturing CE

4.1 Introduction

As evidenced from the above review, scholars have devoted considerable effort to optimise the sustainability in the design stages, providing effective approaches for CE estimation and optimisation. However, the system boundaries of previous optimisation studies are typically limited to the CE generated from manufacturing structure materials (e.g., steel and concrete), while excluding CE from auxiliary materials (e.g., formwork) (X. Zhang & Wang, 2022). There is a scarcity of research considering the trade-off between CE from formwork and structural material. Additionally, the findings from existing studies aim to provide generalised guidance for architects before or during the concept design phase. The implementation of these guidelines is challenging to monitor as the design progresses. There is a notable absence of optimisation methods offering more specific suggestions in the developed design stage.

Therefore, this module seeks to explore the CE reduction potential during the developed design stage, through design optimisation. It considers emissions from both building materials and formwork and introduces variables from both architecture and structure design to maximise the optimisation effects. The content in this chapter has been published in the study of Xiang et al. (2024).

4.2 Optimisation method

The methods employed in this module involves five steps: 1) generate design alternatives using a parametric approach, 2) analysis the response of structure under loadings, 3) detail the structure design according to structure analysis, 4) calculate the CE of design alternatives, and 5) explore the solution with the lowest embodied CE, as illustrated in Figure 4-1.

The analysis and optimisation are restricted to the superstructure, excluding foundations because the design of foundation is highly site-specific and project-specific. Restricting the analysis to superstructures helps to improve the generalisability of the method (Hart et al., 2021). The methods are based on the following postulations, which are normally adopted in prefabrication design:

1) All grids in the framework are rectangular;
2) Secondary beams are evenly distributed in each grid;

3) All walls are directly supported by beams or secondary beams;

4) The cross-section of each structure elements is rectangular and consistent;

5) The cross-section of columns on the same floor is an identical square.

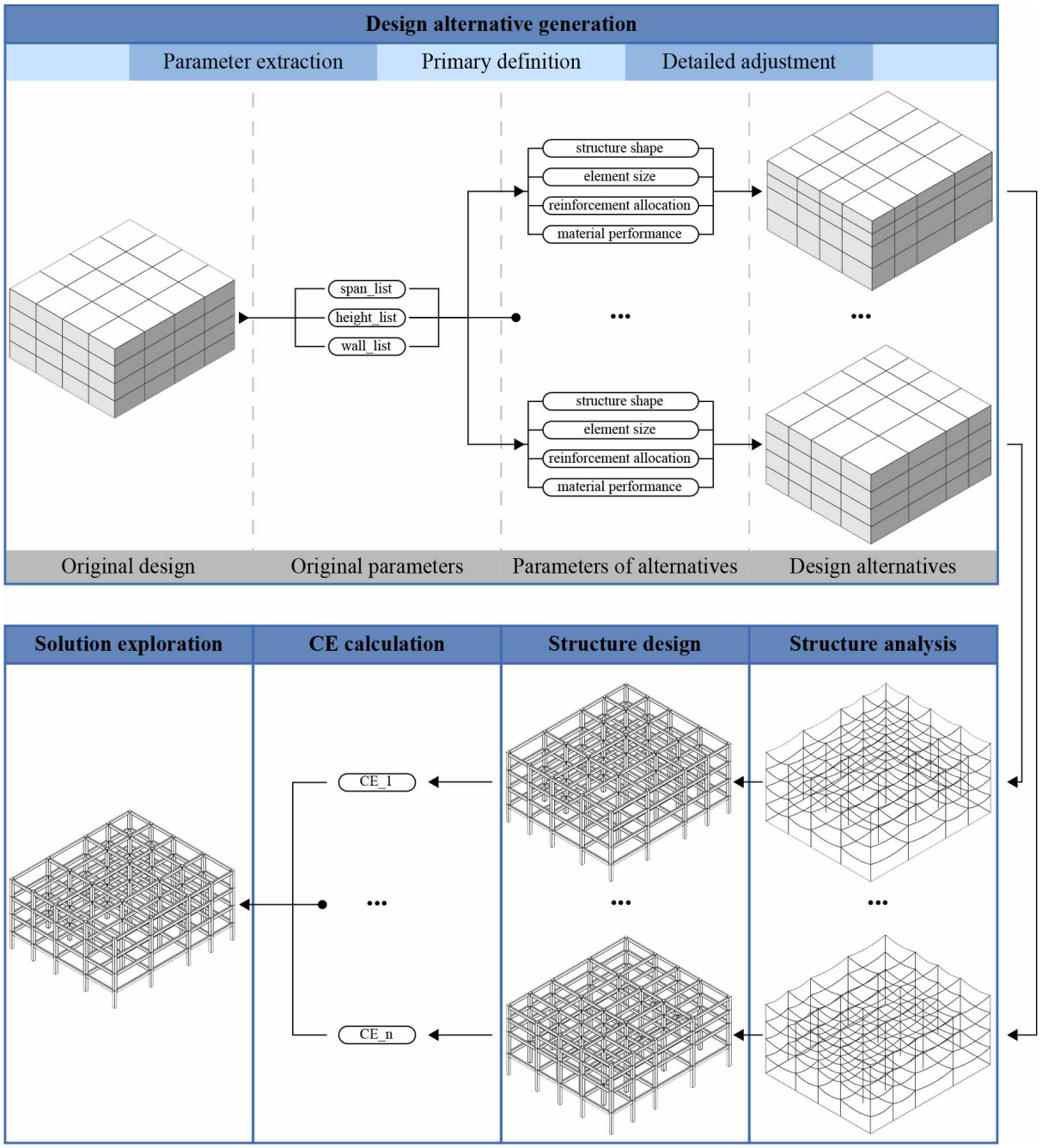

Figure 4-1 Framework of module 2.

4.2.1 Design alternative generation

4.2.1.1 Original design parameter extraction

Module 2 considers design files at the developed design stage as the start point. The geometric features concerning the span length, floor-to-floor height, and the distribution of walls (both internal and external walls) are extracted from design files as lists below:

$$original\_span\_list_d = \{OSL_{d-1}, \dots, OSL_{d-i}, \dots, OSL_{d-n}\}(d = X\ or\ Y) \quad (4\text{-}1)$$

$$original\_height\_list = \{OFH_1, \dots, OFH_i, \dots, OFL_n\} \quad (4\text{-}2)$$

$$original\_wall\_list = \{OW_{1-1-1}, \dots, OW_{f-i-j}, \dots, OW_{m-n-o}\} \quad (4\text{-}3)$$

$$OW_{f-i-j} = \{OWC_{f-i-j-0}, OWC_{f-i-j-1}\} \quad (4\text{-}4)$$

where, $original\_span\_list_d$ is the list of original span length in the d direction; OSL_{d-i} is the original length of the i-th span in the d direction (m); $original\_height\_list$ is the list of original floor-to-floor heights (m); OFH_i is the original floor-to-floor height of the i-th floor (m); $original\_wall\_list$ is the list of original walls, $OWC_{f-i-j-0}$ and $OWC_{f-i-j-1}$ are the coordinates of the start and end points of the j-th wall in the i-th grid on the f-th floor, respectively.

4.2.1.2 Primary definition of design alternatives

Each design alternative is defined by a series of parameters, as listed in Table 4-1 and Figure 4-2. The parameters are categorised into four types, determining the shape of entire structure, the shape of each structure element, the detailed design of each element, and the performance of construction materials, respectively. Design alternatives are generated by varying the value of these parameters within a certain range. The distribution of these parameters is subject to the constraints described by equations (4-5)-(4-13).

$$OSL_{d-i} + min\_TSL_{d-i} \leq DSL_{d-i} \leq OSL_{d-i} + max\_TSL_{d-i} \quad (4\text{-}5)$$

$$OFH_i + min\_TFH_i \leq DFH_i \leq OFH_i + max\_TFH_i \quad (4\text{-}6)$$

$$\sum OSL_{d-i} + min\_TTL_d \leq \sum DSL_{d-i} \leq \sum OSL_{d-i} + max\_TTL_d \quad (4\text{-}7)$$

$$\sum OFH_i + min\_TTH \leq \sum DFH_i \leq \sum OFH_i + max\_TTH \tag{4-8}$$

$$\frac{DSL_{d-i}}{max\_FW} \leq SBN_{f-i} + 1 \leq \frac{DSL_{d-i}}{min\_FW} \tag{4-9}$$

$$\frac{SL_i}{max\_BSDR} \leq BD_i - CCD \times 2 \leq \frac{SL_i}{min\_BSDR} \tag{4-10}$$

$$\frac{BD_i - CCD \times 2}{max\_BDWR} \leq BW_i - CCD \times 2 \leq \frac{BD_i - CCD \times 2}{min\_BDWR} \tag{4-11}$$

$$\frac{SL_i}{max\_SBSDR} \leq SBD_i - CCD \times 2 \leq \frac{SL_i}{min\_SBSDR} \tag{4-12}$$

$$\frac{SBD_i - CCD \times 2}{max\_SBDWR} \leq SBW_i - CCD \times 2 \leq \frac{SBD_i - CCD \times 2}{min\_SBDWR} \tag{4-13}$$

where, min_TSL_{d-i} and max_TSL_{d-i} denote the lower upper boundary of the tolerance for the i-th span in d direction (m); similarly, min_TFH_i and max_TFH_i, min_TTL_d and max_TTL_d, and min_TTH and max_TTH describe the tolerance of the floor-to-floor height of the i-th floor, the tolerance of the overall dimension of structure in d direction, the tolerance of the overall height of structure, respectively (m); DSL_{d-i} signifies the span length of the i-th column grid in d direction (m); max_FW and min_FW represent the maximum and minimum widths of floor slabs, respectively (m); CCD is the concrete cover depth (m); SL_i is the span length of the i-th beam or secondary beam (m); max_BSDR and min_BSDR are the maximum and minimum span-depth ratios of beams, respectively (m); max_BDWR and min_BDWR refer to the maximum and minimum depth-width ratios of beams, respectively; max_SBSDR and min_SBSDR represent the maximum and minimum span-depth ratios of secondary beams; and max_SBDWR and min_SBDWR are the maximum and minimum depth-width ratios of secondary beams, respectively.

Equation (4-5)-(4-8) allows minor changes to the geometric dimensions of the original structure within design alternatives. Typically, architects set identical span length for grids based on their experience and preferences. However, the net distances between columns may vary from the original design due to adjustments in element size (e.g., extending column size for load bearing) and locations (e.g., offsetting columns from the axis). Consequently, minor adjustments to span dimensions (normally less than half of the column edge length) are

common and acceptable in design practices. Comprehensive adjustments to these dimensions may lower embodied CE in manufacture and assembly processes (e.g., by reducing the type and number of formwork) as they may standardise the actual size of elements. Equations (4-9)-(4-13) constrain the solution space, reducing the risk of structurally unfeasible design alternatives, within which the required amount of reinforcement of some elements exceeds the maximum reinforcement due to the geometry of cross section. For the same reason, the sizes of columns in each design alternative are calculated by equations (4-14)-(4-15)

$$EL_f = \sum q_{n-f} \times A_{n-f} \tag{4-14}$$

$$CW_f = \sqrt{\frac{EL_f}{column\_num_f \times (CCS \times \varepsilon_{column})}} + CCD \times 2 \tag{4-15}$$

where, EL_f is the estimated vertical load on the columns of f-th floor (kN); n is the total number of floors; q_{n-f} and A_{n-f} represent the estimated load coefficient (kN/m^2) and the area (m^2) of the $(n-f)$-th floor, respectively; CW_f is the width of columns on the f-th floor (m); $column\_num_f$ is the number of columns on the f-th floor; CCS denotes the axial compressive strength of column concrete (kN/m^2); ε_{column} is the estimated coefficient of compression zone of columns.

Table 4-1 Parameters employed in the generation of design alternatives.

Type of parameters	**Parameter**	**Meaning**
The shape of structure		
	DSL_{d-i}	Designed length of the i-th span in d direction
	DFH_i	Designed floor-to-floor height of the i-th floor
	SBN_{f-i}	The number of secondary beams in the i-th column grid on the f-th floor
	SBO_{f-i}	The orientation of secondary beams in the i-th column grid on the f-th floor
The shape of structure elements		
	BD_i	The designed depth of the i-th beam
	BW_i	The designed width of the i-th beam
	SBD_i	The designed width of the i-th secondary beam

	SBW_i	The designed width of the i-th secondary beam
	FD_i	The designed depth of the i-th floor slab
The details of structure elements		
	CRD_i	The reinforcement design of the i-th column
	CBT_{f-d-i}	The top reinforcement design of the continuous beams on i-th axis in d direction on the f-th floor
	BRD_i	The reinforcement design of the i-th beam
	$CSBT_i$	The top reinforcement design of the i-th group of continuous secondary beams
	$SBRD_i$	The reinforcement design of the i-th secondary beam
	FRD_i	The reinforcement design of the i-th floor slab
The performance of materials		
	CON_{column}	The grade of concrete used in columns
	CON_{beam}	The grade of concrete used in beams
	$CON_{secondary-beam}$	The grade of concrete used in secondary beams
	$CON_{floor-slab}$	The grade of concrete used in floor slabs
	RE_{column}	The grade of tensioned bars used in columns
	RE_{beam}	The grade of tensioned bars used in beams
	$RE_{secondary-beam}$	The grade of tensioned bars used in secondary beams
	$RE_{floor-slab}$	The grade of reinforcement used in floor slabs
	$RE_{column-hop}$	The grade of hooping used in columns
	$RE_{beam-hop}$	The grade of hooping used in beams
	$RE_{secondary-beam-hop}$	The grade of hooping used in secondary beams

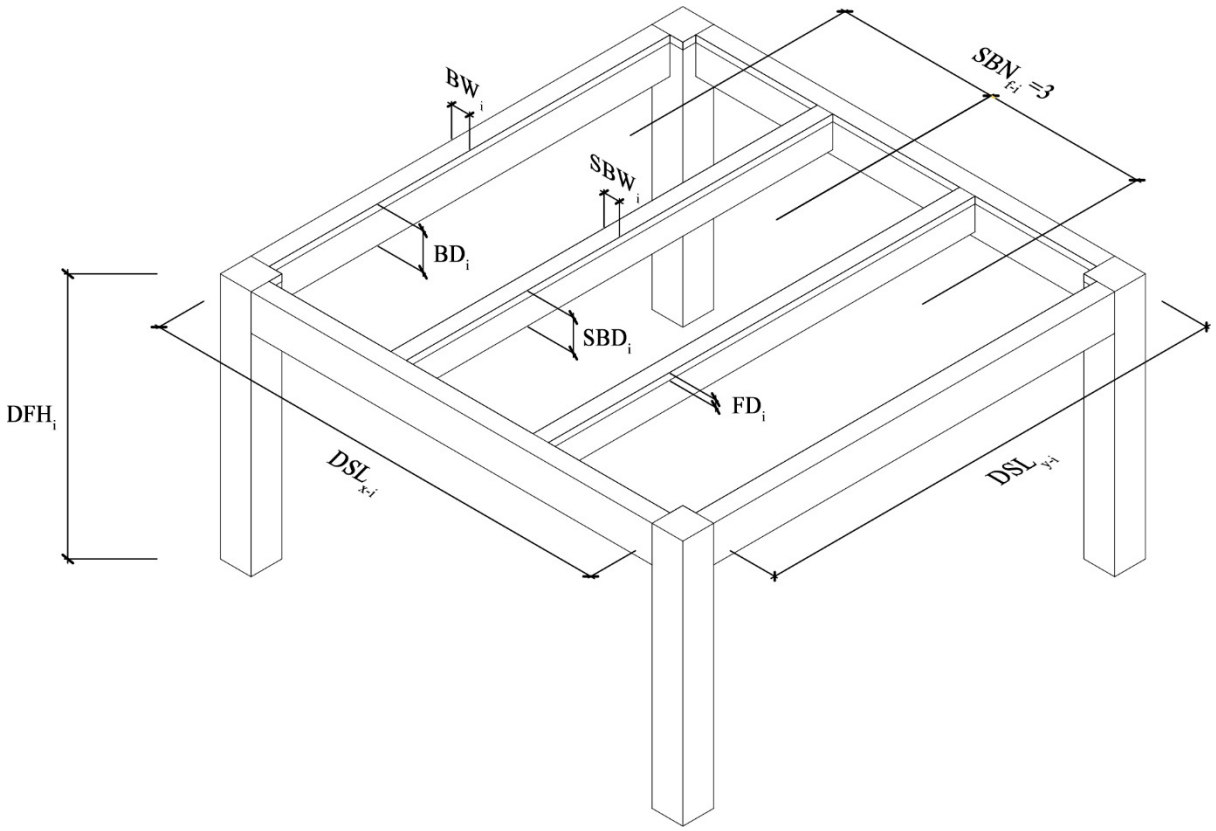

Figure 4-2 Parameter definition in the generation of design alternatives.

Each wall in $original\_wall\_list$ is scaled to an adjusted location according to equations (4-16)-(4-19):

$$ADG_{f-i-j} = ODG_{f-i-j} \times \frac{DSL_{d-i}}{OSL_{d-i}} \tag{4-16}$$

$$AWL_{f-i-j} = OWL_{f-i-j} \times \frac{DSL_{d-i}}{OSL_{d-i}} \tag{4-17}$$

$$adjusted\_wall\_list = \{AW_{1-1-1}, \dots, AW_{f-i-j}, \dots, AW_{m-n-o}\} \tag{4-18}$$

$$AW_{f-i-j} = \{AWC_{f-i-j-0}, AWC_{f-i-j-1}\} \tag{4-19}$$

where, ADG_{f-i-j} is the distance between the j-th adjusted walls in the i-th grid on the f-th floor and the node of corresponding grid of the design alternative (m); ODG_{f-i-j} is the distance between the j-th adjusted walls in the i-th grid on the f-th floor and the node of corresponding grid of the original design (m); AWL_{f-i-j} and OWL_{f-i-j} are lengths of the j-th walls in the i-th grid on the f-th floor of the design alternative and original design,

respectively (m); $adjusted\_wall\_list$ is the list of walls after scaling, $AWC_{f-i-j-0}$ and $AWC_{f-i-j-1}$ are the coordinates of the start and end points of the j-th wall in the i-th grid on the f-th floor in the design alternative, respectively.

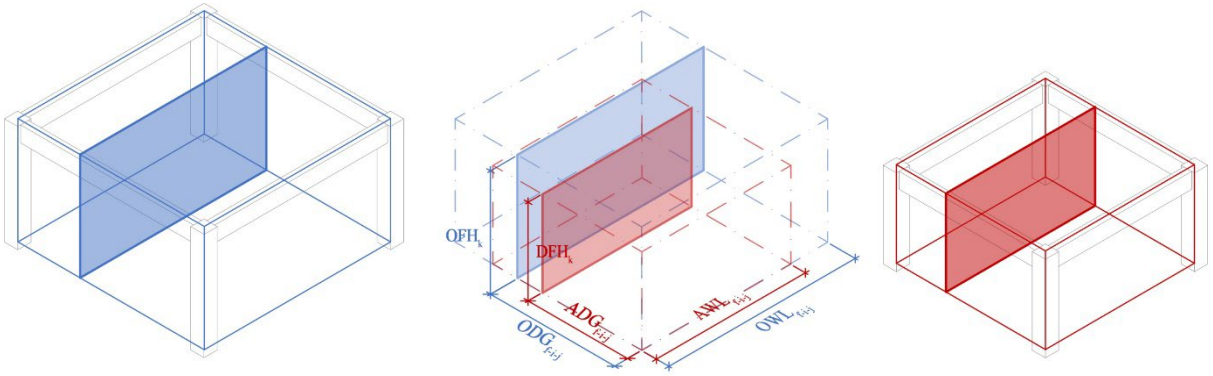

(a) The original design (b) Scale the walls (c) Generate adjusted walls

Figure 4-3 The generation of adjusted walls.

4.2.1.3 Detailed adjustment of design alternatives

Following the primary scaling, the distribution of secondary beams and internal walls are mutually adjusted based on the postulation that the loads of walls are resisted by secondary beams directly. This process is illustrated in Figure 4-4. Firstly, the original distribution of internal walls in the i-th grid is examined to obtain the orientation of majority of internal walls (equal to or greater than 50%). If this orientation differs from SBO_{f-i}, the parameter is adjusted (Figure 4-4 (a)-(b)). Secondary beams in this grid are then evenly distributed according to SBO_{f-i} and SBN_{f-i}. Secondly, the internal walls in the same direction of adjusted SBO_{f-i} are re-allocated to the location of the nearest secondary beams. The distance between the original and re-allocated walls is then calculated according to equations (4-20)-(4-21):

$$DIW_{f-i-j} = \sqrt{\left(COIW_{f-i-j} - CDIW_{f-i-j}\right)^2} \tag{4-20}$$

$$total\_DIW_{f-i} = \sum DIW_{f-i-j} \tag{4-21}$$

where, DIW_{f-i-j} represents the distance between the j-th original and corresponding re-allocated walls in the i-th grid on the f-th floor (m); $COIW_{f-i-j}$ and $CDIW_{f-i-j}$ are coordinates of the j-th original and corresponding re-allocated walls in the i-th grid on the f-

th floor; $total\_DIW_{f-i}$ is the sum of distances between original and corresponding re-allocated walls in the i-th grid on the f-th floor (m).

Thirdly, if DIW_{f-i-j} exceeds a given threshold TIW (indicating that the design alternative generates excessive change to the original design), SBN_{f-i} is adjusted by traversing all feasible value of SBN_{f-i} (in accordance with equation (4-9)). The value with the smallest $total\_DIW_{f-i}$ is selected as the final result. Subsequently, the internal walls in this gird are re-allocated again according to the adjusted SBN_{f-i} and SBO_{f-i}. Lastly, if there are walls in the opposite direction of SBO_{f-i}, additional secondary beams are added beneath them.

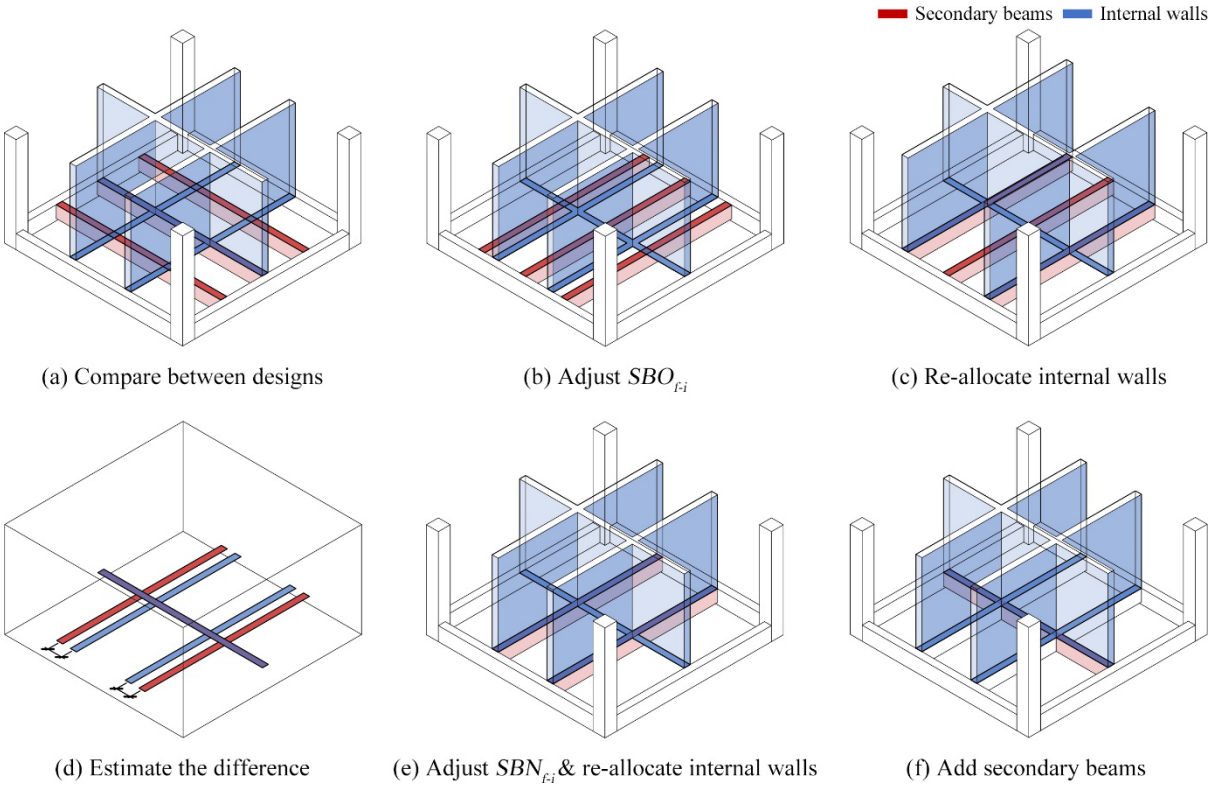

Figure 4-4 The process of re-allocating internal walls and secondary beams.

4.2.2 Analysis of the structure response

The design and structure analysis of precast elements is not much different from that of cast-in-situ reinforced concrete structures (Polat, 2008). Given the maturity of existing methods for precast structure design and considering the focus of this study is on exploring the balance between the use of standardised and custom precast elements, commonly accepted structure analysis and design methods are adopted. Given the studied case introduced in section 4.3.3.1, the analyses and designs in this research adhere to the requirements stipulated by the following

Chinese codes: *GB55001-2021*, *GB55002-2021*, *GB55008-2021*, *GB50011-2010(2016)*, *GB50010-2010(2015)*, *GB50009-2012*, *GB/T51231-2016*, *JGJ1-2014, 13J104*, *15G366-1*, and *22G101-1*. The content in section 4.2.2 and 4.2.3 forego detailed processes in favour of introducing the workflow and significant settings.

The parametric design alternative is converted into a structure model to calculate the expected response of the structure under loadings, as depicted in Figure 4-5. Linear elements (i.e., columns, beams, and secondary beams) are represented by a series of nodes and members, forming a node list ($node\_list$) and a member list ($member\_list$) according to equations (4-22)-(4-25). Each linear element is evenly divided into several (n) members to obtain the internal stress and limiting response. Plane elements (i.e., floor slabs and walls) are subsequently defined by coordinates of vertices, which are represented by the nearest node in $node\_list$, as demonstrated in equations (4-26)-(4-27).

$$LE_i = \{M_{i-1}, \dots, M_{i-j}, \dots, M_{i-n}\} \tag{4-22}$$

$$M_{i-j} = \{MC_{i-j-0}, MC_{i-j-1}\} \tag{4-23}$$

$$node\_list = \{MC_{1-1-0}, MC_{1-1-1} \dots, MC_{i-j-0}, MC_{i-j-1}, \dots, M_{m-n-0}, M_{m-n-1}\} \tag{4-24}$$

$$member\_list = \{M_{1-1}, \dots, M_{i-j}, \dots, M_{m-n}\} \tag{4-25}$$

$$PE_i = \{PEC_{i-1}, PEC_{i-2}, PEC_{i-3}, PEC_{i-4}\} \tag{4-26}$$

$$\{PEC_{i-1}, PEC_{i-2}, PEC_{i-3}, PEC_{i-4}\} \in node\_list \tag{4-27}$$

where, LE_i is the i-th linear element; M_{i-j} represents the j-th member of the i-th linear element; MC_{i-j-0} and MC_{i-j-1} are the coordinates of the two vertices of the member M_{i-j}, respectively; PE_i refers to the i-th plane element; PEC_{i-1}, PEC_{i-2}, PEC_{i-3}, and PEC_{i-4} are coordinates of four vertices of the member PE_i.

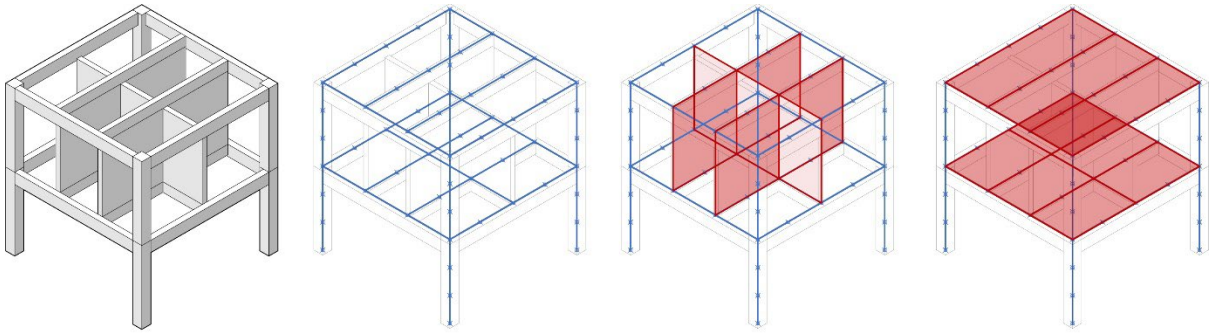

Figure 4-5 The generation of nodes and members for structure analysis.

Regarding the type of joints, widely adopted structural analysis postulations, customary in the field of practice, are employed. Specifically, rigid connections are presumed at the joints of members within the same structure element, column-beam joints, continuous joints of continuous secondary beams and continuous floor slabs, and joints of secondary beams in divergent directions. All remaining joints are postulated as hinged connections.

To represent a close to practice reinforcement design, this study considers dead loads, live loads, snow loads, seismic loads, and the load combinations listed in section 4.3.3.3. Specifically, dead loads for columns, beams, secondary beams, and floor slabs are postulated to be uniformly distributed across these elements. While, dead loads of walls are considered as line load, which are exerted on beams or secondary beams below. Live loads are uniformly distributed across the area of floor slabs, and snow loads are similarly uniformly distributed over the roof. Given the characteristics of the studied case (section 4.3.3.1), seismic loads are calculated using the equivalent base shear method as illustrated in the *GB 50011-2010(2015)*. It is briefly described by equations (4-28)-(4-30).

$$F_{Ek} = \alpha_1 G_{eq} \tag{4-28}$$

$$F_f = \frac{G_f H_f}{\sum G_{f-1} H_{f-1}} F_{Ek}(1 - \delta_n) \tag{4-29}$$

$$F_n' = F_n + \delta_n F_{Ek} \tag{4-30}$$

where, F_{Ek} is the standard value of horizontal seismic action on the entire structure (kN); α_1 represents the horizontal earthquake influence coefficient; G_{eq} is the equivalent gravity load of the whole structure (kN); F_f is the standard value of horizontal seismic action on the f-th floor

(kN); G_f and G_{f-1} correspond to the equivalent gravity loads of structure elements on the f-th and $(f-1)$-th floor, respectively (kN); H_f and H_{f-1} are the heights of f-th and $(f-1)$-th floor, respectively (m); δ_n is the additional seismic action coefficient of the top floor; F_n' represents the standard value of horizontal seismic action on the top floor (kN).

The horizontal seismic action on each floor is distributed among the columns on that floor, as described by equations (4-31)-(4-35):

$$V_{f-i} = \frac{D_{f-i}}{\sum D_{f-j}} F_f \tag{4-31}$$

$$D_{f-i} = \alpha_d \frac{12 stf_{f-i}}{h_{f-i}^2} \tag{4-32}$$

$$\alpha_d = \frac{K_{f-i}}{2 + K_{f-i}} (if\ f > 1) \tag{4-33}$$

$$\alpha_d = \frac{0.5 + K_{f-i}}{2 + K_{f-i}} (if\ f = 1) \tag{4-34}$$

$$K_{f-i} = \frac{\sum stf_{f-i-k}}{stf_{f-i} \times num_{f-i}/2} \tag{4-35}$$

where, V_{fj} is the shear force caused by seismic load on the i-th column on the f-th floor (kN); D_{f-i} represents the adjusted lateral stiffness of the i-th column on the f-th floor (kN/m); $\sum D_{f-j}$ is the sum of the adjusted lateral stiffness of all columns on the f-th floor (kN/m); α_d denotes the correction factor of stiffness; stf_{f-i} is the original linear stiffness of the i-th column on the f-th floor (kN·m); $h_{\mathrm{f-i}}$ is the height of the i-th column on the f-th floor (m); stf_{f-i-k} represents the linear stiffness of the k-th beam connected to the i-th column on the f-th floor (only beams in the same direction as the seismic load is included) (kN·m); num_{f-i} is the number of beams connected to the i-th column on the f-th floor.

A finite element analysis programme developed in Python (Sean Carroll, 2023) is used to estimate the response of structural framework under loadings. This program transforms the effects of loads into equivalent loads on structure nodes (in $node\_list$) and calculates the actions of each member at the node for the detailed design of structure elements.

4.2.3 Detailed design of structure elements

The detailed design of each structure elements is defined by input and output variables listed in Table 4-2. Input variables concerning the geometric features and material selection are inherit from the parameters mentioned in section 4.2.1. The other input variables are determined by combining the available values of building products (e.g., the diameter of rebar). The model traverses the combinations of values and checks for feasible element designs. Each feasible design with a given set of (input) variables is determined by calculating the values of corresponding output variables. Notably, there is no output variable of floor slab designs, meaning that potential combinations of input variables are considered feasible if they can resist the stress (obtained in section 4.2.2).

Table 4-2 Variables adopted in the detailed design of structure elements.

Element type	**Variable Type**	**Variable**	**Definition**
Column	Input	CW	Width of column
		$hooping\_size$	Diameter of hooping
		$rebar\_size$	Diameter of tensioned bar
		con_rebar_size	Diameter of constructional rebar
		CON_{column}	Grade of column concrete
		RE_{column}	Grade of column tensioned bars
		$RE_{column-hop}$	Grade of column hooping
	Output	$rebar\_num$	Number of tensioned rebar on each side
		con_rebar_num	Number of constructional rebar on each side
		$hooping\_num$	Number of hooping limbs
Beam / Secondary beam	Input	$BD/\ SBD$	Depth of beam/secondary beam
		$BW/\ SBW$	Width of beam/secondary beam
		$hooping\_size$	Diameter of hooping
		top_rebar_size	Diameter of tensioned bar on the top
		bot_rebar_size	Diameter of tensioned bar on the bottom
		$CON_{beam}/CON_{secondary-beam}$	Grade of beam/secondary beam concrete
		$RE_{beam}/RE_{secondary-beam}$	Grade of beam / secondary beam tensioned bars

		$RE_{beam-hop}$/ $RE_{secondary-beam-hop}$	Grade of beam/secondary beam hooping
	Output	$rebar\_num\_0$	Number of tensioned bars at node 0 on the top
		$rebar\_num\_mid$	Number of tensioned bars in the middle of top side
		$rebar\_num\_1$	Number of tensioned bars at node 1 on the top
		bot_rebar_num	Number of tensioned bars on the bottom
		$hooping\_num$	Number of hooping limbs
		con_rebar_size	Diameter of constructional rebar
		$con\_rebar\_num\_0$	Number of constructional rebar at node 0 on the top
		$con\_rebar\_num\_mid$	Number of constructional rebar in the middle of top side
		$con\_rebar\_num\_1$	Number of constructional rebar at node 1 on the top
		$con\_rebar\_num\_web$	Number of constructional rebar of web
Floor slab	Input	FD	Depth of floor slab
		FL	Length of floor slab
		FW	Width of floor slab
		$rebar\_spacing$	Spacing of tensioned bars
		$top\_rebar\_size\_x$	Diameter of tensioned bar in the x direction on the top
		$top\_rebar\_size\_y$	Diameter of tensioned bar in the y direction on the top
		$rebar\_size$	Diameter of rebars in the reinforcement mesh
		$CON_{floor-slab}$	Grade of floor slab concrete
		$RE_{floor-slab}$	Grade of floor slab rebar

To improve the efficiency of structure design and optimisation, the exploration of feasible combinations of variables is limited. For columns, beams, and sub-beams, with tensioned bars in given sizes, only the element design with the least quantity of reinforcement is recorded as a feasible alternative. Regarding the design of floor slabs (which has no output variables), with a given interval of tensioned bars, only the element design with the least quantity of reinforcement is recorded as a feasible alternative.

For continual beams and sub-beams, the feasible designs of element are coordinated according to the variables of continual joints to ensure that the rebars on the top are continuous. For simplification, the coordination of designs is limited to adopting rebars of the same size on the top. It can be restricted to adopting the same size and number of rebars on the top if all feasible

combinations of variables are explored. The feasible designs of continual beams and sub-beams are subject to equations (4-36)-(4-41).

$$CEL_i = \{CELE_{i-1}, CELE_{i-2}\} \tag{4-36}$$

$$CEDL_{i-j} = \{CED_{i-j-1}, \dots, CED_{i-j-k}, \dots, CED_{i-j-n}\}(j = 1 \; or \; 2) \tag{4-37}$$

$$CED_{i-j-k} = \{BD_{i-j-k}(SBD_{i-j-k}), \dots, con\_rebar\_num\_web_{i-j-k}\}(j = 1 \; or \; 2) \tag{4-38}$$

$$CTRS_{i-j} = \{top\_rebar\_size_{i-j-1}, \dots, top\_rebar\_size_{i-j-k}, \dots, top\_rebar\_size_{i-j-n}\}(j = 1 \; or \; 2) \tag{4-39}$$

$$top\_rebar\_size^*_{i-j-k} \in CTRS_{i-1} \cap CTRS_{i-2} \tag{4-40}$$

$$CEDL^*_{i-j} = \{\dots, CED^*_{i-j-k}, \dots\} \tag{4-41}$$

where, CEL_i is two continually connected beams or sub-beams ($CELE_{i-1}$ and $CELE_{i-2}$) at the node i; $CEDL_{i-j}$ represents the list of all feasible designs of the continual element $CELE_{i-1}$ or $CELE_{i-2}$; CED_{i-j-k} is the k-th feasible design of the element $CELE_{i-j}$, which is consisted of input and output variables mentioned before; $CTRS_{i-j}$ denotes the list of all feasible top rebar size of the element $CELE_{i-1}$ or $CELE_{i-2}$; the value of $top\_rebar\_size_{i-j-k}$ is marked as $top\_rebar\_size^*_{i-j-k}$ if it exists in the intersection of $CTRS_{i-1}$ and $CTRS_{i-2}$; correspondingly, the element design containing $top\_rebar\_size^*_{i-j-k}$ is marked as CED^*_{i-j-k}, which further constitutes the list of coordinated design for continual beams or sub-beams ($CEDL^*_{i-j}$).

Regarding the joints of prefabricated elements, tensioned bars of columns are connected by rebar couplers. Discontinuous rebars (due to different number of rebars in columns or different column sizes) are anchored to the column-beam joint. Similarly, continuous tensioned bars on the top of beams and secondary beams are connected by rebar couplers. Discontinuous tensioned bars on the top and tensioned bars on the bottom are anchored to the column-beam joint (for beams) or beam-secondary-beam joint (for secondary beams). The tensioned bars of floor slabs on the bottom are anchored to the floor-beam joint or floor-secondary-beam joint. The support rebars on the top extend to the continuously connected floor slabs if allowed or are anchored to the floor-beam joint or floor-secondary-beam joint otherwise.

4.2.4 Calculation of embodied carbon

The system boundary of this article encompasses the embodied carbon emitted from materials of superstructures and formwork used in both off-site manufacture and onsite construction. The precast elements considered include columns, beams, secondary beams, floor slabs, internal walls, external walls. The CE of these elements is calculated using equation (4-42):

$$CE_{ELE-i} = Q_{CON-i}Coe_{CON} + Q_{RE-i}Coe_{RE} + Q_{RE-COU-i}Coe_{RE-COU} \quad (4\text{-}42)$$

where, CE_{ELE-i} represents the CE of the i-th element (kg CO_2e); Q_{CON-i}, Q_{RE-i}, and $Q_{RE-COU-i}$ are the quantity of concrete (m^3), reinforcement (kg), and rebar coupler (kg) consumed by the i-th element, respectively; Coe_{CON}, Coe_{RE}, and Coe_{RE-COU} are the CE coefficient of the concrete (kg CO_2e/m^3), reinforcement (kg CO_2e/kg), and rebar coupler (kg CO_2e/kg), respectively.

Formwork is categorized into two parts:1) precast formwork and 2) cast-in-situ formwork, as shown in Figure 4-6. Precast elements are postulated to be manufactured by production lines in the factory, where elements are placed on casting beds (G. Liu et al., 2019). Thus, the top and bottom surfaces are excluded from the calculation of formwork area. The cast-in-situ parts of each floor are postulated to be constructed after assembling all precast elements. Consequently, the top, bottom and some surrounding surfaces of cast-in-situ parts are not considered in the calculation of formwork area.

Each piece of formwork required to manufacture a specific precast element (FW_i) is defined by equation (4-43):

$$FW_{i-j} = \{[length_{i-j}, width_{i-j}], [\dots, (open_{i-j-k}, position_{i-j-k}), \dots]\} \quad (4\text{-}43)$$

where, $length_{i-j}$ and $width_{i-j}$ are the length (m) and width (m) of the j-th surface of the i-th elements to which the formwork is attached, respectively; $open_{i-j-k}$ and $location_{i-j-k}$ represent the size and position of the k-th opening on this piece of formwork, respectively.

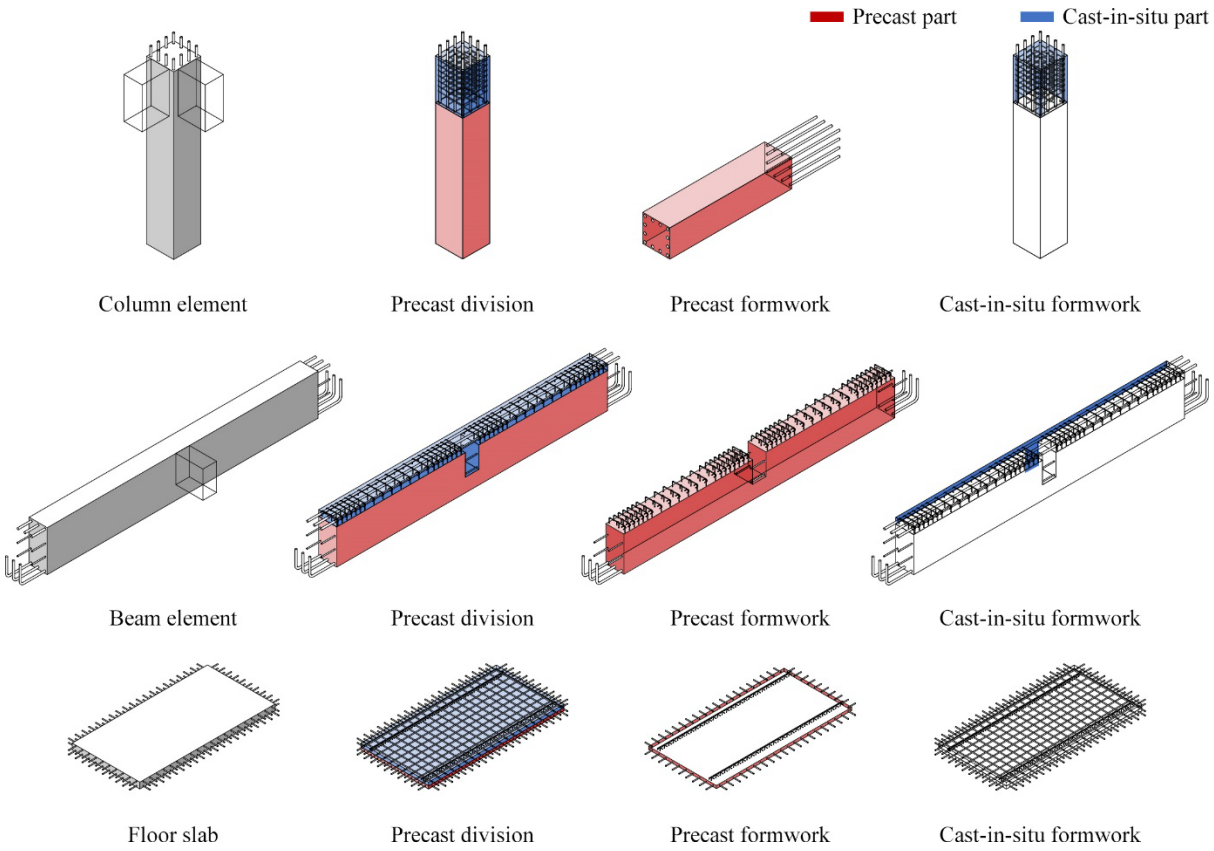

Figure 4-6 The division of precast and cast-in-situ formwork.

To maximise the formwork reusing, an off-line mode is adopted, i.e., all required formwork pieces are assumed to be known prior to manufacturing. Formwork pieces that share the similar sizes and identical openings are considered the same and form a new list RFW. The final formwork to be manufactured and is decided by equations (4-44)-(4-46):

$$RFW_l = \{\dots, FW_{i-j}, \dots\} \tag{4-44}$$

$$MFW_l = \{[length_l, width_l], [\dots, (open_{l-k}, position_{l-k}), \dots], cycle_l\} \tag{4-45}$$

$$m\_num_l = cycle_l / max\_reuse\_cycle \tag{4-46}$$

where, RFW_l is the l-th list of formwork pieces share the similar characteristics; MFW_l represents the l-th piece of formwork that is going to be manufactured, $length_l$ and $width_l$ are the length and width of the l-th piece of formwork, they are determined by the maximum length and width of formwork pieces in RFW_l; $open_{l-k}$ and $position_{l-k}$ depict the size and position of the k-th opening on this piece of formwork, respectively. Notably, $open_{l-k}$ is dictated by the largest size of the k-th opening on formwork pieces in RFW_l if the opening is for rebar

extension; $cycle_l$ refers to the required cycle times of the l-th piece of formwork; m_num_l is number of the l-th piece of formwork requires to be produced; max_reuse_cycle is the maximum reuse cycles of the formwork piece.

Precast elements are postulated to be manufactured separately (i.e., one element a time). Thus, the associated required pieces of formwork are counted by each element. In contrast, the cast-in-situ parts are assumed to be constructed floor by floor. Thus, the required pieces of cast-in-situ formwork are counted by each floor. Given that different contractors are responsible for the manufacture of precast elements and on-site construction, precast and cast-in-situ formwork are calculated separately.

The CE of each piece of formwork (CE_{FW-i}) is calculated using equation (4-47):

$$CE_{FW-i} = (length_i \times width_i - \sum A_{open_{i-j}})Coe_{FW-i} \quad (4\text{-}47)$$

where, $\sum A_{open_{i-j}}$ is the sum of area of openings on the i-th piece of formwork (m^2); Coe_{FW-i} is the CE coefficient of formwork material (kg CO_2e/m^2).

The embodied carbon emitted from materials of structure (CE_{STU}) is calculated using equation (4-48):

$$CE_{STU} = \sum CE_{ELE-i} + \sum CE_{FW-j} \quad (4\text{-}48)$$

4.2.5 Exploration of optimisation results

The objective of optimisation problem is to minimize the embodied CE of design alternatives (CE_{STU}) defined by parameters listed in Table 4-1. This study employs a genetic algorithm (GA) to search for the minimum value of CE_{STU} and corresponding setting of parameters. The whole problem is first defined in standard Python 3.9, and then Geatpy 2.7.0 – a genetic and evolutionary algorithm toolbox for Python (Geatpy team, 2022) – is used to explore the optimisation results. Detailed settings are provided in section 4.3.3.3.

A Monte Carlo analysis is adopted to estimate the uncertainties in CE and assess the potential for CE reduction during the developed design stage. Specifically, 1000 design alternatives are randomly generated to obtain a comprehensive view. Given that the distribution pattern of

parameters is unknow in real-world practice, the value of each parameter is randomly distributed within the available range.

4.3 Module validation

4.3.1 Validation of alternative generation

Given the research hypotheses mentioned in section 1.3.2, the design alternatives generated via parametric design approach object to equations (4-49) and (4-50):

$$Parameter_i \neq Parameter_j \tag{4-49}$$

$$CE_i \neq CE_j \tag{4-50}$$

where, $Parameter_i$ and $Parameter_j$ are the parameter sets of design alternatives i and j, respectively; CE_{i} and CE_j are the CE of design alternatives i and j, respectively. In the set of all design alternatives, there should be at least 1 pair of i and j that fulfil the above equations.

Additionally, the design alternatives should share the similar geometric characteristics as the original design, so that the design optimisation would not sacrifice the sake for architectural performance.

4.3.2 Validation of carbon reduction

For the novelty of the proposed method, the carbon reduction efficiency should object to the following equation:

$$CE_{optimal} < CE_{conventional} \tag{4-51}$$

where, CE_{optimal} and $CE_{\mathrm{conventional}}$ are the embodied CE of the optimal solution found by GA and conventional design optimisation method, respectively. Considering the design optimisation adopted in design practice, the conventional design optimisation method is defined as design employing the principle of standardisation, which is stated in section 1.2.2. A detailed setting of this baseline value is introduced in section 4.3.3.4.

4.3.3 Module application

4.3.3.1 Sample building

This study employs the module on a real-world case to estimate the applicability of the proposed approach. The studied case is a four-storey reinforced-concrete office building located in Nanjing, China, as illustrated in Figure 4-7. The project has an area of 2971.16 m^2 and a height of 20.4m. It is a representative case for precast concrete projects in China, involving precast solid columns, precast composite beams, precast composite floor slabs, and autoclaved aerated concrete wall slabs. The structure is designed with a seismic precautionary intensity of degree 7, belongs to designed earthquake group 1, and has a site classification of I_1. The stairs, lifts and envelope are excluded from analysis and optimisation, because these parts are considered the same in all design alternatives (as elaborated in section 4.2.1, where the geometric features of all design alternatives remain the same). The results shown in sections 4.4 further validate this assumption, showing that excluding these parts would not generate significant difference to the prefabrication design optimisation.

4.3.3.2 Data collection

The data collected include: 1) the geometric features of studied case; 2) constraints and requirements on structure design and analysis; 3) carbon emission factor of materials. The geometric features are extracted from design files (i.e., the design drawings in developed design). Detailed reviews and content analysis is conducted on those drawings to obtain the variables in $original\_span\_list_x$, $original\_span\_list_y$, $original\_height\_list$, $original\_height\_list$, and OW_{f-i-j}. The drawings of sample building are examined and verified by all participants to ensure the data quality.

Regarding the data for structure design and analysis, national codes, regulations, and technical standards are the main sources. Cited files include but are not limited to *GB55001-2021, GB55002-2021, GB55008-2021, GB50011-2010(2016), GB50010-2010(2015), GB50009-2012, GB/T51231-2016, JGJ1-2014, 13J104, 15G366-1, and 22G101-1*. This study employs CE data from *China Products Carbon Footprint Factors Database* (CCG, 2022) and Calculation standard of building carbon emissions GB/T51366-2019 (2014).

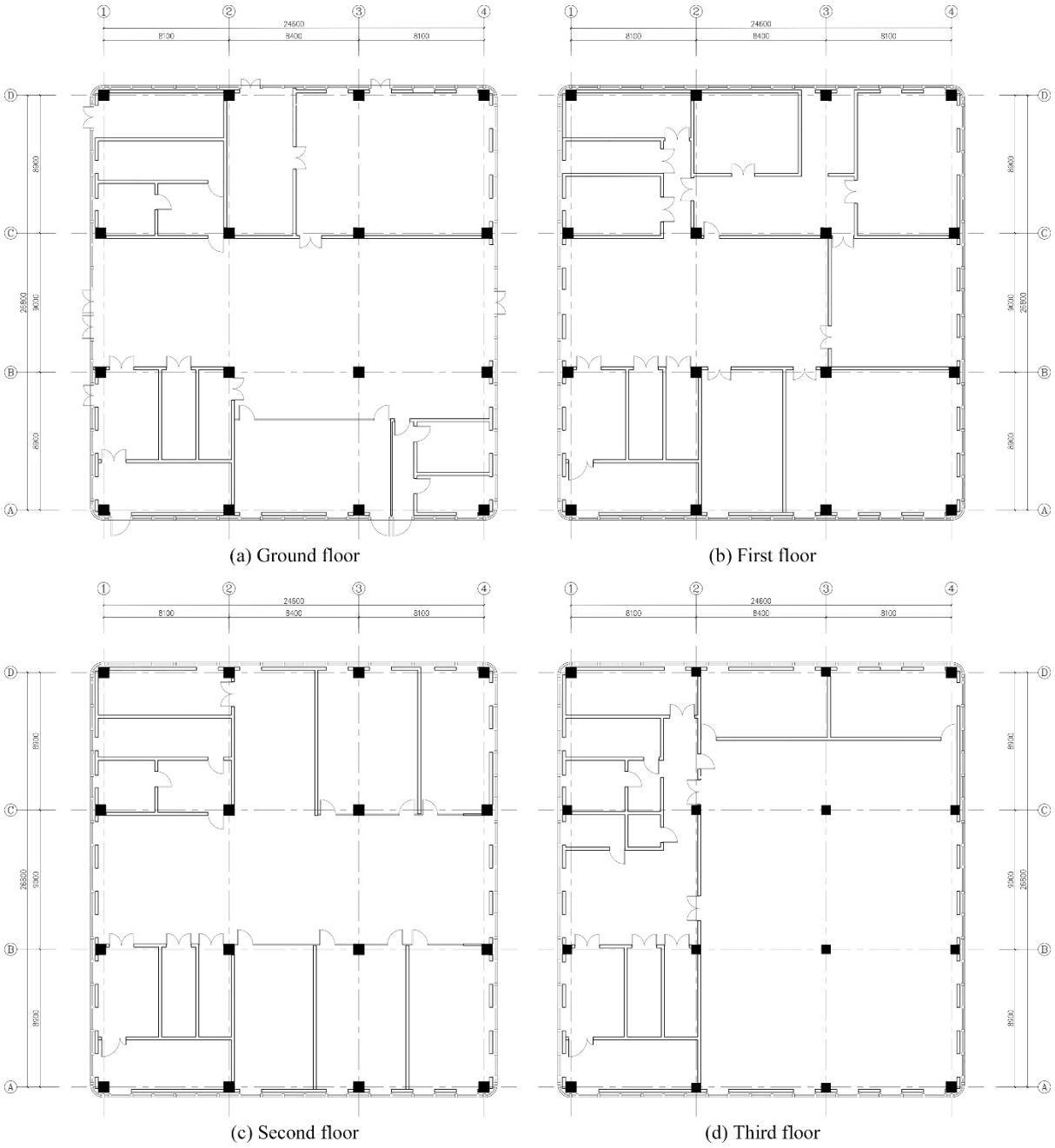

Figure 4-7 The plan of the studied case.

4.3.3.3 Parameter settings

Table 4-3 lists the setting of parameters in the structure optimisation of the case study. For better practicability, discrete variables are employed. Specifically, continuous variables concerning the dimensions of framework (e.g., the span length of each grid) and structural elements (e.g., the depth of beams) are transformed into discrete variables with a step of 0.05m, the minimum unit in real-world practice. The tolerance of dimensions in either X- or Y-direction and building height are set to 0 to eliminate the carbon reduction effects from a

decreasing building area. Notably, parameters from min_FW to max_SBDWR are set based on the experienced value and codes mentioned before. These parameters are also validated to ensure that the dimensions and weight of elements fulfil the requirement of transportation and hanging.

The formwork is assumed to be made of aluminium alloy in cast-in-situ construction and steel in precast manufacture. The maximum reuse cycle (max_reuse_cycle) for both precast and cast-in-situ formwork is set at 50. This value references the average reuse cycle of 3mm steel formwork in precast factory and the maximum reuse cycle of cast-in-situ metal formwork. While precast formwork can sometimes be used up to 100 times (Dong et al., 2015), it does not generate significant influence on the results of this study, as a few of precast formwork is reused for more than 50 times (according to the results in section 4.4).

Table 4-3 Parameter settings of structure optimisation.

Categorize	**Parameter**	**Value**	**Unit**
Original designs			
	$original\_span\_list_x$	{8.10,8.40,8.10}	m
	$original\_span\_list_y$	{8.90,9.00,8.90}	m
	$original\_height\_list$	{4.80,4.80,4.80,6.00}	m
Variable domains			
	Available diameter of tensioned bars	{16,18,20,22,25,28,32}	mm
	Available diameter of rebars in floor slabs	{8,10,12,16,18,20}	mm
	Available diameter of hooping	{8,10,12}	mm
	Available diameter of constructional rebars	{8,10,12}	mm
	Available rebar spacing of floor slabs	{0.10,0.15,0.20}	m
	$min\_TSL_{d-i}(d = x\ or\ y)$	−0.30	m
	$max\_TSL_{d-i}(d = x\ or\ y)$	0.30	m
	min_TFH	−0.15	m
	max_TFH	0.15	m
	$min\_TTL_d(d = x\ or\ y)$	0.00	m
	$max\_TTL_d(d = x\ or\ y)$	0.00	m
	min_TTH	0.00	m
	max_TTH	0.00	m
	min_FW	1.80	m
	max_FW	3.00	m
	min_BSDR	10.00	-

	max_BSDR	12.00	-
	min_BDWR	1.50	-
	max_BDWR	3.00	-
	min_SBSDR	12.00	-
	max_SBSDR	14.00	-
	min_SBDWR	1.50	-
	max_SBDWR	3.00	-
Identical settings			
	CON_{column}	C35	-
	CON_{beam}	C35	-
	$CON_{sub-beam}$	C35	-
	$CON_{floor-slab}$	C35	-
	RE_{column}	HRB400	-
	RE_{beam}	HRB400	-
	$RE_{sub-beam}$	HRB400	-
	$RE_{floor-slab}$	HRB400	-
	$RE_{column-hop}$	HRB335	-
	$RE_{beam-hop}$	HRB335	-
	$RE_{sub-beam-hop}$	HRB335	-
	CCD	0.02(0.15 for floor slabs)	m
	Density of steel	7.85	ton/m^3
	Density of concrete	2.42	ton/m^3
	Density of cast-in-situ formwork (aluminium alloy)	25.00*	kg/m^2
	Density of precast formwork (steel)	50.00	kg/m^2
	Density of wall slabs (autoclaved aerated concrete wall slabs)	525.00	kg/m^3
	Coe_{CON}	317.50	kg CO_2e/m^3
	Coe_{RE}	2.34	kg CO_2e/kg
	Coe_{RE-COU}	2.34	kg CO_2e/kg
	$Coe_{FW-cast-in-situ}$	7.95	kg CO_2e/kg
	$Coe_{FW-precast}$	2.67	kg CO_2e/kg
	Coe_{ACWS} (CE coefficient of the autoclaved aerated concrete wall slabs)	297.80	kg CO_2e/m^3
	Coefficient of live load	2.50	kN/m^2
	Coefficient of snow load	0.65	kN/m^2
	max_reuse_cycle	50	-

* Baosheng Zhou (2019)

The analysis of structure calculates the response of structure elements in five typical load combinations, as listed in Table 4-4. The combination coefficients of loads are obtained from *GB50009-2012* and common practice in real-word projects. Structure analysis employs the maximal envelope of element response across these five load combinations.

Table 4-4 Load combinations.

Num	**Combination coefficient of loads**				
	Dead load	Live load	Snow load	Seismic load in X direction	Seismic load in Y direction
1	1.3	0.65	0.65×0.7	1.4	0
2	1.3	0.65	0.65×0.7	-1.4	0
3	1.3	0.65	0.65×0.7	0	1.4
4	1.3	0.65	0.65×0.7	0	-1.4
5	1.3	1.5	1.5×0.7	0	0

The computations were performed on a personal desktop equipped with an i7-12700k CPU and 48GB RAM (3200MHz). Given the typical time consumption observed in practice (Jusselme et al., 2020), an upper limit of 48 hours is set for the optimisation period. Consequently, four simplification postulations are adopted to yield feasible solutions within this timeframe: 1) the cross section of beams in the same span is identical; 2) the cross section of secondary beams in the same span is identical; 3) the depth of beams connected to more than four secondary beams adopt the maximum value; 4) the width of secondary beams adopts the maximum value if the depth is smaller than the lower boundary defined by equation (4-12) (the depth of secondary beams may reduce to a small value if it exceeds the depth of beams that it is connected to). Postulations 1-2 aim to curtail the number of variables, thus reducing the computing time. Postulations 3-4 aim to reduce the risk of structurally unfeasible design alternatives, similar to the goal of constraints delineated by equations (4-9)-(4-13).

After simplification, 728 variables are employed to ensure that the design alternative can be defined under the most unfavourable situation. The GA settings are listed in Table 4-5. Notably, this study employs a prophet population with four individuals to expedite optimisation. The prophet population, a function embedded in Geatpy 2.7.0, allows the input of several sets of pre-determined variables presumed to yield good performance. The algorithm assesses the performance of prophet population before generating the original population and adopts the chromosomes of prophet population as a guidance during optimisation (Geatpy team, 2022). The prophet population adopted in this research represents designs with the fewest number of

elements, which aligns with principle of standardisation. All the other variables are set to be identical for simplification.

Table 4-5 Parameter settings of GA.

Parameter	Value
Population size	60
Prophet population size	4
Probability of performing crossover	0.7
Probability of mutation	0.07
Termination criteria	Generation = 100

4.3.3.4 Baseline scenario

A baseline scenario is established to estimates CE originating from a design strictly adhering to the principle of standardisation. This scenario involves adopting uniform cross-section dimensions and minimising the number of building elements. Specifically, the baseline scenario maintains the original framework dimensions. Floor slabs are designed with the maximum possible width to minimize the number of slabs and secondary beams. Meanwhile, formwork is designed and manufactured by the on-line mode, i.e., the dimensions of formwork pieces are unknown in advance. Specifically, each required piece of formwork is initially compared to a list of existing formwork pieces. If no existing formwork piece can replace the required one, a new piece is added.

Table 4-6 listed the parameters adopted in the baseline scenario. These parameters, grounded in practical experience and referenced value from *Reinforced Concrete Structure Construction Manual* (China Nonferrous Engineering Co., 2016), are estimated for least favourable conditions in the whole structure to avoid structural unfeasibility. Civil engineers have verified these parameters before estimation. Any parameters not specified in this table are assumed to be the same as those in Table 4-3. Design details are generated via the process mentioned in section 4.2. Notably, the baseline scenario avoids manual design to eliminate biases from design experience and personal preferences. This approach ensures that the comparison represents the effectiveness of the optimisation strategy.

Table 4-6 Parameter settings of the baseline scenario.

Parameter	Value (m)
CW	0.6
con_rebar_size	0.020-0.025

BD/SBD	0.85/0.75
BW/SBW	0.40/0.35
$top\_rebar\_size/bot\_rebar\_size$	0.018-0.022

4.4 Validation results and analysis

4.4.1 The efficiency of optimisation

The optimisation lasts 45.93 hours. A feasible solution (the local-optimum result found by GA optimisation with CE of 8.05×10^5 kg CO_2e) is achieved by the 25th generation, in roughly 11.48 hours. Figure 4-8 shows that the average objective value rapidly drops within the first 20 generations and stabilises after the 30th generation (approximately 14 hours), indicating a rapid data convergence. The initial generation's best objective value is 8.18 × 105 kg CO2e. Monte Carlo analysis suggests this value would increase to about 9.30 × 105 kg CO2e (13.70% higher) with entirely random design alternatives. In the case of fully random population, achieving a similar outcome (i.e., attaining the best objective value of 8.18 × 105 kg CO2e) typically requires over 80 generations (around 36 hours). Additionally, the model is more likely to become trapped in a larger local optimum due to the reduced population diversity during optimisation. These results implies that the introduction of prophet population significantly improves optimisation efficiency.

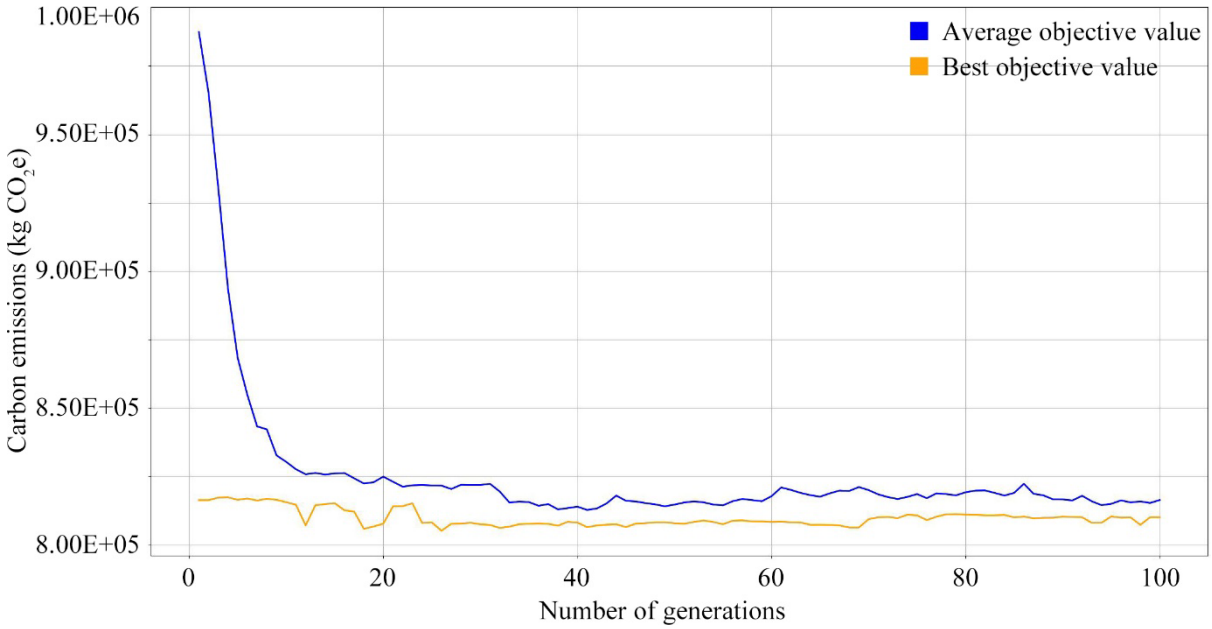

Figure 4-8 The variation of objective values across generations.

Ultimately, the optimisation yields at least 7 solutions with lower CE, indicating the exploration of 7 superior solutions. This is a conservative estimation of the optimisation performance because only solutions surpassing the current best solution are recorded. Detailed information of the feasible solution regarding the response of structure, design of elements and formwork, material consumption of each element, etc., is provided in the Appendix A-D.

4.4.2 The effectiveness of design alternative generation

Figure 4-9 illustrates the CE distribution among design alternatives with randomly selected parameters (from Monte Carlo analysis), the feasible solution, and the baseline scenario. Emissions are categorised into six parts according to their sources. Specifically, the CE from concrete and reinforcement accounts for emissions from their use in columns, beams, secondary beams, and floor slabs, respectively. CE from wall slabs, cast-in-situ formwork, and precast formwork refer to emissions from autoclaved aerated concrete, steel formwork, and aluminium alloy, respectively.

The total CE for designs with randomly selected parameters ranges from 9.39 to 11.45 × 10^5 kg CO_2e. These variances are smaller than those reported in previous findings (Cavalliere et al., 2019; X. Zhang & Wang, 2022) due to constraints on the most influential parameters (e.g., dimensions of the floor plan and the floor-to-floor height). Compared with the CE of feasible solution, the distribution range suggests a CE variance of 16.64 - 42.24%. It highlights the necessity for providing continual design guidance and monitoring the implementation of sustainable design decisions throughout the design process. Without such guidance, benefits from early-stage decisions could be negated by unsustainable choices in later stages.

The CE in the baseline scenario is lower or about equal to the minimum CE from the Monte Carlo analysis across all categories, as shown in Figure 4-9. This pattern indicates that adopting conventional standardisation principle significantly reduces embodied CE and material consumption. It aligns with the finding that architects and civil engineers tend to propose reasonably good designs based on their experience (Y. Zhou et al., 2023). However, solely relying on the standardisation leaves a gap in achieving the lowest embodied CE. Employing less standardised designs is likely to result in greater carbon reductions.

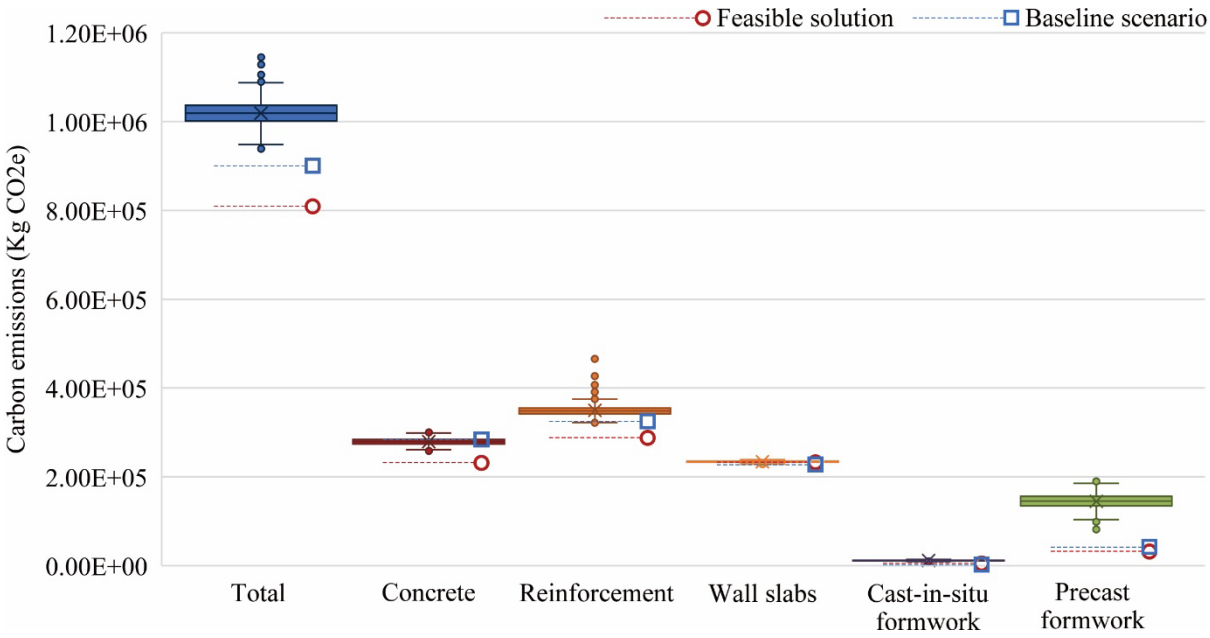

Figure 4-9 Distribution of CE from the whole structure, concrete, reinforcement, wall slabs, and formwork.

4.4.3 The effectiveness of embodied carbon reduction

Figure 4-10 and Table 4-7 provide a detailed breakdown of carbon emissions for the baseline scenario and feasible solution. Reinforcement, concrete, and wall slabs are the main sources of embodied carbon, accounting for approximately 36%, 30%, and 27% of the total CE, respectively. The contribution of formwork to CE is relatively minimal, only 5.5%. The feasible solution reduces CE from concrete, reinforcement, and precast formwork by 14.32%, 16.71%, and 10.39%, respectively, while it increases emissions from wall slabs and cast-in-situ formwork by 1.17% and 71.88%, respectively. Variations in CE from concrete, reinforcement, wall slabs, precast formwork, and cast-in-situ formwork result in CE changes of -4.49%, -6.31%, +0.30%, +0.48%, and -0.48% in the entire structure, respectively. Overall, the feasible solution achieves a 10.51% reduction in embodied CE compared to the baseline scenario.

These finding fulfils the equation (4-51) and implies that the proposed design optimisation method provides a better carbon reduction than existing design method (i.e., standardisation). This finding implies that optimising the dimensions of precast elements beyond standardisation can further reduce material-related CE. Despite the feasible solution employs 66.7% more cast-in-situ formwork and 11.55% less precast formwork compared to the baseline, it only results in a 0.48% increase and a 0.48% decrease in total CE, respectively. Previous research indicates

that off-site construction in prefabrication reduces formwork quantity (Cheng et al., 2022; Dong et al., 2015; Wong & Tang, 2012). For instance, the adoption of casting bed significantly reduces formwork area, as introduced in section 4.2.4. Thus, the impact of formwork is less pronounced in comparisons among precast designs than between precast and cast-in-situ constructions. Consequently, the advantage of standardisation in reducing formwork CE is not as significant as expected. In contrast, the reduced use of building materials in the feasible solution achieves a greater carbon reduction (10.5%), making it more sustainable than the baseline scenario.

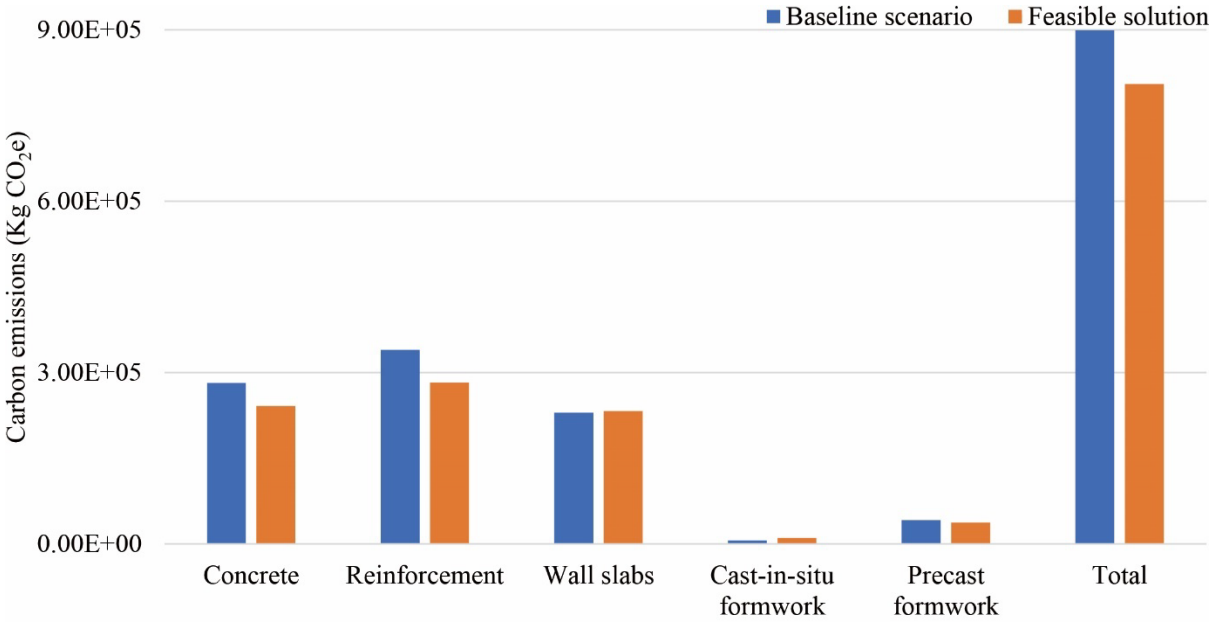

Figure 4-10 Comparison between CE of the baseline scenario and feasible solution.

Table 4-7 CE of solutions from each source (kg CO_2e).

Source of CE	**Baseline scenario**	**Feasible solution**	**Difference between feasible solution and baseline value**	**Difference in the total CE**
Concrete	281876.29	241498.49	-14.32%	-4.49%
Reinforcement	339820.98	283033.92	-16.71%	-6.31%
Wall slabs	230207.74	232902.54	1.17%	0.30%
Cast-in-situ formwork	5948.79	10224.50	71.88%	0.48%
Precast formwork	41774.88	37435.79	-10.39%	-0.48%
Total	899628.68	805095.24	-10.51%	-10.51%

4.4.4 Analysis on standardisation

To estimate the influence of standardisation principle, Table 4-8 presents a macro-level comparison (from the perspective of dimensions) of the standardisation levels between the feasible solution and baseline scenario. While the feasible solution has the same number of columns and beams as the baseline scenario, it features more secondary beams and floor slabs. Furthermore, the feasible solution has more element types across all three categories of elements. These findings indicate that the baseline scenario employs more standardised element size and the minimum number of building elements, align with assumptions stated in section 4.3.3.4.

Notably, both the feasible solution and baseline scenario have over 20 types of floor slabs, exceeding expectation. This arises from the arrangement of secondary beams, which are evenly distributed across each span. Consequently, the size of floor slabs is influenced by both the span length and the width of beams and secondary beams, leading to non-negligible disparity. It indicates a comprehensive consideration of span length and element size is crucial for higher standardisation, underscoring the importance of tolerance in span design as mentioned in section 4.2.1.2. However, in this case, the feasible solution does not address the issue (although the tolerance is applied). This is due to two reasons: 1) the macro-level element type has minor impact on CE, and 2) the discontinuous value of span length prevents a standardised solution for all the floor slabs.

Table 4-8 Estimation of the geometric standardisation.

	Columns	**Beams & Secondary beams**	**Floor slabs**
Feasible solution			
Element type	4	11	29
Element number	64	221	250
Baseline scenario			
Element type	2	8	27
Element number	64	215	238

Given the benefits of standardisation in reducing element type and number and its drawbacks in CE, this study analyses the design of each piece of formwork to elucidate this contradiction. Figure 4-11 and Figure 4-12 illustrate the reuse cycles for precast and cast-in-situ formwork, respectively. Reuse cycles of each formwork category are represented by a violin plot (on the left), a boxplot (on the right), and a scatter plot (dots on the right). The violin plot and boxplot

display the distribution of reuse cycles, ranging from 0 to 50 times. In the scatter plot, each dot represents an individual formwork piece, with its vertical coordinate indicating the reuse cycle.

Regarding the precast formwork, the average reuse cycles for beams & secondary beams, columns, and floors formwork in the baseline scenario and feasible solution are 26.77, 18.29, 29.52 and 16.95, 14.22, 16.51, respectively. Generally, precast formwork in the baseline scenario is reused for more times than in the feasible solution. As illustrated in Figure 4-11, many pieces of precast formwork are reused less than 20 times in the feasible solution, leading to lower average reuses cycles compared to the baseline scenario. Such data reflects that standardisation enhances the reuse of formwork pieces to a certain extent.

However, the quantity of formwork and its associated CE in feasible solutions is 10.39% lower than in the baseline scenario. This indicates that the reuse cycle of formwork pieces does not directly influence formwork quantity. The scatter plot in Figure 4-11 shows that many formwork pieces in the baseline scenario are still seldom reused, contributing to a large formwork quantity. This pattern may be attributed to the fact that both the dimensions and openings contribute to formwork diversity and quantity. Although standardisation tends to uniform the formwork dimensions, it often overlooks variations in the size and position of openings. As a result, elements with the same dimensions but different openings require different formwork sets, increasing the total number of formwork pieces.

Meanwhile, the common use of on-line mode in formwork production prohibits the maximum reuse of formwork pieces. Since a formwork piece can cater to elements of its size or smaller, the requirement for additional formworks increases when smaller elements are manufactured first. Conversely, employing the off-line mode in formwork manufacture (where the dimensions and openings are determined based on the characteristics of all required formwork pieces) can yield more adaptable formwork pieces. This approach facilitates the reuse of formwork in creating elements with similar dimensions and openings. Thus, this mode can decrease the total formwork needed and potentially offer a more effective way to lower both formwork quantity and associated CE.

As for the reuse cycles of cast-in-situ formwork, most formwork pieces are exactly reused 4 times, as illustrated in Figure 4-12. This is due to the assumption that cast-in-situ concrete is constructed floor by floor (stated in section 4.4), which caps the maximum reuse cycle of cast-in-situ formwork at 4 times. Besides, both the construction plan and diversity of element

dimensions influence the result, Specifically, adopting different column sizes for the ground floor and other floors in the feasible solution results in fewer reuse cycles and more formwork pieces. These finding suggest that benefits of standardisation are more significant in larger projects with more floors, where cast-in-situ formwork can be reused for more times.

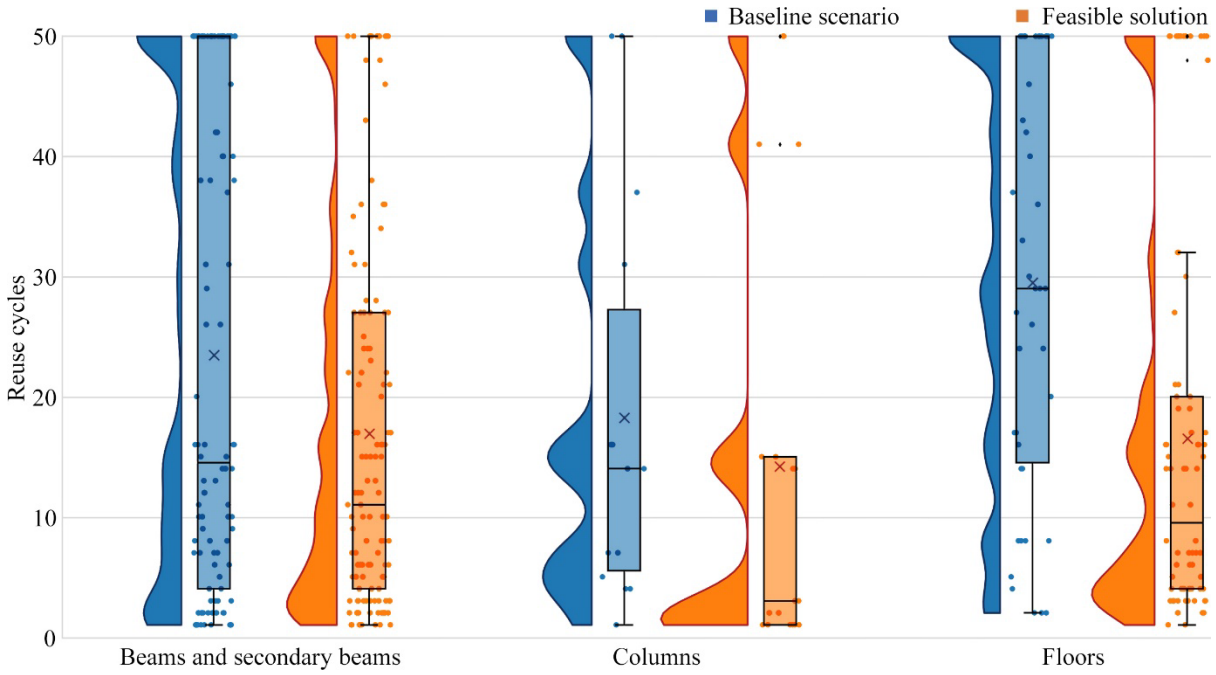

Figure 4-11 Reuse cycles of precast formwork.

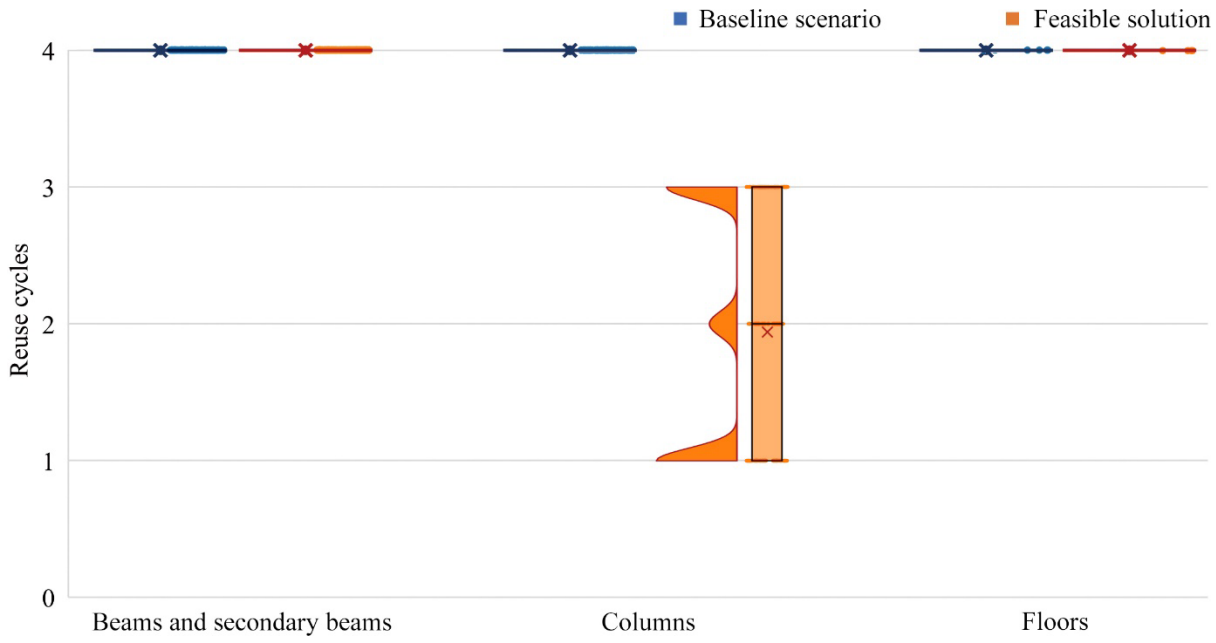

Figure 4-12 Reuse cycles of cast-in-situ formwork.

4.5 Summary

This section presents a parametric design optimisation method for reducing the embodied CE from building materials and casting formwork during the developed design stage. Using a parametric approach, the method generates design alternatives based on the original architecture design. Automatic structure analysis and detailed design are then employed to determine the dimensions and material allocation of structure elements. With the objective of minimising CE from building materials and formwork, a GA is utilised to explore solutions with the lowest CE.

Applying the method to a case project in China verifies its effectiveness in making minor adjustments to the original design and reducing CE. The optimised design alternative results in a 10.51% decrease in embodied CE, achieved through reductions in the quantity of concrete, reinforcement, and casting formwork by 14.32%, 16.71%, and 10.39% respectively.

5 Optimisation of transportation CE

5.1 Introduction

The transportation of prefabricated elements crucially impacts the CE of projects. However, limited attention has focused on the CE calculation in the transportation stage. Existing studies roughly simulated the transportation process as transferring homogeneous non-solid material by a fleet of identical vehicles in a stable environment, which deviates from the real-world transportation situation. As a result, the CE calculation method using actual transportation conditions demands further exploration and, more so, for the prefabricated construction context. This pursuit can be divided into two requirements: 1) the simulation of transportation status and 2) the CE calculation based on specific situations. To address the issue, this study adopts the bin packing (BP) problem for the micro-level analysis on the transportation of prefabricated elements in this section. The content in this chapter has been published in the study of Xiang et al. (2022).

5.2 Optimisation method

The methods employed in this module involve four steps: 1) model the transportation status of prefabricated elements as a classic three-dimensional BP problem, 2) calculate the transportation CE using the modal analysis model, 3) explore the solution to the BP problem, and 4) compare the results to other methods for validation. The research content related to each step is explained in detail below.

5.2.1 Bin packing problem design

5.2.1.1 Review of Bin packing problem

The BP problem refers to packing a set of items into a minimum number of bins so that the sum of the item sizes in each bin is no greater than the bin capacity (Coffman et al., 2013). The problem can be categorised into one-, two-, and three-dimensional conditions for different practical applications (Solomon & Weiner, 1986). Specifically, one-dimensional BP problems have many applications to problems of data management, scheduling, and resource allocation (Hall et al., 1988); two-dimensional BP problems are used to solve problems in the cutting of corrugated or decorated material (wood, glass, cloth industries), and the newspapers paging (Lodi, Martello, & Monaci, 2002); and three-dimensional BP problems are applied in cutting

and loading contexts (e.g., cutting of foam rubber in arm-chair production, container and pallet loading, and packaging design) and scheduling problems (Faroe et al., 2003; Lodi, Martello, & Vigo, 2002).

BP problems can be classified by several factors according to the problem type, as shown in Table 5-1 (Dyckhoff, 1990; Shang et al., 2020; Wäscher et al., 2007). Generally, all BP problems could be considered combinations of these factor alternatives (Shang et al., 2020). Wäscher et al. (2007) 's research introduced the detailed definitions of specific BP problems and their corresponding factors.

Table 5-1 The classification of bin packing problems

Factors	**Sub-factors**	**Alternatives**
Dimension	Dimension	One, two, three dimensional
Item features	Item shape	Regular, irregular
	Item assortment	Identical items, weekly heterogeneous assortment, strongly heterogeneous assortment
	Item rotation	Rotatable, non-rotatable
Bin features	Bin number	One, more than one
	Bin size	All dimensions fixed, one or more variable dimensions
	Bin assortment	Identical bins, weekly heterogeneous assortment, strongly heterogeneous assortment
Packing process	Packing status	Orthogonal, non-orthogonal
	Packing mode	Online, offline
	Packing target	Specific bin length, area, or volume, specific bin filling rate, output value maximisation, input value minimisation
Limitation	Limitation	Item value, item adjacency, item location

The BP problem is known to be NP-hard, which means that the existence of an efficient (polynomial-time) algorithm is unlikely. Consequently, computation times are expected to grow exponentially as the problem size increases. This characteristic motivates the search for heuristic, or approximate, solutions to instances of the problem (Hall et al., 1988). Generally, most algorithms are employed to find reasonable, feasible solutions in an acceptable timescale rather than to search for every possible solution or combination (Munien & Ezugwu, 2021).

The solution for BP problems can technically be divided into two steps: 1) exploring the suitable method to place the item, and 2) searching for the optimum placing result. In the same way, the development of solution algorithms can be summarised as 1) developing more accurate placing algorithms and 2) introducing more efficient searching algorithms (Shang et

al., 2020). Considering the existing advance in computer science, which could provide approximate or even exact optimal solutions, a promising research direction is to apply the solutions in practical scenarios (Shang et al., 2020).

Regarding applying BP solutions in transportation, scholars focus on modelling and solving actual problems in the logistics industry. The BP solution was originally applied to optimise the transportation plan of variable-sized items. Specifically, the prototype problem is defined as packing a subset of given rectangular three-dimensional boxes into a given rectangular container for the smallest container number and thus the lowest transportation cost (A. Lim et al., 2005). The subsequent research added more constraints on the packing method to solve specific issues, pushing the BP solutions closer to reality. For instance, Baldi et al. (2012) studied the method of packing compulsory and non-compulsory items for the minimum total net cost. Other constraints include the weight balance (Moon & Nguyen, 2014), product order and destination (Erbayrak et al., 2021), transportation route (Cruz Reyes et al., 2007), and time window (Q. Liu et al., 2021).

5.2.1.2 Problem description

The transportation of prefabricated elements is considered a three-dimensional BP problem with guillotine constraints. Specifically, this problem involves packing a set of three-dimensional rectangular boxes orthogonally into rectangular containers while satisfying the requirement that the packing is guillotine cuttable (i.e., there exists a series of face parallel straight cuts that can recursively cut the container into pieces so that each piece contains a box and that no box has been intersected by a cut (Amossen & Pisinger, 2010)). Compared with simple orthogonal three-dimensional BP problems (which are usually adopted onsite (H. Wang et al., 2021)), the guillotine constraints allow for moving the prefabricated elements from the top of vehicles, thus reducing the time and difficulty of loading or unloading (Shang et al., 2020).

In this problem, prefabricated elements are considered a set of rectangular boxes, each of which has seven parameters, as shown in equations(5-1)-(5-6). These equations are represented based on precast concrete elements and can be applied to other volumetric or panelised prefabricated element types (e.g., timber elements and steel elements) by adjusting the corresponding values.

$$B = \{b_1, \dots, b_i, \dots, b_n\} \tag{5-1}$$

$$b_i = \{l_i, w_i, h_i, r_{i-L}, r_{i-W}, r_{i-H}, weight_i\} \quad (5\text{-}2)$$

$$l_i = l_{i-1} + l_{i-2} + l_{i-3} + l_{i-4} \quad (5\text{-}3)$$

$$w_i = w_{i-1} + w_{i-2} + w_{i-3} + w_{i-4} \quad (5\text{-}4)$$

$$h_i = h_{i-1} + h_{i-2} + h_{i-3} + h_{i-4} \quad (5\text{-}5)$$

$$weight_i = l_{i-2} \times w_{i-2} \times h_{i-2} \times \rho_{material} \quad (5\text{-}6)$$

where n is the number of boxes; B is the set of n boxes; b_i is the i-th box in the set; l_i, w_i, and h_i are the length, width, and height (m) of b_i, respectively; r_{i-L}, r_{i-W}, and r_{i-H} are binary variables that determine whether the box can be rotated around the length (X), width (Y), and height (Z) axes, respectively. The value equals 1 if the box can be rotated and 0 otherwise; $weight_i$ is the weight of b_i (ton); l_{i-1}, l_{i-3}, w_{i-1}, w_{i-3}, h_{i-1}, and h_{i-3} are the extension length of the rebar on each side (m), respectively; l_{i-2}, w_{i-2}, and h_{i-2} are the length, width, and height of precast concrete (m), respectively; l_{i-4}, w_{i-4}, and h_{i-4} are the interval between adjacent elements in each dimension (m); and $\rho_{material}$ is the density of element material (ton/m^3), which is set to 2.5 ton/m^3 in precast concrete elements. The weight of extended rebar is excluded in the calculation because their weight only contributes to a minor part of the prefabricated elements' weight, thus leading to the negligible variance of the result. Figure 5-1 describes the variables mentioned above.

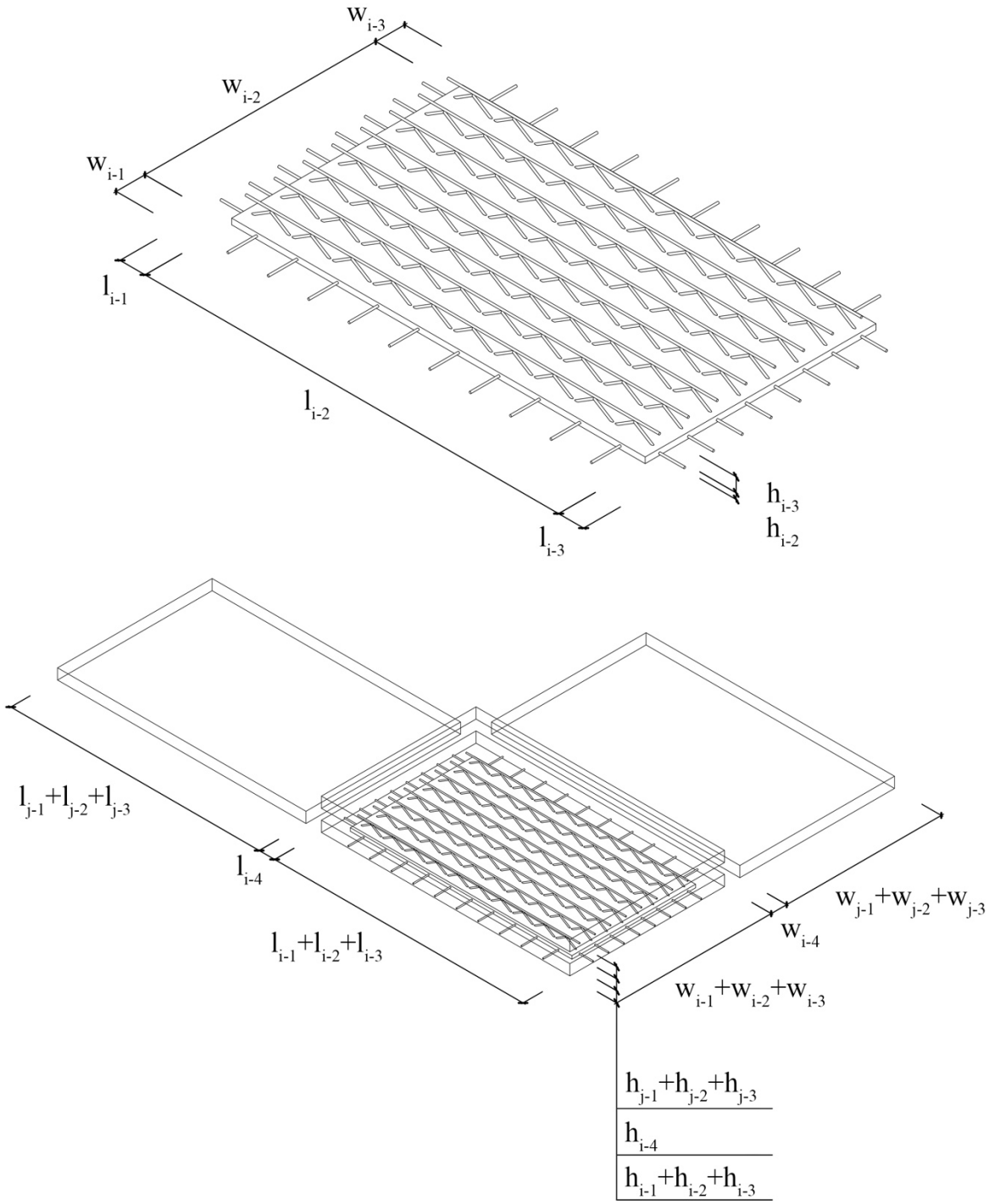

Figure 5-1 Variables of the prototype prefabricated element.

The transportation space of vehicles is considered a set of rectangular containers with four parameters, as shown in equations (5-7)-(5-10).

$$F = \{V_1, \dots, V_i, \dots, V_m\} \tag{5-7}$$

$$V_i = \{C_{i-1}, \dots, C_{i-j}, \dots, C_p\} \tag{5-8}$$

$$C = \{C_{1-1}, \dots, C_{i-j}, \dots, C_{m-p}\} \quad (5\text{-}9)$$

$$C_{i-j} = \{L_{i-j}, W_{i-j}, H_{i-j}, Load_{i-j}\} \quad (5\text{-}10)$$

where m is the number of vehicles, F is the set of m vehicles in the transportation fleet; V_i is the i-th vehicle in F; C_{i-j} is the j-th container of the i-the vehicle; p is the number of containers in V_i; C is the set of containers; L_{i-j}, H_{i-j}, and W_{i-j} are length, width, and height of C_{i-j} (m), respectively; and $Load_{i-j}$ is the load capacity of C_{i-j} (ton).

The objective of the BP problem is to pack all the boxes in set B into a suitable container set C, thus minimising the total carbon emissions of fleet F. This aim is represented by equation (5-11) below:

$$min[CE(F)] \quad (5\text{-}11)$$

where $CE(F)$ is the CE of fleet F (kg CO_2e). The calculation method of CE is given in section 5.2.2.

This packing problem has the following constraints:

C-1: All the boxes are packed orthogonally, i.e., every face of boxes is parallel to the faces of the containers.
C-2: The rotation of each box is strictly limited by the parameter of r_{i-X}, r_{i-Y}, and r_{i-Z}.
C-3: All the boxes are fully supported by either other boxes or the container, i.e., the bottom of each box is not allowed to hang in the air.
C-4: The packing is guillotine cuttable.
C-5: All the boxes must be packed.
C-6: Boxes are placed into containers without exceeding the length, width, height, and weight of each container.
C-7: The layer of packed boxes cannot exceed the limitation of corresponding codes (specific codes are cited in section 5.3.3.3).

5.2.1.3 Variable determination

The packing of boxes is considered a recursion of a four-step process: 1) select a specific box, 2) select an available space to place the box, 3) place the box, and 4) update the available space.

Correspondingly, the key to solve this problem is to determine 1) the order of boxes, 2) the available space, 3) the method to place the box, and 4) the update method of residual spaces.

The order of boxes O is determined by a set of float-type variables N, according to equations (5-12)-(5-16). These equations allow for determining the order of boxes without the limitation of box number, and the equations can therefore be used in a recursion process.

$$N = \{N_1, \dots, N_i, \dots, N_n\} \tag{5-12}$$

$$N_i \in [0,1] \tag{5-13}$$

$$box\_num_i = N_i \times length(B') \tag{5-14}$$

$$B' \in B \tag{5-15}$$

$$O = \{box\_num_1, \dots, box\_num_i, \dots, box\_num_n\} \tag{5-16}$$

where B' is the set of residual boxes (boxes that are not placed); $length(B')$ is the number of items in B'; and box_num_i represents the selected sequence number of box in B' (e.g., 5 means the fifth box in B').

The selection of available spaces is combined with the determination of the box placing method. Given a box b_i, the set of available space to place box b_i is S', and the selection of a specific space is determined by a float-type variable P_i. It works as shown in equations (5-17)-(5-19)

$$P_i \in [0,1] \tag{5-17}$$

$$space\_num_i = P_i \times length(S') \tag{5-18}$$

$$P = \{P_1, \dots, P_i, \dots, P_n\} \tag{5-19}$$

where $space\_num_i$ represents the selected sequence number of space in S' (e.g., 5 means the fifth space in S'); $length(S')$ is the number of items in S'; and P is the set of P_i. Regarding the placing method, the *bottom-up left-justified* method is employed (i.e., always placing the box at the lowest and the leftmost corner of a space) (Baker et al., 1978). In this method, six placing alternatives exist, as shown in Figure 5-2. Each alternative generates a corresponding available space in the set of available space S. Thus, the selection among these six alternatives can also be represented by P_i.

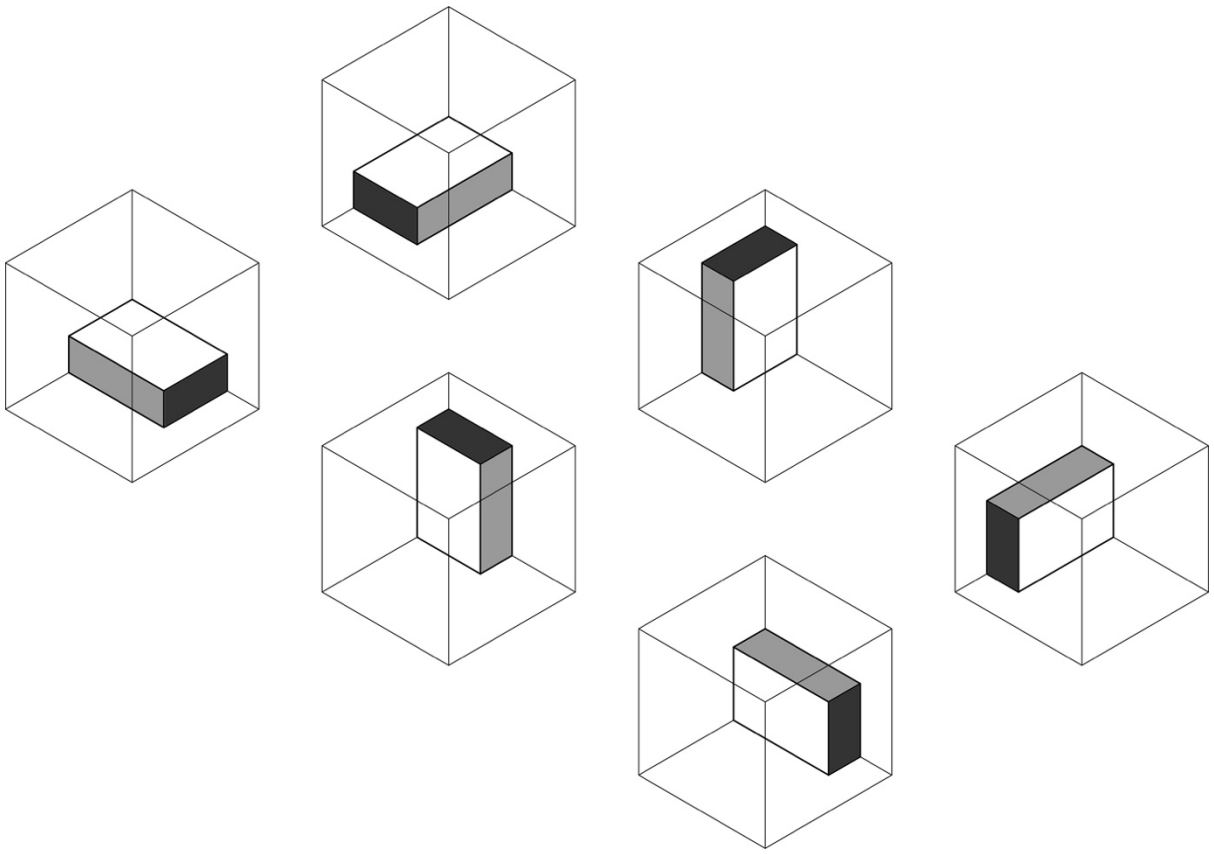

Figure 5-2 Placing alternatives of boxes.

A discrete variable set T determines the selection among different vehicle types once a new vehicle is added. It is calculated in equations (5-20)-(5-21).

$$T = \{T_1, \dots, T_i, \dots, T_m\} \tag{5-20}$$

$$T_i \in \{1, 2, \dots, type\_num\} \tag{5-21}$$

where T_i represents the type of i-th vehicle in the fleet F; and $type\_num$ is the total number of available vehicle types.

Concerning the update of residual space, once a box is placed, the selected space will be divided into several smaller and discrete sub-spaces in two ways due to the constraints of C-3 and C-4 (Figure 5-3). The selection of these two methods is represented by a set of binary variables G, as shown in equations (5-22)-(5-23).

$$G = \{G_1, \dots, G_i, \dots, G_n\} \tag{5-22}$$

$$G_i \in \{0,1\} \tag{5-23}$$

where G_i represents the selection of the place generation method in the i-th time box placing.

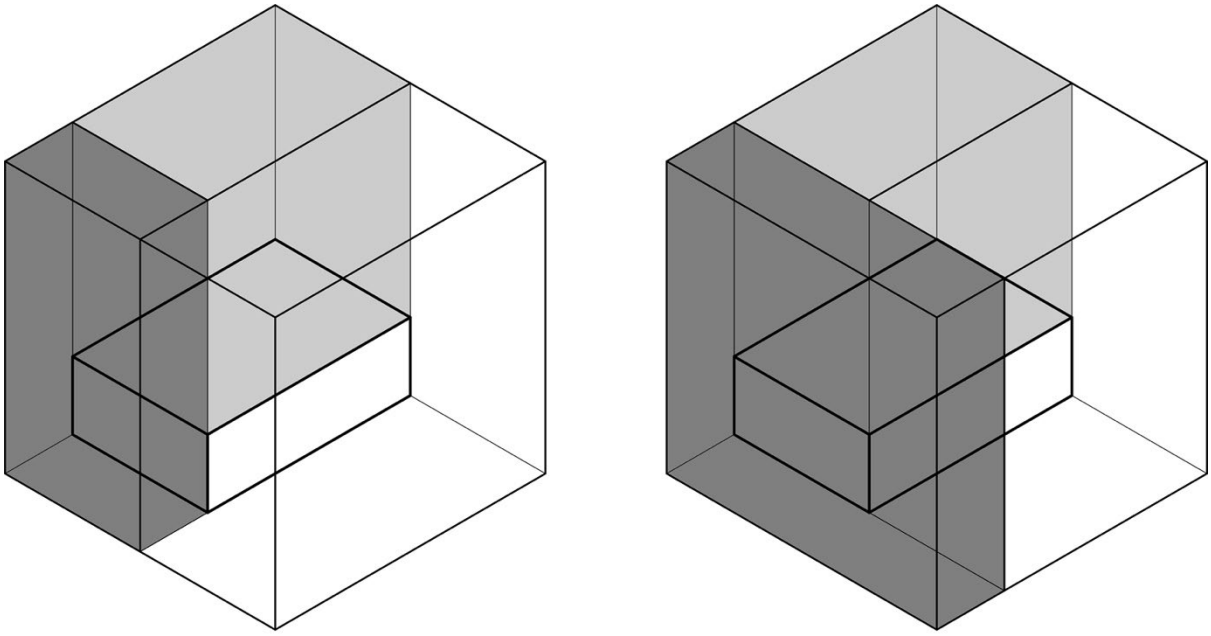

Figure 5-3 Space generation method when G_i=0 (a) and G_i=1 (b)

Therefore, the objective of this algorithm is to search for the variable sets N, P, and G that have the lowest CE. Correspondingly, equation (5-11) can be transformed into the following equation to represent the objective of this bin packing problem:

$$min[CE(N, P, T, G)] \tag{5-24}$$

5.2.1.4 Algorithm development

The algorithm defined each box b_i in the box set B by a parameter set b_i' as below:

$$b_i' = \{l_i, w_i, h_i, v\_num_i, x_i, y_i, z_i, r_{i-X}, r_{i-Y}, r_{i-Z}, weight_i\} \tag{5-25}$$

where v_num_i is the number of vehicles in which b_i is placed; and x_i, y_i, and z_i represent the coordinates of b_i's bottom-left corner.

The set of containers C is transformed to the set of spaces S, as defined in the equations (5-26)-(5-28), as below:

$$S = \{S_1, \dots, S_i, \dots, S_q\} \tag{5-26}$$

$$S_i = \{v\_num_i, L_i, W_i, H_i, X_i, Y_i, Z_i, Load_i, M_i, Layer_i\} \quad (5\text{-}27)$$

$$M_i \in \{0,1,2,3,4,5\} \quad (5\text{-}28)$$

Where q is the number of spaces; S_i is the i-th space in the space set S; L_i, W, and H_i are the length, width, and height (m) of S_i, respectively; $Load_i$ is the load capacity (ton) of S_i; M_i is a variable that represents the box placing method when S_i is used to place a box, as shown in Figure 5-2; and $Layer_i$ is the layer number of S_i.

The pseudo-code of the BP algorithm is given as below:

For each box b_i in the box set B**:**
  define b_i by parameters as b_i'
  add b_i' to the residual box set B'
End
For $number$ in the range [1, $length(B)$]**:**
  select a box b_{number}' in B' according to N_{number}
  While b_{number}' is not placed**:**
    For each space S_i in the space set S**:**
      If b_{number}' can be placed in S_i by the method of M**:**
        let $S_i(M_i) = M$
        add S_i to S'
      End
    End
    If S' is not an empty set**:**
      select a space S_{number} in S' according to P_{number}
      place b_{number}' in S_{number} according to $S_{number}(M_{number})$
      If the $S_{number}(Layer_{number})$ does not exceed the limitation**:**
        generate the new space S_{new} according to G_{number}
        add S_{new} to S
      End
      remove b_{number}' from B'
      identify b_{number}' as a placed box
    Else:
      vehicle_num += 1
      add a new vehicle and its corresponding space to S according to $T_{vehicle\_num}$
    End
  End
End

5.2.2 Carbon emissions calculation

5.2.2.1 Calculation boundary

The research boundary of this article is the process of transporting the prefabricated elements from the factory to the construction site by vehicle. The emission process in this stage includes running exhaust, start exhaust, brake wear, tire wear, etc. (EPA, 2020c). Considering that running exhaust emissions (i.e., the archetypal mobile source emissions that generate during the operation of internal-combustion engines after the engine and emission control systems have stabilized at the specific operating temperature (EPA, 2020c)) contribute to 98.85% of CE (EPA, 2020a), this study focuses only on emissions in this stage.

5.2.2.2 Data source

MOVES3 (*The United States Environmental Protection Agency's Motor Vehicle Emission Simulator*) is selected as the data source for the CE calculations in the case study of five Chinese projects (section 5.3.3.1). It is a set of modelling tools for estimating air pollution emissions produced by on-road and nonroad mobile sources (EPA, 2020a). Although *MOVES3* was developed based on the emission data in California, USA, previous studies have reported the tool remains accurate in calculations outside California, especially in China (Yue et al., 2013; L. Zhang et al., 2017). Considering that the national modal emission model in China is rare (Huang et al., 2010), employing *MOVES3* for CE calculations is reasonable in this country.

5.2.2.3 Quantitative calculation

This study employs the calculation method for heavy-duty vehicles (with a gross vehicle weight rating of more than 8500 lbs) in the *Overview of EPA's Motor Vehicle Emission Simulator* (EPA, 2020c). The total running carbon emissions CE (kg CO_2e) of the fleet F is calculated by equation (5-29), as shown below:

$$CE = \sum \left[Time_i \times \sum \left(OMF_{i-j} \times f_j \right) \right] \tag{5-29}$$

where $Time_i$ is the operating hours of the i-th vehicle (V_i) in the fleet F (h); OMF_{i-j} is the fraction of time that V_i spent in the operating mode j; and f_j is the CE rate of operating mode j (ton/h).

MOVES3 classifies the CE rates of operating mode f using scaled tractive power (STP), as shown in equations (5-30)-(5-34).

$$STP_t = \frac{res_{roll} v_t + res_{rotate} v_t^2 + res_{aero} v_t^3 + mass \times v_t(\alpha_t + g \times sin\,\theta_t)}{f_{scale}} \quad (5\text{-}30)$$

$$res_{roll} = mass \times g \times \mu_{rolling} \times cos\,\theta_t \quad (5\text{-}31)$$

$$res_{aero} = \frac{1}{2} \times \mu_{aero} \times \rho_{aero} \times area \quad (5\text{-}32)$$

$$mass_i = f_{scale_i} + load_i \quad (5\text{-}33)$$

$$load_j = \sum_{b_i'(v_i=j)} b_i'(weight_i) \quad (5\text{-}34)$$

where STP_t is the STP at time t (kW/ton); res_{roll} is the rolling resistance coefficient (kW·sec/m); res_{rotate} is the rotational resistance coefficient (kW·sec^2/m^2); res_{aero} is the aerodynamic drag coefficient (kW·sec^3/m^3); $mass$ is the total mass of the individual vehicle (ton); v_t is the instantaneous vehicle velocity at time t (m/s); α_t is the instantaneous vehicle acceleration (m/s^2); g is the acceleration due to gravity (9.8 m/s^2); θ_t is the road grade at time t; f_{scale} is the fixed mass of the vehicle (ton); $\mu_{rolling}$ is the rolling resistance coefficient of the vehicle (N/kN); μ_{aero} is the aero drag coefficient of the vehicle; ρ_{aero} is the density of the air (1.29 kg/m^3); and $area$ is the windward area of the vehicle (m^2).

The carbon emission rate of operating mode j (f_j) is linearly related to the STP of the operating mode (EPA, 2020a), and f_j can be calculated using equation (5-35).

$$f_j = k_f \times STP_j + f\_0 \quad (5\text{-}35)$$

where STP_j is the STP of operating mode j (kW/ton); f_0 is the emission rate of the vehicle operating with the STP value of 0 (kg CO_2e/h); and k_f is the coefficient factor of STP and emission rate (1000·kg^2 CO_2e/kWh), which can be obtained through regression analysis on the emission data of *MOVES3*.

5.2.3 Exploration of solutions

This study employs a genetic algorithm (GA) to search for solutions to the bin packing problem defined in section 3.1. The bin packing problem is first modelled in standard Python 3.8. Then, Geatpy 2.6.0—a genetic and evolutionary algorithm toolbox for Python (Geatpy team, 2022)—is used to explore the result of equation (*5-24*).

5.3 Module validation

5.3.1 Validation of bin packing solutions

In the assumption that prefabricated elements are transported by identical vehicles on a straight road with stable features at a stable speed, and the freight does not change the windward area, equation (5-30) can be transformed as shown below:

$$STP_t = \frac{\left(mass \times g \times \mu_{rolling} \times cos\,\theta_t + Cv_t^2 + mass \times g \times sin\,\theta_t\right) \times v_t}{f_{scale}} \tag{5-36}$$

$$= \frac{(\mu_{rolling} \times cos\,\theta_t + sin\,\theta_t) \times v_t g}{f_{scale}} load + \frac{(\mu_{rolling} \times cos\,\theta_t + sin\,\theta_t) \times v_t g}{f_{scale}} f_{scale} + \frac{Cv_t^3}{f_{scale}} \tag{5-37}$$

$$= D \times load + E \tag{5-38}$$

where,

$$D = \frac{\left(\mu_{rolling} \times cos\,\theta_t + sin\,\theta_t\right) \times v_t g}{f_{scale}} \tag{5-39}$$

$$E = \left(\mu_{rolling} \times cos\,\theta_t + sin\,\theta_t\right) \times v_t g + \frac{Cv_t^3}{f_{scale}} \tag{5-40}$$

Accordingly, equation (5-29) can be rewritten as follows:

$$CE = \sum [Time_i \times f_i] \tag{5-41}$$

$$= Time_i \times \sum \left[k_f \times \left(STP_j - STP_{min}\right) + f\_min\right] \tag{5-42}$$

$$= Time_i \times \sum \left[k_f \times (D \times load + E - STP_{min}) + f\_min\right] \tag{5-43}$$

$$= Time_i \sum \left(k_f \times D \times load\right) + T_i \sum \left[f\_min + k_f(E - STP_{min})\right] \quad (5\text{-}44)$$

$$= Time_i \times k_f \times D \times \sum load + \left[k_f(E - STP_{min}) + f\_min\right] \times Time_i \times m \quad (5\text{-}45)$$

Equations (5-34) and (5-41) can be re-interpreted as equations (5-46) and (5-47), respectively:

$$STP = STP_{elements} + STP_{vehicles} \quad (5\text{-}46)$$

$$CE = CE_{elements} + CE_{vehicles} \quad (5\text{-}47)$$

where $STP_{elements}$ is the STP to move only prefabricated elements to the construction site (kW/ton); $STP_{vehicles}$ is the STP to move vehicles without freight to the construction site (kW/ton); $CE_{elements}$ is the CE generated by moving only prefabricated elements to the construction site (kg CO_2e); and $CE_{vehicles}$ is the carbon emissions generated by moving vehicles without freight to the construction site (kg CO_2e).

As the total weight of prefabricated elements is a fixed value, the objective defined by equation (*5-22*) can then be transformed as

$$min\ (m) \quad (5\text{-}48)$$

The objective defined by equation (5-48) is the same as the aim of classical bin packing problems, and thus it can be solved using classical bin packing algorithms. This study adopts the results of the *three-dimensional residual-space optimised algorithm (3D-RSO)* (Shang et al., 2020) as the benchmark. The pseudo-code of this algorithm is given below:

For each box b_i in the box set B**:**
  define b_i by parameters as b_i'
  add b_i' to the residual box set B'
End
sort B' in descending order according to the maximum possible bottom area of each box
While B' is not an empty set**:**
  select the first box b_1' in B'
  For each space S_i in the space set S**:**
    If b_1' can be placed in S_i by a method**:**
      calculate the performance of residual space after placing b_1' by this method
      add S_i to S'
    End
  End
  If S′ is not an empty set**:**

---

sort S′ in descending order according to the performance of residual space
select the first space $S_1{}'$ in S'
place $b_1{}'$ in $S_1{}'$ according to the corresponding method
generate new space S_{new} with the largest residual space
add S_{new} to S
remove $b_1{}'$ from B'
Else:
add a new vehicle and its corresponding space to S
End
End

The 3D-RSO algorithm employs predefined formulas to determine the box order, box placing method, and generation method of new spaces after box placing, thus producing an acceptable result very quickly (less than 1 second). However, a global optimum of solutions can hardly be achieved without heuristic algorithms. Therefore, the criterion in bin packing solutions validation is that the results from the algorithm with GA (GA-based algorithm) should be equal to or better than the results of the 3D-RSO algorithm. This requirement is represented by the following equations:

$$m_{GA} \leq m_{3D-RSO} \tag{5-49}$$

$$CE_{GA} \leq CE_{3D-RSO} \tag{5-50}$$

where m_B and m_{3D-RSO} are the number of vehicles of GA-based algorithm and 3D-RSO algorithm, respectively; and CE_{GA} and CE_{3D-RSO} are the CE of GA-based algorithm and 3D-RSO algorithm (kg CO_2e), respectively.

5.3.2 Validation of CE calculation and optimisation

The CE calculation and optimisation are validated through conducting quantitative comparisons between the results of different calculation methods. The benchmarked calculation method and emission rate are selected from the *China Products Carbon Footprint Factors Database* (CCG, 2022; LÜ et al., 2021) and the Calculation standard of building carbon emissions (2014) *GB/T51366-2019*. The CE is calculated based on these two sources using the following equations:

$$CE_{benchmark} = \sum Mal_i \times Dis_i \times Coe_i \tag{5-51}$$

$$Coe_i = \frac{Fac_i}{Load_{average} \times Load\_rate_i} \quad (5\text{-}52)$$

where $CE_{benchmark}$ is the benchmarked CE value (kg CO_2e); Mal_i is the material quantity transported by method i (ton); Dis_i is the transport distance (km); Coe_i is the CE coefficient of the transport method [kg CO_2e/(ton·km)]; Fac_i is the CE factor of the transport method i (kg CO_2e/km); $Load_{average}$ is the average load capacity (ton); and $Load\_rate_i$ is the average loading rate.

5.3.3 Module application

5.3.3.1 Sample buildings

This article employs five real-built cases using the precast concrete structure to validate the transportation carbon emissions calculation of prefabricated elements. The five buildings are all located in China: two residential buildings (Project A and B), one apartment building (Project C), one office building (Project D), and one education building (Project E), as shown in Figure 5-4 and Table 5-2 Summary of sample buildings. Considered element types include prefabricated floor slab (floor), shear wall slab (wall), column, and beam.

Figure 5-5 provides information on the geometric features of prefabricated elements in these five projects. In the figure, the x-axis represents the dimension of length (m) and the y-axis represents the dimension of width and height (m). Specifically, the l_i and w_i of each prefabricated element are shown by the x- and y-coordinates of a dot, respectively. The value of h_i is given by the height of a vertical bar (corresponding to the dot) at the bottom of each figure. Figure 5-5 also shows the distribution of elements' size by colour transparency. A darker colour means a greater gathering of points and bars (i.e., more prefabricated elements are in such a specific size).

Table 5-2 Summary of sample buildings

Description	Project A	Project B	Project C	Project D	Project E
Types	Residence	Residence	Apartment	Office	School
Floor area (m^2)	454.79	751.54	2083.54	3298.96	1371.43
Layer number	20	18	17	6	6

Floor to floor height (m)	2.90	2.90	3.50	3.82	3.25
Element types, pieces, and weight (ton) per floor	Floor slab×59 42.71 Shear wall slab×10 17.26	Floor slab×110 74.68 Shear wall slab×20 32.36	Floor slab×168 194.93 Shear wall slab×69 236.01 Column×10 34.04 Beam×41 13.67	Floor slab×155 219.08 Column×20 65.42 Beam×119 429.15	Floor slab×90 89.59 Column×44 104.79
Total weight of prefabricated elements per floor (ton)	59.97	107.04	478.65	713.65	194.38

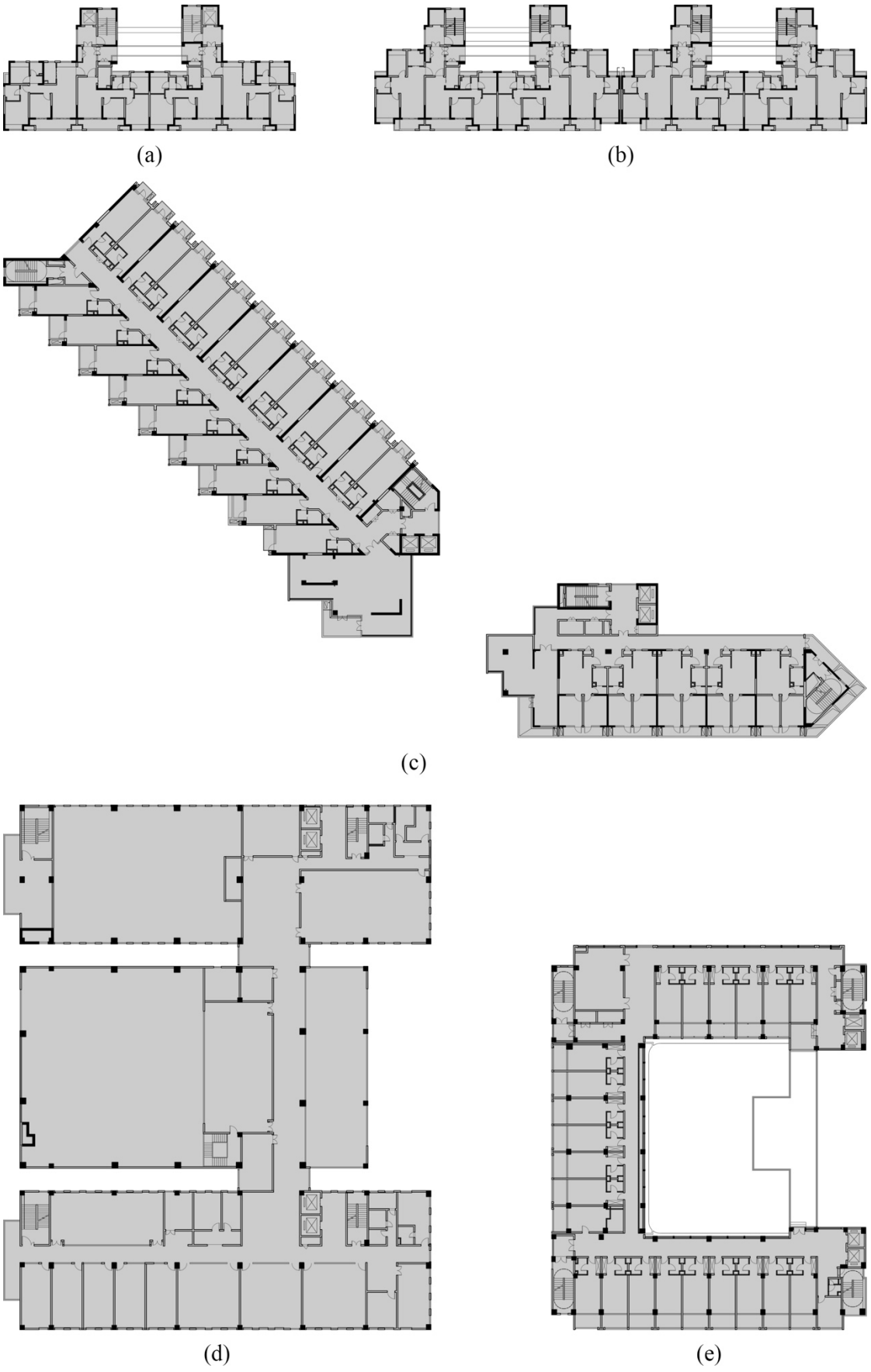

Figure 5-4 Plan layout of Project A (a), B (b), C (c), D (d), and E (e)

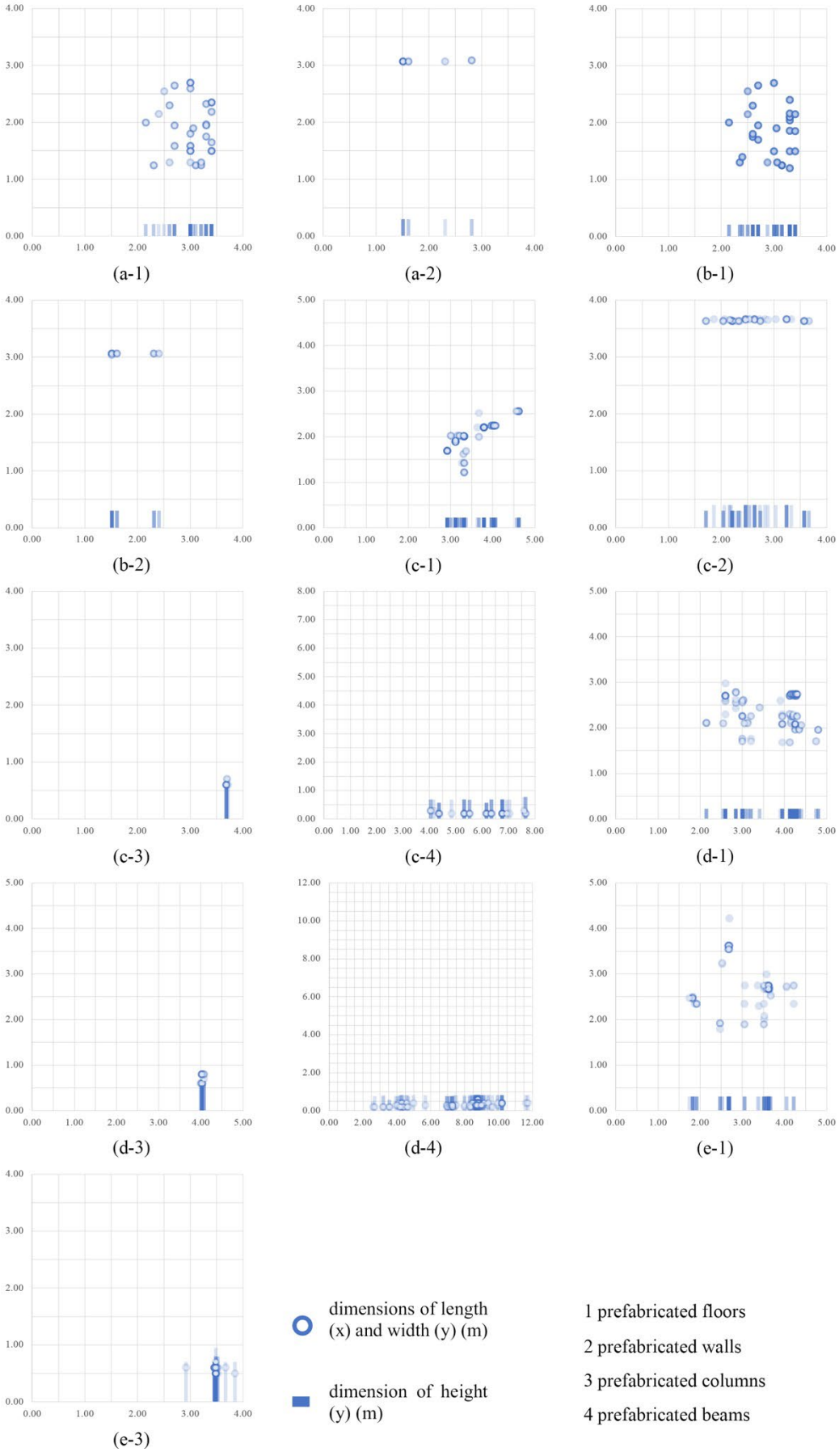

Figure 5-5 Features of prefabricated elements in Project A (a), B (b), C (c), D (d), and E (e)

5.3.3.2 Data collection

The data collected in this study include 1) prefabricated element data, including the type, size, weight of elements used in the project; 2) CE data, including emission factor and application conditions adopted in either method; 3) vehicle data, including the type, size, load capacity, and resistance factor of vehicles; and 4) transportation data, including transportation constraints and road features.

The data of prefabricated elements are extracted from the design files (i.e., the design drawings and schedules). Content analysis is then conducted on those drawings to obtain the value of variables concerning l_i, w_i, h_i, and $weight_i$. The drawings of projects are examined and verified by all participants to ensure data quality.

This study employs CE data from *MOVES3*. Specific value set are selected according to the parameters of alternatives vehicles listed in Table 5-3. The table also includes the sources of vehicle and transportation data.

5.3.3.3 Parameter Settings

The transportation CE calculation is conducted based on the following conditions:

1) All the prefabricated elements are transported in Jiangsu Province, China, on a sector of the G40 road without the consideration of vehicle rotation.

2) All the vehicles are moving at a stable speed at 0 ℃ with standard atmospheric pressure.

3) All the prefabricated elements of a project are first divided by floors and then divided by their types into different batches (e.g., the floor batch of the first floor).

4) Elements in the same batch are packed by the off-line mode, i.e., all the elements are known before packing.

Considering the transportation code and current situation in China, this study set two vehicle alternatives. Vehicle 1 has a size of 13.75m×3m×4m (Length×Width×Height) and a 15.3-ton self-weight. Vehicle 2 has a size of 17.5m×3m×4m and a 16.8-ton self-weight. The upper limitation of the gross mass of these two vehicles are both 49 ton; thus, the load capacity of vehicles 1 and 2 are 33.7 ton and 33.2 ton, respectively. The transportation space of each vehicle is represented by two rectangular containers, as shown in Figure 5-6.

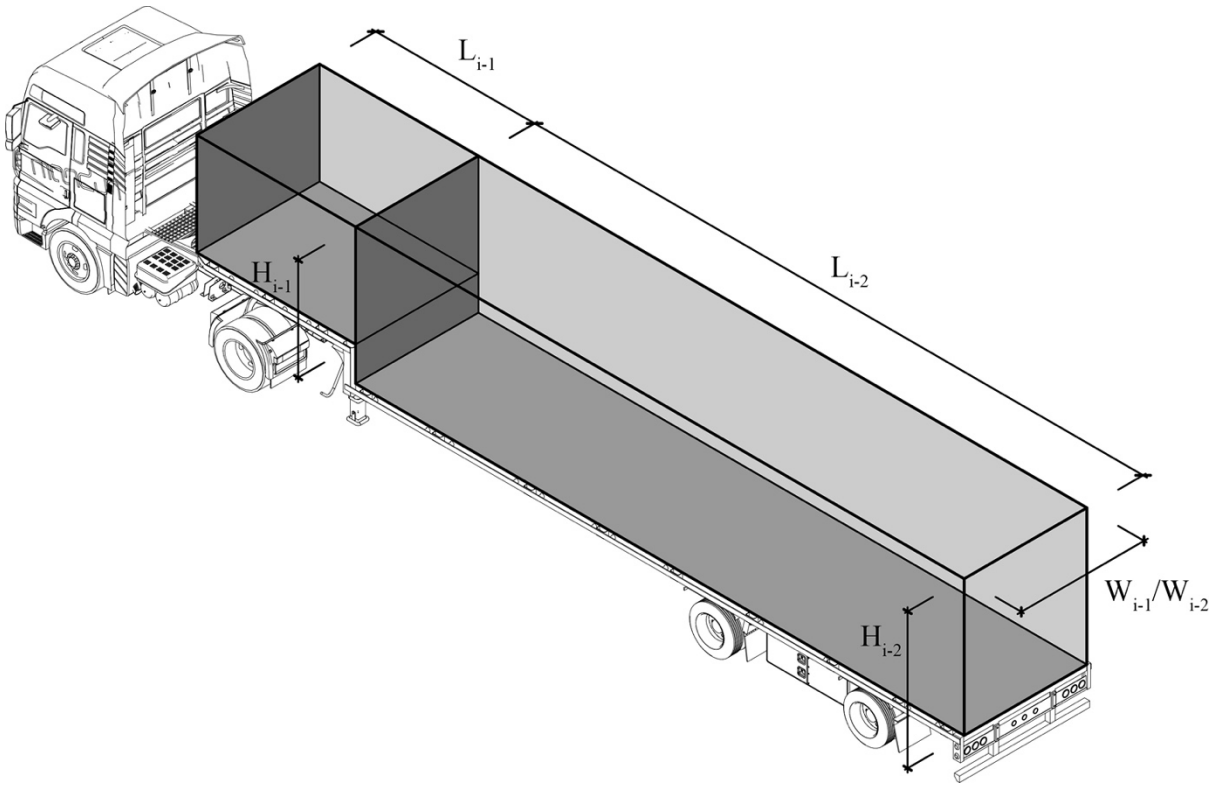

Figure 5-6 Space division of the vehicle

Figure 5-7 gives information on the packing status of different element types. All types of elements are packed horizontally and allow for rotation around one dimension. A detailed description of calculation parameters is provided in Table 5-3.

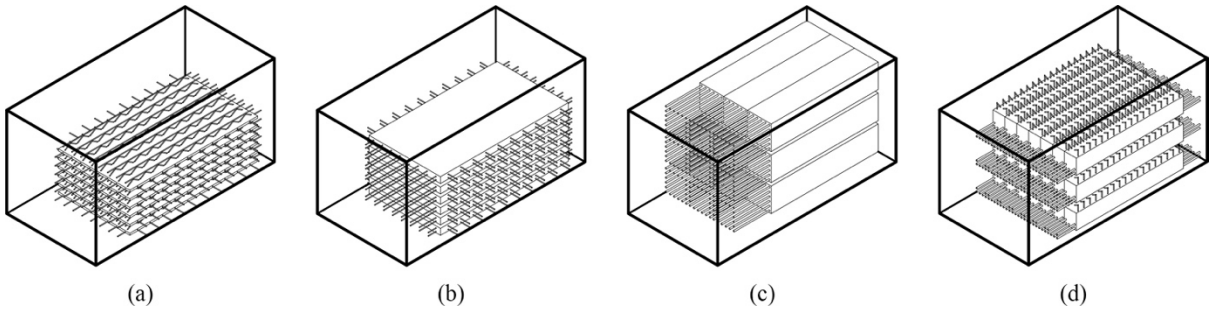

Figure 5-7 Packing status of prefabricated floors (a), walls (b), columns (c), and beams (d)

Table 5-3 Variable settings of the CE calculation

Settings			**Value**	**Data source**
Vehicle				
Vehicle 1	Size	Length (m)	13.75	A*, B*, C*
		Width (m)	3	
		Height (m)	4	

	Load	$Load_1$ (ton)	33.7	
	Weight	f_{scale} (ton)	15.3	
	Resistance	$\mu_{rolling}$ (N/kN)	6.8	
		μ_{aero}	0.75	
	Fuel		Diesel	
	Space			
	Space 1	Length (m)	4	
		Width (m)	3	
		Height (m)	2.4	
		$Load_{1-1}$ (ton)	33.7	
	Space 2	Length (m)	9.75	
		Width (m)	3	
		Height (m)	3	
		$Load_{1-2}$ (ton)	33.7	
Vehicle 2	Size	Length (m)	17.5	A*, B*, C*
		Width (m)	3	
		Height (m)	4	
	Load	$Load_2$ (ton)	32.2	
	Weight	f_{scale} (ton)	16.8	
	Resistance	$\mu_{rolling}$ (N/kN)	6.8	
		μ_{aero}	0.75	
	Fuel		Diesel	
	Space			
	Space 1	Length (m)	4	
		Width (m)	3	
		Height (m)	2.4	
		$Load_{2-1}$ (ton)	32.2	
	Space 2	Length (m)	13.5	
		Width (m)	3	
		Height (m)	2.7	
		$Load_{2-2}$ (ton)	32.2	
Transportation				
Constraints	Floor	Stack mode	Horizontal	D*, E*
		$Layer_i$	≤ 6	
		r_{i-L}	0	
		r_{i-W}	0	
		r_{i-H}	1	
	Wall	Stack mode	Horizontal	
		$Layer_i$	≤ 6	
		r_{i-L}	0	
		r_{i-W}	0	
		r_{i-H}	1	
	Column	Stack mode	Horizontal	
		$Layer_i$	≤ 3	
		r_{i-L}	1	
		r_{i-W}	0	
		r_{i-H}	0	
	Beam	Stack mode	Horizontal	
		$Layer_i$	≤ 2	

		r_{i-L}	0	
		r_{i-W}	0	
		r_{i-H}	1	
Road	$\tan\theta_t$ and slope in percentage	-0.005	3.88%	F*, G*
		-0.004	30.62%	
		0.000	45.54%	
		0.006	13.57%	
		0.007	6.39%	
	Distance	Distance (km)	50	
Speed	Speed	v_t (km/h)	59.08	H*
Loading status	Loading rate	$Load\_rate_i$	0.40-0.65	A*
CE calculation				
	BP method	k_f (1000·kg^2 CO_2e/kWh)	9.82×10^{-3}	I*
		f_0 (kg CO_2e/h)	13.57	
	Validation method 1	Coe_i_1 [kg CO_2e/(ton·km)]	0.047	H*, J*
	Validation method 2	Coe_i_2 [kg CO_2e/(ton·km)]	0.059	K*

A* School of Transporation and Logistics of Southwest Jiaotong University (2020)
B* Delgado & Li (2017)
C* China Automotive Technology and Research Center (2018)
D* China Institute of Building Standard Design & Research (2015)
E* Technical specification for precast concrete structures (2014)
F* Togpographic-map.com (2022)
G* Google Maps (2022)
H* LÜ et al. (2021)
I* EPA (2020a)
J* CCG (2022)
K* Calculation standard of building carbon emissions (2014)

This study employs a personal laptop to run all the algorithms; the laptop device specification includes an Intel Core i7-8665U CPU and 16 GB installed RAM. For an objective comparison among algorithms and projects, this study uses the identical parameter settings in the computing of each transportation task, as mentioned in this section.

Table 5-4 Parameter setting of GA-based bin packing algorithm

Parameter	**Value**
Population size	3, 200
Probability of performing crossover	0.7
Mutation operator F	0.5
Termination criteria	Generation = 1200

5.4 Validation Results

5.4.1 Bin packing solutions

The GA-based BP algorithm generally shows better performance than the 3D-RSO algorithm in packing prefabricated elements of five sample buildings, as shown in Figure 5-8. The number of vehicles employed by the GA-based algorithm is equal to or less than 3D-RSO algorithms using either vehicle 1 or 2, filling the demand of equation (5-49). Generally, the larger the total number of vehicles used, the larger the difference between those two algorithms.

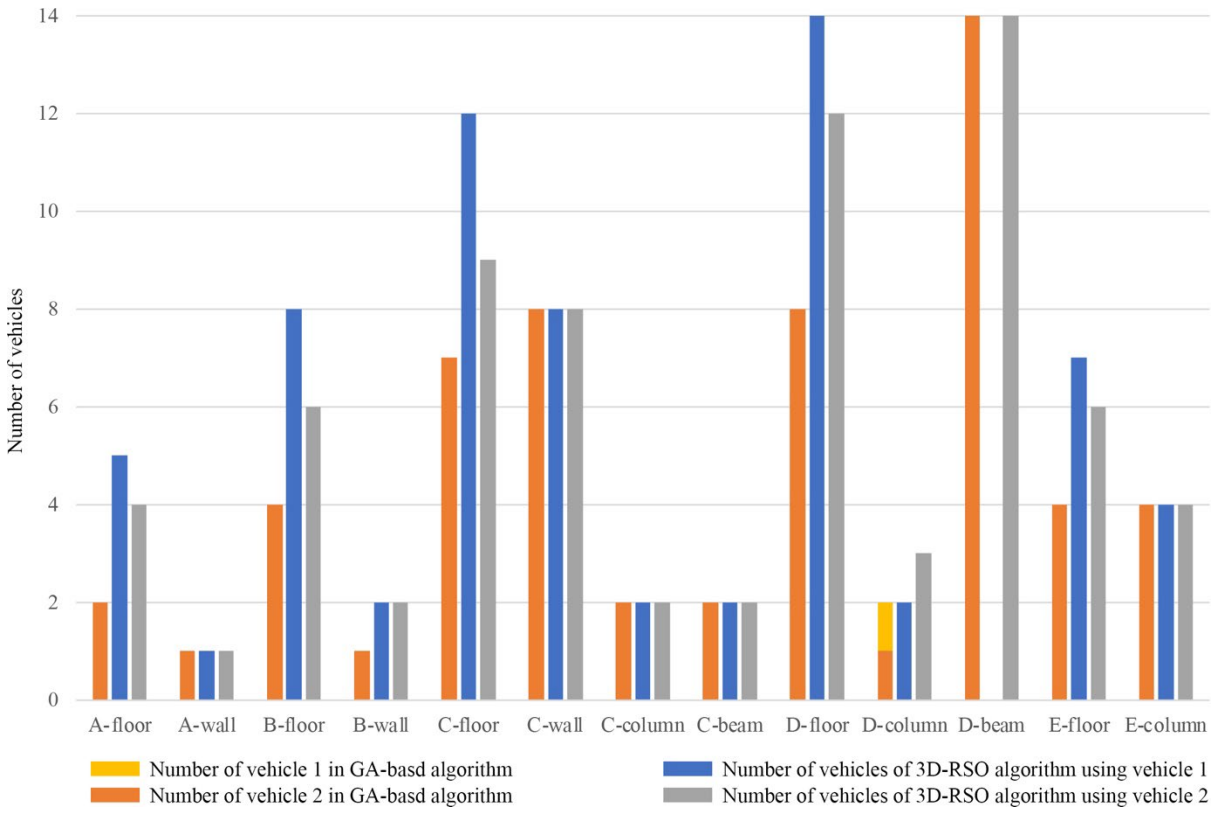

Figure 5-8 Number of vehicles in GA-based BP algorithm and 3D-RSO algorithm

Meanwhile, the 3D-RSO algorithm employs more vehicles, in most cases, when using vehicle 1 than vehicle 2. As shown in Table 5-3, vehicle 1 has a larger load capacity and a smaller space size than vehicle 2. Therefore, element size rather than element weight has a dominant effect on vehicle numbers in the transportation CE analysis on the sample buildings. Notably, the 3D-RSO algorithm using vehicle 1 in the transportation of prefabricated beams of Project D does not produce any data because the elements' size exceeds the dimensions of the available spaces in vehicle 1.

5.4.2 CE calculation

Figure 5-9 compares the variation of transportation CE with loading rate among the BP method and two validation methods. Results show that the CE of these three methods are linearly related to the loading rate. In the analysis of vehicle 1, the slopes of the BP method, validation method 1 with Coe_i_1 (0.047), and validation method 2 with Coe_i_2 (0.059) are 20.02, 79.20, and 99.42, respectively. The interceptions of the three methods are 34.51, 0, and 0, respectively. The line of BP method is interpreted as following: when transporting prefabricated elements on a 50 km section on the G40 road by vehicle 1, the CE of driving an empty vehicle is 34.51 (kg CO_2e); for every 1% increase in the loading rate (i.e., every 0.337-ton increase in the loading weight), the CE increases by 0.2002 (kg CO_2e). Similarly, lines of validation methods 1 and 2 mean the CE of driving an empty vehicle is 0 (kg CO_2e), and every 1% increase in the loading rate will increase the CE by 0.7920 and 0.9942 (kg CO_2e), respectively. The same analysis can be applied in the case of vehicle 2, where the slopes of the BP method, validation method 1, and validation method 2 are 11.42, 75.67, and 94.99, respectively, and the interceptions are 33.26, 0, and 0, respectively.

The line of the BP method intersects with the lines of validation methods 1 and 2 at points around 57% and 47%, respectively. Considering a $\pm$10% interval, the intersection range will be around 50%-65% (0.047) and 37%-50% (0.059), respectively. These ranges mean that the CE calculation result of the BP method is consistent with the result of the *China Products Carbon Footprint Factors Database* (CCG, 2022; LÜ et al., 2021) and the *Calculation Standard of Building Carbon Emissions GB/T51366-2019* (Calculation standard of building carbon emissions GB/T 51366-2019, 2014) when the average loading rate is at 50%-65% and 37%-50%, respectively. School of Transportation and Logistics of Southwest Jiaotong University (2020) reported that the average loading rate of heavy-duty vehicles in Jiangsu province is between 40% and 65%, which indicates that the average carbon emissions factor Coe_i_1 (0.047) is very likely measured with a 0.40-0.65 loading rate ($Load\_rate_i$), which covers the intersection range of 50% - 65%. Therefore, the calculation result of the BP method could very likely be close to the average real-world emissions. However, the average loading rate of building materials is between 69% and 99%, which is outside the intersection range of the BP method and Coe_i_2 (0.059). As a higher loading rate should lead to a lower carbon emission factor Coe_i, a greater loading rate (69%-99% vs. 40%-65%) with a higher factor value

(0.059 vs. 0.047) suggests that the emission factor of 0.059 may not be consistent with the real-world emissions.

Additionally, the variance between the BP-algorithm-based method and Chinese official emission factor (Coe_i_1) (CCG, 2022) (validation method 1) becomes significant with the loading rate shifting this range. According to equation (5-51), the CE result from the validation method 1 is linearly related to the weight of elements but without an original emission value (i.e., the interception is 0 in Figure 5-9). This pattern indicates that the validation method 1 evenly distributes the CE generated by the vehicles themselves to each unit of prefabricated elements. The validation method 1 is suitable for estimating CE at a macro level (e.g., calculating the transportation CE of a city by multiplying the emission factor and cargo throughout) (LÜ et al., 2021). It is not, however, reasonable (accurate) in the micro-level application, especially when the loading rate is extremely low or high. In contrast, by considering the CE of vehicles, the BP-algorithm-based method provides a more stable performance across different loading rates, making it more suitable for micro-level CE calculations.

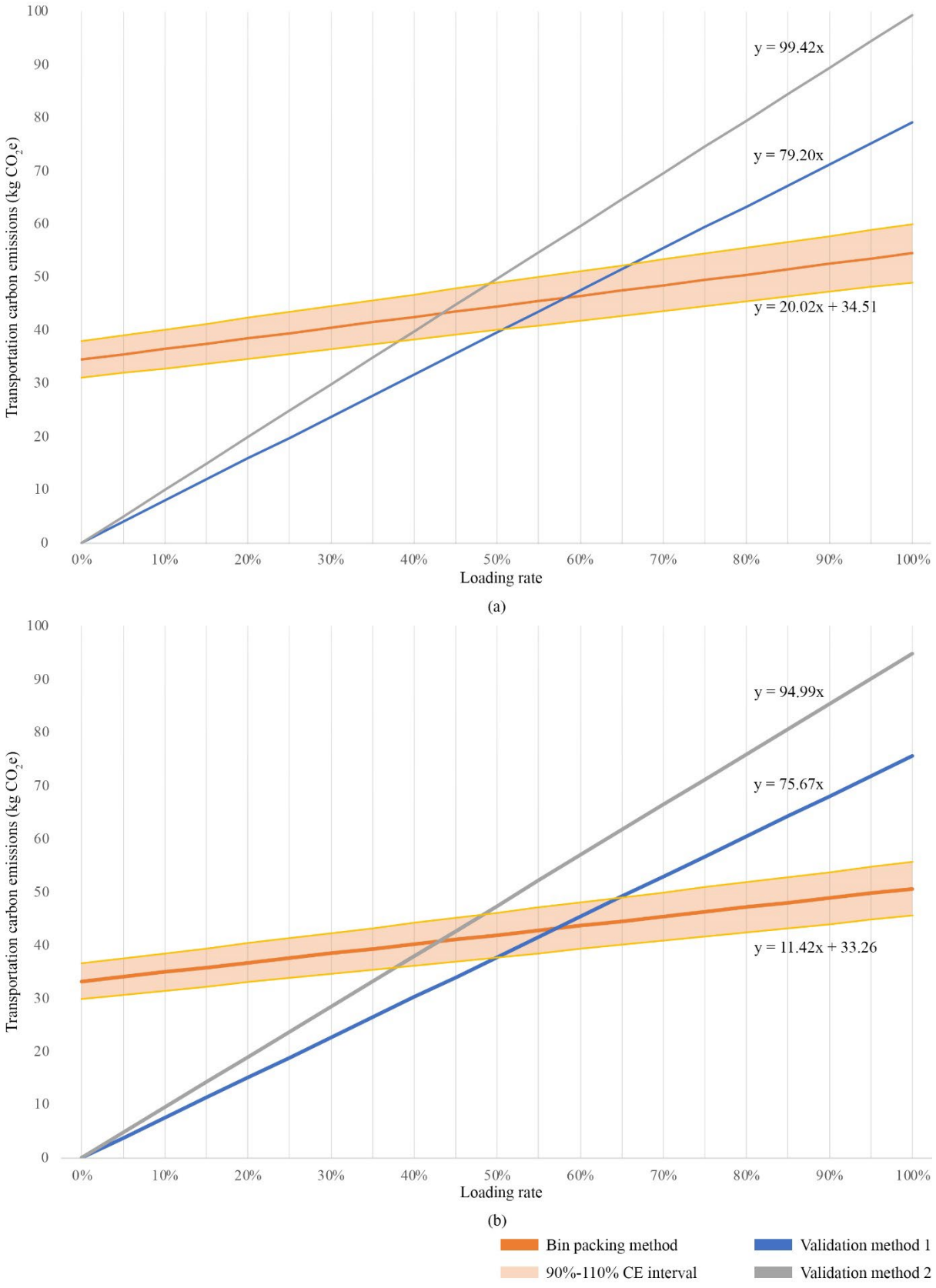

Figure 5-9 CE variation with loading rate of vehicle 1 (a) and vehicle 2 (b)

5.4.3 Transportation CE of prefabricated elements

This study estimates the transportation CE of prefabricated elements in five projects (13 transportation tasks) using the GA-based BP algorithm, 3D-RSO algorithm using vehicle 1, 3D-RSO algorithm using vehicle 2, validation method 1 using the emission factor of 0.047 [kg $CO_2e/(ton \cdot km)$], and validation method 2 using the emission factor of 0.059 [kg $CO_2e/(ton \cdot km)$], as shown in Table 5-5 and Figure 5-10. Appendix E-G provide the detailed solutions for the GA-based BP algorithm and 3D-RSO algorithms.

Generally, the GA-based BP algorithm has the lowest CE compared to other methods. This result fulfils equation (5-50) so that the GA-based algorithm has a lower or equal CE to the 3D-RSO algorithm. The result also remains consistent with section 5.4.1, underscoring that the GA-based method employs the least number of vehicles in the same situation comparing to other methods. However, no stable relationship exists between the results of 3D-RSO algorithms and validation methods 1 and 2.

Table 5-6 estimates the carbon reduction effects of GA-based algorithm and 3D-RSO algorithms. Given that validation method 1 represents the average transportation efficiency of prefabricated elements (as mentioned in section 5.4.2), validation method 1 is set as the benchmark in this table. The data shows that the GA-based algorithm has 10-30% lower emissions than validation method 1 in most transportation tasks. Similar as before, the emission difference between 3D-RSO and validation methods 1 is not consistent. These results show that employing GA-based algorithm in transportation optimisation can lead to an average of 10-30% carbon reduction.

Table 5-5 Transportation CE of prefabricated elements in Projects A-E (kg CO_2e)

Project	Elements	GA-based algorithm	3D-RSO algorithm (vehicle 1)	3D-RSO algorithm (vehicle 2)	Validation method 1 (0.047)	Validation method 2 (0.059)
A	Floor	89.63	197.91	156.16	100.38	126.01
	Wall	42.67	44.83	42.67	40.85	51.29
B	Floor	173.45	320.42	239.98	175.50	220.31
	Wall	53.72	88.23	84.03	76.03	95.45
C	Floor	338.29	529.87	404.82	458.09	575.05
	Wall	393.77	409.83	393.77	554.62	696.23
	Column	84.94	88.01	84.94	79.97	100.39
	Beam	94.98	100.26	94.98	123.61	155.16
D	Floor	384.61	613.23	517.67	514.83	646.28

	Column	104.93	106.17	135.18	153.74	193.00
	Beam	697.82	-	697.82	1008.50	1265.99
E	Floor	181.51	290.93	248.04	210.53	264.28
	Column	189.73	197.26	189.73	246.25	309.12

Table 5-6 CE difference to the Validation method 1 (%)

Project	**Elements**	**GA-based algorithm**	**3D-RSO algorithm (vehicle 1)**	**3D-RSO algorithm (vehicle 2)**
A	Floor	-10.71	97.16	55.57
	Wall	4.46	9.74	4.46
B	Floor	-1.17	82.58	36.74
	Wall	-29.34	16.05	10.52
C	Floor	-26.15	15.67	-11.63
	Wall	-29.00	-26.11	-29.00
	Column	6.21	10.05	6.21
	Beam	-23.16	-18.89	-23.16
D	Floor	-25.29	19.11	0.55
	Column	-31.75	-30.94	-12.07
	Beam	-30.81	-	-30.81
E	Floor	-13.78	38.19	17.82
	Column	-22.95	-19.89	-22.95

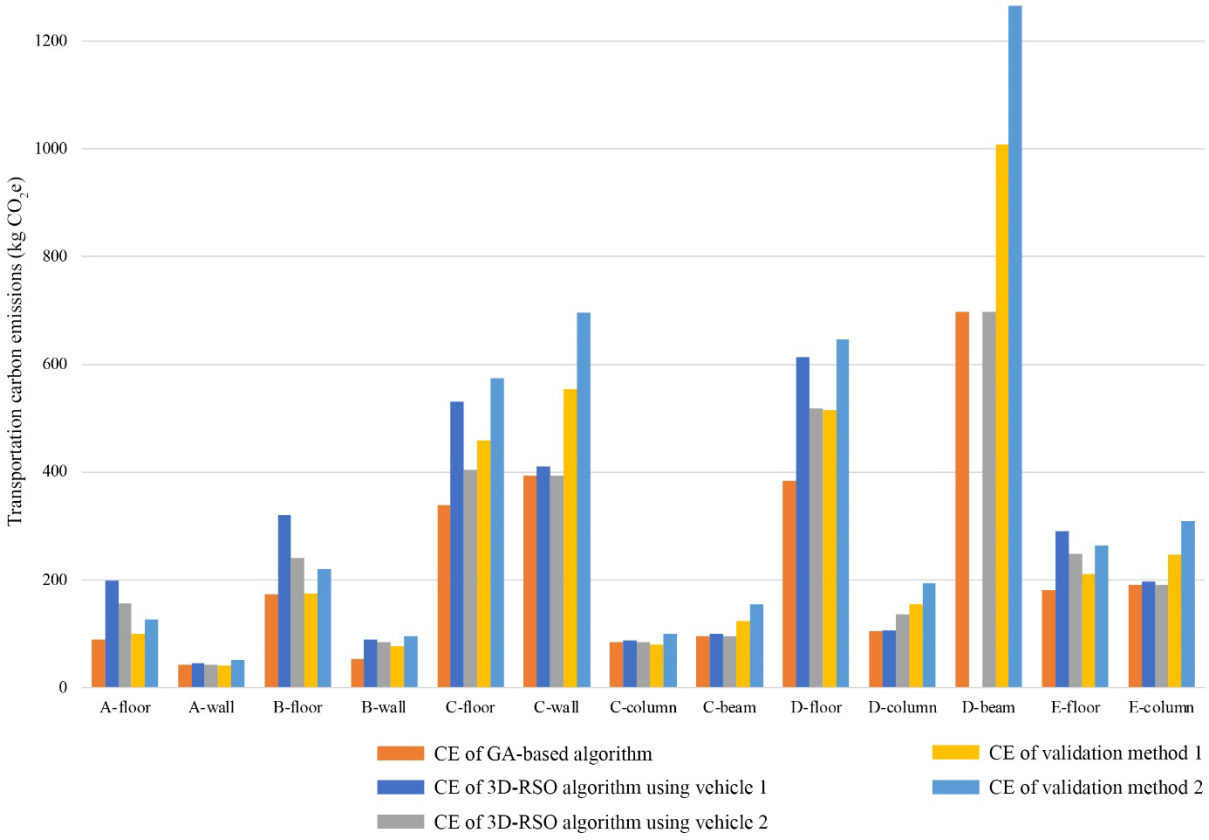

Figure 5-10 Transportation CE of prefabricated elements in Projects A-E

As the total CE is mainly affected by the quantity of transported elements, it is more objective to compare the CE per unit of prefabricated elements. Therefore, Figure 5-11 compares the average CE per unit weight of elements; the dotted lines of 2.35 and 2.95 are two benchmark values calculated using Coe_i_1 (0.047) and Coe_i_2 (0.059) (i.e., the CE of transporting one ton of prefabricated elements for 50km), respectively. The CE values are categorised into four groups according to the element types: prefabricated floors, walls, columns, and beams. The GA-based algorithm provides the lowest CE in most tasks, except in the transportation of prefabricated walls in Project-A and prefabricated columns in Project-D, where the result (2.45 and 2.49) is minorly higher than the benchmark result of 2.35.

Regarding the result of 3D-RSO algorithms, when vehicle 1 is adopted, the CE is higher than 2.35 in all five transportation tasks of prefabricated floors and two of three wall transportation tasks. In contrast, results of this method are lower than 2.35 in two of three column transportation tasks and in both beam transportation tasks. When vehicle 2 is adopted, the CE results are higher than 2.35 in three of five floor transportation tasks, two of three wall transportation tasks, and one of three column transportation tasks. The results are lower than 2.35 in other cases. Generally, the benchmark of 2.95 is higher than the results of all the other methods in most cases, as explained in section 5.4.2 when the emission factor of 0.059 is higher than real-world emissions.

Looking into the average CE values, the trend is generally consistent with the task-specific data i.e., the result of the GA-based algorithm is the lowest among all results. The results of the 3D-RSO algorithm using vehicle 1 are higher than 2.35 and 2.95 in the transportation of prefabricated floors and are lower than those two benchmarks in the transportation of prefabricated walls, columns, and beams. This result suggests that employing GA-based algorithms can reduce transportation CE in all the element types, while 3D-RSO algorithms are more sustainable in transporting prefabricated walls, columns, and beams.

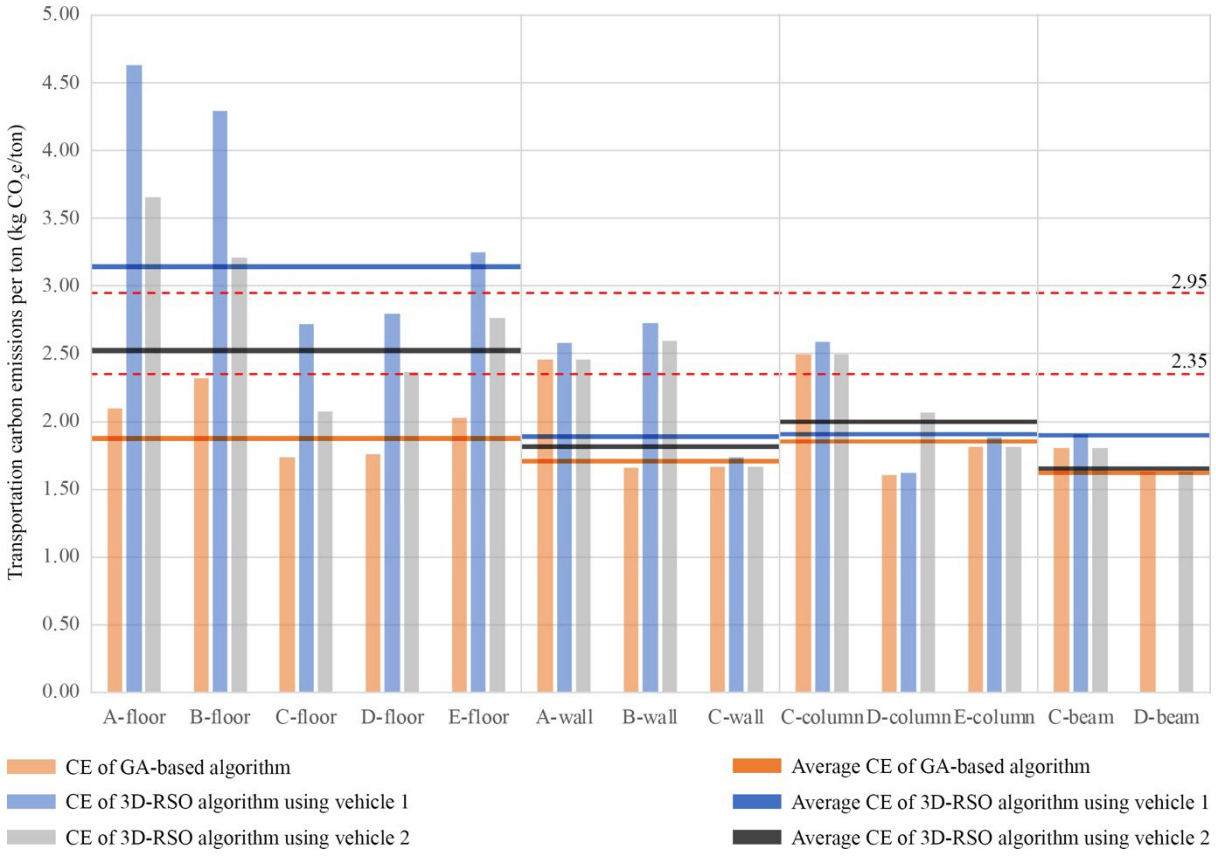

Figure 5-11 Transportation CE per ton of different element types

The difference in CE per unit prefabricated element can be explained by the difference in loading rate, as shown in Figure 5-12, where the transportation CE per unit element decreases with the growth of the loading rate. Figure 5-13 illustrates the loading rate of each transportation task. The GA-based algorithm obtains the highest average loading rate among all four element categories. The loading rate of the 3D-RSO algorithm using vehicle 2 ranks the second in prefabricated floors, walls, and beams and ranks the third in columns. This sequence is consistent with the sequence of the CE per unit element (i.e., a higher loading rate appears accompanied by a lower CE per unit element).

Besides, the average loading rate of elements varies with the element type, where the prefabricated floor has the lowest loading rate with the largest difference among the three algorithms. Prefabricated columns, however, have a smaller algorithm difference, while prefabricated walls and beams have the highest average loading rate.

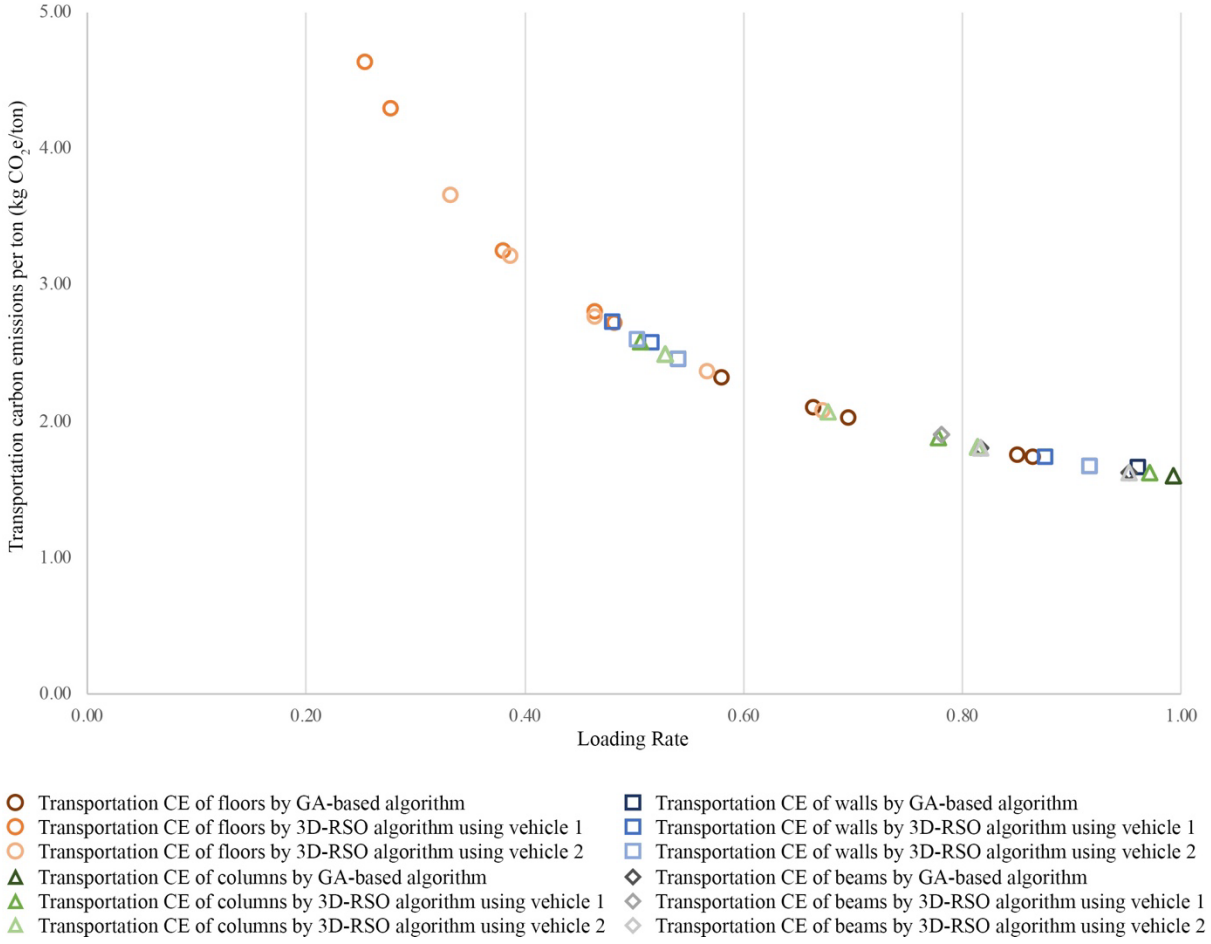

Figure 5-12 The variation of CE of per ton elements with loading rate of vehicle

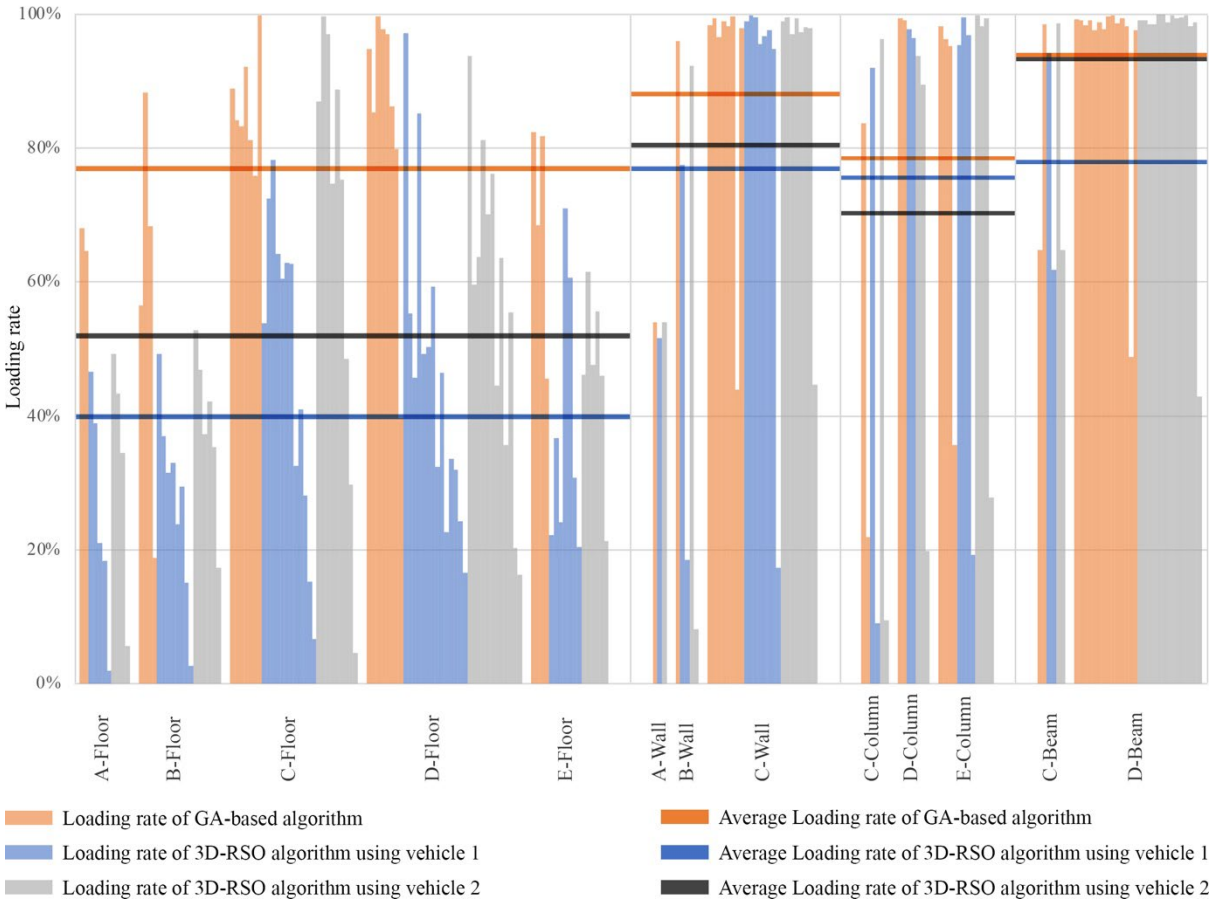

Figure 5-13 Loading rate of different element types

5.4.4 Algorithm performance

Figure 5-14 shows the solving process of the GA-based bin packing algorithm, in which the y-axis represents the value of the objective function (i.e., the CE per hour (kg CO_2e/h)), and the x-axis represents the generation in computing. The algorithm achieves the lowest CE value within the first 600 generations in all 13 transportation tasks. Specifically, the optimum solutions are obtained within the first 50 generations in the transportation of prefabricated walls, columns, and beams, while the computing of prefabricated floors' transportation takes approximately 250 to 550 generations.

The average value in each generation is not a smooth curve in b-1 and d-3. Meanwhile, in a-1 and e-1, the average does not tend to the optimum value. This situation is because the objective function is not fully continuous. As shown in equation (5-45), the transportation CE is dominated by the number of vehicles, a discrete variable. Therefore, the average value may be stuck at a local-optimum value. This reason also explains the existence of fluctuations of optimal values in the figures a-1, b-1, b-2, d-1, and e-1.

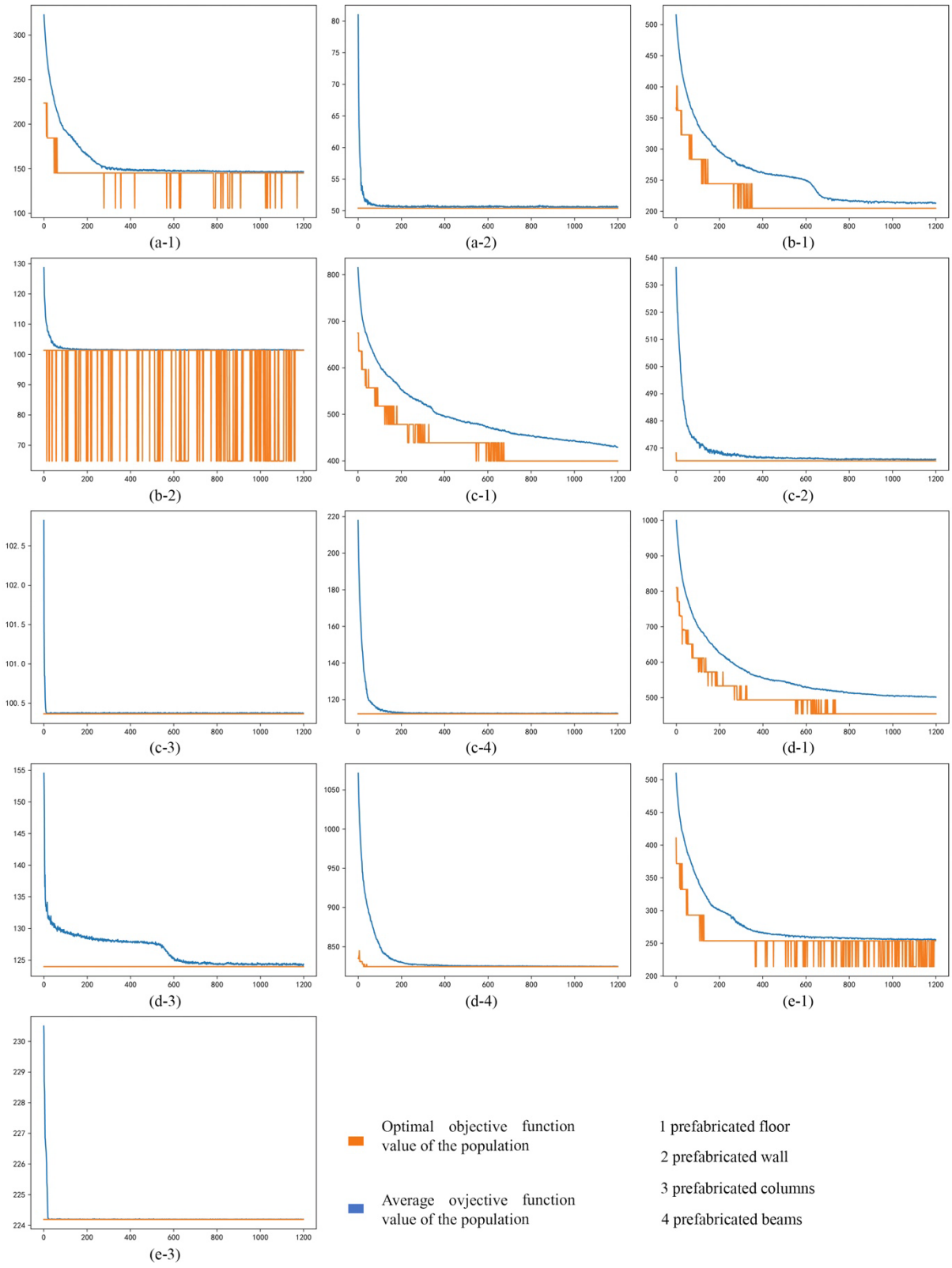

Figure 5-14 Objective function value variation with the generation (x-axis is the value of objective function and y-axis is the number of generations)

Figure 5-15 illustrates the computing time of the GA-based and 3D-RSO algorithms. The GA-based algorithm takes much more time than the 3D-RSO algorithms. Additionally, the total

computing time and the computing time per piece element of the GA-based algorithm is growing with the total piece number increasing from 1880.13s (10 pieces in C-column) to 85542.05 (168 pieces in C-floor) and from 188.01s per piece (C-column) to 509.18s per piece (C-floor), respectively. In contrast, the variation in total computing time of the 3D-RSO algorithm is not significant across all 13 transportation tasks, between 0.26s and 0.35s, leading to a negative relationship between the computing time per element piece and the number of prefabricated elements.

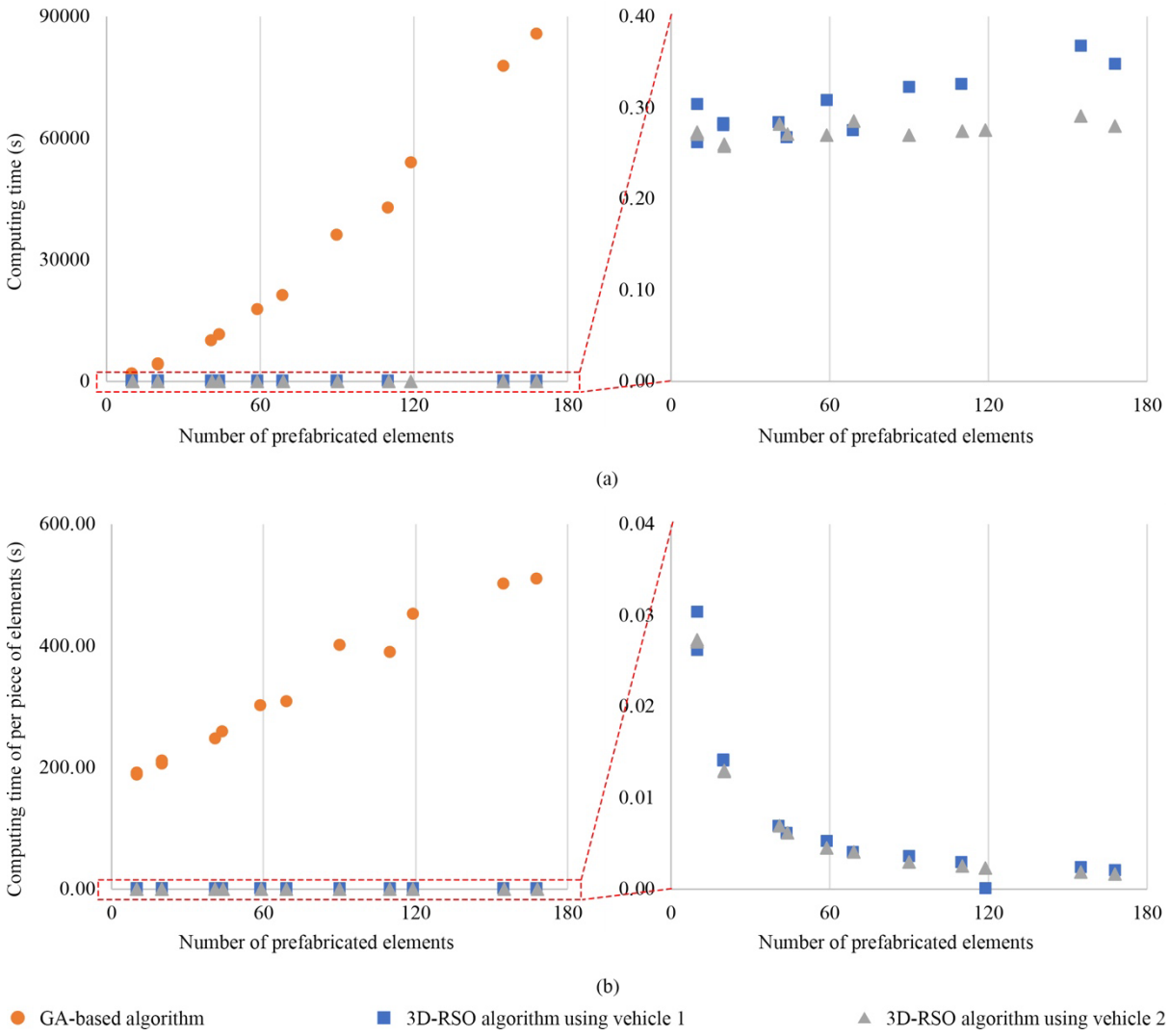

Figure 5-15 Variation of the total computing time with the number of prefabricated elements (a) and Variation of the computing time per element piece with the number of prefabricated elements (b)

Figure 5-16 illustrates the trade-off of computing time and CE when replacing the 3D-RSO algorithm with the GA-based algorithm, in which a closer distribution to the right bottom

corner means a more efficient replacement and the opposite when a dot is approaching the left top corner. Generally, the replacement of 3D-RSO algorithm using vehicle 1 shows a more significant advantage than the 3D-RSO algorithm using vehicle 2 because of a larger CE reduction with a similar increase in computing time. Regarding the difference across element types, the CE reduction is more significant in the transportation of floors while less significant in the other three, especially in the transportation of columns and beams. This finding indicates that it is more efficient to employ the GA-based algorithm than the 3D-RSO algorithm in the transportation planning of prefabricated floors.

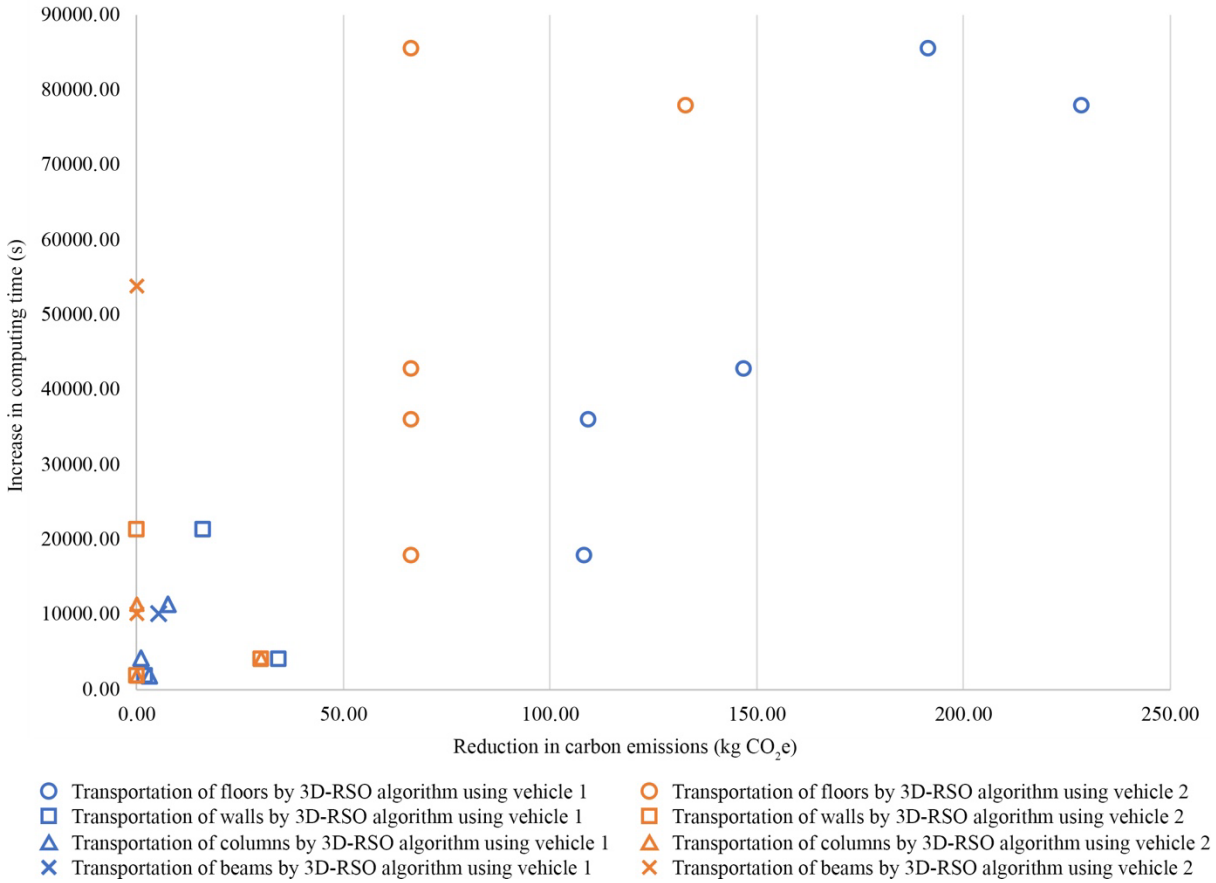

Figure 5-16 Variation of the increase in computing time with the reduction in total carbon emissions

5.5 Summary

This section presents a micro-level transportation CE optimisation method that estimates and reduces the emissions based on the features of prefabricated elements and vehicles. The method simulates the transportation status of prefabricated elements as BP problems. Then, a modal analysis model is employed to calculate the CE of each vehicle based on vehicle type, road

condition, and freight weight. Considering the minimum transportation CE as objective, a GA is employed to search for the optimal solution and its corresponding CE values.

Application in five case studies demonstrates the method's effectiveness in reducing transportation CE across different prefabricated element types. The optimised results achieve the lowest CE in all the transportation tasks. Although it requires longer computing time, this method remains feasible for real-world transportation optimisation.

6 Communication of optimisation results

6.1 Introduction

Sections 4 and 5 describe the development of modules 2 and 3 for reducing CE in the manufacturing and transportation of prefabricated projects. Applying such modules in the practices demands the data extraction from design files and presentation of optimised solutions to the designers. Therefore, modules 1 and 4 are developed in this section. Specifically, Module 1 is designed to extract design parameters ($original\_span\_list_d$, $original\_height\_list$, and $original\_wall\_list$) from original design. Meanwhile, module 4 visualises the feasible design alternative identified by module 2 and the feasible transportation plan determined by module 3 into a designer-friendly format. Developing these two modules necessitates a clear definition of EIF for both input and output design files. Consequently, developing module 1 and 4 involves two steps: 1) identifying EIF used in design practice, and 2) developing tools for processing design files in the target EIF.

6.2 Identification of EIF in design practice

Given hypothesis 6 (section 1.3.2), which posits that design content influence the selection of EIF used in design, this section explores the relationship between design tasks and EIF via the survey and statistical analysis of design practice and EIF usage. Specifically, five steps are involved: 1) A questionnaire survey with design experts in the Chinese construction industry; 2) analysis of variance (ANOVA) to explore the design features of experienced designers in sustainable and prefabricated constructions; 3) Relevance analysis to identify key factors influencing the selection of EIF; 4) Logistic regression analysis to quantify the contribution of these factors; 5) Multiple-correspondence analysis (MCA) to visualise the contributions of key factors. The content of this section has been published in the study of Xiang, Mahamadu, & Florez-Perez (2024).

6.2.1 Questionnaire survey

6.2.1.1 Questionnaire design

The questionnaire is divided into three parts, as given in the Appendix H: 1) Respondents' demographic information (e.g., jobs, qualifications, industry experience, and organisation characteristics); 2) Participants' design habits (e.g., used design software, design optimisation

method, and design considerations); and 3) The characteristics of participants' design activities (e.g., EIF used during design). Given the dominance of Chinese in the industry, all questions are presented in Chinese.

The questionnaire includes two types of questions: multiple choice and Likert-scale. As architects and civil engineers often have multiple and varied design responsibilities in China, Multiple choice and Likert-scale questions are preferred over single choice questions to minimise personal biases from summarising complex scenarios into one primary statue. For the same reason, factor ranking, as seen in previous studies (H. Guo et al., 2019), is omitted. Using Likert-scale questions instead of ranking permits equivalent weighting of items, potentially yielding more accurate descriptions. Quantitative descriptions are added in selections to help participants select the most fitting response for their situation.

6.2.1.2 Data collection

Target participants are experienced construction industry professionals including designers, engineers, and contractors, due to the professional nature of questions. Initially, 30 experts were identified and invited via literature review, consulting of data from Ministry of Housing and Urban Rural Development of China, and Linkedln groups. Subsequently, a snowball sampling method was used to expand participant pool. Participants were invited to fill and share the anonymous questionnaire via Microsoft Forms from June to November 2023. The data collection method and process were approved and qualified by the University College London on 02/11/2022.

6.2.1.3 Data processing

Survey results are automatically extracted from Microsoft Forms into a Microsoft Excel file. A python script is employed to convert all the answers into selections of single choice questions. For instance, the question "what is your responsibility in the design" is divided into five sub-questions covering involvement in architecture, structure, building system, building products, and other design areas. The selection of choice is represented in numerical categories from 1 to 7. A detailed list of variable names and categories are given in the Appendix H.

6.2.2 Data analysis

6.2.2.1 Analysis of variance

ANOVA is used to estimate differences among designers with varied design experience in sustainable and prefabricated projects. Comparing the "average" selection of designers reveals qualitative patterns in design activities. Table 6-1 listed the variables employed in ANOVA. Specifically, each analysis estimates a pair of variables: one for design experience and one for design activity.

Table 6-1 Variables adopted in ANOVA.

Design experience	**Design activities**	
Sustainable percentage	Cost increase	
Prefabrication percentage	Time increase	
Sustainability	Formats of design files	2D graph 3D model 3D BIM 4D BIM VR
	Preferred format of design constraints	Preference in text Preference in tables Preference in 2D Preference in 3D Preference in BIM
	Preferred format of design reference	Prefer in text Prefer in tables Prefer in 2D Prefer in 3D Prefer in BIM
	Sustainability analysis method	Never consider sustainability Qualitative Quantitative
	CE analysis system boundary	Never consider CE Construction material CE Maintenance material CE Construction CE Operational CE Demolition CE Indirect CE
	Design optimisation method	Never optimise Experience based Less than 5 alternatives More than 5 alternatives

6.2.2.2 Relevance analysis

The questionnaire results involve two types of variables: ordinal categorical variable and nominal categorical variable. Specifically, ordinal categorical variables have a clear to their categories. These are used for questions such as “how often do you use the following design software”. Conversely, nominal categorical variables represent answers to questions like “what kind of building do you usually design”.

Kendall's Tau-b is employed to measure the relevance between two ordinal categorical variables. The calculation involves the following equations:

$$\tau_B = \frac{n_c - n_d}{\sqrt{(n_0 - n_1)(n_0 - n_2)}} \tag{6-1}$$

$$n_0 = n(n-1)/2 \tag{6-2}$$

$$n_1 = \sum_i t_i(t_i - 1)/2 \tag{6-3}$$

$$n_2 = \sum_j u_j(u_j - 1)/2 \tag{6-4}$$

where, τ_B is Kendall's Tau-b coefficient; n_c is the number of concordant pairs; n_d represents the number of discordant pairs; n is sample size; t_i is the number of tied values in the i^{th} group of ties for the first quantity; u_j is the number of tied values in the j^{th} group of ties for the second quantity.

Theil’s U, also known as the Uncertainty Coefficient, is employed to assess the degree of association between two nominal categorical variables and between a nominal and an ordinal categorical variable. This coefficient quantifies the reduction in uncertainty of one random variable when another is known. Theil’s U is calculated using the following equations:

$$U(X|Y) = \frac{H(X) - H(X|Y)}{H(X)} \tag{6-5}$$

$$H(X) = -\sum p(x)\, log\, p(x) \tag{6-6}$$

$$H(X|Y) = -\sum p(y,x)\, log\left(\frac{p(y,x)}{p(y)}\right) \quad (6\text{-}7)$$

where, $U(X|Y)$ is the uncertainty coefficient of X with given Y; $H(X)$ is the information entropy of X; $H(X|Y)$ is the conditional information entropy of X with given Y; $p(x)$ is the probability of event X; $p(y,x)$ is the joint probability of X and Y; $p(y)$ is the probability of event Y.

Since Kendall's Tau-b coefficient and Uncertainty Coefficient share a similar scale, the relevance between two variables is estimated as follows (Botsch, 2011):

$|\tau_B$ or $U(X|Y)| \leq 0.10$: very weak

$0.10 < |\tau_B$ or $U(X|Y)| \leq 0.20$: weak

$0.20 < |\tau_B$ or $U(X|Y)| \leq 0.30$: moderate

$0.30 < |\tau_B$ or $U(X|Y)|$: strong

In this study, variables with an absolute coefficient greater than 0.1 are deemed relevant.

6.2.2.3 Logistic regression analysis

Three categories of dependent variables are selected: 1) Data format used in the design process (i.e., *2D graph*, *3D model*, and *3D BIM*); 2) Preferred data format for preliminary design information from previous stages (i.e., *Preference in 2D*, *Preference in 3D*, and *Preference in BIM*); and 3) Preferred data format for decision-assistive design reference information (i.e., *prefer in 2D graph*, *prefer in 3D model*, and *prefer in BIM model*). Candidate independent variables are chosen based on their relevance estimated in section 6.2.2.2.

Initially, these candidates are filtered based on the existence of a reasonable relationship between dependent and independent variables. For example, the source of design constraints (e.g., *Codes*, *Experienced parameters*, and *Construction situation*) are considered independent variables for preferred data format for preliminary design information from previous stages while excluded for data format used in the design process. Filtered candidates are then used to develop multinomial logistics regression models in SPSS. A step-in strategy is employed to automatically identify contributing factors to dependent variables. Notably, the ordinal logistic

regression model is denied because pilot analysis indicates it fails the test of parallel lines assumption.

6.2.2.4 Multiple-correspondence analysis

As an extension of correspondence analysis, MCA allows to analyse relationship patterns among several categorical dependent variables via point proximities on a low-dimensional map (Abdi & Valentin, 2007). This study employs MCA to explore concurrent patterns in various design activities and information formats. Dependent variables, along with their corresponding independent variables, as outlined in section 6.2.2.3, form several variable sets. These sets are utilized to analyse the characteristics of design activities using specific EIFs.

6.2.3 Findings from questionnaire survey and data analysis

6.2.3.1 Descriptive results

By the end of survey period, 137 questionnaires were submitted, with 131 identified valid responses. Submissions from six respondents were excluded due to insufficient experience in design and construction. Participants' responsibilities comprised architecture design (83), structure design (24), building system design (9), building products design (8), and other design fields (18). Participants are involved in various design stages, including preliminary studies (45), concept design (58), developed design (74), technical design (60), product design (29), and other design phases (6). Figure 6-1 illustrates the division of these design stages in China based on the corresponding design tasks. Detailed definitions of terms used can be found in the publications by Hollberg (2016), RIBA (2020), and Jin et al. (2022).

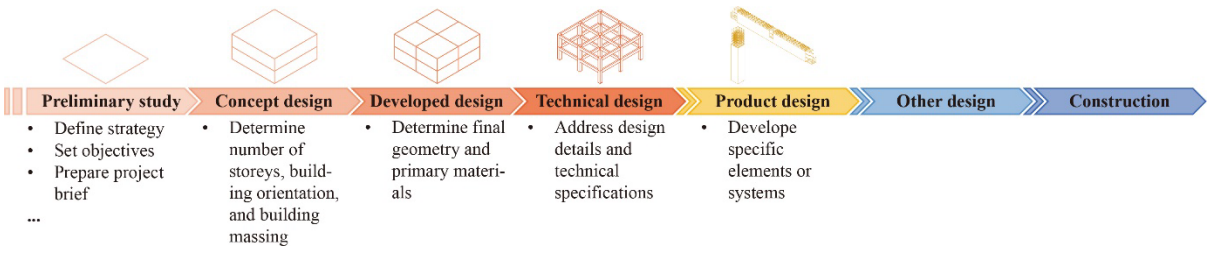

Figure 6-1 Division of design stages.

Notably, the sums of these results (142 and 272) exceed the total number of valid responses (131), indicating that some participants are hold multiple roles in practice. This pattern is also observed in other multiple-choice questions. The distribution of participants' experience in the

construction industry is as follows: less than 2 years (16.79%), 3-5 years (31.30%), 6-11 years (21.37%), 11-20 years (21.37%), and more than 20 years (9.16%). Of the participants, 22 (16.79%) obtained national qualifications, including 3 class-2 certified architects, 12 class-1 certified architects, 5 class-1 certified civil engineers, 1 certified constructor, and 1 certified utility engineer.

As illustrated in Figure 6-2, more than 70% of participants (93) have the experience in prefabrication design and 18% of them (23) design prefabricated projects for 40% of their design tasks. Regarding their experience in sustainable design, 72% (95) used to design sustainable buildings (projects have a particular emphasis on the carbon emissions and energy demand), and 23% (30) are experienced in this area (i.e., design sustainable buildings for more than 40% of the time).

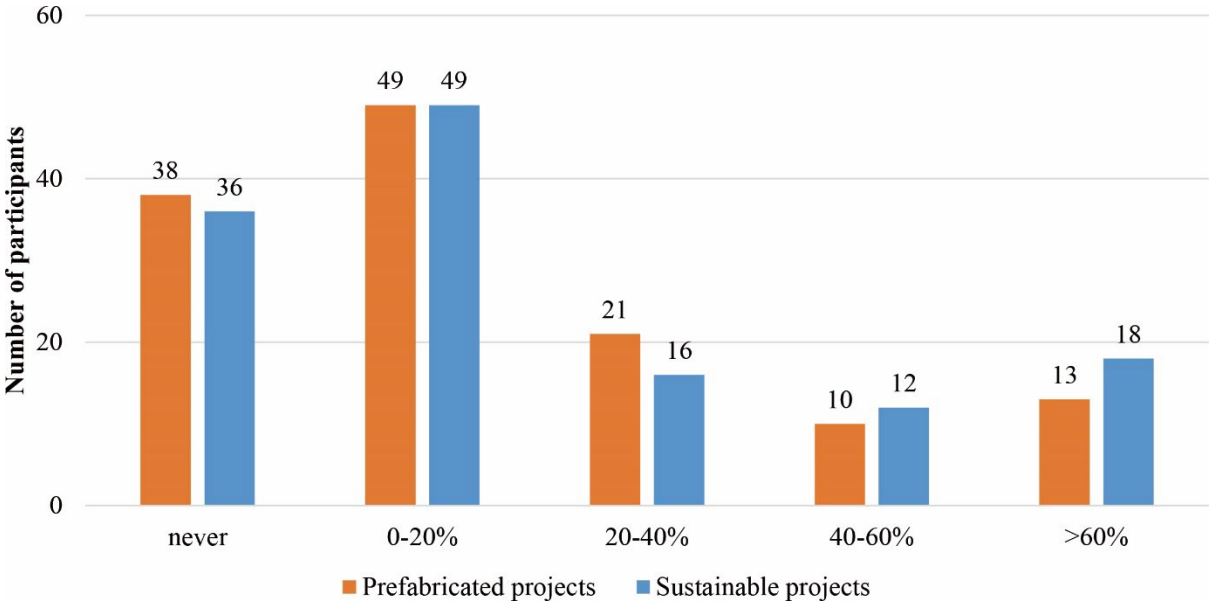

Figure 6-2 Design experience in prefabricated and sustainable projects.

Figure 6-3 shows the participants' tolerance on the trade-offs between sustainability and cost and time. Specifically, 87% of participants accept a less-than-30% increase in project budget when designing sustainable buildings. However, the tolerance on time increase is less featured than that on cost increase. 65% of participants accept to spend less than 12 hours for increasing the sustainability of their design, and 95% of them accept to spend less than 72 hours. More than 90% of participants (118) consider design optimisation a useful method for carbon reduction and 43% (56) think it is very useful in design practice.

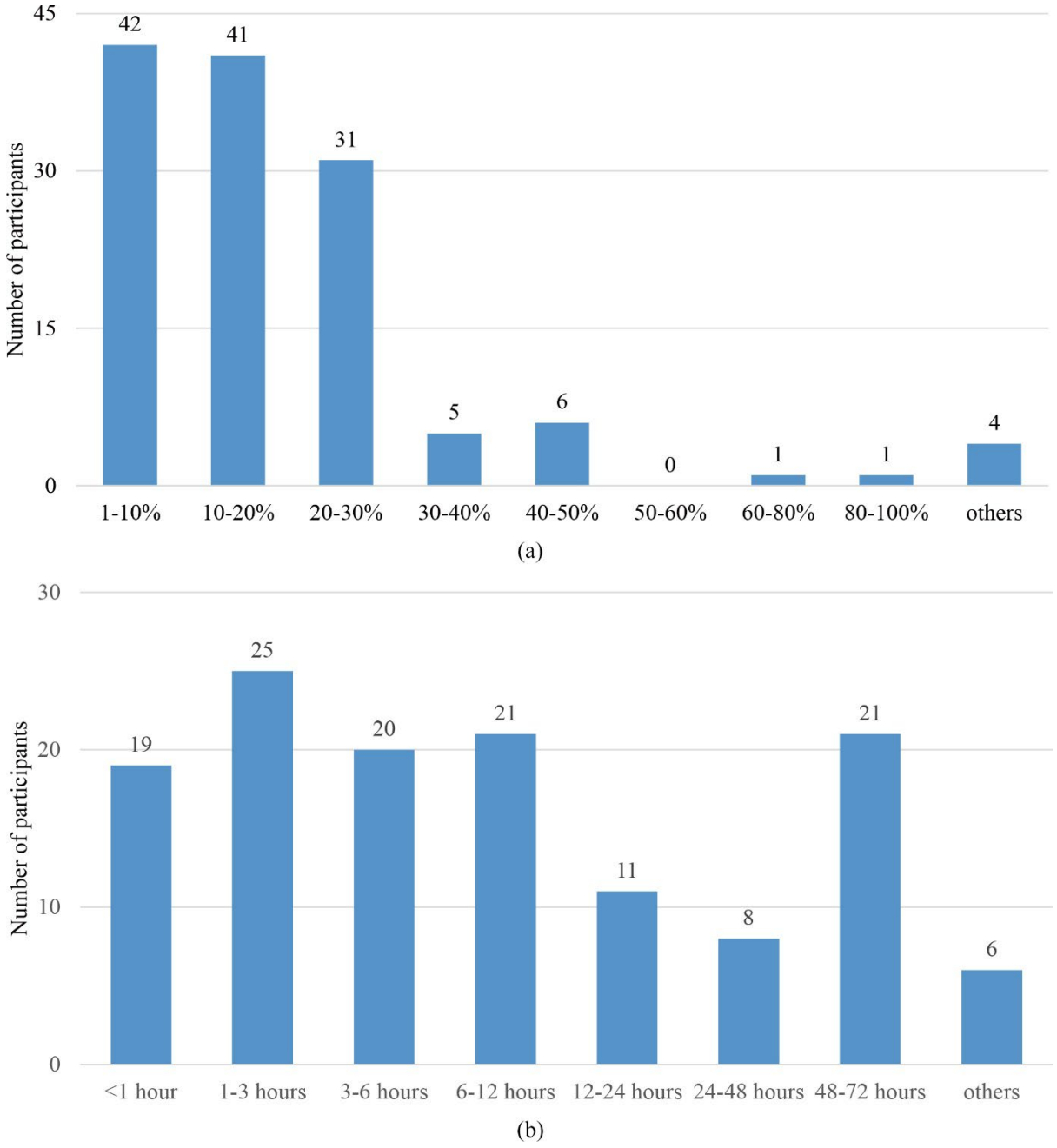

Figure 6-3 The tolerance on time and cost increase.

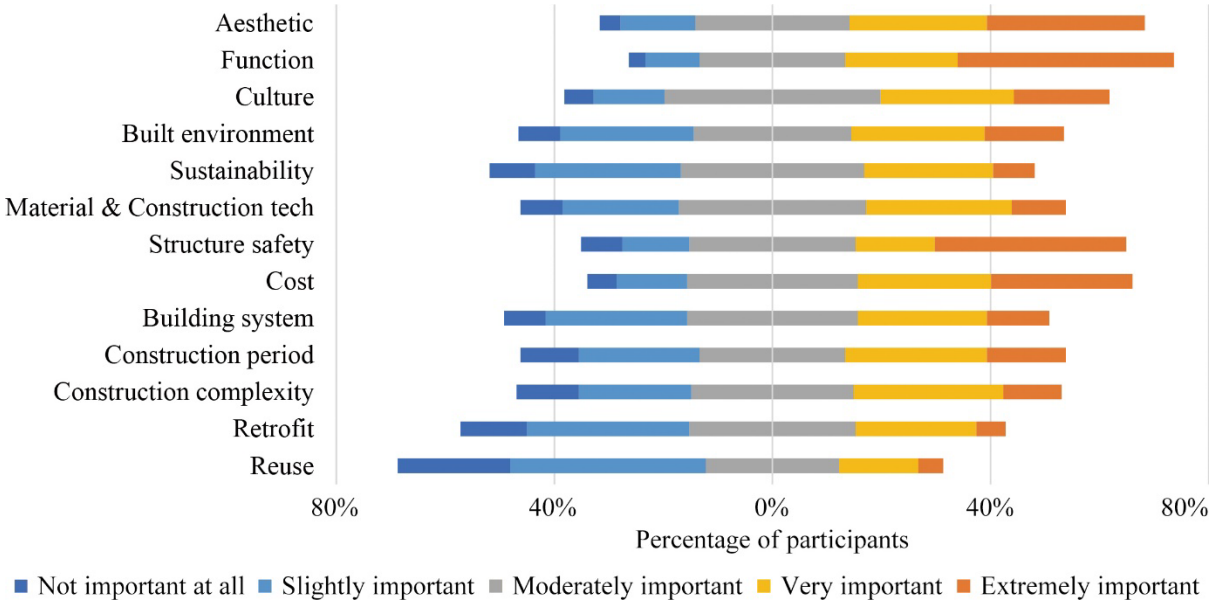

Figure 6-4 Considerations in the design process.

Figure 6-4 displays the various considerations during the design process. Designers primarily focused on aesthetics and visual appeal, functionality and space requirements, environmental and cultural context, structural stability and safety, and cost-effectiveness and budget constraints. Considerations with the least influence on design includes building retrofitting feasibility, building demolition and reuse of building materials, and sustainability and building efficiency.

Regarding the design content, over half of the participants are involved in determining geometric features (54.20%), space division (62.60%), and selecting building materials (63.36%). Approximately 40% participants are responsible for selecting building products (39.69%), construction technology (40.46%), and designing building elements (45.80%). 23.66% of participants were involved in selecting building equipment. 87.79% of respondents report optimising their designs in practice, with 57.25% (75 designers) relying on personal experience and 13.74% (18 designers) using optimisation algorithms. Typically, most designers explore the optimum result among less than 5 design alternatives, while only 21 respondents consider more than 5 design alternatives.

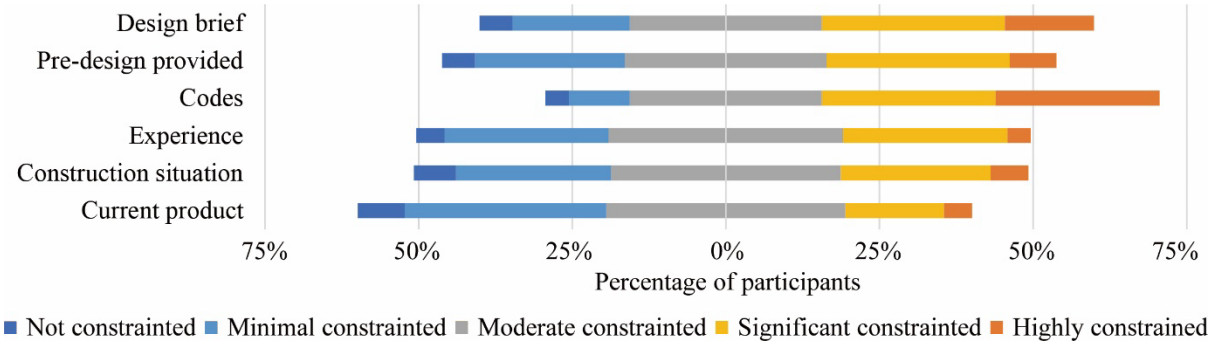

Figure 6-5 Impact of constraints on design practice.

Figure 6-5 shows that codes, regulations, and technical standards significantly constrain design content, as reported by designers. The design brief imposes the second-strict limitation, followed by designs from previous stages, commonly used parameters or values, and construction equipment and conditions. The availability and characteristics of building products have minimal influence on the design decisions of designers.

Figure 6-6 illustrates the EIFs used by designers during the design process. 2D drawing is the predominate format of design files, followed by 3D model and 3D BIM model. Multi-dimensional BIM model and virtual reality or immersive visualisation are the least used data formats. Regarding the design constraints (a detailed description is given in the question 17 to 19 in the Appendix H), most of them are presented in descriptive text, tables, and 2D drawings. Constraints in 3D models and BIM models are seldom encountered in practice. Designers show similar preferences for data formats used in design constraints and references (a detailed description is given in the question 20 and 21 in the Appendix H). In most cases, designers prefer using 3D models and 2D drawings, followed by tables and BIM models. Descriptive text is the least welcomed format for both design constraint and references. Most design output are presented in 2D drawings with BIM model being the least-used data format for design results.

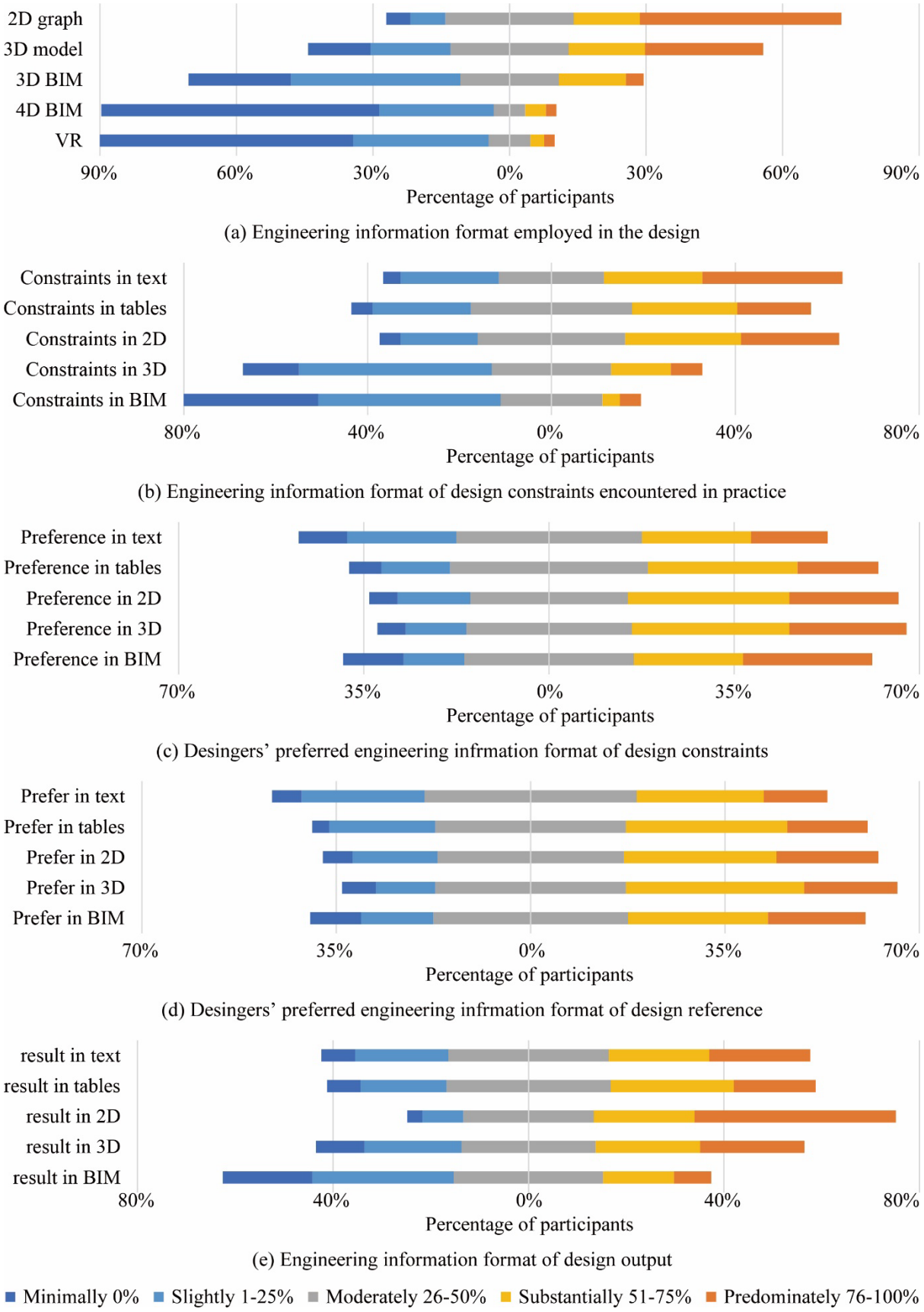

Figure 6-6 Engineering information formats encountered in the design process.

6.2.3.2 Analysis of variance

Figure 6-7 to Figure 6-16 display the results of ANOVA. The horizontal axes of figures categorise participants by their design experience levels while the vertical axes delineate the characteristics of design activities, referenced in Appendix H. Each bar across the different categories represents the proportion of respondents who selected a particular characteristic, measured as a percentage. This visual distribution illustrates how frequently each design activity characteristic is associated with the respective levels of design experience among the participants. Although 33 pairs of variables are estimated in the ANOVA (as listed in Table 6-1), only 7 pairs are valid. Pairs failing the test for variances homogeneity or lacking statistical significance are excluded from this section.

Figure 6-7 illustrates a significant difference in the choices of *Prefabrication percentage_5* compared to the other groups, with an increase in the percentage of *Cost increase_8* and *Cost increase_7* increases and a decrease in that of *Cost increase_1*. This pattern suggests that designers with extensive prefabrication experience (over 60% of their projects are prefabricated) are more tolerant of budget increases for carbon reduction. Similarly, Figure 6-8 indicates that, designers who work on sustainable projects for more than 40% of their time are more tolerant of project cost increases.

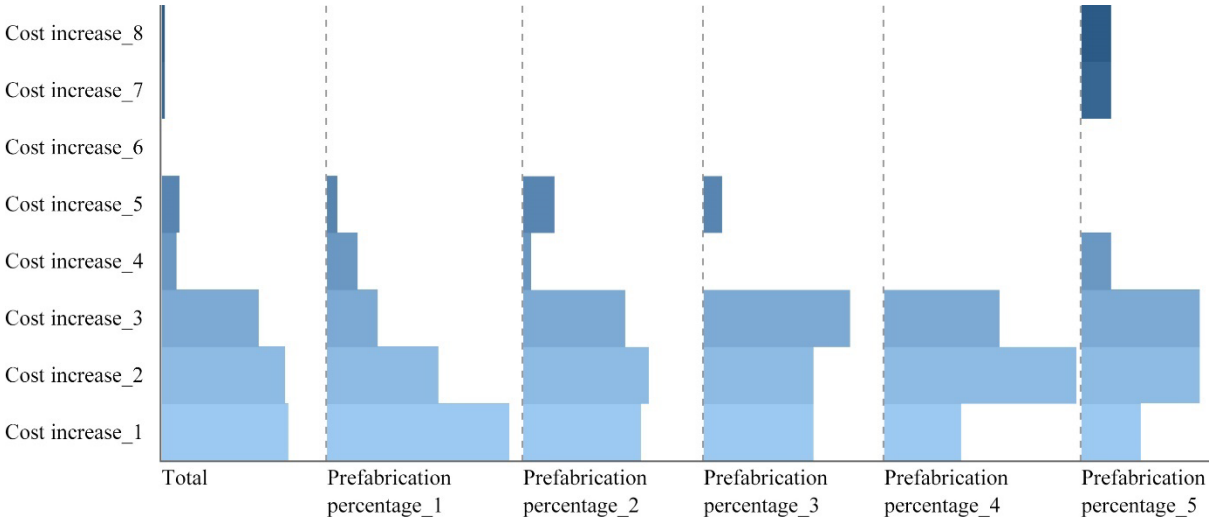

Figure 6-7 The influence of experience in prefabrication design on the tolerance of cost increase.

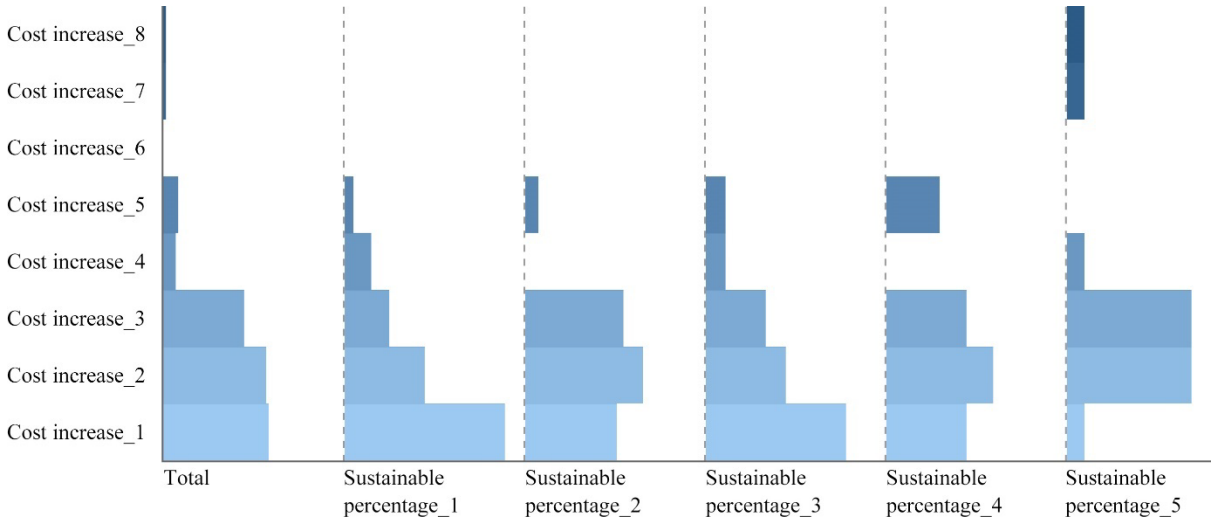

Figure 6-8 The influence of experience in sustainable project design on the tolerance of cost increase.

However, experience in either prefabricated or sustainable projects does not significantly affect tolerance for extending the design period. Despite so, Figure 6-9 reveals that prioritising sustainability during design impacts the tolerance for longer design periods. Specifically, designers who deem sustainability and energy efficiency as very or extremely important are more accepting of extend design periods, averaging 6-24 hours.

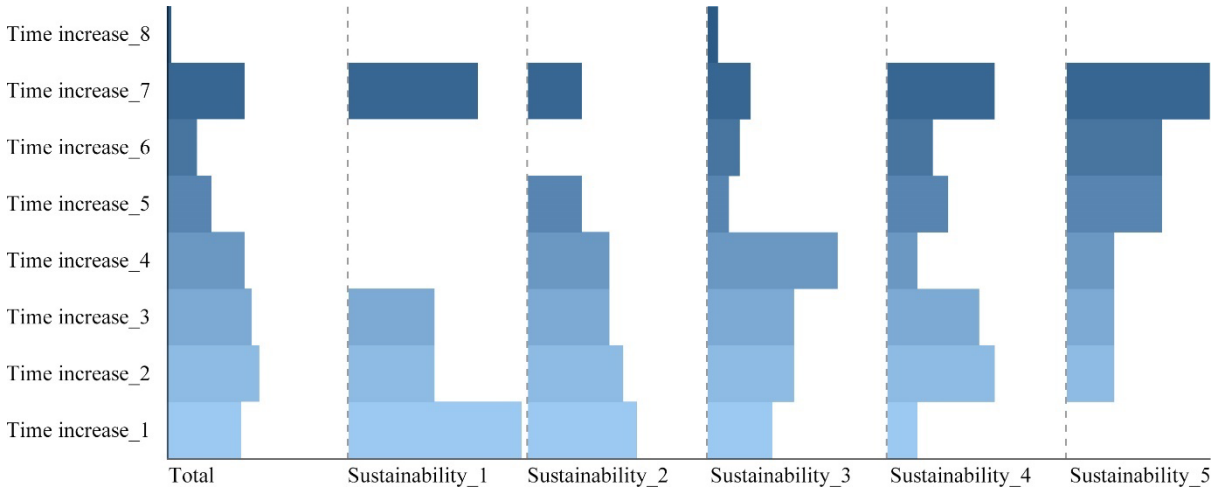

Figure 6-9 The influence of considering sustainability during design on the tolerance of time increase.

Regarding the design information formats, experienced prefabrication designers (*Prefabrication percentage_5*) tend to use 3D BIM models more frequently, as illustrated in Figure 6-10. Similarly, designers experienced in sustainable projects (*Sustainable*

percentage_5) show a greater preference for using 3D models compared to others, as indicated in Figure 6-11. Figure 6-12 to Figure 6-16 show that an emphasis on the sustainability leads to an increased usage of 3D and BIM models, along with a preference for receiving design constraints in 2D, 3D, and BIM format.

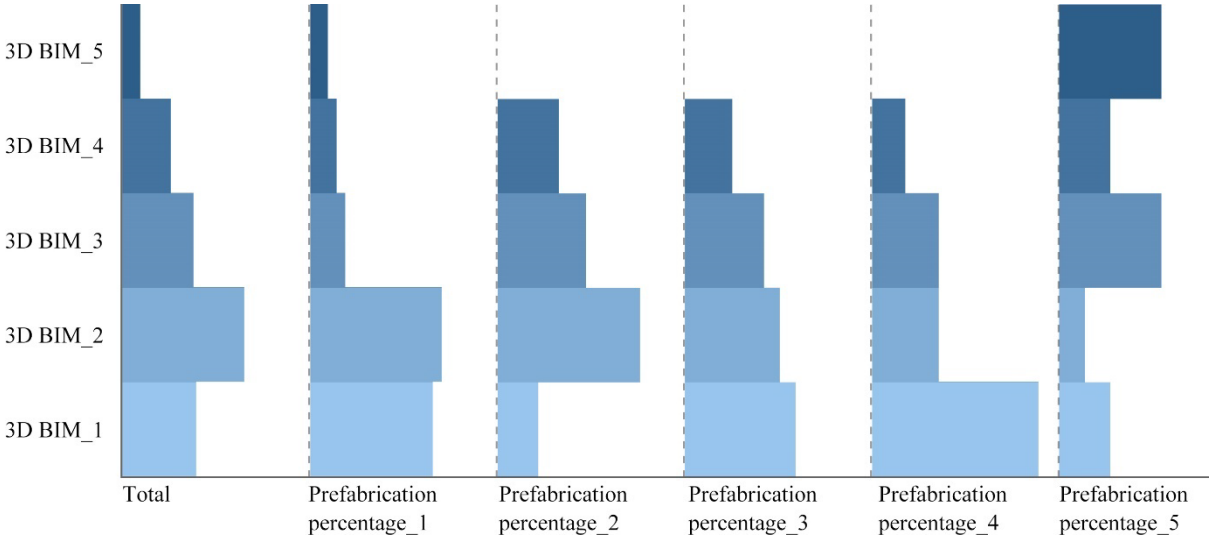

Figure 6-10 The influence of experience in prefabrication design on BIM model usage.

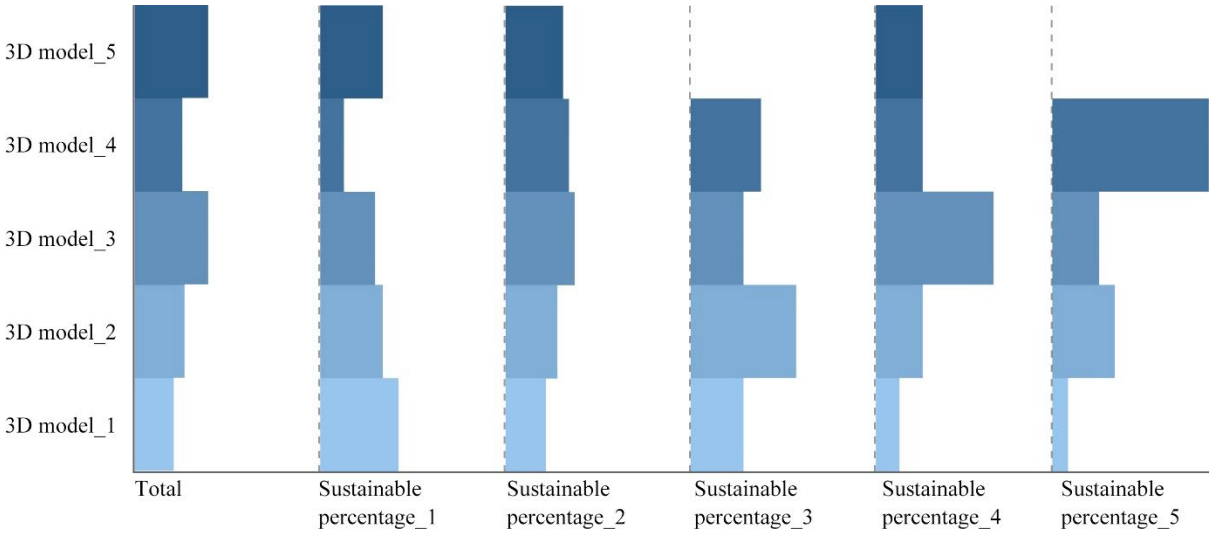

Figure 6-11 The influence of experience in sustainable project design on 3D model usage.

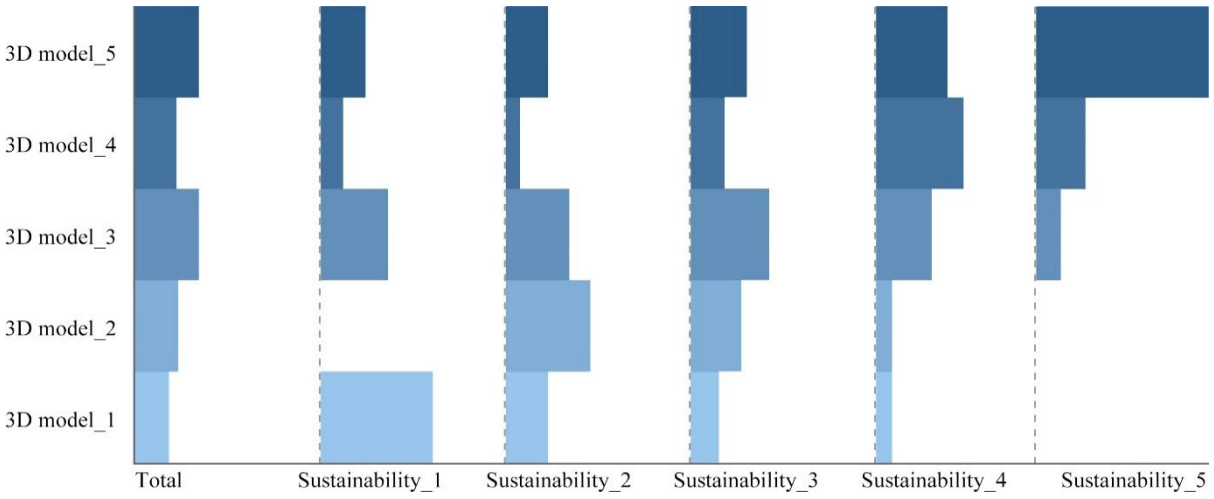

Figure 6-12 The influence of considering sustainability during design on 3D model usage.

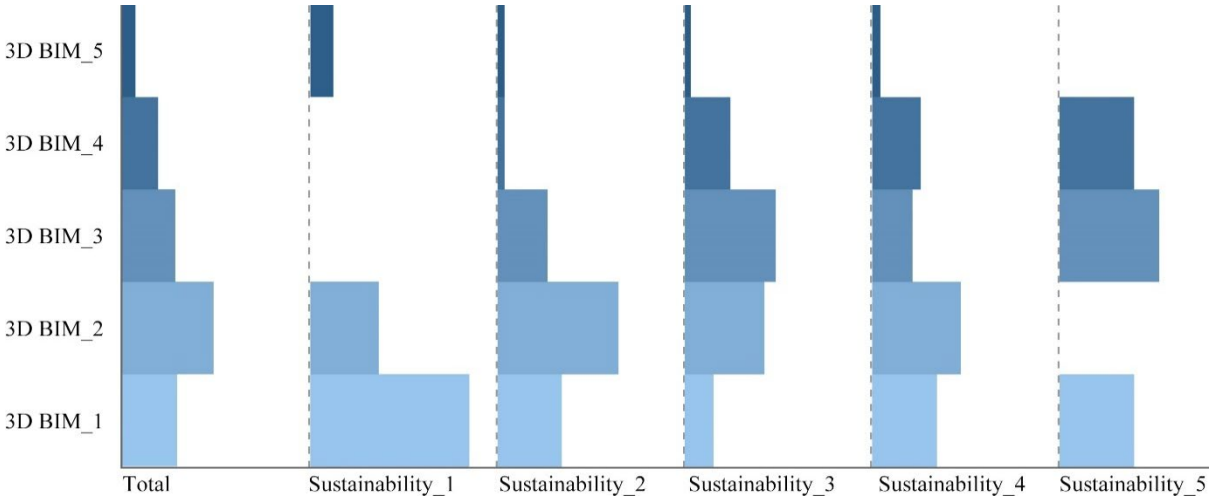

Figure 6-13 The influence of considering sustainability during design on BIM model.

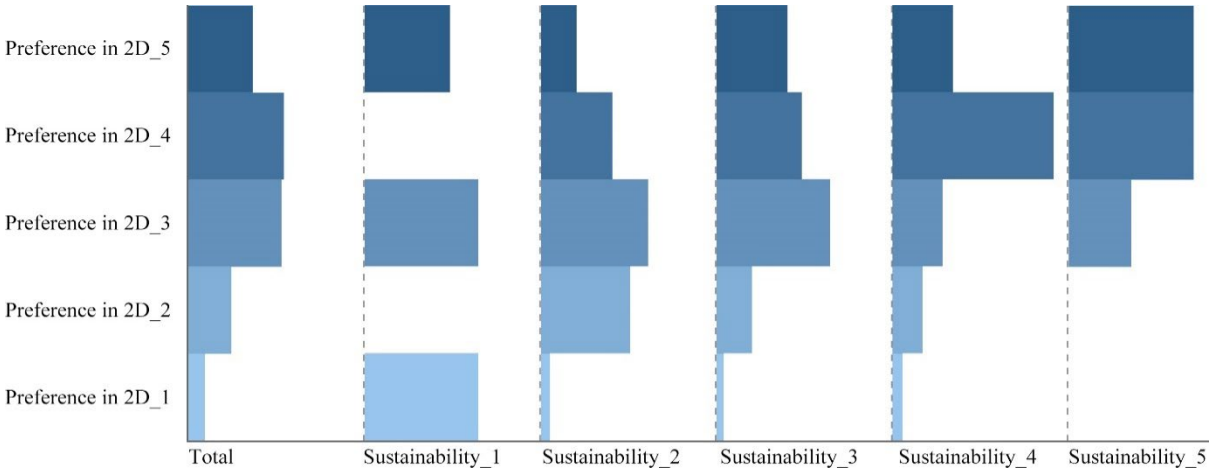

Figure 6-14 The influence of considering sustainability during design on the preferring design constraints in 2D graph.

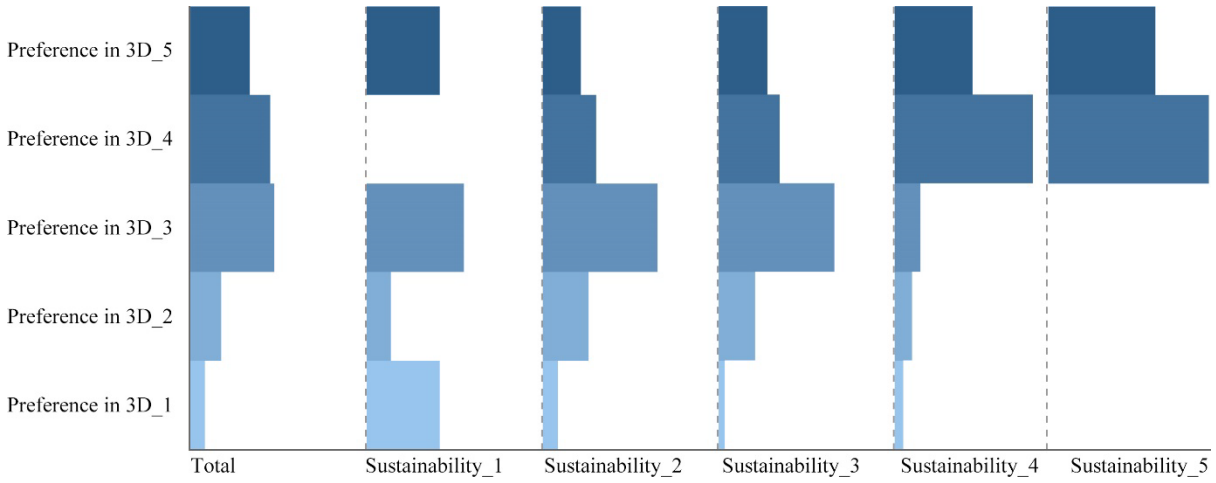

Figure 6-15 The influence of considering sustainability during design on the preferring design constraints in 3D model.

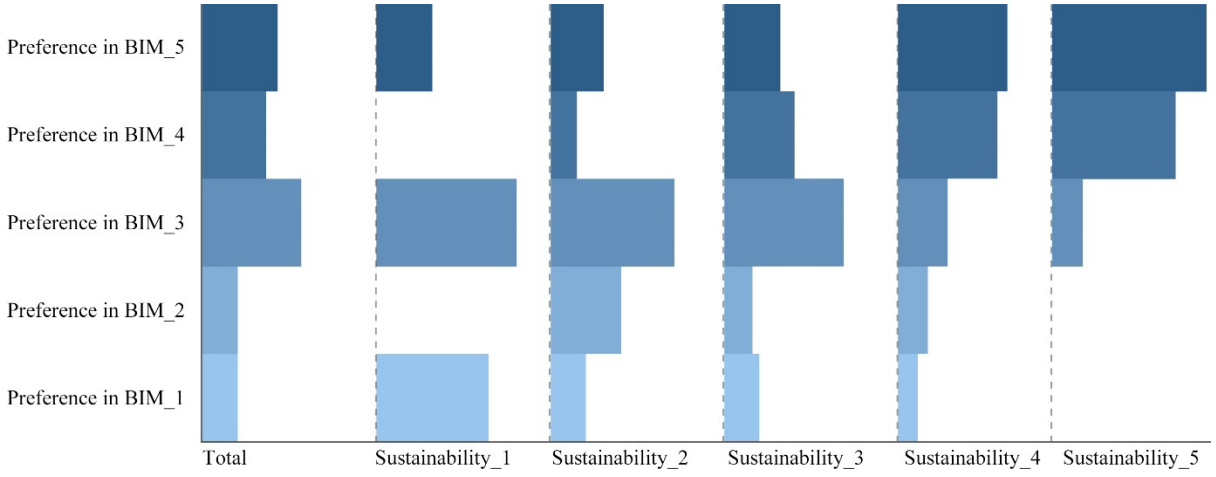

Figure 6-16 The influence of considering sustainability during design on the preferring design constraints in BIM model.

6.2.3.3 Results of relevance analysis

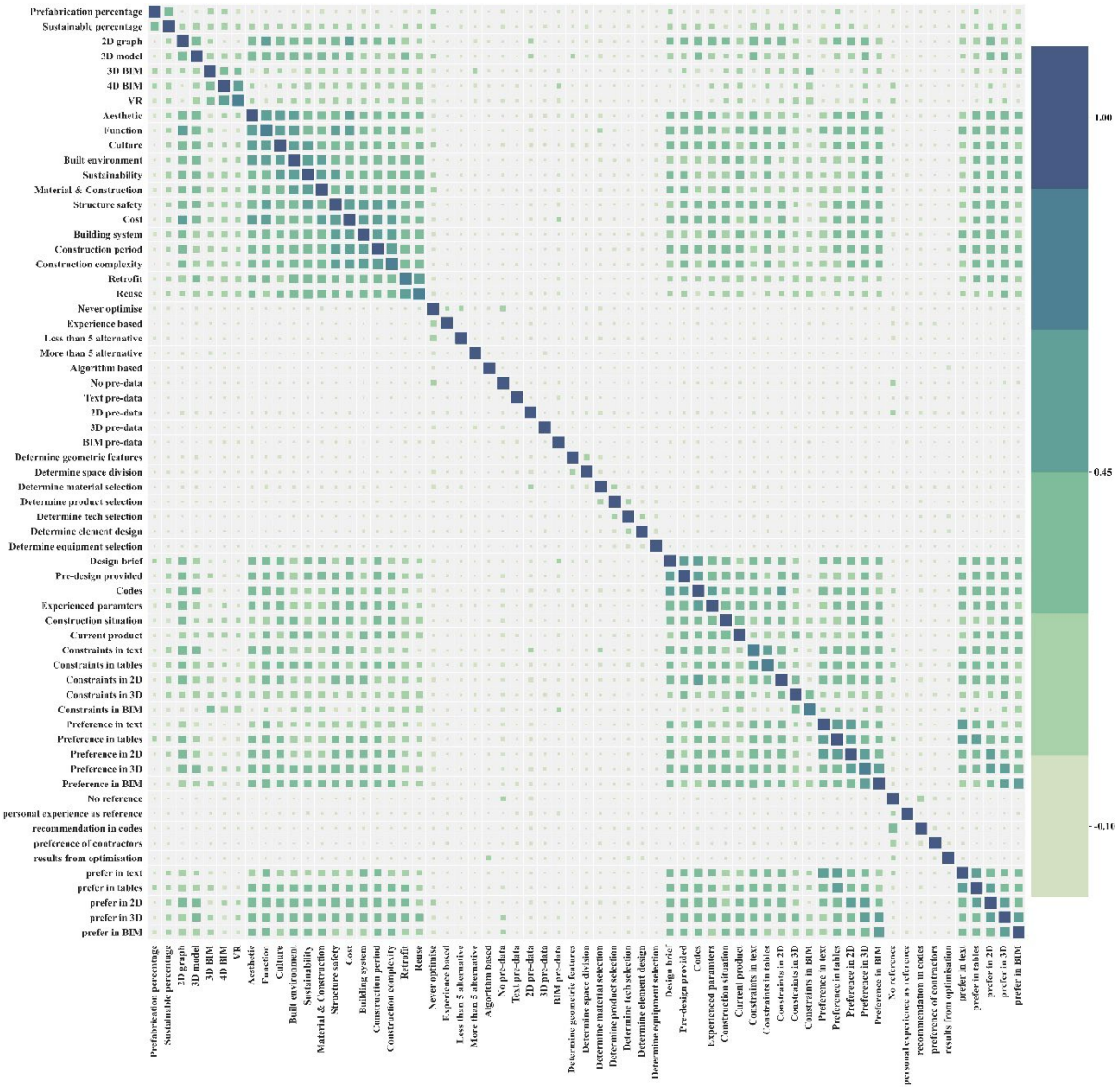

Figure 6-17 The heatmap of relevant factors.

Figure 6-17 is a cropped segment from the full-size heatmap (seen in Appendix I), depicting the contribution of candidate independent variables. Notably, the analysis excludes the relevance between variables within the same category, as it does not indicate the factors' contribution to the EIF. An example of this relevance is that the preferred formats of design reference (from *prefer in text* to *prefer in BIM*) are highly inter-related. Following this relevance analysis, dependant variables and their corresponding candidate independent variables are identified and listed in Table 6-2.

Table 6-2 Candidate independent variables adopted in analysis.

Factors	**Candidate independent variables**	**Contribution to the format of design files**	**Contribution to the preferred format of design constraints**	**Contribution to the preferred format of design reference**
Project experience	Prefabrication percentage Sustainable percentage	√	√	√
Design considerations	Aesthetic Function Culture Built environment Sustainability Material & Construction Structure safety Cost Building system Construction period Construction complexity Retrofit Reuse	√	√	√
Design content	Determine geometric features Determine space division Determine material selection Determine product selection Determine tech selection Determine element design Determine equipment selection Other design	√	√	√
Optimisation method	Never optimise Experience based Less than 5 alternatives More than 5 alternatives Algorithm based Other method	√		√

Formats of design files	2D graph 3D model 3D BIM 4D BIM VR		√	√
Pre-design data	No pre-data Text pre-data 2D pre-data 3D pre-data BIM pre-data Other pre-data	√	√	
Design constraints	Design brief Pre-design provided Codes Experienced parameters Construction situation Current product		√	
Formats of design constraints	Constraints in text Constraints in tables Constraints in 2D Constraints in 3D Constraints in BIM		√	
Design reference	No reference Personal experience as reference Recommendation in codes Preference of contractors Results from optimisation Other reference			√

6.2.3.4 Results of logistic regression

This study employs 5-point Likert scale questions. However, this approach leads to singularity in the Hessian matrix during logistic regression analysis, suggesting the needs to merge some categorical variables. Consequently, responses to the 5-point Likert scale questions are consolidated into fewer categories, as detailed in Table 6-3.

Table 6-3 The adjustment of Likert scale points

Num	Questions	Original Likert scale	Adjusted Likert scale
12	From your experience, what is the level of	1 - Not important at all 2 - Slightly important	2 - Slightly important

	importance placed on the following in your design activities?	3 - Moderately important	3 - Moderately important
		4 - Very important	4 - Very important
		5 - Extremely important	
15	Please score the frequency of using the following types of model/drawing in the design (express in term of percentages of time used)? 2D graph, 3D BIM	1 - 0%	2 - 0-25%
		2 - 1-25%	
		3 - 26-50%	3 - 26-50%
		4 - 51-75%	4 - 51-100%
		5 - 76-100%	
15	Please score the frequency of using the following types of model/drawing in the design (express in term of percentages of time used)? 3D model	1 - 0%	1 - 0%
		2 - 1-25%	2 - 1-25%
		3 - 26-50%	3 - 26-50%
		4 - 51-75%	4 - 51-100%
		5 - 76-100%	
17	To what extent do the following constraints limit your design	1 - 0%	2 - 0-25%
		2 - 1-25%	
		3 - 26-50%	3 - 26-50%
		4 - 51-75%	4 - 51-100%
		5 - 76-100%	
18	Which data formats are typically used to express those design constraints? Please indicate the approximate frequency of using the following data format.	1 - 0%	2 - 0-25%
		2 - 1-25%	
		3 - 26-50%	3 - 26-50%
		4 - 51-75%	4 - 51-100%
		5 - 76-100%	
19	Please indicate the preference for using design constraints in the following data format	1 - Strongly prefer not to	2 - Prefer not to
		2 - Prefer not to	
		3 - Neutral	3 - Neutral
		4 - Prefer to use	4 - Prefer to use
		5 - Strongly prefer to use	
21	Please indicate the preference for using reference in the following forms.	1 - Strongly prefer not to	2 - Prefer not to
		2 - Prefer not to	
		3 - Neutral	3 - Neutral
		4 - Prefer to use	4 - Prefer to use
		5 - Strongly prefer to use	

Table 6-4 presents the parameter estimation of logistic regression models, where parameters that have significant contributions to dependent variables are highlighted. Notably, there are two regression models in analysing the factors contributing to preferring 3D design constraints

due to their similar performance. Taking the regression model for 2D drawings in the design files as an example, the model is interpreted with its corresponding parameters as followers:

Using 2D drawings 51-100% of the time, initiating designs with 2D drawings, adopting over five design alternatives during optimization, and highly valuing functionality, space requirements, cost-effectiveness, and budget constraints were set as reference categories. The results indicate:

- A reduced emphasis on construction cost is associated with a 4.597 to 12.185 times increased likelihood of designers using 2D drawings for only 26-50% of their time.
- Rating the importance of functionality and space requirement as moderate or slight increases the likelihood of using 2D drawings 26-50% of the time by factors of 17.315 and 22.664, respectively.
- Absence of preliminary 2D drawing data and a slight emphasis on construction budget are linked to an increased likelihood (by factors of 23.899 and 23.807, respectively) of designers using 2D drawings for less than 25% of their time.
- Using fewer than five design alternatives during optimization corresponds to a reduced likelihood (0.056 times) of using 2D drawings less than 25% of the time.

To prevent repetition and verbosity in model interpretation, the influences are concisely summarised in Table 6-5 and stated as follows:

- Emphasising functionality, space requirements, cost-effectiveness, and budget constraints, coupled with providing basic data in 2D and optimising design wither fewer than five alternatives, are likely to increase the use of 2D drawings in the design.
- Preferring to express design constraints in 2D format is associated with frequent use of 2D drawings, prioritising functionality and space requirements, strict adherence to the design brief, and omitting determination of construction technology.
- A preference for 2D drawings for design reference data is linked to a focus on functionality, space requirements, and structural stability safety.
- An increased likelihood of using 3D models correlates with a focus on aesthetics and visual appeal, functionality, and space requirement.
- The considerations of structural stability and safety, integration of building systems, and equipment and conditions during construction, and the frequency of using 3D models

during design is positively related to preferring the provision of design constraints in 3D models.

- A preference for 3D design references is more likely when emphasising on functionality, space requirements, and the complexity of project delivery and not involving determining the selection of building product.
- Increased use of BIM model is associated with greater attention to the complexity of project delivery and experience with prefabrication design.
- Valuing aesthetics and visual appeal, structural stability and safety, the integration of building systems, and equipment and conditions in the construction, adherence to the design provided by previous stages, and the frequency of using 3D models is positively related to preferring adopting design constraints in BIM model. Conversely, the frequent use of 2D drawings is negatively associated with preferring design constraints in BIM model.
- Preferring BIM model for design references is likely linked to an emphasis on functionality, space requirements, and the complexity of project delivery and involving determining construction technology.
- A lesser preference for BIM design references is more likely when focusing on structural stability and safety, involving determining building product, and adopting personal experience as design reference.

Table 6-4 Parameter estimation of regression model.

		B	S.E.	Significance	Exp(B)
Reference category is 4 in 2D graph					
2	intercept	-2.585	0.992	0.009	
	[Function = 2]	1.960	1.352	0.147	7.097
	[Function = 3]	2.224	1.140	0.051	9.244
	[Function = 4]	0			
	[Cost = 2]	3.395	1.325	0.010	29.807
	[Cost = 3]	1.520	1.224	0.214	4.572
	[Cost = 4]	0			
	[>5 alternatives = 0]	-2.891	1.034	0.005	0.056
	[>5 alternatives = 1]	0			
	[2D pre-data=0]	3.174	0.954	0.001	23.899
	[2D pre-data=1]	0			
3	intercept	-2.978	1.019	0.003	
	[Function = 2]	3.121	0.997	0.002	22.664
	[Function = 3]	2.852	0.716	0.000	17.315
	[Function = 4]	0			
	[Cost = 2]	2.500	0.947	0.008	12.185

	[Cost = 3]	1.525	0.745	0.041	4.597
	[Cost = 4]	0			
	[>5 alternatives = 0]	-0.246	0.981	0.802	0.782
	[>5 alternatives = 1]	0			
	[2D pre-data=0]	0.873	0.846	0.302	2.393
	[2D pre-data=1]	0			

Reference category is 4 in Preference in 2D

2	intercept	-2.482	0.609	0.000	
	[2D graph=2]	1.347	0.943	0.153	3.845
	[2D graph=3]	1.347	0.796	0.091	3.846
	[2D graph=4]	0			
	[Function=2]	0.535	0.941	0.570	1.707
	[Function=3]	-0.054	0.916	0.953	0.948
	[Function=4]	0			
	[Design brief=2]	1.956	0.735	0.008	7.068
	[Design brief=3]	0.196	0.753	0.795	1.216
	[Design brief=4]	0			
	[Determine tech selection=0]	0.551	0.620	0.374	1.735
	[Determine tech selection=1]	0			
3	intercept	-2.417	0.587	0.000	
	[2D graph=2]	1.931	0.974	0.047	6.893
	[2D graph=3]	2.419	0.813	0.003	11.236
	[2D graph=4]	0			
	[Function=2]	-0.699	1.039	0.501	0.497
	[Function=3]	1.739	0.797	0.029	5.692
	[Function=4]	0			
	[Design brief=2]	1.932	0.812	0.017	6.904
	[Design brief=3]	1.806	0.693	0.009	6.088
	[Design brief=4]	0			
	[Determine tech selection=0]	-1.259	0.613	0.040	0.284
	[Determine tech selection=1]	0			

Reference category is 4 in Prefer in 2D

2	intercept	-2.867	0.584	0.000	
	[Function=2]	3.001	0.963	0.002	20.106
	[Function=3]	2.174	0.872	0.013	8.793
	[Function=4]	0			
	[Structure safety=2]	2.980	0.903	0.001	19.680
	[Structure safety=3]	0.968	0.882	0.273	2.632
	[Structure safety=4]	0			
3	intercept	-1.222	0.306	0.000	
	[Function=2]	0.910	0.996	0.361	2.483
	[Function=3]	1.935	0.695	0.005	6.924
	[Function=4]	0			
	[Structure safety=2]	1.578	0.787	0.045	4.844

	[Structure safety=3]	0.680	0.620	0.273	1.974
	[Structure safety=4]	0			

Reference category is 4 in 3D model

1	intercept	-2.509	0.521	0.000	
	[Aesthetic=2]	3.291	1.399	0.019	26.867
	[Aesthetic=3]	0.860	1.084	0.428	2.363
	[Aesthetic=4]	0			
	[Function=2]	2.059	1.448	0.155	7.837
	[Function=3]	2.224	1.222	0.069	9.240
	[Function=4]	0			
2	intercept	-2.170	0.443	0.000	
	[Aesthetic=2]	2.798	1.388	0.044	16.417
	[Aesthetic=3]	-0.076	1.094	0.944	0.926
	[Aesthetic=4]	0			
	[Function=2]	1.704	1.531	0.266	5.496
	[Function=3]	3.490	1.214	0.004	32.794
	[Function=4]	0			
3	intercept	-1.401	0.322	0.000	
	[Aesthetic=2]	0.138	1.535	0.929	1.148
	[Aesthetic=3]	-0.069	0.952	0.942	0.933
	[Aesthetic=4]	0			
	[Function=2]	3.002	1.455	0.039	20.128
	[Function=3]	3.535	1.129	0.002	34.292
	[Function=4]	0			

Reference category is 1 in Preference in 3D*

2	intercept	-4.558	1.011	0.000	
	[Structure safety=2]	1.782	0.840	0.034	5.941
	[Structure safety=3]	1.137	0.844	0.178	3.118
	[Structure safety=4]	0			
	[3D model=1]	2.201	1.016	0.030	9.035
	[3D model=2]	1.598	0.942	0.090	4.941
	[3D model=3]	1.574	0.872	0.071	4.828
	[3D model=4]	0			
	[Construction situation=2]	3.266	0.927	0.000	26.201
	[Construction situation=3]	0.731	1.117	0.513	2.076
	[Construction situation=4]	0			
3	intercept	-4.175	0.787	0.000	
	[Structure safety=2]	2.186	0.799	0.006	8.904
	[Structure safety=3]	2.390	0.617	0.000	10.910
	[Structure safety=4]	0			
	[3D model=1]	2.257	0.880	0.010	9.559
	[3D model=2]	1.477	0.817	0.071	4.378
	[3D model=3]	1.780	0.660	0.007	5.931
	[3D model=4]	0			

	[Construction situation=2]	1.944	0.773	0.012	6.988
	[Construction situation=3]	1.896	0.708	0.007	6.657
	[Construction situation=4]	0			

Reference category is 4 in Preference in 3D*

2	intercept	-4.710	1.043	0.000	
	[3D model=1]	2.964	1.077	0.006	19.378
	[3D model=2]	1.878	0.920	0.041	6.540
	[3D model=3]	1.991	0.894	0.026	7.322
	[3D model=4]	0			
	[Construction situation=2]	3.609	0.952	0.000	36.943
	[Construction situation=3]	0.570	1.100	0.605	1.767
	[Construction situation=4]	0			
	[Building system=2]	0.755	0.810	0.351	2.128
	[Building system=3]	0.997	0.904	0.270	2.711
	[Building system=4]	0			
3	intercept	-5.988	1.146	0.000	
	[3D model=1]	3.522	1.058	0.001	33.844
	[3D model=2]	2.190	0.826	0.008	8.938
	[3D model=3]	2.769	0.741	0.000	15.944
	[3D model=4]	0			
	[Construction situation=2]	2.175	0.847	0.010	8.801
	[Construction situation=3]	1.823	0.741	0.014	6.192
	[Construction situation=4]	0			
	[Building system=2]	2.639	0.922	0.004	13.995
	[Building system=3]	3.761	0.940	0.000	42.993
	[Building system=4]	0			

Reference category is 4 in Prefer in 3D

2	intercept	-2.929	0.803	0.000	
	[Function=2]	3.544	0.998	0.000	34.591
	[Function=3]	1.632	0.766	0.033	5.114
	[Function=4]	0			
	[Construction complexity=2]	3.069	0.948	0.001	21.526
	[Construction complexity=3]	1.520	0.967	0.116	4.571
	[Construction complexity=4]	0			
	[Determine product selection=0]	-1.228	0.700	0.080	0.293

	[Determine product selection=1]	0			
3	intercept	-1.162	0.420	0.006	
	[Function=2]	2.190	0.925	0.018	8.938
	[Function=3]	1.762	0.583	0.003	5.826
	[Function=4]	0			
	[Construction complexity=2]	2.013	0.633	0.001	7.485
	[Construction complexity=3]	1.197	0.589	0.042	3.311
	[Construction complexity=4]	0			
	[Determine product selection=0]	-1.380	0.528	0.009	0.252
	[Determine product selection=1]	0			

Reference category is 4 in 3D BIM

2	intercept	-1.660	0.562	0.003	
	[Construction complexity=2]	1.865	0.600	0.002	6.454
	[Construction complexity=3]	0.307	0.681	0.652	1.359
	[Construction complexity=4]	0			
	[Prefabrication percentage=1]	1.423	0.623	0.022	4.148
	[Prefabrication percentage=2]	-0.445	0.638	0.485	0.641
	[Prefabrication percentage=3]	0			
3	intercept	-1.377	0.480	0.004	
	[Construction complexity=2]	1.229	0.532	0.021	3.417
	[Construction complexity=3]	1.008	0.497	0.042	2.739
	[Construction complexity=4]	0			
	[Prefabrication percentage=1]	1.340	0.578	0.020	3.821
	[Prefabrication percentage=2]	0.663	0.487	0.173	1.940
	[Prefabrication percentage=3]	0			

Reference category is 4 in Preference in BIM

2	intercept	-4.357	1.188	0.000	
	[Aesthetic=2]	2.892	1.382	0.036	18.020
	[Aesthetic=3]	-0.692	1.033	0.503	0.500
	[Aesthetic=4]	0			

	[Structure safety=2]	-0.532	1.253	0.671	0.588
	[Structure safety=3]	1.441	1.097	0.189	4.227
	[Structure safety=4]	0			
	[Building system=2]	1.499	1.113	0.178	4.478
	[Building system=3]	1.915	0.998	0.055	6.784
	[Building system=4]	0			
	[2D graph=2]	0.593	1.454	0.683	1.810
	[2D graph=3]	-1.517	1.216	0.212	0.219
	[2D graph=4]	0			
	[3D model=1]	-1.107	1.515	0.465	0.331
	[3D model=2]	1.466	1.284	0.254	4.331
	[3D model=3]	2.431	1.256	0.053	11.373
	[3D model=4]	0			
	[Pre-design provided=2]	0.332	0.951	0.727	1.394
	[Pre-design provided=3]	-0.485	0.921	0.599	0.616
	[Pre-design provided=4]	0			
	[Construction situation=2]	3.613	1.116	0.001	37.065
	[Construction situation=3]	1.484	1.017	0.144	4.410
	[Construction situation=4]	0			
3	intercept	-8.700	1.874	0.000	
	[Aesthetic=2]	-0.721	1.478	0.626	0.486
	[Aesthetic=3]	-1.791	1.084	0.099	0.167
	[Aesthetic=4]	0			
	[Structure safety=2]	-1.091	1.142	0.339	0.336
	[Structure safety=3]	2.545	0.959	0.008	12.740
	[Structure safety=4]	0			
	[Building system=2]	4.959	1.369	0.000	142.520
	[Building system=3]	4.428	1.345	0.001	83.725
	[Building system=4]	0			
	[2D graph=2]	-1.813	1.557	0.244	0.163
	[2D graph=3]	-3.737	1.321	0.005	0.024
	[2D graph=4]	0			
	[3D model=1]	2.822	1.573	0.073	16.813
	[3D model=2]	3.480	1.328	0.009	32.454
	[3D model=3]	5.391	1.563	0.001	219.322
	[3D model=4]	0			
	[Pre-design provided=2]	3.103	1.080	0.004	22.274
	[Pre-design provided=3]	2.346	0.996	0.019	10.440
	[Pre-design provided=4]	0			
	[Construction situation=2]	2.952	1.094	0.007	19.136

	[Construction situation=3]	2.886	1.002	0.004	17.914
	[Construction situation=4]	0			

Reference category is 4 in Prefer in BIM

2	intercept	-1.386	0.626	0.027	
	[Function=2]	3.651	1.066	0.001	38.524
	[Function=3]	3.998	1.080	0.000	54.515
	[Function=4]	0			
	[Structure safety=2]	-1.039	1.163	0.372	0.354
	[Structure safety=3]	-1.134	1.063	0.286	0.322
	[Structure safety=4]	0			
	[Construction complexity=2]	1.873	1.059	0.077	6.510
	[Construction complexity=3]	-0.246	0.899	0.784	0.782
	[Construction complexity=4]	0			
	[Determine product selection=0]	-2.496	0.807	0.002	0.082
	[Determine product selection=1]	0			
	[Determine tech selection=0]	2.397	0.754	0.001	10.994
	[Determine tech selection=1]	0			
	[personal experience as reference=0]	-1.322	0.654	0.043	0.266
	[personal experience as reference=1]	0			
3	intercept	-2.410	0.696	0.001	
	[Function=2]	2.011	0.994	0.043	7.474
	[Function=3]	2.696	0.836	0.001	14.815
	[Function=4]	0			
	[Structure safety=2]	-2.698	1.069	0.012	0.067
	[Structure safety=3]	-0.737	0.767	0.336	0.479
	[Structure safety=4]	0			
	[Construction complexity=2]	3.520	0.927	0.000	33.772
	[Construction complexity=3]	1.251	0.687	0.068	3.495
	[Construction complexity=4]	0			
	[Determine product selection=0]	-1.051	0.619	0.090	0.349
	[Determine product selection=1]	0			
	[Determine tech selection=0]	1.561	0.605	0.010	4.764

[Determine tech selection=1]	0			
[personal experience as reference=0]	0.648	0.590	0.272	1.912
[personal experience as reference=1]	0			

Table 6-5 Qualitative relationships between dependant and independent variables.

Dependant variable	**Independent variable**	
	Positively related	**Negatively related**
2D graph	Function Cost 2D pre-data	> 5 alternatives
Preference in 2D	2D graph Function Design brief	Determine tech selection
Prefer in 2D	Function Structure safety	
3D model	Aesthetic Function	
Preference in 3D	3D model Structure safety Building system Construction situation	
Prefer in 3D	Function Construction complexity	Determine product selection
BIM model	Prefabrication percentage Construction complexity	
Preference in BIM	Aesthetic Structure safety Building system 3D model Pre-design provided Construction situation	2D graph
Prefer in BIM	Function Construction complexity Determine tech selection	Structure safety Determine product selection Personal experience as reference

6.2.3.5 Results of multiple-correspondence analysis

The results of MCA visualise the relationships between the independent and dependent variables within each regression model. As depicted in Figure 6-18 to Figure 6-20, the MCA plots display data matrixes, where categories of categorical variables are represented in a two-dimensional space. The proximity between categories indicates their similarity across the analysed variables. Categories in close proximity suggest a strong association, whereas those further apart indicate dissociated.

Taking Figure 6-18-a as an example, the cluster of points representing *Cost_4*, *Function_4*, and *2D graph_4* suggests that designers who employ 2D drawings for more than half of the time in design are likely to place significantly emphasis on functionality, space requirements, cost-effectiveness, and budget constraints. Conversely, designers who exhibit less concern for these aspects (*Cost_3*, *Function_3*, *Cost_2*, *Function_2*) are less likely to frequently use 2D drawings (as shown by *2D graph_3*, *2D graph_2*). Overall, the interpretations of Figure 6-18 to Figure 6-20 align with the qualitative relationships discussed in section 6.2.3.4, hence detailed interpretations are not reiterated here.

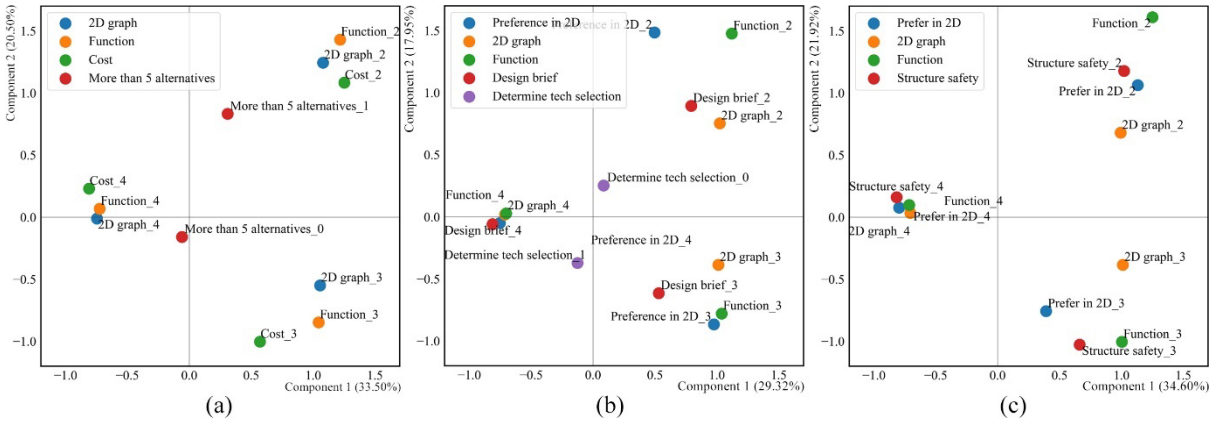

Figure 6-18 Multi-correspondence analysis on 2D drawings used in design files (a), constraints (b), and reference (c).

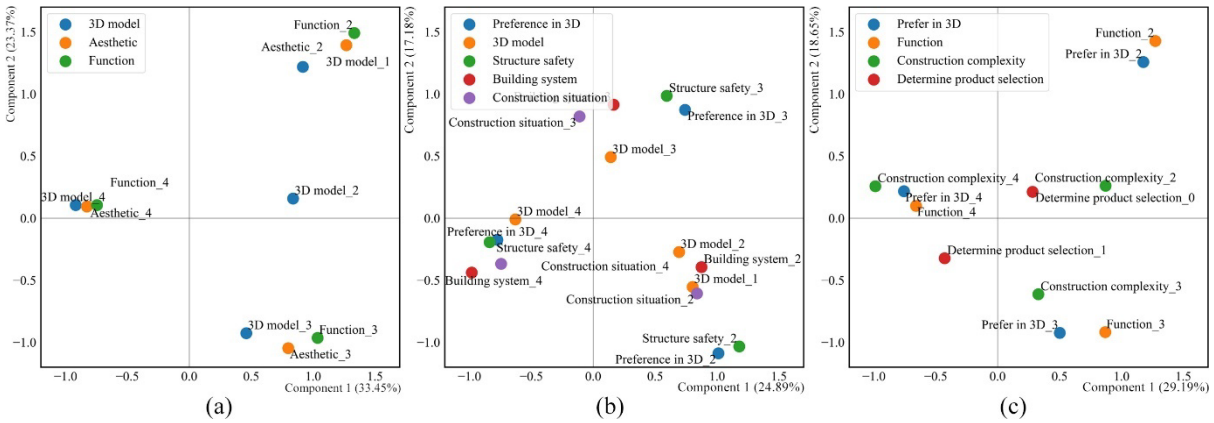

Figure 6-19 Multi-correspondence analysis on 3D models used in design files (a), constraints (b), and reference (c).

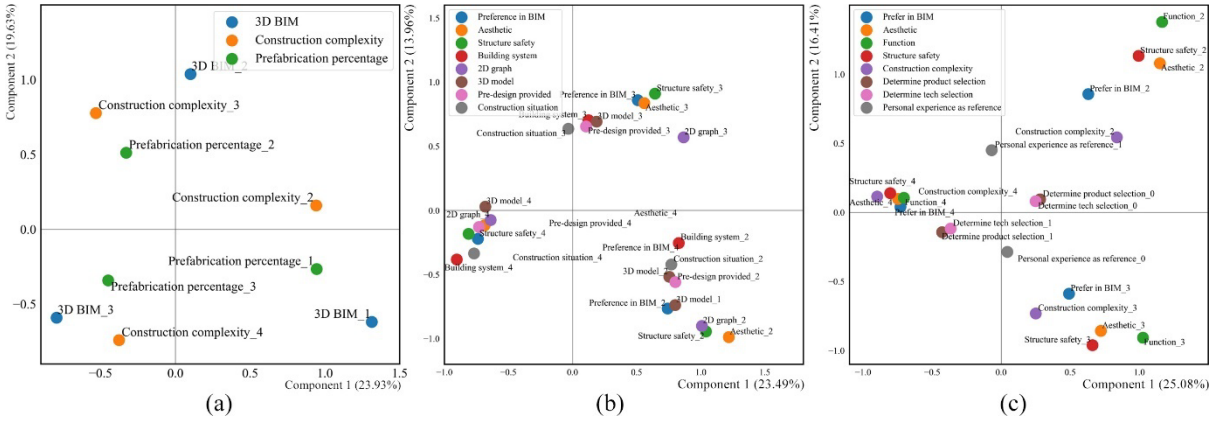

Figure 6-20 Multi-correspondence analysis on BIM models used in design files (a), constraints (b), and reference (c).

6.2.4 Analysis of the findings

6.2.4.1 Analysis of descriptive results and ANOVA

In this research, architects and civil engineers comprised approximately 70% of the respondents. Around 17% of the participants held national qualifications. These demographic distributions align with the typical composition of designers in many design firms. Despite the inevitable sampling bias, the demographic distribution suggests a representative sampling. The composition of respondents also impacts the statistics regarding design considerations, as illustrated in Figure 6-4. Specifically, the aesthetics and visual appeal, functionality and space requirements, environment and cultural context, and cost-effectiveness and budget reflect the main considerations of architects. The emphasis on structural stability and safety and cost are commonly emphasised within the design of structure engineers. Consequently, these factors are more prominent than the others.

Generally, participants exhibit a positive attitude towards employing design optimisation in practice, laying a foundation for applying the proposed carbon reduction method. Additionally, designers are willing to invest additional time in design for enhanced sustainability, accepting a design period extension of 12-72 hours. However, designers' tolerance for cost increases is limited, suggesting that suitable solutions should not compromise economic performance for carbon reduction. Tolerance of project cost increases and design period extensions grows with experience in prefabricated and sustainable project design.

Despite years of promotion, design via BIM model remains relatively unpopular across designers (Herr & Fischer, 2019; Ma et al., 2022). Figure 6-6-a shows that 58.78% of the designers use BIM models less than 25% of the time, while only 18.32% use it for over 50% of their time. The lag in BIM model becomes more obvious when considering multidimensional models (involving time, budget, etc., as new dimensions). A significant 86.26% of participants rarely use such information format in their practice. 2D drawings continue to be the most prevalent data format in the design process. Notably, 58.78% of respondents report using this data format for over half of their working hours. This trend aligns with findings of Sweany et al. (2016) and Alruwaythi et al. (2019), suggesting a slower-than-expected technological evolution, particularly in comparison to the early adoption of 2D CAD (Y. Liu et al., 2017).

The usage rate of 2D, 3D, and BIM formats in design outputs aligns with those in the design process, as shown in Figure 6-6-e and Figure 6-6-a. The consistent use of these formats throughout the design process reflects that design information is usually conveyed in its original format, suggesting that designers seldom integrate information into BIM models. Since designers often base their work on outcomes from previous stages (Tribelsky & Sacks, 2010), the usage rates of the above three data formats in design constraints (usually the start point of design, Figure 6-6-b) are similar to those in design outputs (Figure 6-6-e). Furthermore, Figure 6-5 points out that codes and design brief are also the main sources of design constraints. These files typically contain text, tables, photos, and 2D graphs, making text and tables as commonly used as 2D data in design constraints.

Figure 6-6-c and Figure 6-6-d reveal that 3D data is the most preferred data format for data extraction, followed by 2D graphs and tabular values. Previous studies (Dadi, Goodrum, Taylor, & Carswell, 2014; Dadi, Goodrum, Taylor, & Maloney, 2014; Dadi, Taylor, et al., 2014; Shi, Du, Asce, et al., 2020) corroborate these findings, attributing the preference to 3D's superiority over 2D in information retrieval. However, despite the perceived usefulness of BIM model in previous studies (Chinese Building Industry BIM Application Analysis Report Editorial Committee, 2022), it is less favoured than traditional formats like tables, 2D, and 3D data in both design constraints and references. The reluctance to handle BIM models may stem from their complexity than from performance of different data formats. Processing BIM model typically demands higher-performance hardware and more time (Cai & Zhou, 2023). Additionally, extracting necessary data from these highly integrated information models

requires more effort (Jiao Chen et al., 2021). Since data extracted from BIM models is often presented in traditional formats (2D, 3D, or tables), designers tend to opt for more efficient alternatives, i.e., conventional data formats.

Although ANOVA indicates that design experience and an emphasis on sustainability influence the choice of EIF, it does not sufficiently identify the best data format for sustainable design optimisation. For instance, 2D, 3D, and BIM formats all appear to be viable options for sustainable project design. Therefore, regression analysis, which quantifies the contribution of multiple variables, is necessary.

6.2.4.2 Analysis of relevance and logistic regression

The relevance analysis (Figure 6-17 and Table 6-2) indicates that factors of experience in project design, design considerations, design contents, design optimisation methods, and files encountered during the design significantly influence the choice of EIFs. This finding partially aligns with Dadi, Goodrum, Taylor, & Carswell (2014), who noted that the experience of using 2D CAD data affects the efficiency of processing 2D data. However, this research does not observe the influence of working period as claimed by the authors. Additionally, variables related to design considerations and contents are more influential than other demographic characteristics (e.g., design responsibility, involved design phases, and characteristics of employers) in constructing logistic regression models. This predominance in relevance analysis stems from the fact that designers typically engage in multiple design tasks and design phases. Hence, design considerations and contents are more apt descriptors of their design activities.

Regarding the EIFs (Table 6-4 and Table 6-5), 2D and 3D data are commonly used in traditional architecture design tasks. Specifically, 2D data is particular prevalent in the developed design phase, when functionality and space requirement are key considerations. The positive influence of aesthetics and functionality implies that 3D format is likely adopted in both the conceptual (determine the geometrical features of projects) and developed design stage (coordinate architecture and engineering information spatially) (RIBA, 2020). In these stages, 3D model enables designers to quickly visualise their concepts (Charef et al., 2018), allowing customers and professionals to accurately assess project performance and development (Antwi-Afari et al., 2018). Compared to architects, designers specialising in structural, engineering, and construction management demonstrate a stronger preference for acquiring basic design information from earlier stages in 3D models rather than 2D drawings. Their work heavily

relies on the provided fundamental designs, encompassing multi-dimensional spatial information, making the ease of accessing complex data in 3D models highly appealing (Dadi, Goodrum, Taylor, & Maloney, 2014). For the same reason, designers prioritise functionality, space requirement, and project delivery complexity tend to prefer receiving design references in the 3D models.

As shown in Table 6-5, the employment of BIM model correlates with experience in designing prefabricated projects and a focus on project delivery complexity. However, characteristics of conventional architecture design (e.g., emphasis on functionality), structure design (e.g., emphasis on structure stability), and engineering design (e.g., emphasis on building systems integration) show little influence on BIM model selection. This pattern suggests no evidence of BIM model being more prevalent in any particular conventional design task than the others. Considering the frequency of participants reporting BIM model usage in design practice (Figure 3), it appears BIM model is seldom adopted across these three design tasks. Y. Liu et al. (2017) explained this pattern by noting that the benefits of BIM are hard to realise in conventional design tasks, where conventional design tools suffice, and the complexity of BIM modelling is a disadvantage. In contrast, designing for prefabricated constructions demands detailed design of prefabricated elements to meet manufacture and assembly requirements (S. Gao et al., 2019). The creation and transfer of these details often exceed the capabilities of conventional formats like 2D drawings and 3D models, necessitating the use of BIM model (Yuan et al., 2018). Consequently, the increase concerns on prefabrication and project delivery lead to an increased adoption of BIM model.

The factors influencing the preference for receiving design constraints in BIM model are similar to those for 3D model; designers working with complex information from earlier stages tend to favour BIM model for data retrieval. BIM model's capability to store both geometric and non-geometric information enables later-stage designers to access accurate and consistent design information (Tan et al., 2021). Concerning negatively correlated factors, designers who rely on personal experience demonstrate less preference for BIM model as design references, indicating a reluctance among experienced designers to this modern tool. This finding aligns with Ahmed's (2018) observation that habitual resistance is a key barrier to BIM implementation. Evidence also suggests that designers involved in selecting building products and structural design are less inclined to use BIM model for design references. The

unavailability of product BIM models (Yuan et al., 2018) may lead these designers to prefer conventional formats (e.g., 2D graphs), reinforcing their resistance to adopting BIM model.

The observed relationships between design activities and EIF indicate that conventional data formats (i.e., 2D and 3D) are sufficient for design information processing in conventional design tasks. Conversely, BIM model is more likely to be adopted in design tasks that require the integration of multi-disciplinary information. Therefore, a promising application for BIM model lies in the technical design stage of prefabricated projects, where the building structure is detailed into the design of prefabricated elements (RIBA, 2020).

The technical design stage may also serve as a start point of introducing BIM model in the design process. Compared to the concept and developed design stages, designers have access to finalised design information in the technical design, enhancing the accuracy and consistency of BIM modelling. Additionally, project delivery conditions and multidisciplinary coordination (e.g., collision test), which exceed the capabilities of conventional data formats, are more likely to be addressed in this stage, emphasising the needs of BIM model. Therefore, in a proposed BIM application, design tasks in the concept and developed design stage are processed using current data format. Subsequently, these design contents are transformed and integrated into BIM model during the technical stage and maintained in this format until delivery.

Consistency between the EIFs used in design and the preferred data formats for design constraints is observed in Table 6-4 and Table 6-5. Specifically, frequent use of 2D and 3D formats is associated with a preference for receiving design constraints in these respective formats. Considering that BIM models are visualised in three dimensions, the positive correlation with using 3D model and the negative correlation with using 2D drawings for preferring BIM in design constraints strengthen the above finding. In summary, acceptance of a specific data format increases with growing usage experience.

6.2.4.3 Analysis of multiple-correspondence analysis

MCA (Figure 6-18 to Figure 6-20) visualise the extent to which the design activities explain the selection or preference of data formats. A greater aggregation of points indicates a stronger explanatory power of variables. Generally, the points in Figure 6-18-a and Figure 6-19-a show more aggregation than those in Figure 6-20-a. This suggests that the use of 2D and 3D data is more driven by design task requirements compared to the use of BIM model. The primary

motivations for adopting BIM model likely stem from external sides such as policy, codes, and economic incentives rather than practical design improvement.

As depicted in Figure 6-18 to Figure 6-20, variables are more clustered in extreme categories like grade 4, while more dispersed in the others (e.g., grade 2 and 3). This pattern is also evident in the parameter estimations of regression models (Table 6-4). Selecting non-reference categories (e.g., grade 2 or 3) of the independent variables significantly influences the predicted category of dependent variables. However, variations in choices among these non-reference categories (such as the distinction between choosing Grade 2 and Grade 3) appear to have a less pronounced effect. Although the predictive performance of these regression models is limited, they effectively demonstrate the qualitative influence of independent variables, supporting the above analysis.

6.3 Data processing for optimisation model

6.3.1 Pipeline of the optimisation model

Given the EIFs employed in practice (as stated in sections 6.2.3 and 6.2.4), the pipeline of the proposed design optimisation method is depicted in Figure 6-21. Initially, the original design is input in either 2D drawings or 3D models. Rhinoceros 3D and grasshopper are then used to process these design files and extract the original design parameters. Subsequently, the design parameters are saved in Microsoft excel files, with the suffix of .xlsx. After that, the optimisation programme is executed in Python. The feasible solution identified by GA is depicted by a set of design parameters, which are then processed by Rhinoceros 3D and grasshopper to generate a digital 3D model for results visualisation. Utilising Rhino-inside-Revit, a plugin-tools for Autodesk Revit, these 3D models can be converted into BIM models within the Revit environment. Both 3D and BIM models serve to provide design assistance to designers at the developed design stage.

Importantly, the optimisation process does not occur within a single design software environment, such as Rhinoceros 3D and grasshopper, because optimisation plugins (e.g., octopus) lack the capability to explore feasible results defined by parameters mentioned in sections 4 and 5. In essence, the embedded optimisation tools in design software lack the computational power to handle numerous parameters. Therefore, the micro-level design optimisation is segmented into three steps, as mentioned above: 1) extracting design data using

design software, 2) exploring the feasible solution by coding, and 3) visualising the results by design software.

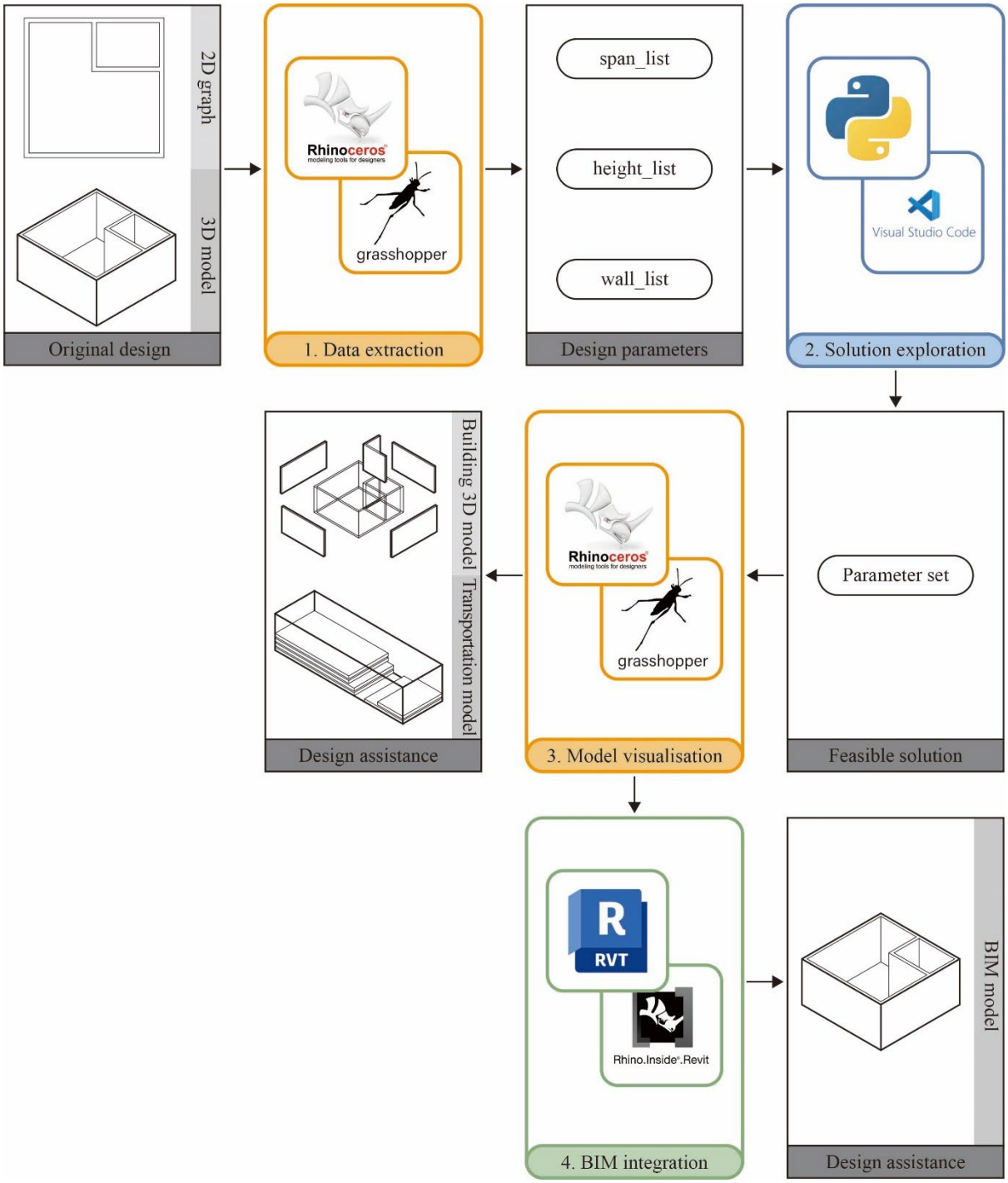

Figure 6-21 Pipeline of the proposed design optimisation method.

6.3.2 Data extraction

Based on the findings from section 6.2.3, 2D drawing and 3D model are the preferred EIFs in the developed design stage. The optimisation, therefore, begins with the original design in these two formats. These files are processed in the following steps:

1) First, the data is imported into Rhino for data extraction, as illustrated in Figure 6-22. In rhino, 2D drawings are converted into a 3D version via aligning the drawings according to the elevation. Notably, building elements, like columns and walls, are segmented into distinct layers for differing.
2) Subsequently, grasshopper scripts (Figure 6-23) are employed to extract original design parameters like $original\_span\_list_d$, $original\_height\_list$, $original\_wall\_list$, as detailed in section 4.2.1. In this step, design elements (e.g., axis, columns, and walls) in 2D drawing or 3D model are categorised into breps (Boundary Representation). These elements are then identified and re-constructed as lines, as illustrated in Figure 6-24. Finally, the coordination and parameters of design elements are exported into several tables with .xlsx extension.

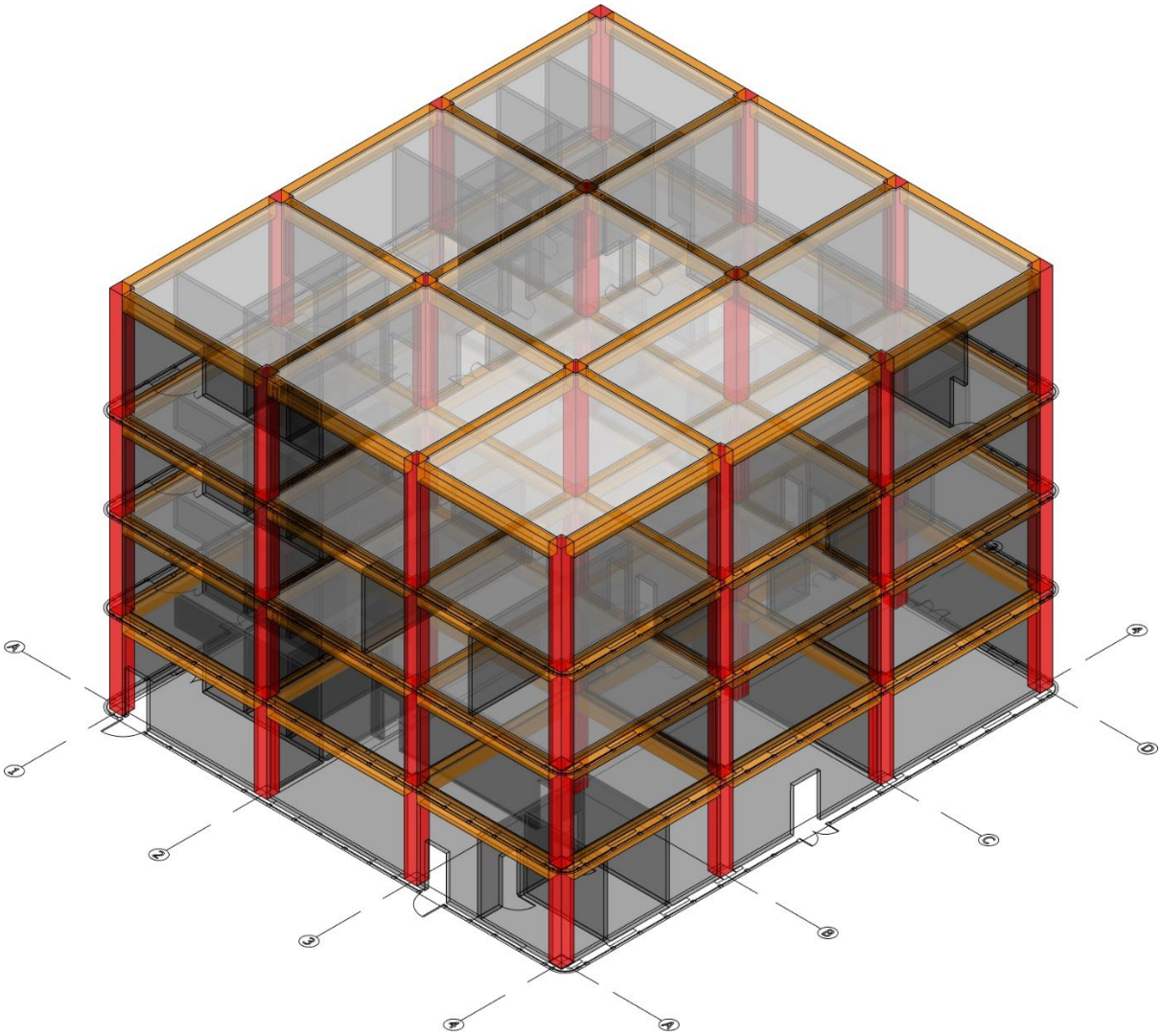

Figure 6-22 Original design data of the studied case.

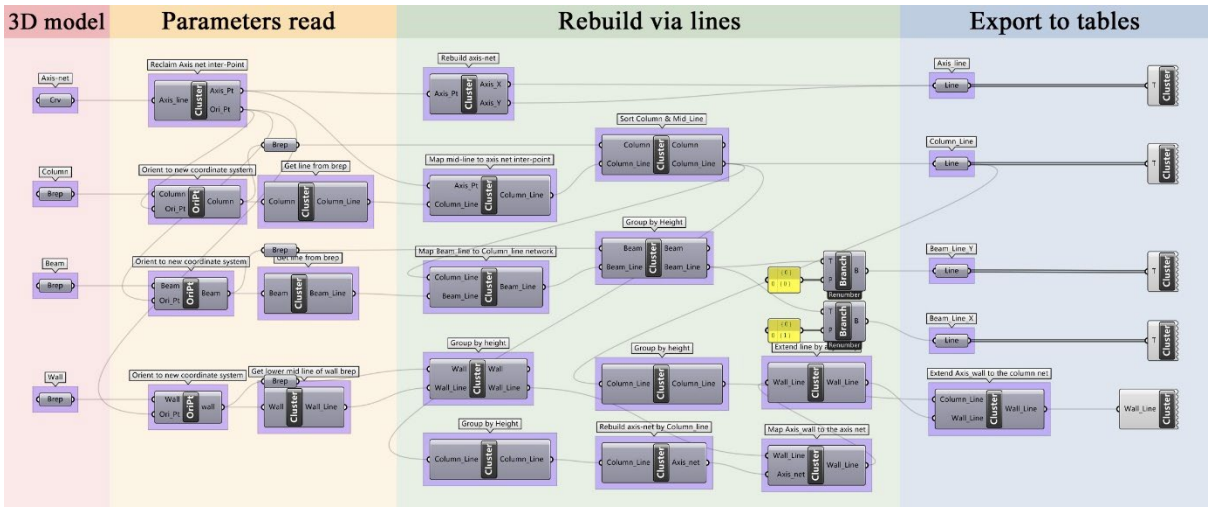

Figure 6-23 Data extraction program in grasshopper.

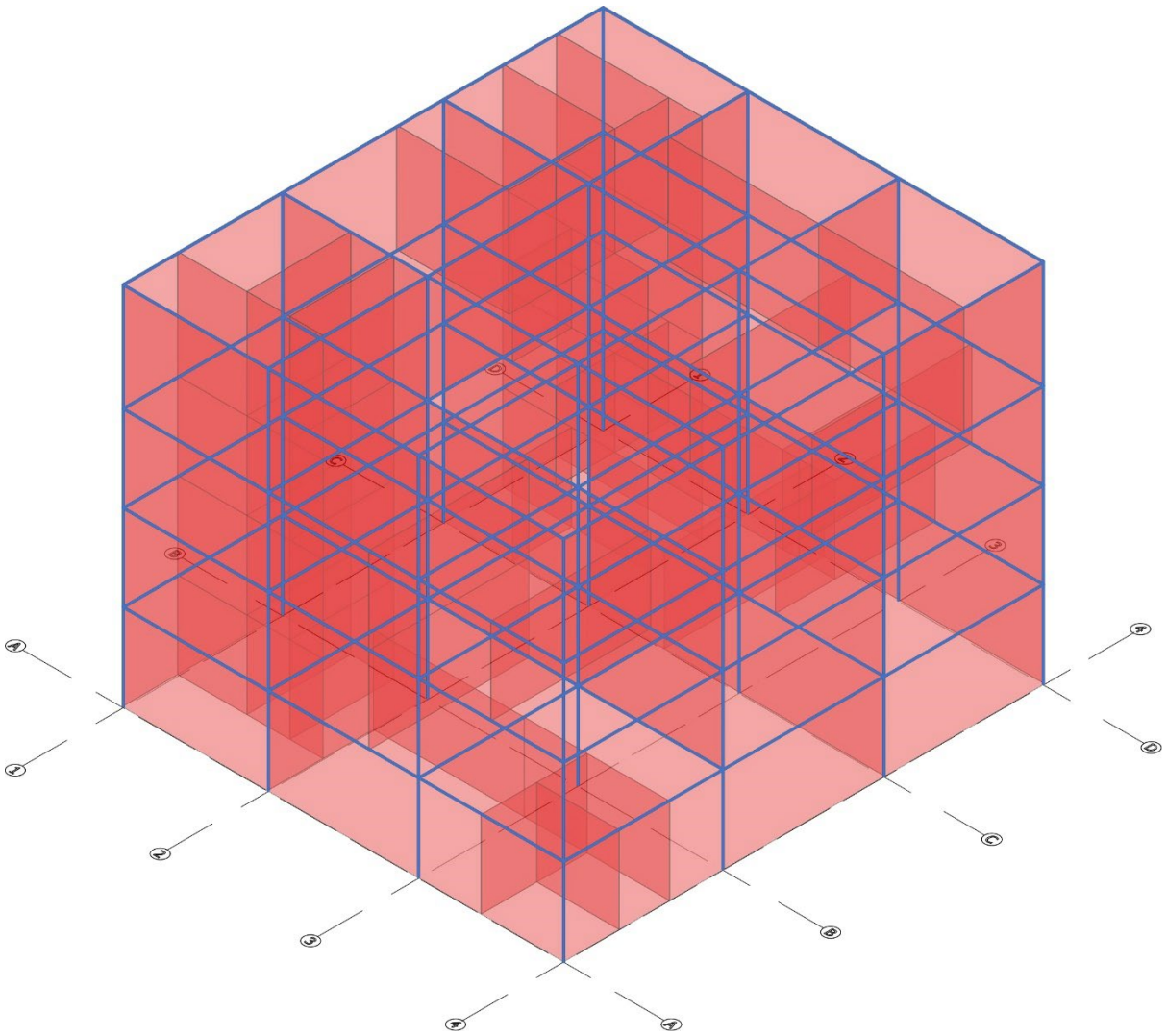

Figure 6-24 Simplified model after parameter extraction.

6.3.3 Feasible solution visualisation

6.3.3.1 Visualisation of the feasible design alternative

Parameters from the feasible design alternative are fed into a visualisation programme coded in grasshopper, as illustrated in Figure 6-25. Firstly, building elements, like columns, beams, secondary beams, and floor slabs, are rebuilt as sets of breps in Rhino. These breps depict the dimensions and positioning of building elements. Subsequently, rebar designs of building elements are labelled with tags on each building element. These tags are displayed in varied orientation and directions to represent the structure design across element sections. They can be individually for clearer visualisation of design details. Figure 6-26 shows the visualised model with full tags in Rhino.

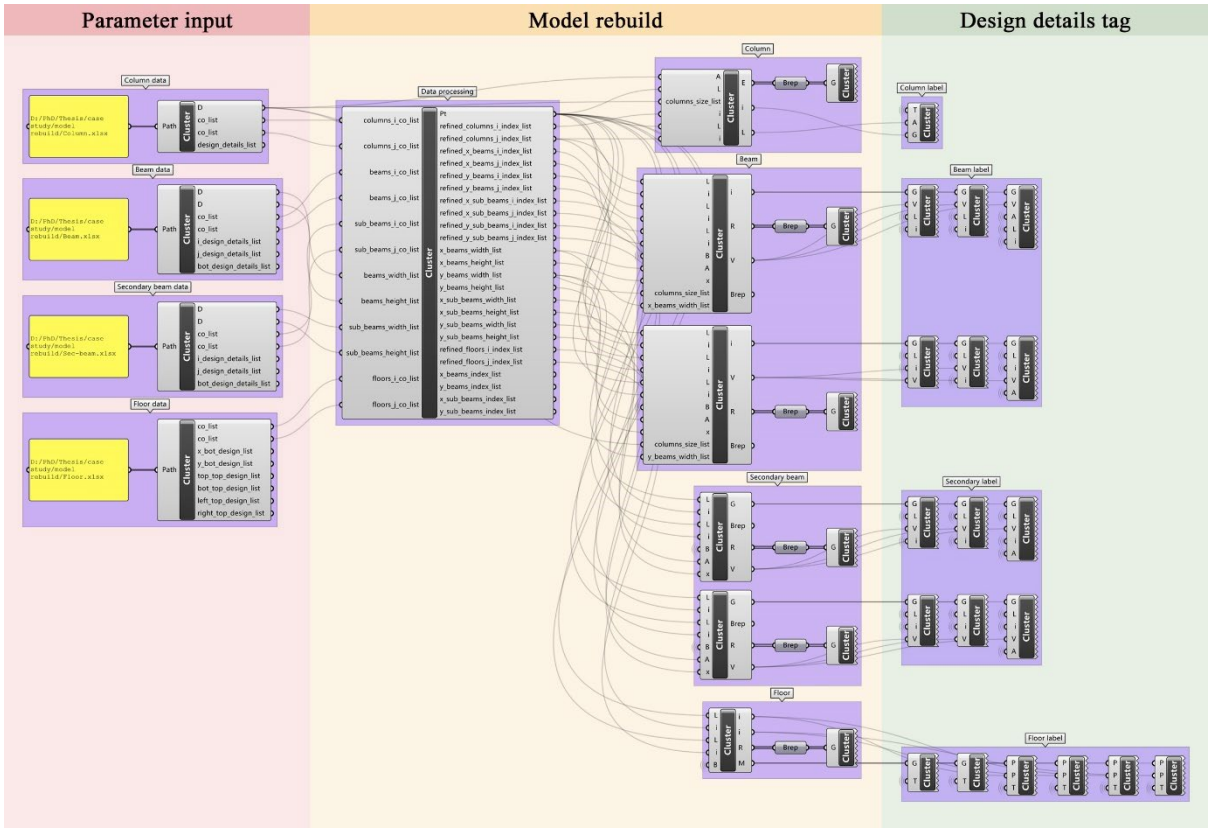

Figure 6-25 Design parameter visualisation programme in grasshopper.

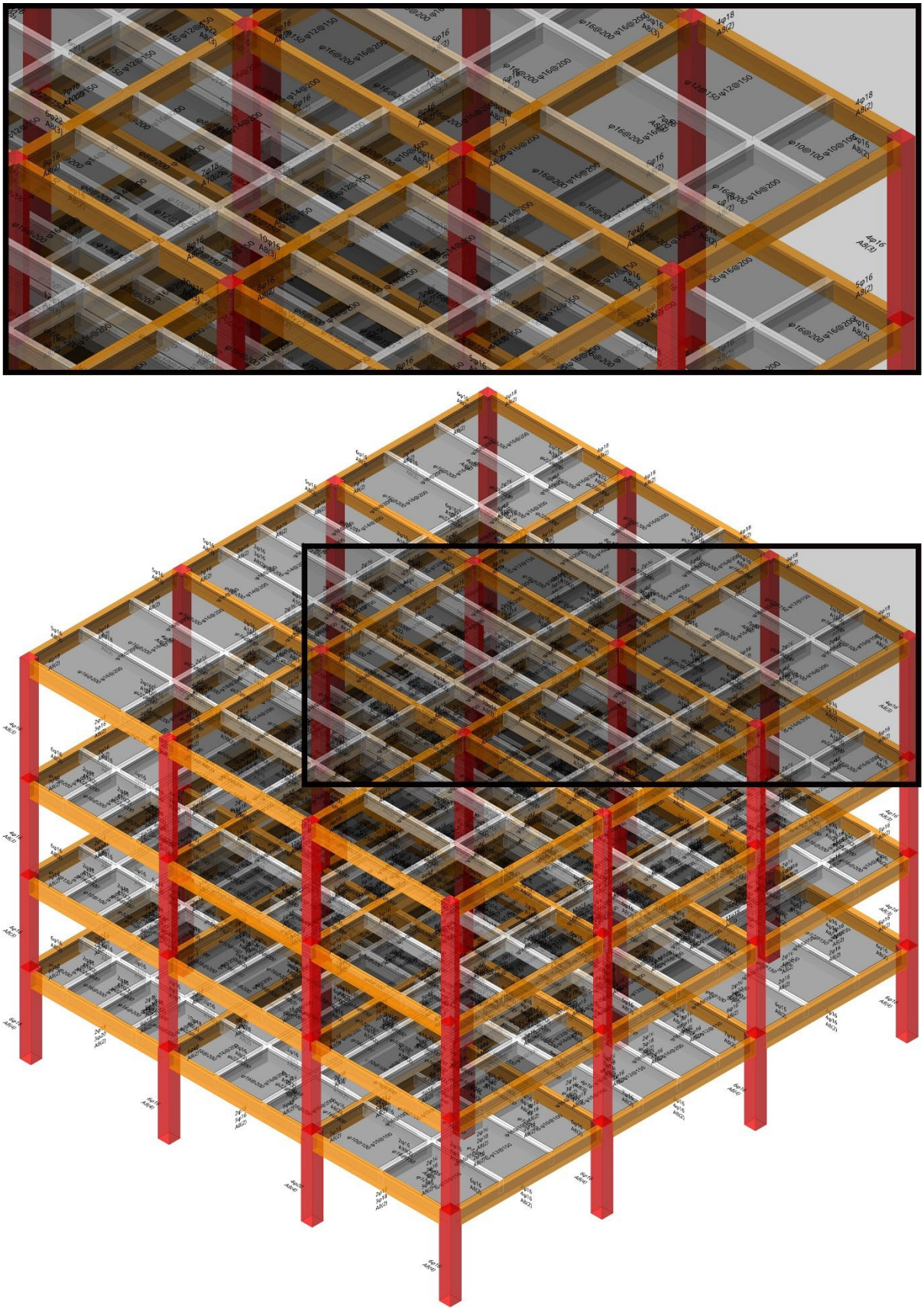

Figure 6-26 Visualisation of the feasible solution.

6.3.3.2 Visualisation of the feasible transportation plan

The transportation plan is visualised using a programme coded in grasshopper, as illustrated in Figure 6-27. Firstly, the parameters of transportation plan are visualised via a set of edges. These edges depict the external boundaries of precast elements and the available space on tracks. Then, design parameters of precast elements are input to visualise the details of each element. Tags mark the ID and corresponding weight of each element. Figure 6-28 to Figure 6-30 display the visualised transportation plan for the studied case.

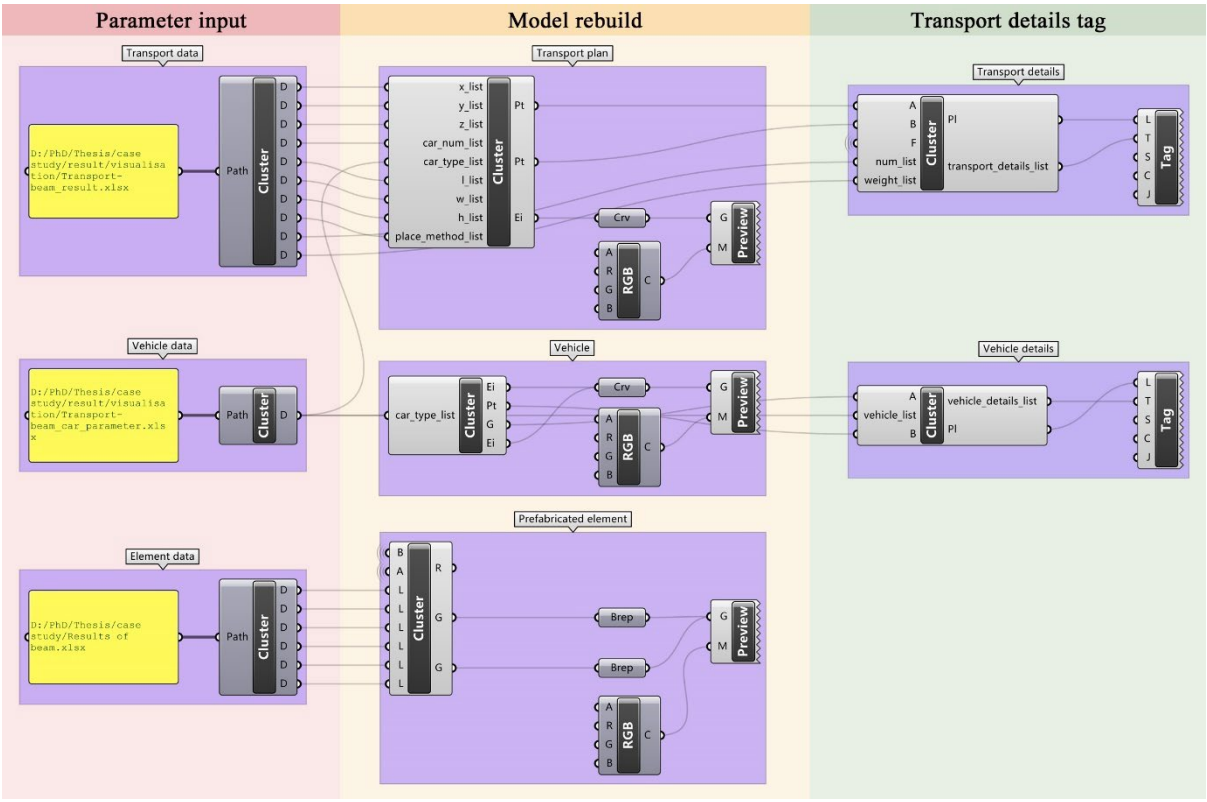

Figure 6-27 Transportation parameter visualisation programme in grasshopper.

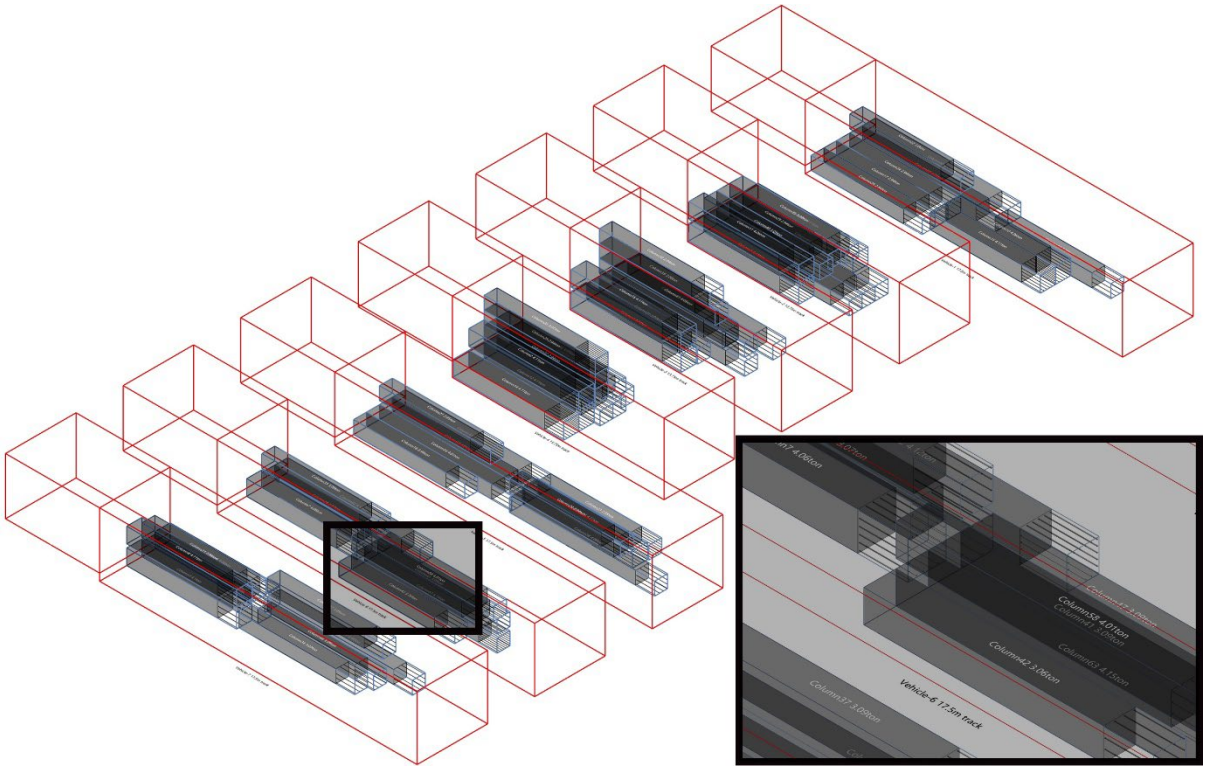

Figure 6-28 Visualisation of column transportation.

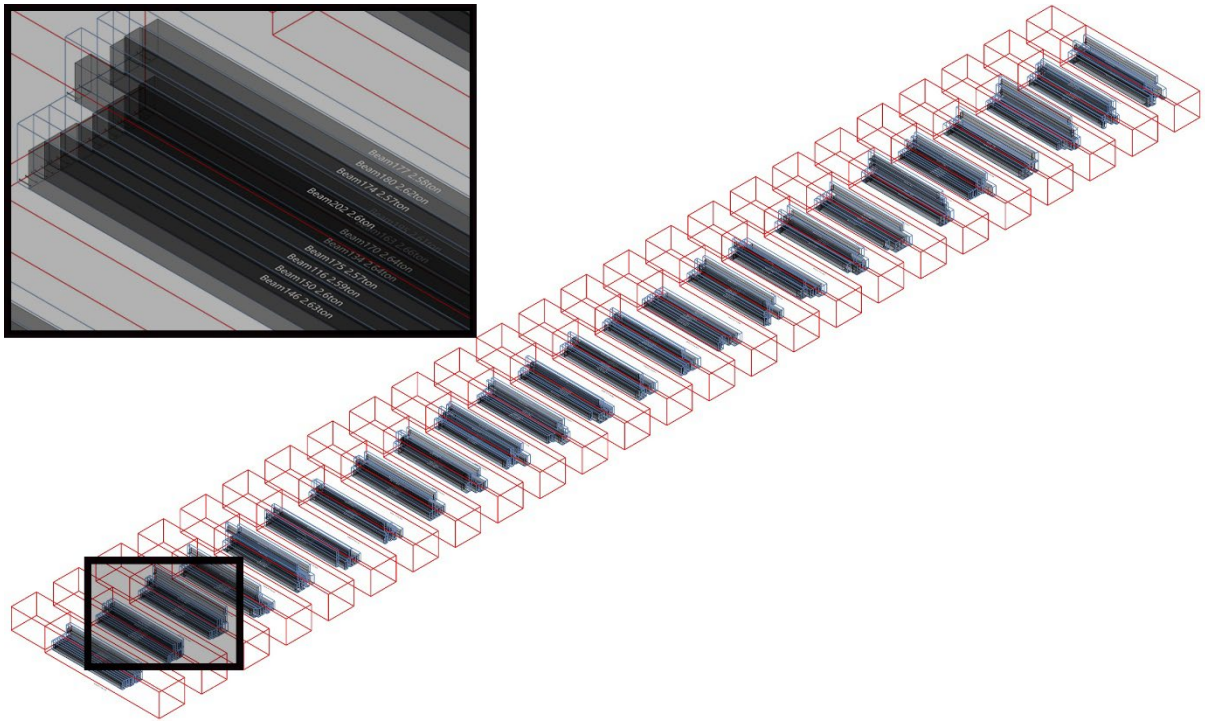

Figure 6-29 Visualisation of beam transportation.

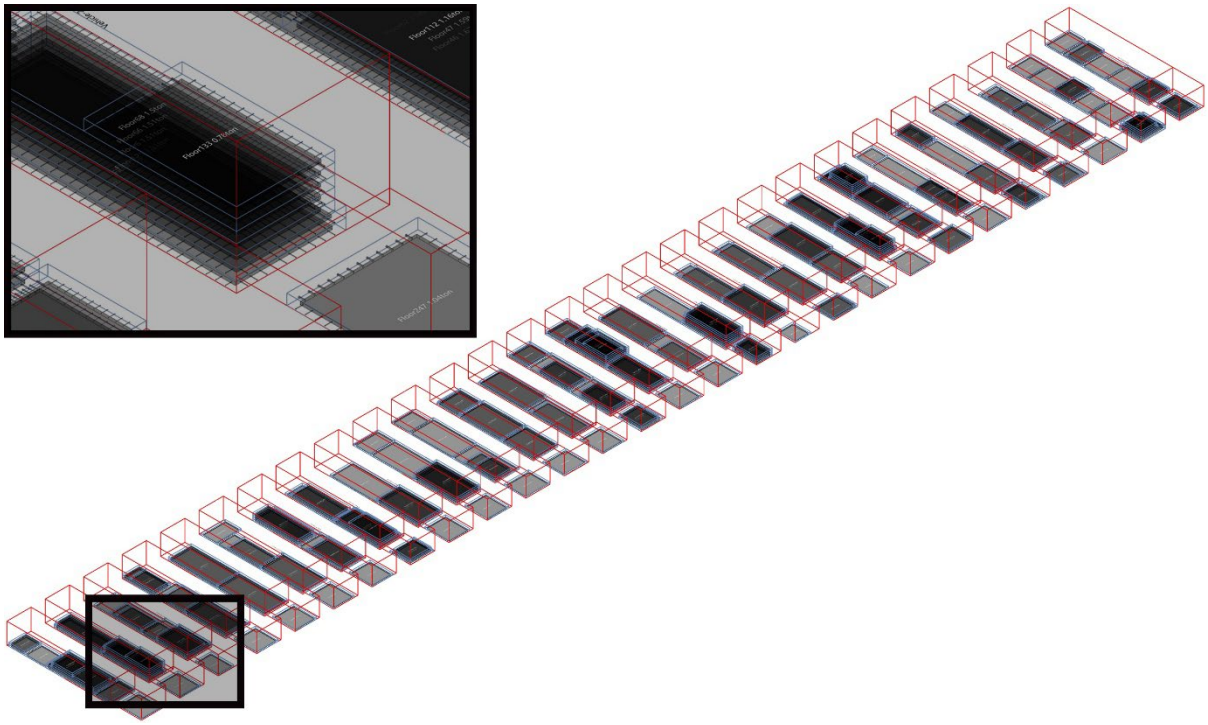

Figure 6-30 Visualisation of floor slab transportation.

6.4 Summary

This section develops tools for design data extraction and optimised results visualisation. It identifies the EIF used across concept, developed, and technical design stages through a questionnaire survey among Chinese designers and a statistical analysis on their responses. Findings from ANOVA, relevance analysis, logistic regression, and multiple correspondence analysis reveal that 2D and 3D files are preferred for creating and comparing design alternatives during the concept and developed design stages. On the contrast, BIM is welcomed for coordinating multi-disciplinary data in the later stages of project development. Based on these results, grasshopper plug-in tools are developed to extract design parameters from 2D and 3D design files and visualise the optimised results in 3D models.

7 Implementation and validation of the optimisation model

7.1 Introduction

To implement the proposed design optimisation model, this study employs modules 1-4 developed in sections 4-6 in a real-world case, as introduced in 4.3.3.1. After that, a two-step validation, including internal and external validation, is used to verify the model's carbon reduction effectiveness and practicality, respectively.

7.2 Model implementation

7.2.1 Scenario settings

The studied case is a four-storey reinforced-concrete office building located in Nanjing, China, as illustrated in Figure 7-1. The project has an area of 2971.16 m^2 and a height of 20.4m. It is a representative case for precast concrete projects in China, involving precast solid columns, precast composite beams, precast composite floor slabs, and autoclaved aerated concrete wall slabs. The structure is designed with a seismic precautionary intensity of degree 7, belongs to designed earthquake group 1, and has a site classification of I_1. The stairs, lifts and envelope are excluded from analysis and optimisation, because these parts are considered the same in all design alternatives (as elaborated in section 3, where the geometric features of all design alternatives remain the same).

A baseline scenario is established to quantify the optimisation effects of the proposed approach. Specifically, the architecture and structure design of the baseline scenario is the same as those mentioned in section 4.3.3.4. Regarding the transportation of prefabricated elements, the assumed conditions align with those described in section 5.3.3.3. Given the average loading rate of prefabricated elements in Jiangsu Province, China, is 0.40-0.65, the baseline transportation CE is calculated using equations (5-51) and (5-52) with an emission rate of 0.047 kg CO_2e/(ton·km).

The design and delivery of the studied case follow the following Chinese code: *GB55001-2021, GB55002-2021, GB55008-2021, GB50011-2010(2016), GB50010-2010(2015), GB50009-2012, GB/T51231-2016, JGJ1-2014, 13J104, 15G366-1, and 22G101-1*. The emission factors are cited from *China Products Carbon Footprint Factors Database* (CCG, 2022) and

Calculation standard of building carbon emissions GB/T51366-2019 (2014). These constraints are consistent with those in sections 4 and 5.

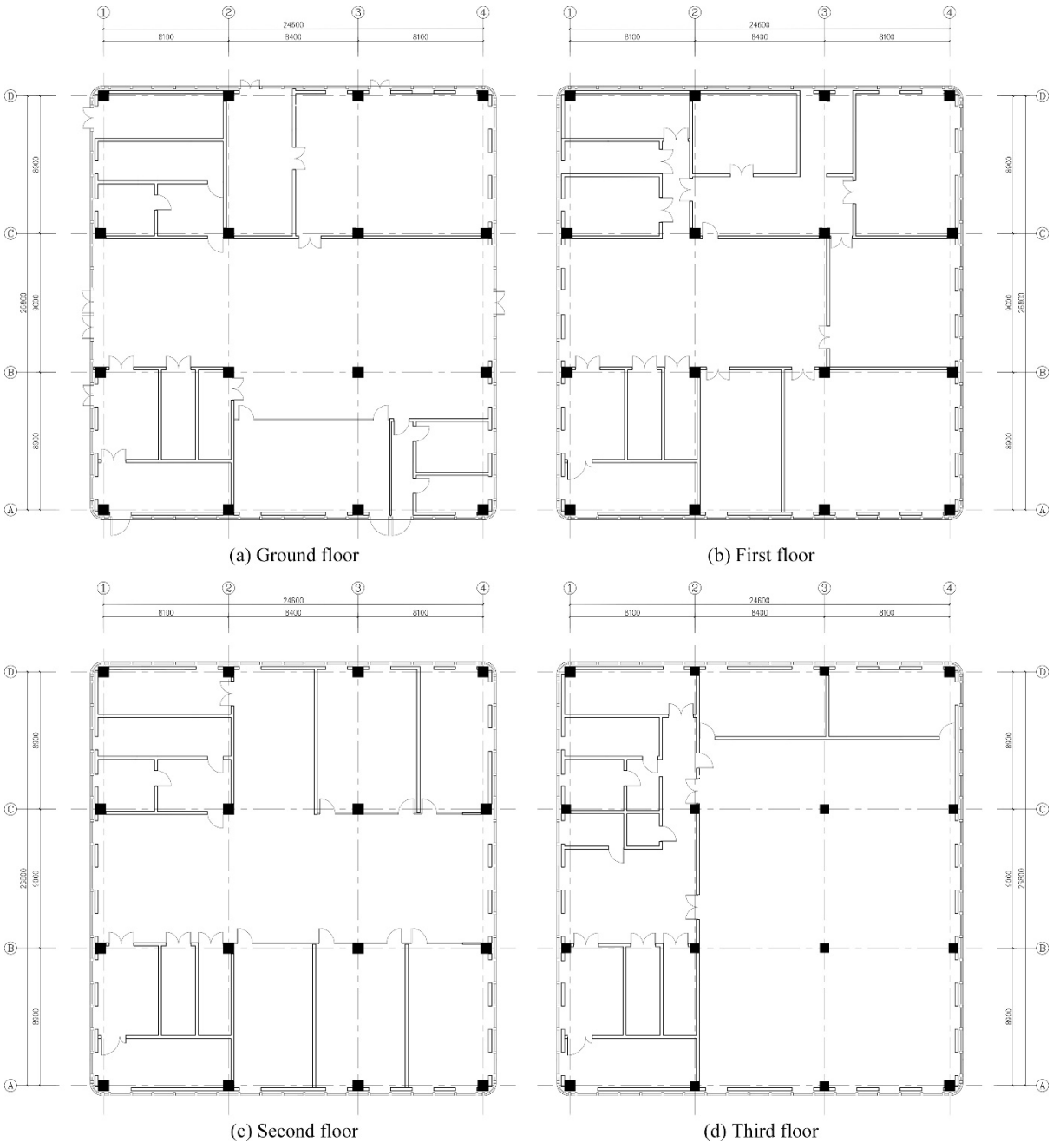

Figure 7-1 The plan of the studied case.

7.2.2 Optimisation effect

The optimisation last for 56.5 hours on a personal desktop with an i7-12700k CPU and 48GB RAM (3200MHz). A feasible solution achieves a CE of 8.08×10^5 kg CO_2e. Figure 7-2 and Table 7-1 shows the carbon reduction achieved through design optimisation. The feasible

solution reduces CE from building materials, formwork, and transportation by 11.09%, 0.13%, and 30.82%, respectively, representing a 10.06% decrease in embodied CE. Compared to element transportation, the manufacturing process contribute to a significantly larger part of embodied emissions, consistent with assumptions in section 3.3.2. Optimising emissions from manufacturing and transportation in two separate steps have a minor influence on overall carbon reduction, suggesting the effectiveness of proposed optimisation method.

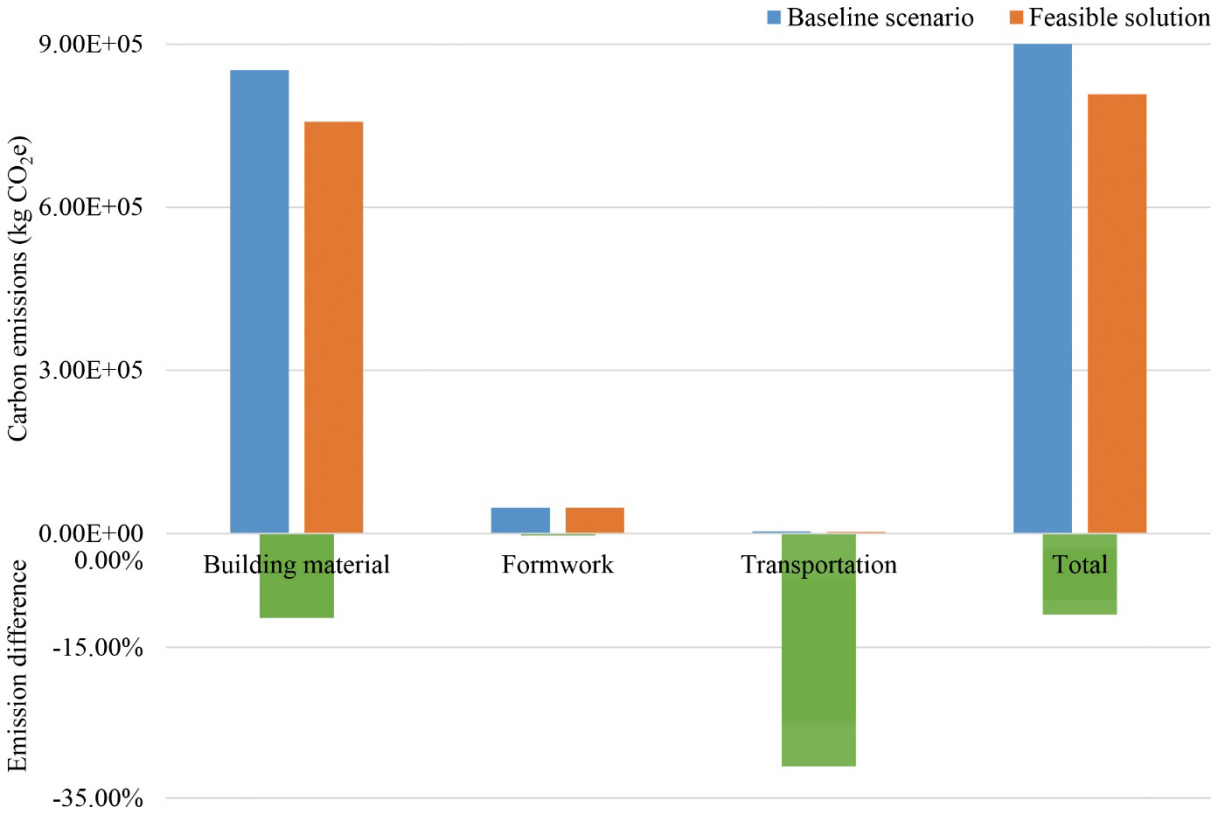

Figure 7-2 Carbon reduction from optimisation.

Table 7-1 CE of baseline scenario and feasible solution (kg CO_2e).

	Building material	**Formwork**	**Transportation**	**Total**
Baseline scenario	851905.01	47723.67	3952.16	903580.84
Feasible solution	757434.95	47660.29	2733.92	807829.16
Emission difference	-11.09%	-0.13%	-30.82%	-10.60%

Notably, the ratios of manufacturing and transportation CE differ from previous studies (Teng & Pan, 2020), with manufacturing contributing significantly more in the studied case. The discrepancy stems from the system boundary, which excludes emissions from onsite construction and transporting onsite construction materials from factory to the construction site.

Additionally, the transportation distance is set as 50km. Longer transportation distances would increase the contribution of transportation emissions (Dixit et al., 2013). This variance is detailed discussed in section 8.1.1.

Despite so, the studied case results indicate the effectiveness of applying the proposed method in sustainable design optimisation. For both the baseline scenario and the feasible solution, similar quantities of onsite construction and transportation are excluded, involving the assembly of approximately 1680 tons of precast elements and transportation of about 520 tons of cast-in-situ reinforced concrete. With uniform construction and transportation processes, CE from these excluded parts has minimal difference. Therefore, the potential for carbon reduction in these areas is limited, leading to minor impacts on overall carbon reduction.

Figure 6-26 and Figure 6-28 to Figure 6-30 illustrates the visualised feasible design alternative and transportation plans. They are the final output of the optimisation model. Detailed optimisation results of element design and transportation plan are given in Appendix A-C and Appendix J, respectively.

7.3 Research validation

7.3.1 Internal validation

Carbon reduction effectiveness is verified via internal validation. As described in section 4.3 and 5.3, several baseline scenarios are set to represent common practices in prefabricated element manufacturing and transportation. The effectiveness of the optimisation models is quantitatively estimated via comparing CE between the proposed optimisation model and baseline scenarios, as illustrated in Table 7-2.

Results from case studies in sections 4 and 5 show that CEs from the optimisation model are lower than those from the baseline scenario, indicating the models' capability to reduce emissions in the manufacturing and transportation stages. Exceptions are witnessed in Case A – Wall and Case C – Column in section 5. The higher emissions from the optimisation model stem from the baseline scenario estimating transportation CE using the macro-level emission factors, which may deviate from the real-world conditions, as stated in section 5.4. When the baseline scenario is changed to the 3D-RSO algorithm using vehicle 1 (which is closer to practice), the optimised ratios become -4.82% and -3.49%, respectively.

Section 7 evaluates the integrated model using a similar approach. Results demonstrate that the sequential use of optimisation models for manufacturing and transportation reduces the overall embodied CE of prefabricated projects by 10.60%. Therefore, the design optimisation method proposed in section 3 is considered theoretically effective.

Table 7-2 CE of the baseline scenario and feasible solution in case studies (kg CO_2e).

	Baseline scenario	**Feasible solution**	**Optimised ratio**
Section 4 Manufacturing CE			
Case A	899628.68	805095.24	-10.51%
Section 5 Transportation CE			
Case A - Floor	100.38	89.63	-10.71%
Case A - Wall	40.85	42.67	4.46%
Case B - Floor	175.50	173.45	-1.17%
Case B - Wall	76.03	53.72	-29.34%
Case C - Floor	458.09	338.29	-26.15%
Case C - Wall	554.62	393.77	-29.00%
Case C - Column	79.97	84.94	6.21%
Case C - Beam	123.61	94.98	-23.16%
Case D - Floor	514.83	384.61	-25.29%
Case D - Column	153.74	104.93	-31.75%
Case D - Beam	1008.50	697.82	-30.81%
Case E - Floor	210.53	181.51	-13.78%
Case E - Column	246.25	189.73	-22.95%
Section 7 Manufacturing and transportation CE			
Case A	903580.84	807829.16	-10.60%

7.3.2 External validation

The model practicality is verified via external validation i.e., questionnaire survey mentioned in section 6.2.1. In the questionnaire, questions 15-18 estimates the necessity of employing design optimisation. Questions 19-20 assess designers' acceptance of the optimisation performance. Questions 22, 23, and 27 test the adjustability of variables (design parameters) introduced in sections 4 and 5 within design practices.

Responses to questions 15 and 16 in the questionnaire show that over 85% and 73% of respondents consider sustainability and CE during design, respectively. Responses to questions 17 and 18 reveal that around 90% of respondents have used and are willing to employ design optimisation. These findings underscore a practical demand for sustainable design optimisation in the construction industry, highlighting the importance of this study.

Responses to questions 22, 23, and 27 indicate that the variables employs in optimisation models for prefabricated element manufacturing (section 4.2) and transportation (section 5.2)

are flexible in design practices. Additionally, responses to question 28 shows that, most designers rely on referenced data rather than personal experience. This finding suggest that designers are likely to consider the values from the feasible solution (provided by the optimisation model) when determining those flexible variables. Therefore, optimising designs by adjusting such variables is practical in real-world design process.

Responses to question 19 suggest that 87% of respondents are willing to increase project costs by up to 30% for improved sustainability. The feasible solution from the proposed optimisation method reduces the usage of building materials, formwork, and transportation vehicles, leading to a reduced cost in element manufacturing, onsite construction, and transportation. Therefore, it aligns with the requirements of designers. However, responses to question 20 indicate that most designers prefer to spend less than 12 hours on design optimisation. The full optimisation period of the proposed method exceeds this limit by twice, suggesting a need for improved efficiency. However, as it requires no manual oversight, this duration is equivalent to two working days, making it somewhat acceptable. This issue could be solved via employing higher-performed hardware and improving the algorithm. Detailed solutions for this issue are discussed in the section 8.

Analysis in section 6.2.3 and 6.2.4 reveals that designers of prefabricated projects a prefer working with 2D graphs and 3D models. The data extraction and visualisation process mentioned in sections 6.3.2 and 6.3.3 demonstrates that the proposed optimisation method can interpret original design parameters from 2D and 3D files and visualise the feasible solution in 3D models. Additionally, with "*Rhino-inside-Revit*", the feasible solution can be integrated into Autodesk Revit, realising the application in BIM software. This finding suggests that is capable of processing commonly used design files and offering guidance in designers' preferred formats. Therefore, the proposed method is considered practical for real-world applications.

7.4 Summary

This section verifies the practicality and effectiveness of the proposed optimisation model. Applying the model to a four-floor Chinese office building shows that the model can reduce embodied emissions from building materials, formwork, and transportation by 11.09%, 0.13%, and 30.82%, respectively, representing a 10.06% decrease in embodied CE. Responses from a questionnaire survey among Chinese designers indicate that the variables employed in the

optimisation model are adjustable in design practice, and designers are willing to adopt this model for reducing embodied emissions.

8 Discussion

8.1 Comparison with previous findings

8.1.1 Carbon reductions

The optimisation model achieves a 11.09% reduction in building materials and corresponding CE, suggesting the model's effectiveness in reducing embodied CE of prefabricated projects. This reduction is less significant than replacing reinforced concrete by sustainable building materials, like timber (Hart et al., 2021) or supplementary cementing materials (Gan et al., 2017), which leads to 35% and 20% less embodied emissions, respectively. However, fully replacing reinforced concrete is not practical in Chinese construction industry as stated in section 1.2.1. Therefore, a carbon reduction at 11.09% in building materials is more reasonable and practical in current prefabricated project design optimisation.

Beyond carbon reduction by replacing cast-in-situ construction by prefabrication, which claims 5-15% less emissions (Hao et al., 2020; Mao et al., 2013), the proposed optimisation model points out an additional reduction potential through the optimisation of prefabricated element design. Given that all the design variables employed are adjustable in design practice (section 7.3.2) and the optimised design alternative shares the similar architecture design with the original design (section 4.2.1), this addition carbon reduction effect is considered promising in most prefabricated projects in China.

Regarding the emissions from formwork, the optimisation model reduces 0.13% emissions. This value is significantly lower than formwork reduction from replacing cast-in-situ construction by prefabrication (Cheng et al., 2022; Dong et al., 2015; Wong & Tang, 2012). This variance stem from the absolute smaller quantity in prefabricated construction than cast-in-situ construction, as stated in section 4.4.3. Despite so, considering the high cost of mental formwork (Hyun et al., 2018), the minor reduction in formwork quantity leads to considerable savings in construction cost, defending its values in prefabrication design optimisation.

The transportation emissions are decreased by 30.08% through design optimisation. However, it only contributes to 1.27% of the total carbon reductions. This stems from the minor contribution of transportation emissions to the overall embodied CE, which is 0.34%-0.44%. This contribution is significantly smaller than findings of Du et al. (2019) and Hao et al. (2020), which are around 1-5%. It is because only the transportation of prefabricated element is

considered (section 3.3.1). By including an estimated transportation emissions of building materials (40km distance for concrete, 500km for the other materials, and an emission ratio at 0.047 kg CO_2e/(ton·km) (Calculation standard of building carbon emissions GB/T 51366-2019, 2014)), the transportation emissions of the baseline scenario and feasible solution are increased by 1.70 and 1.60 × 10^5 kg CO_2e, increasing the contribution of transportation emissions to 1.8% and 1.9% respectively. These results are similar to previous studies (Du et al., 2019; Hao et al., 2020).

However, the results are still far smaller than the finding of Dong et al. (2015), who claimed a 18% contribution of transportation emissions. The reason for their high transportation emission mainly from the long transportation distance in Hong Kong, where prefabricated elements and building materials are all imported from the China mainland. Jafary Nasab et al. (2020)'s finding suggests that importing building materials and transporting them in a long distance will significantly increase transportation emissions.

8.1.2 Results communication

Data from the questionnaire survey (section 6.2.3) reveal a unique pattern of BIM model utilisation for building design in China. Despite being promoted for years (J. Li et al., 2020; Yu Yang et al., 2024), the BIM model is the least used and least welcomed engineering information format among designers, consistent with data reported by Deng et al. (Deng et al., 2020). However, this data contrasts with regions like Singapore and the UK, where BIM utilisation rates exceed 80% (Teo et al., 2016) and 60% (UKBIMA, 2021), respectively, despite similar promotion efforts.

One potential reason for this discrepancy is the lack of detailed and clear requirements for BIM usage in China. For example, the UK government mandated BIM use for all public projects worth £5M and over starting in 2016 (Olanrewaju et al., 2022). To achieve this, the UK established a BIM application framework, specifying BIM information and formatting requirements, including the level of model detail, model information, model definition, and model information exchanges, through ISO 19650 (Specification for information management for the capital/delivery phase of construction projects using building information modelling: PAS 1192-2:2013, 2013) and previously the PAS 1192 standards (ISO 19650: Organization and digitization of information about buildings and civil engineering works, including building information modelling (BIM) — Information management using building information

modelling, 2018). Similarly, Singapore mandated that all new architectural plans be submitted in BIM format in 2013 (Liao et al., 2021). The Singapore government outlined the deliverables, process and personnel/professionals involved in BIM usage and clarified the roles and responsibilities of designers via Singapore BIM Guide (Singapore BIM Guide - Version 2.0, 2013). The government also developed the platform CORENET X for BIM model submission and inspection (BCA, 2023). In contrast, such requirements are less stringent in China, where the goal was merely to use BIM in 90% of projects funded by national capital or aiming for green building certification by 2020 (MOHURD, 2015). The depth and scale for BIM application in these project remains unclear, leading to "token" use of BIM models (Deng et al., 2020).

This phenomenon underscores the lack of BIM standards and corresponding workflows (Tan et al., 2019), which may influence practice and preference for engineering information format used by designers. On the one hand, Chinese construction industry still relies on manual 2D drawing reviews by government agencies, with BIM models serving more as a secondary or extra format (Wei & Hu, 2014). The national design framework development goal for 2023 remained focused on achieving the digital checking of conventional drawings (Notice from the Ministry of Housing and Urban-Rural Development on Promoting the Standardization, Normalization, and Facilitation of Engineering Construction Project Approvals, 2023). The use of BIM models for design review and building delivery is encouraged but not mandated. Consequently, using BIM models becomes a voluntary for most designers, facing resistance due to habitual practices (Ahmed, 2018) and its disadvantages in conventional design tasks (Y. Liu et al., 2017).

On the other hand, existing BIM standards focuses primarily on the model at delivery rather than throughout the entire life cycle. For instance, the Nanjing government mandated design checking via BIM models and has established standards for BIM model delivery (Nanjing Municipal Bureau of Planning and Natural Resources, 2021). However, a comprehensive framework for model development across design stages is lacking, allowing designers to use conventional design tools and rebuild BIM models for compliance after design. Without a clear definition of details (e.g., LOD) during design, BIM model often serve as a 3D visualisation tool, inevitably losing out to more flexible data format.

However, the current lack of detailed standards allows for a careful consideration of the application approach for BIM. Given the lessons learned from Singapore and Hong Kong,

where using BIM sometimes become compliance-driven (Liao et al., 2021; Yu Yang et al., 2024), enhancing BIM's desirability, practicality, and ease of use is a significant goal. A flexible use of possible EIF for higher design and optimisation efficiency is anticipated.

8.2 The integration of macro-level and micro-level analysis

Comparing CE during element manufacturing and transportation reveals significant difference between macro-level and micro-level analysis. Generally, macro-level analysis, which factors overall material consumption and average emission ratio, effectively estimates design sustainability and provides considerable carbon reduction. This approach, requiring a less complex model and shorter analysis period, is more efficient than micro-level analysis. Nevertheless, macro-level results are less accurate and sustainable compared to micro-level analysis, which introduces detailed variables including building element features, connection method, vehicle characteristic, and transportation routines. Therefore, integrating these two approaches may yield better performance in sustainability analysis and optimisation.

Specifically, the principle of macro-level standardisation aims to minimise the number and type of precast elements. Applying this method in design can effectively reduce embodied CE in prefabricated project, as illustrated in Figure 4-9. However, it may also lead to the adoption of a larger element size, causing lower material efficiency and more consumption of building materials. Since formwork accounts for a minor percentage of embodied CE, savings from reduced formwork may not offset increased CE from materials. Thus, a better application of standardisation in precast projects may involve strategies beyond using entirely identical elements. Designers should categorise building elements according to their structural capacity and design specific cross-section accordingly. This approach allows unifying similar elements into a uniform size to reduce variety and formwork-related CE. Additionally, it helps minimise the use of over-sized cross-section, thereby reducing CE from building materials.

Similarly, employing identical emission factors in transportation analysis is effective for analysing CE of a large area but are not accurate enough for a single project. Micro-level analysis on element transportation shows that there are significant differences in the average loading rate and CE per unit elements across different element types (Figure 5-11 and Figure 5-13). Given that the carbon emission per unit of elements decreases with the growth in loading rate (Figure 5-12), a possible solution towards more accurate CE results using the emission factor method is to provide different emission factors for different element types. Such factors

would be more convenient to implement in a general CE estimation because calculations based on emission factors saves time for bin packing problem modelling and solving.

8.3 Micro-level carbon reduction strategies

Conducting micro-level analysis on embodied CE points out novel carbon reduction strategies in design and construction practices. The micro-level analysis on the formwork design shows that standardising geometric size does not directly influence formwork quantity or variety. Therefore, solely consider applying standardisation, even with the aforementioned approach, may not necessarily leads to lower formwork consumption. A micro-level optimisation, considering both building materials and formwork design, is essential for lower embodied CE in precast projects. Additionally, the differing results between off-line and online formwork design modes suggest that improving the adaptability of formwork may provide a better CE reduction than standardisation. In other words, conventional estimation of standardisation, focusing solely on element size, may not be sufficient accurate. Formwork consumption and adaptability may serve as better criteria for standardisation estimation.

The diversity in the reuse cycles of formwork (Figure 4-11 and Figure 4-12) challenges previous findings that using metal formwork necessarily reduces embodied CE (Dong et al., 2015; Wong & Tang, 2012). Metal formwork generates higher manufacturing CE but offers greater reuse cycles, potentially lowering lifecycle CE. However, substituting timber formwork with steel formwork only reduces CE after 50 times reuse (given the density of timber formwork at 15kg/m2, the CE coefficient at 0.81 kg CO_2e/kg, and the maximum reuse recycle at 5 times). Considering that most formwork pieces in this study are reused fewer than 50 times, replacing all the timber formwork with steel formwork increases overall CE, unless most steel formwork pieces are reused over 50 times in subsequent projects.

This finding underscores two strategies for reducing formwork CE in precast construction. The first strategy involves establish a pool of existing formwork pieces. In this regards, architects and civil engineers could consider the dimensions of existing formwork when designing elements in new projects, thereby maximising formwork reuse. Alternatively, the formwork pieces with few reuse cycles (e.g., less than 10 times) could be made from timber. Both strategies require detailed formwork estimations during the design phase, underscoring the importance of conducting micro-level design analysis.

Additionally, micro-level analysis points out the scalability benefits in sustainability optimisation of prefabricated project. As illustrated in Figure 4-12, the majority of formwork pieces are exactly reused 4 times. This is due to the assumption that cast-in-situ concrete is constructed floor by floor, which caps the maximum reuse cycle of cast-in-situ formwork at 4 times. However, adopting different column size for the ground floor and other floors in the feasible solution results in fewer reuse cycles and more formwork pieces. This finding suggests that the advantages of standardisation may be more pronounced in projects with more floors and larger plan areas, where the cast-in-situ parts are constructed in more times.

Regarding transportation CE, Figure 5-8 and Figure 5-13 illustrate that the differences in the vehicle number and the loading rate between the GA-based algorithm and the 3D-RSO algorithm increase with the growth in the number of prefabricated elements because this study employs an off-line packing mode. In this mode, a greater number of prefabricated elements provide algorithms with a larger solution space to explore the suitable element that fits the residual space, thus reducing the space waste and reducing the total number of vehicles. This effect therefore magnifies the performance difference between algorithms. Meanwhile, the accumulation of performance differences also grows with the element quantity and could lead to significant variance in the end—for example, the GA-based algorithm requires 33%-50% fewer vehicles than the 3D-RSO algorithm in the transportation of prefabricated floors in Project D (119 pieces) but the same number of vehicles in the transportation of prefabricated walls in Project A (10 pieces). Considering that a higher loading rate leads to a lower transportation CE per unit of prefabricated elements (Figure 5-12), the trend mentioned in the previous paragraph provides a potential method to reduce the transportation CE of prefabricated elements by considering a larger number of elements in one transportation batch.

8.4 Potential improvement of optimisation efficiency

As mentioned in section 7.3, the runtime of optimisation exceeds conventional (24-34 hours (Jusselme et al., 2020)) and expected optimisation period. Besides integrating macro-level and micro-level analysis methods, employing a simplified model also serves an effective method for rapid optimisation. Regarding the optimisation for manufacturing CE, the slight difference in the CE across generations suggests that solutions from the prophet generation might yield comparable CE reduction. They may serve as a close-to-feasible solution for rapid design optimisation.

Concerning the transportation CE optimisation, Figure 5-16 illustrates that the CE reduction caused by replacing the 3D-RSO algorithm with the GA-based algorithm is most obvious in the transportation of prefabricated floors and less significant in the other three categories. This variance suggests that the advantages of the GA-based algorithm (increasing the loading rate, thus reducing the CE) are less significant in some element types, and thus the disadvantage of a long computing period becomes more significant. Therefore, it is more reasonable to employ the 3D-RSO algorithm rather than the GA-based algorithm in these tasks for rapid computing without sacrificing significant performance.

However, the effectiveness of the simplified methods may vary under different architectural designs. Therefore, the optimisation effect of the prophet generation is not guaranteed. Additionally, the constraints of coding efficiency and computing power limits the optimisation effects. Only a limited number of design alternatives (6000) are estimated in the optimisation (in section 4) within a feasible timeframe, forcing the adoption of simplification postulations as mentioned in 4.3. The potential for CE reduction using more complex parameter combinations is yet to be explored. Moreover, the current feasible solution is not necessarily the global optimum due to the inherent characteristic of GA. There may remain potential for further reductions under the current settings. Consequently, using GA in future studies for lower embodied CE is still necessary.

8.5 Summary

This section discusses the research findings and their implications. The emission contributions of building materials, casting formwork, and transportation vehicles are consistent with previous studies yet differ in detail because of considering micro-level construction conditions. Introducing micro-level variables enhances the application of conventional design principles and offers novel carbon reduction strategies, like increasing the adaptability of casting formwork and maximising the use of existing formwork pieces, promoting sustainable practices in prefabricated constructions.

9 Conclusion

Prefabrication is widely considered an effective method to reduce embodied CE in the construction industry. Scholars have put considerable effort on optimising prefabrication design at early design stages for lower emissions. However, existing studies rely on macro-level analysis and lack supervisions on the implementation of carbon reduction strategies. Consequently, the effects of their strategies are not guaranteed in practice. Therefore, this study presents a micro-level design optimisation method of prefabricated projects for practical carbon reduction strategies in Chinese construction industry, where precast reinforced concrete is the main forms of prefabrication.

9.1 Response to research questions and objectives

To achieve the goal, three research questions are raised:

1) How can embodied CE from prefabricated constructions be calculated more accurately using current estimation methods and accessible data?
2) What is the practical approach of predicting and optimising embodied CE of prefabricated projects in the design stage?
3) To what extent can design optimisation be applied and what is the most appropriate way of implementing optimisation as a guidance to designers in prefabricated design?

To address the aim, the following objectives are undertaken:

1) Identify the stages, impact variables, calculation method, and available database for calculating embodied CE of prefabricated constructions.
2) Analyse embodied CE of prefabricated construction using micro-level design variables.
3) Generate design alternatives and compare their CE to identify the most sustainable design.
4) Develop a practical method to communicate the optimisation outputs to designers effectively.

9.1.1 Estimating embodied CE using available data

9.1.1.1 Identify the system boundaries of prefabrication embodied CE optimisation

Research objective 1 "Identify the stages, impact variables, calculation method, and available database for calculating embodied CE of prefabricated constructions." is addressed via a literature review focusing on project embodied CE.

The review results show that manufacturing and transportation stages contributes to more than 90% of embodied CE, in which building materials, formwork, and fuel for transporting prefabricated element emerge as the primary carbon sources. These elements offer the greatest carbon reduction potential. Therefore, this study defines the system boundary to include embodied CE from producing building materials and formwork as well as transporting prefabricated elements.

Emissions from building materials and formwork are typically analysed using emission factor method, where material quantity and CE coefficient are the main variables. The *China Products Carbon Footprint Factors Database* (CCG, 2022) and Calculation standard of building carbon emissions (2014) *GB/T51366-2019* provide emission factors for building materials and formwork materials used in prefabricated construction.

Regarding transportation CE, the *China Products Carbon Footprint Factors Database* (CCG, 2022; LÜ et al., 2021) and Calculation standard of building carbon emissions (2014) *GB/T51366-2019* introduce the emission factor method, considering material quantity, transport distance, and CE coefficient. These two sources also provide the emission coefficients for transportation emission estimation. Additionally, *MOVES3* introduces the transportation emission calculation method that factors vehicles features, driving patterns, road conditions, and freight weight. The necessary data for employing this method can be found in the *Preliminary Report on the Freight Industry* (School of Transporation and Logistics of Southwest Jiaotong University, 2020), *Market Analysis and Fuel Efficiency Technology Potential of Heavy-Duty Vehicles in China* (Delgado & Li, 2017), *China Green Freight Assessmen*t (China Automotive Technology and Research Center, 2018), and *Exhaust Emission Rates for Heavy-Duty Onroad Vehicles in MOVES3* (EPA, 2020a).

9.1.1.2 Improve existing embodied CE estimation methods

Research objective 2 “Analyse embodied CE of prefabricated construction using micro-level design variables” is addressed via improving existing embodied CE estimation methods.

Current CE estimation methods and databases, as mentioned in section 9.1.1.1, predominantly rely on statistical analysis. While suitable for macro-level (such as city and region) emission estimation, these methods and data lack the accuracy needed for project-specific analysis. A promising strategy to address such issue involves integrating those statistical emission factors with process-based life-cycle analysis of material quantities. This strategy analyses the design and construction process at a micro-level, introducing detailed design/construction variables to estimate accurate material quantities. The refined material quantities are then used along with statistical emission factors to estimate embodied CE.

Specifically, the estimation of building material quantities for manufacturing CE calculation is conducted via quantitative analysis of the prefabricated element design. The material quantity of each element is estimated based on its features, considering specific element cross-sections and connection junctions. This research considers the quantity of casting formwork via construction simulation based on element dimensions. Each piece of formwork is comprehensively considered using an off-line production mode, i.e., assuming the dimensions of all elements are known in advance and maximising the reuse of formwork pieces.

After obtaining the refined quantities of building materials and formwork pieces, the manufacture CE is calculated via multiplying these quantities by corresponding emission factors from The *China Products Carbon Footprint Factors Database* (CCG, 2022) and Calculation standard of building carbon emissions (2014) *GB/T51366-2019*.

For transportation analysis, a 3D BP algorithm is employed to simulate the loading status of prefabricated elements on each vehicle. This simulation provides the freight weight for each vehicle. Using the analysis method from *MOVES3*, the transportation CE is accurately estimated.

9.1.2 Predicting and optimising embodied CE at design stage

The research question 3 “What is the practical approach of predicting and optimising embodied CE in the design stage?” and the corresponding research objective 3 “Generate design

alternatives and compare their CE to identify the most sustainable design." are addressed using the parametric design approach and GA.

Given the features of project design, an original architectural design representing geometric dimensions serves as the optimisation starting point. The geometric features of this original design are converted into a set of numeric parameters. The uncertain design variables necessary for structure and prefabricated element design are defined as parameters within specific ranges. Design alternatives, based on the original design, are generated via varying the uncertain design parameters.

The structure design of each alternative is performed based on the guidance and requirements of the Chinese codes *GB55001-2021*, *GB55002-2021*, *GB55008-2021*, *GB50011-2010(2016)*, *GB50010-2010(2015)*, *GB50009-2012*, *GB/T51231-2016*, *JGJ1-2014, 13J104*, *15G366-1*, and *22G101-1*. After determining the detailed design of each design alternative, the corresponding CE is estimated using the refined emission analysis method mentioned in section 9.1.1.2. Finally, a GA is employed to explore the feasible solution with the lowest CE.

9.1.3 Communicating the optimisation results

To address question 4 "What is the most appropriate form of providing design guidance to designers? and research objective 4 "Develop a practical method to communicate the optimisation outputs to designers effectively." a questionnaire survey is conducted among Chinese designers.

The survey results indicate a high likelihood of original designs being presented in 2D drawings and 3D models. Designers prefer to receive design assistance in 3D models. Consequently, a viable application of the proposed design optimisation method involves extracting original design parameters from 2D drawings and 3D models, and presenting feasible solutions in 3D models.

Based on this finding, a design parameter extraction tool and an optimisation visualisation tool are developed in Rhino 3D and Grasshopper. Specifically, the data extraction tool extract original design parameters from 3D models and stored these parameters in files with suffix of .xlsx. These parameters are then input into the design optimisation model mentioned in section 9.1.2 to obtain the optimised design solution, which is defined by a set of parameters.

The parameters of optimised design solution are then input into the visualisation tool to generate the 3D model of project design and transportation plans.

9.2 Research findings

Based on the responses in section 9.1, this study presents a micro-level carbon optimisation model for reducing CE from building materials, formwork, and fuel consumption during element transportation. Applying this method to a case project shows that the proposed design optimisation method achieved reductions in CE from building materials, formwork, and prefabricated element transportation by 11.09%, 0.13%, and 30.82%, respectively, representing a 10.06% decrease in the overall embodied CE. The findings indicate that the proposed design optimisation model is effective in reducing the embodied CE of prefabricated projects.

Additionally, codes are developed in Rhino grasshopper for data extraction and visualisation of feasible solutions. Application of these codes in the studied case demonstrates that the proposed design optimisation model can extract necessary parameters from original design, whether in 2D drawing or 3D model. The feasible solution identified by the model can be expressed in 3D model, encompassing extensive information on structural design and the transportation plan. These results indicate significant potential for the proposed optimisation model's application in current design practices.

A questionnaire survey is conducted to verify the method's practicality and exploring an application approach in current design practices. Analysis on the responses reveals a considerable demand for sustainable design optimisation in Chinese construction industry. The effects and efficiency of the proposed optimisation method meet most requirements of designers. It is practical for designers to employ the proposed method for determining critical design variables for a lower embodied CE. Therefore, the proposed design optimisation method is deemed practical for application in Chinese construction industry.

9.3 Research implications

This study reviews existing strategies and approaches for sustainable design optimisation. Through introducing real-world conditions and constraints, the practicality and potential defects of these strategies are estimated. Being provided with a comprehensive view, scholars

can use the estimation results as guidance when selecting carbon analysis and estimation methods.

Additionally, this study conducts micro-level design optimisation of prefabricated element design and transportation. Comparison between macro-level and micro-level analysis reveals that simply applying macro-level sustainable strategies might not guarantee reduced CE. The uncertainty of micro-level decisions may offset the expected carbon reduction from broad principles. Therefore, the significance of introducing micro-level analysis in the design and construction process is highlighted. This approach could offer scholars a novel and thorough understanding of carbon reduction strategies and helps to refine conventional design and transportation methods. The new carbon reduction horizons are highly plausible to be discovered by applying these strategies practically and comprehensively.

Regarding element design, this research provides a practical perspective on the principle of standardisation. Designers can apply this principle as a general guideline for sustainable precast project design. Additionally, introducing micro-level variables links detailed design and formwork reuse, unveiling novel carbon reduction strategies through formwork design, manufacturing, and assembly. These strategies can complement existing carbon reduction methods, enabling designers and researchers to lessen the environment impact of precast projects.

Meanwhile, the proposed optimisation method equips architects and civil engineers with specific design details. This data could guide the design towards lower CE, preventing potential CE increases from inappropriate decisions in design development. It, therefore, facilitates the implementation of early-stage design decisions and addresses gaps left by previous early-stage tools. Additionally, the model analyses the design of formwork pieces, offering manufacturer efficient formwork blueprints, thereby enhancing the reusability of formwork pieces and reducing construction cost.

As for element transportation, this study provides a transportation CE optimisation method for prefabricated construction by integrating the bin packing problem and modal CE analysis model. The introduced transportation CE analysis method considers real-world constraints in the transportation CE calculation of prefabricated elements. It adopts element size, element quantity, and vehicle type as variables in transportation CE estimation, by which CE analysis is quantitatively linked to architecture design and construction organisation. Scholars,

architects, and civil engineers can therefore employ the method to reduce project-specific transportation CE values.

Additionally, the BP algorithm provides contractors with a detailed packing solution via the variable set of each element. Contractors can use these variables to guide transportation planning, thus achieving the smallest vehicle number. Since the transportation cost is positively related to the vehicle number, the BP algorithm could also cause a reduction in transportation costs and construction fees.

9.4 Research contributions

9.4.1 Theoretical contributions

This research challenges the effects of macro-level analysis in prefabrication design. Conventional methods, like standardisation in design optimisation and emission factor method in transportation CE analysis, are not accurate enough in estimating prefabricated projects. Therefore, scholars are encouraged to incorporate more practical and detailed data into design analysis. Shifting from macro-level estimations (based on traditional quota methods) to micro-level simulations of design and construction could reveal new decarbonisation opportunities in design practices.

The analysis on EIF utilisation in design reveals the qualitative impact of design activities. Beyond technical advantages, the requirement and preference of designers are highlighted to be considered in determining design EIF. Scholars can leverage these findings to identify the most suitable EIF for various design tasks, paving the way for future studies on sustainable design tools developments and promotions.

9.4.2 Practical contributions

This research contributes to the decarbonisation of construction projects by exploiting innovative carbon reduction strategies. Given that these strategies targets at optimising decisions made in the development stage, their reduction potential is likely to be replicable in other projects. Concurrently, these strategies offer design solutions that reduce building material consumption and transportation quantities, thereby reducing capital investment and aligning with the commercial imperatives in prefabrication scenarios.

The proposed optimisation model equips architects and civil engineers with continuous decision-making support throughout the design process. This support facilitates the implementation of early-stage design decisions and may provide additional CE reduction as design evolves. As a supplementary optimisation process, this method could be integrated seamlessly into the existing workflow, fostering the application of sustainable construction in practice. It serves a promised solution for designers and manufacturers to reduce embodied CE of prefabricated projects comprehensively.

Although this study focuses on precast construction in China, the benefits are expected to be broadly applicable. Precast project design and delivery in China is similar to those in regions like Europe, Hong Kong, and Singapore, where comparable structural design codes, methods, and processes are used. Therefore, the hypothesis and preconditions in this study are achievable, indicating the potential applicability of the proposed optimization model. In this context, the study could contribute to the advancement of sustainable construction worldwide.

9.5 Limitations and future studies

Despite the above contributions, this study yields some limitations. Firstly, the design optimisation is conducted solely from the perspective of CE. A comprehensive target integrating improving construction quality and shortening construction period remains to be considered in future studies.

Secondly, despite utilising micro-level analysis on the design and construction process of prefabricated project, the optimisation model involves approximations. Such cases include simplification assumptions mentioned in sections 4.3.3.3 and 5.3.3.3. A more complex variable set and close-to-reality model settings should be considered for real-world applications.

Thirdly, the optimisation is applied in one representative case, verifying the efficiency and practicality of the proposed method. Applying the optimisation model on more case would better validate the claim of this study.

Lastly, the exploration of feasible solutions is constrained by algorithm efficiency and computing power. Given the main focus of this study is reducing embodied CE and applying the method in design practice, the optimisation efficiency remains to be further improved. Future works are encouraged to consider more performance indicators, introduce more accurate

analysis models, improve the algorithm efficiency, and integrate the optimisation model with building information modelling.

Reference

Abanda, F. H., Oti, A. H., & Tah, J. H. M. (2017). Integrating BIM and new rules of measurement for embodied energy and CO2 assessment. *Journal of Building Engineering*, *12*(October 2016), 288–305. https://doi.org/10.1016/j.jobe.2017.06.017

Abd Rashid, A. F., & Yusoff, S. (2015). A review of life cycle assessment method for building industry. *Renewable and Sustainable Energy Reviews*, *45*, 244–248. https://doi.org/10.1016/j.rser.2015.01.043

Abdi, H., & Valentin, D. (2007). Multiple Correspondence Analysis. *Encyclopedia of Measurement and Statistics*, *2*(4), 651–657. http://www.utd.edu/

Abdollahzadeh, N., & Biloria, N. (2022). Urban microclimate and energy consumption: A multi-objective parametric urban design approach for dense subtropical cities. *Frontiers of Architectural Research*, *11*(3), 453–465. https://doi.org/10.1016/j.foar.2022.02.001

Abey, S. T., & Anand, K. B. (2019). Embodied Energy Comparison of Prefabricated and Conventional Building Construction. *Journal of The Institution of Engineers (India): Series A*, *100*(4), 777–790. https://doi.org/10.1007/s40030-019-00394-8

Ahmed, S. (2018). Barriers to Implementation of Building Information Modeling (BIM) to the Construction Industry: A Review. *Journal of Civil Engineering and Construction*, *7*(2). https://doi.org/https://doi.org/10.32732/jcec.2018.7.2.107

Alkhadashi, A., Mohammad, F., Zubayr, R. O., Aoun Klalib, H., & Balik, P. (2022). Multi-objective design optimisation of steel framed structures using three different methods. *International Journal of Structural Integrity*, *13*(1), 92–111. https://doi.org/10.1108/IJSI-07-2021-0080

Al-Obaidy, M., Courard, L., & Attia, S. (2022). A Parametric Approach to Optimizing Building Construction Systems and Carbon Footprint: A Case Study Inspired by Circularity Principles. *Sustainability (Switzerland)*, *14*(6). https://doi.org/10.3390/su14063370

Alotaibi, B. S., Khan, S. A., Abuhussain, M. A., Al-Tamimi, N., Elnaklah, R., & Kamal, M. A. (2022). Life Cycle Assessment of Embodied Carbon and Strategies for Decarbonization

of a High-Rise Residential Building. *Buildings*, *12*(8). https://doi.org/10.3390/buildings12081203

Alruwaythi, O., Asce, M., & Goodrum, P. (2019). *A Difference in Perspective: Impact of Different Formats of Engineering Information and Spatial Cognition on Craft-Worker Eye-Gaze Patterns*. https://doi.org/10.1061/(ASCE)

Alwan, Z., & Ilhan Jones, B. (2022). IFC-based embodied carbon benchmarking for early design analysis. *Automation in Construction*, *142*. https://doi.org/10.1016/j.autcon.2022.104505

Amossen, R. R., & Pisinger, D. (2010). Multi-dimensional bin packing problems with guillotine constraints. *Computers and Operations Research*, *37*(11), 1999–2006. https://doi.org/10.1016/j.cor.2010.01.017

Anastasiades, K., Goffin, J., Rinke, M., Buyle, M., Audenaert, A., & Blom, J. (2021). Standardisation: An essential enabler for the circular reuse of construction components? A trajectory for a cleaner European construction industry. I: *Journal of Cleaner Production* (Bd. 298). Elsevier Ltd. https://doi.org/10.1016/j.jclepro.2021.126864

Andersson, N., & Lessing, J. (2017). The Interface between Industrialized and Project Based Construction. *Procedia Engineering*, *196*, 220–227. https://doi.org/10.1016/j.proeng.2017.07.193

Antwi-Afari, M. F., Li, H., Pärn, E. A., & Edwards, D. J. (2018). Critical success factors for implementing building information modelling (BIM): A longitudinal review. I: *Automation in Construction* (Bd. 91, s. 100–110). Elsevier B.V. https://doi.org/10.1016/j.autcon.2018.03.010

Anvari, B., Angeloudis, P., & Ochieng, W. Y. (2016). A multi-objective GA-based optimisation for holistic Manufacturing, transportation and Assembly of precast construction. *Automation in Construction*, *71*(Part 2), 226–241. https://doi.org/10.1016/j.autcon.2016.08.007

Anwar, N., & Najam, F. A. (2017). Structures and Structural Design. I: *Structural Cross Sections* (s. 1–37). Elsevier. https://doi.org/10.1016/b978-0-12-804443-8.00001-4

Arehart, J. H., Pomponi, F., D'Amico, B., & Srubar, W. V. (2022). Structural material demand and associated embodied carbon emissions of the United States building stock: 2020–2100. *Resources, Conservation and Recycling*, *186*. https://doi.org/10.1016/j.resconrec.2022.106583

Arslan, D., Sharples, S., Mohammadpourkarbasi, H., & Khan-Fitzgerald, R. (2023). Carbon Analysis, Life Cycle Assessment, and Prefabrication: A Case Study of a High-Rise Residential Built-to-Rent Development in the UK. *Energies*, *16*(2). https://doi.org/10.3390/en16020973

Baker, B. S., Coffman, E. G., & Rivest, R. L. (1978). Orthogonal Packings in Two Dimensions. *Proceedings - Annual Allerton Conference on Communication, Control, and Computing*, *9*(4), 626–635. https://doi.org/10.1137/0209064

Baldi, M. M., Crainic, T. G., Perboli, G., & Tadei, R. (2012). The generalized bin packing problem. *Transportation Research Part E: Logistics and Transportation Review*, *48*(6), 1205–1220. https://doi.org/10.1016/j.tre.2012.06.005

Baosheng Zhou. (2019). Analysis on the construction and quality management of aluminum-alloy formwork in construction projects. *Building technology research*, *2*(3). https://doi.org/10.32629/btr.v2i3.1971

Basbagill, J., Flager, F., Lepech, M., & Fischer, M. (2013). Application of life-cycle assessment to early stage building design for reduced embodied environmental impacts. *Building and Environment*, *60*, 81–92. https://doi.org/10.1016/j.buildenv.2012.11.009

Basbagill, J. P., Flager, F. L., & Lepech, M. (2014). A multi-objective feedback approach for evaluating sequential conceptual building design decisions. *Automation in Construction*, *45*, 136–150. https://doi.org/10.1016/j.autcon.2014.04.015

Basic, S., Hollberg, A., Galimshina, A., & Habert, G. (2019). A design integrated parametric tool for real-time Life Cycle Assessment - Bombyx project. *IOP Conference Series: Earth and Environmental Science*, *323*(1). https://doi.org/10.1088/1755-1315/323/1/012112

Battisti, A., Persiani, S. G. L., & Crespi, M. (2019). Review and mapping of parameters for the early stage design of adaptive building technologies through life cycle assessment tools. *Energies*, *12*(9). https://doi.org/10.3390/en12091729

BCA. (2023). *CORENET X*. https://www1.bca.gov.sg

Bernett, A., Kral, K., & Dogan, T. (2021). Sustainability evaluation for early design (SEED) framework for energy use, embodied carbon, cost, and daylighting assessment. *Journal of Building Performance Simulation*, *14*(2), 95–115. https://doi.org/10.1080/19401493.2020.1865459

Bo, W. (2018). Analysis of Prefabricated Building Design Points. *Building Technique Development*, *45*(16), 5–6. https://doi.org/10.3969/j.issn.1001- 523X.2018.16.003.

Botsch, R. (2011). *Chapter 12: Significance and measures of association*. Scopes and Methods of Political Science. https://polisci.usca.edu/apls301/Text

BP. (2021). *Statistical Review of World Energy 2021* (Bd. 70). https://www.bp.com/content/dam/bp/business-sites/en/global/corporate/pdfs/energy-economics/statistical-review/bp-stats-review-2021-full-report.pdf

BRE Global Limited. (2024). *BREEAM*. https://breeam.com/

Brown, N. C., & Mueller, C. T. (2019). Quantifying diversity in parametric design: A comparison of possible metrics. *Artificial Intelligence for Engineering Design, Analysis and Manufacturing: AIEDAM*, *33*(1), 40–53. https://doi.org/10.1017/S0890060418000033

Bröchner, J., Josephson, P.-E., & Kadefors, A. (2002). Swedish construction culture, management and collaborative quality practice. *Building Research & Information*, *30*(6), 392–400. https://doi.org/10.1080/09613210210159866

Singapore BIM Guide - Version 2.0, Cornet. https://www.corenet.gov.sg/general/bim-guides/singapore-bim-guide-version-20.aspx

Cabeza, L. F., Boquera, L., Chàfer, M., & Vérez, D. (2021). Embodied energy and embodied carbon of structural building materials: Worldwide progress and barriers through literature map analysis. *Energy and Buildings*, *231*. https://doi.org/10.1016/j.enbuild.2020.110612

Cabeza, L. F., Rincón, L., Vilariño, V., Pérez, G., & Castell, A. (2014). Life cycle assessment (LCA) and life cycle energy analysis (LCEA) of buildings and the building sector: A

review. *Renewable and Sustainable Energy Reviews*, *29*, 394–416. https://doi.org/10.1016/j.rser.2013.08.037

Cai, B., & Zhou, Q. (2023). Application of Gpu parallel in BIM model lightweight. *2023 5th International Conference on Communications, Information System and Computer Engineering, CISCE 2023*, 415–418. https://doi.org/10.1109/CISCE58541.2023.10142347

Cang, Y., Luo, Z., Yang, L., & Han, B. (2020). A new method for calculating the embodied carbon emissions from buildings in schematic design: Taking "building element" as basic unit. *Building and Environment*, *185*(August), 107306. https://doi.org/10.1016/j.buildenv.2020.107306

Cascone, S. (2023). Digital Technologies and Sustainability Assessment: A Critical Review on the Integration Methods between BIM and LEED. I: *Sustainability (Switzerland)* (Bd. 15, Nummer 6). MDPI. https://doi.org/10.3390/su15065548

Cavalliere, C., Habert, G., Dell'Osso, G. R., & Hollberg, A. (2019). Continuous BIM-based assessment of embodied environmental impacts throughout the design process. *Journal of Cleaner Production*, *211*, 941–952. https://doi.org/10.1016/j.jclepro.2018.11.247

CCG. (2022). *China Products Carbon Footprint Factors Database*. http://lca.cityghg.com

Chan, M., Masrom, M. A. N., & Yasin, S. S. (2022). Selection of Low-Carbon Building Materials in Construction Projects: Construction Professionals' Perspectives. *Buildings*, *12*(4). https://doi.org/10.3390/buildings12040486

Charef, R., Alaka, H., & Emmitt, S. (2018). Beyond the third dimension of BIM: A systematic review of literature and assessment of professional views. *Journal of Building Engineering*, *19*, 242–257. https://doi.org/10.1016/j.jobe.2018.04.028

Chastas, P., Theodosiou, T., & Bikas, D. (2016). Embodied energy in residential buildings-towards the nearly zero energy building: A literature review. *Building and Environment*, *105*, 267–282. https://doi.org/10.1016/j.buildenv.2016.05.040

Chau, C. K., Leung, T. M., & Ng, W. Y. (2015). A review on life cycle assessment, life cycle energy assessment and life cycle carbon emissions assessment on buildings. *Applied Energy*, *143*(1), 395–413. https://doi.org/10.1016/j.apenergy.2015.01.023

Chen, Jiao, Luo, Y., Zhang, H., & Du, W. (2021). Quality evaluation of lightweight realistic 3D model based on BIM forward design. *Computer Communications*, *174*, 75–80. https://doi.org/10.1016/j.comcom.2021.04.017

Chen, Jindao, Shi, Q., Shen, L., Huang, Y., & Wu, Y. (2019). What makes the difference in construction carbon emissions between China and USA? *Sustainable Cities and Society*, *44*(April 2018), 604–613. https://doi.org/10.1016/j.scs.2018.10.017

Chen, S., Teng, Y., Zhang, Y., Leung, C. K. Y., & Pan, W. (2023). Reducing embodied carbon in concrete materials: A state-of-the-art review. *Resources, Conservation and Recycling*, *188*. https://doi.org/10.1016/j.resconrec.2022.106653

Chen, W., Yang, S., Zhang, X., Jordan, N. D., & Huang, J. (2022). Embodied energy and carbon emissions of building materials in China. *Building and Environment*, *207*(PA), 108434. https://doi.org/10.1016/j.buildenv.2021.108434

Chen, Ying, & Zhu, Y. (2010). Models for life-cycle enegy consumption and environmental emissions in residential buildings. *Journal of Tsinghua Univeristy(Science and Technology)*, *50*(3), 5.

Chen, Yonghong, & Ding, C. (2023). Multidimensional evolutionary analysis of China's BIM technology policy based on quantitative mapping. *Architectural Engineering and Design Management*. https://doi.org/10.1080/17452007.2023.2291585

Chen, Yonghong, Yang, Y., Luo, L., & Ding, C. (2023). Impacts of BIM policy on the technological progress in the Architecture, Engineering, and Construction (AEC) industry: evidence from China. *Journal of Asian Architecture and Building Engineering*. https://doi.org/10.1080/13467581.2023.2278888

Cheng, B., Huang, J., Lu, K., Li, J., Gao, G., Wang, T., & Chen, H. (2022). BIM-enabled life cycle assessment of concrete formwork waste reduction through prefabrication. *Sustainable Energy Technologies and Assessments*, *53*. https://doi.org/10.1016/j.seta.2022.102449

China Automotive Technology and Research Center. (2018). China Green Freight Assessment. *Bejing Operations*. https://theicct.org/sites/default/files/China_Freight_Assessment_English_20181022.pdf

China Institute of Building Standard Design & Research. (2015). *Drawing Collection for National Building Standard Design*. http://www.chinabuilding.com.cn

China Nonferrous Engineering Co., Ltd. (2016). *Reinforced Concrete Structure Construction Manual* (5. udg.). China Architecture Publishing & Media Co., Ltd.

Chinese Building Industry BIM Application Analysis Report Editorial Committee. (2022). *China Construction Industry BIM Application Analysis Report (2022)* (1. udg., Bd. 1). China Architecture & Building Press.

Christen, A., Coops, N. C., Crawford, B. R., Kellett, R., Liss, K. N., Olchovski, I., Tooke, T. R., Van Der Laan, M., & Voogt, J. A. (2011). Validation of modeled carbon-dioxide emissions from an urban neighborhood with direct eddy-covariance measurements. *Atmospheric Environment*, *45*(33), 6057–6069. https://doi.org/10.1016/j.atmosenv.2011.07.040

Chung, J. W., LEE, B. H., Lee, S. S., Kim, D. J., Park, J. Y., & Goo, Y. M. (2012). STUDY ON ANALYSIS OF REAL ROAD DRIVING CHARACTERISTICS OF HEAVY-DUTY GAS DELIVERY TRACTOR. *International Journal of Automotive Technology*, *13*(2), 293–300. https://doi.org/10.1007/s12239

Coenders, J. L. (2021). Next generation parametric design. *Journal of the International Association for Shell and Spatial Structures*, *62*(2), 153–166. https://doi.org/10.20898/j.iass.2021.018

Coffman, E. G., Csirik, J., Galambos, G., Martello, S., & Vigo, D. (2013). Bin packing approximation algorithms: Survey and classification. I: *Handbook of Combinatorial Optimization* (Bd. 1–5, s. 455–531). https://doi.org/10.1007/978-1-4419-7997-1_35

Copiello, S. (2017). Building energy efficiency: A research branch made of paradoxes. I: *Renewable and Sustainable Energy Reviews* (Bd. 69, s. 1064–1076). Elsevier Ltd. https://doi.org/10.1016/j.rser.2016.09.094

Creswell, J. W., & Creswell, J. David. (2013). Research Design: Qualitative, Quantitative and Mixed Methods Approaches. I: A. E. H. Salmon, C. D. E. C. Neve, E. A. M. O'Heffernan, P. E. D. C. Felts, & C. E. A. Marks (Red.), *SAGE Publications, Inc.* (Fifth Edit, Bd. 53, Nummer 9).

Cruz Reyes, L., Nieto-Yáñez, D. M., Rangel-Valdez, N., Herrera Ortiz, J. A., González B, J., Castilla Valdez, G., & Delgado-Orta, J. F. (2007). *An Algorithm for the Packing in Product Transportation Problems with Multiple Loading and Routing Variants* (A. Gelbukh & Á. F. Kuri Morales, Red.; s. 1078–1088). Springer Berlin Heidelberg.

Dadi, G. B., Goodrum, P. M., Taylor, T. R. B., & Carswell, C. M. (2014). Cognitive Workload Demands Using 2D and 3D Spatial Engineering Information Formats. *Journal of Construction Engineering and Management*, *140*(5). https://doi.org/10.1061/(asce)co.1943-7862.0000827

Dadi, G. B., Goodrum, P. M., Taylor, T. R., & Maloney, W. F. (2014). Effectiveness of communication of spatial engineering information through 3D CAD and 3D printed models. *Visualization in Engineering*, *2*(1). https://doi.org/10.1186/s40327-014-0009-8

Dadi, G. B., Taylor, T. R. B., Goodrum, P. M., & Maloney, W. F. (2014). Performance of 3D computers and 3d printed models as a fundamental means for spatial engineering information visualization. *Canadian Journal of Civil Engineering*, *41*(10), 869–877. https://doi.org/10.1139/cjce-2014-0019

Davidson, C. H., Davidson, P. L., & Ruberg, K. (1988). EXPERT SYSTEMS AND THE USE OF INFORMATION IN BUILDING DESIGN AND CONSTRUCTION. I: *91 JOURNAL OF DOCUMENTATION* (Bd. 44, Nummer 2).

Delgado, O., & Li, H. (2017). *Market Analysis and Fuel Efficiency Technology Potential of Heavy-Duty Vehicles in China* (Nummer July). www.theicct.org

Deng, Y., Li, J., Wu, Q., Pei, S., Xu, N., & Ni, G. (2020). Using network theory to explore bim application barriers for BIM sustainable development in China. *Sustainability (Switzerland)*, *12*(8). https://doi.org/10.3390/SU12083190

Desouza, C. D., Marsh, D. J., Beevers, S. D., Molden, N., & Green, D. C. (2020). Real-world emissions from non-road mobile machinery in London. *Atmospheric Environment*, *223*(July 2019), 117301. https://doi.org/10.1016/j.atmosenv.2020.117301

Adoption of Building Information Modelling for Capital Works Projects in Hong Kong, Pub. L. No. DEVB(W) 430/80/01. https://www.corenet.gov.sg

Dixit, M. K. (2017). Life cycle embodied energy analysis of residential buildings: A review of literature to investigate embodied energy parameters. *Renewable and Sustainable Energy Reviews*, *79*(October 2016), 390–413. https://doi.org/10.1016/j.rser.2017.05.051

Dixit, M. K. (2019). Life cycle recurrent embodied energy calculation of buildings: A review. *Journal of Cleaner Production*, *209*, 731–754. https://doi.org/10.1016/j.jclepro.2018.10.230

Dixit, M. K., Culp, C. H., & Fernández-Solís, J. L. (2013). System boundary for embodied energy in buildings: A conceptual model for definition. *Renewable and Sustainable Energy Reviews*, *21*, 153–164. https://doi.org/10.1016/j.rser.2012.12.037

Dixit, M. K., Fernández-Solís, J. L., Lavy, S., & Culp, C. H. (2012). Need for an embodied energy measurement protocol for buildings: A review paper. *Renewable and Sustainable Energy Reviews*, *16*(6), 3730–3743. https://doi.org/10.1016/j.rser.2012.03.021

Dong, Y. H., Jaillon, L., Chu, P., & Poon, C. S. (2015). Comparing carbon emissions of precast and cast-in-situ construction methods - A case study of high-rise private building. *Construction and Building Materials*, *99*(2015), 39–53. https://doi.org/10.1016/j.conbuildmat.2015.08.145

Du, Q., Bao, T., Li, Y., Huang, Y., & Shao, L. (2019). Impact of prefabrication technology on the cradle-to-site CO2 emissions of residential buildings. *Clean Technologies and Environmental Policy*, *21*(7), 1499–1514. https://doi.org/10.1007/s10098-019-01723-y

Dubljević, S., Tepavčević, B., Markoski, B., & Anđelković, A. S. (2023). Computational BIM tool for automated LEED certification process. *Energy and Buildings*, *292*. https://doi.org/10.1016/j.enbuild.2023.113168

Dunant, C. F., Drewniok, M. P., Eleftheriadis, S., Cullen, J. M., & Allwood, J. M. (2018). Regularity and optimisation practice in steel structural frames in real design cases. *Resources, Conservation and Recycling*, *134*, 294–302. https://doi.org/10.1016/j.resconrec.2018.01.009

Dyckhoff, H. (1990). A typology of cutting and packing problems. *European Journal of Operational Research*, *44*(2), 145–159. https://doi.org/10.1016/0377-2217(90)90350-K

El-Diraby, T., Krijnen, T., & Papagelis, M. (2017). BIM-based collaborative design and socio-technical analytics of green buildings. *Automation in Construction*, *82*, 59–74. https://doi.org/10.1016/j.autcon.2017.06.004

Elo, S., & Kyngäs, H. (2008). The qualitative content analysis process. *Journal of Advanced Nursing*, *62*(1), 107–115. https://doi.org/10.1111/j.1365-2648.2007.04569.x

Eltaweel, A., & SU, Y. (2017). Parametric design and daylighting: A literature review. I: *Renewable and Sustainable Energy Reviews* (Bd. 73, s. 1086–1103). Elsevier Ltd. https://doi.org/10.1016/j.rser.2017.02.011

EPA. (2023). *Overview of Greenhouse Gases*. https://www.epa.gov/ghgemissions

EPA, U. S. E. P. A. (2020a). *Exhaust Emission Rates for Heavy-Duty Onroad Vehicles in MOVES3*. https://www.epa.gov/sites/default/files/2020-11/documents/420r20018.pdf

EPA, U. S. E. P. A. (2020b). *Exhaust Emission Rates for Light-Duty Onroad Vehicles in MOVES3*. https://www.epa.gov/sites/production/files/2020-11/documents/420r20019.pdf

EPA, U. S. E. P. A. (2020c). *Overview of EPA ' s MOtor Vehicle Emission Simulator (MOVES3)*. https://nepis.epa.gov/Exe/ZyPDF.cgi?Dockey=P1011KV2.pdf

Erbayrak, S., Özkır, V., & Mahir Yıldırım, U. (2021). Multi-objective 3D bin packing problem with load balance and product family concerns. *Computers and Industrial Engineering*, *159*(June). https://doi.org/10.1016/j.cie.2021.107518

EN 15978:2011: Sustainability of construction works - Assessment of environmental performance of buildings. Calculation method, European Committee for Standardization. https://doi.org/10.3403/30204399

Eurostat. (2023, 10. august). *Glossary:Carbon dioxide equivalent*. Eurostat. https://ec.europa.eu/eurostat

Fang, Y., Ng, S. T., Ma, Z., & Li, H. (2018). Quota-based carbon tracing model for construction processes in China. *Journal of Cleaner Production*, *200*, 657–666. https://doi.org/10.1016/j.jclepro.2018.08.028

Farinha, C., Brito, J. de, & Veiga, M. Do. (2021). Life cycle assessment. I: *Eco-Efficient Rendering Mortars* (s. 205–234). Woodhead Publishing. https://doi.org/10.1016/B978-0-12-818494-3.00008-8

Faroe, O., Pisinger, D., & Zachariasen, M. (2003). Guided local search for the three-dimensional bin-packing problem. *INFORMS Journal on Computing*, *15*(3), 267–283. https://doi.org/10.1287/ijoc.15.3.267.16080

Feng, K., Chen, S., & Lu, W. (2019). Machine learning based construction simulation and optimization. *Proceedings - Winter Simulation Conference*, *2018-Decem*, 2025–2036. https://doi.org/10.1109/WSC.2018.8632290

Fenner, A. E., Razkenari, M., Hakim, H., & Kibert, C. (2017). *A Review of Prefabrication Benefits for Sustainable and Resilient Coastal Areas*.

Fonseca Arenas, N., & Shafique, M. (2023). Recent progress on BIM-based sustainable buildings: State of the art review. *Developments in the Built Environment*, *15*. https://doi.org/10.1016/j.dibe.2023.100176

Fu, F. (2018). Design and Analysis of Complex Structures. I: *Design and Analysis of Tall and Complex Structures* (s. 177–211). Elsevier. https://doi.org/10.1016/B978-0-08-101018-1.00006-X

Fujita, E. M., Campbell, D. E., Zielinska, B., Chow, J. C., Lindhjem, C. E., DenBleyker, A., Bishop, G. A., Schuchmann, B. G., Stedman, D. H., & Lawson, D. R. (2012). Comparison of the MOVES2010a, MOBILE6.2, and EMFAC2007 mobile source emission models with on-road traffic tunnel and remote sensing measurements. *Journal of the Air and Waste Management Association*, *62*(10), 1134–1149. https://doi.org/10.1080/10962247.2012.699016

Gan, V. J. L., Cheng, J. C. P., Lo, I. M. C., & Chan, C. M. (2017). Developing a CO2-e accounting method for quantification and analysis of embodied carbon in high-rise buildings. *Journal of Cleaner Production*, *141*, 825–836. https://doi.org/10.1016/j.jclepro.2016.09.126

Gao, S., Jin, R., & Lu, W. (2019). Design for manufacture and assembly in construction: a review. *Building Research and Information*, *0*(0), 1–13. https://doi.org/10.1080/09613218.2019.1660608

Gao, Yu;, Li, Z., Zhang, H., Yu, B., & Wang, J. (2018). A carbon emission analysis model for prefabricated construction based on LCA. *Journal of Engineering Management*, *32*(2), 30–33. https://doi.org/10.13991/j.cnki.jem.2018.02.006

Gao, Yue, & Tian, X. L. (2020). Prefabrication policies and the performance of construction industry in China. *Journal of Cleaner Production*, *253*, 120042. https://doi.org/10.1016/j.jclepro.2020.120042

Gascón Alvarez, E., Stamler, N. L., Mueller, C. T., & Norford, L. K. (2022). Shape optimization of chilled concrete ceilings – Reduced embodied carbon and enhanced operational performance. *Building and Environment*, *221*. https://doi.org/10.1016/j.buildenv.2022.109330

Gauch, H. L., Dunant, C. F., Hawkins, W., & Cabrera Serrenho, A. (2023). What really matters in multi-storey building design? A simultaneous sensitivity study of embodied carbon, construction cost, and operational energy. *Applied Energy*, *333*, 120585. https://doi.org/10.1016/j.apenergy.2022.120585

Gauch, H. L., Hawkins, W., Ibell, T., Allwood, J. M., & Dunant, C. F. (2022). Carbon vs. cost option mapping: A tool for improving early-stage design decisions. *Automation in Construction*, *136*. https://doi.org/10.1016/j.autcon.2022.104178

Geatpy team. (2022). *Geatpy*. http://geatpy.com

Gerth, R., Boqvist, A., Bjelkemyr, M., & Lindberg, B. (2013). Design for construction: Utilizing production experiences in development. *Construction Management and Economics*, *31*. https://doi.org/10.1080/01446193.2012.756142

Gibb, A. G. (1999). Off-site fabrication: prefabrication, pre-assembly and modularisation. I: *John Wiley & Sons*.

Giesekam, J., Barrett, J. R., & Taylor, P. (2016). Construction sector views on low carbon building materials. *Building Research and Information*, *44*(4), 423–444. https://doi.org/10.1080/09613218.2016.1086872

Giesekam, J., Barrett, J., Taylor, P., & Owen, A. (2014). The greenhouse gas emissions and mitigation options for materials used in UK construction. *Energy and Buildings*, *78*, 202–214. https://doi.org/10.1016/j.enbuild.2014.04.035

Google Maps. (2022). *Map of China*. https://www.google.com/maps

Gray, J. R., & Grove, S. K. (2020). *The Practice of Nursing Research: Appraisal, Synthesis, and Generation of Evidence* (9. udg., Bd. 1). Elsevier.

Guilherme Fleith de Medeiros, & Moacir Kripka. (2014). Optimization of reinforced concrete columns according to different environmental impact assessment parameters. *Engineering Structures*, *59*, 185–194. https://doi.org/10.1016/j.engstruct.2013.10.045

Guo, C., Xu, J., Yang, L., Guo, X., Liao, J., Zheng, X., Zhang, Z., Chen, X., Yang, K., & Wang, M. (2019). Life cycle evaluation of greenhouse gas emissions of a highway tunnel: A case study in China. *Journal of Cleaner Production*, *211*, 972–980. https://doi.org/10.1016/j.jclepro.2018.11.249

Guo, H., Yu, R., & Fang, Y. (2019). Analysis of negative impacts of BIM-enabled information transparency on contractors' interests. *Automation in Construction*, *103*, 67–79. https://doi.org/10.1016/j.autcon.2019.03.007

Hall, N. G., Ghosh, S., Kankey, R. D., Narasimhan, S., & Rhee, W. S. T. (1988). Bin packing problems in one dimension: Heuristic solutions and confidence intervals. *Computers and Operations Research*, *15*(2), 171–177. https://doi.org/10.1016/0305-0548(88)90009-3

Han, M., Lao, J., Yao, Q., Zhang, B., & Meng, J. (2020). Carbon inequality and economic development across the Belt and Road regions. *Journal of Environmental Management*, *262*(October 2019), 110250. https://doi.org/10.1016/j.jenvman.2020.110250

Hao, J. L., Cheng, B., Lu, W., Xu, J., Wang, J., Bu, W., & Guo, Z. (2020). Carbon emission reduction in prefabrication construction during materialization stage: A BIM-based life-cycle assessment approach. *Science of the Total Environment*, *723*, 137870. https://doi.org/10.1016/j.scitotenv.2020.137870

Hardison, D., Hallowell, M., & Littlejohn, R. (2020). Does the format of design information affect hazard recognition performance in construction hazard prevention through design reviews? *Safety Science*, *121*, 191–200. https://doi.org/10.1016/j.ssci.2019.09.008

Hart, J., D'Amico, B., & Pomponi, F. (2021). Whole-life embodied carbon in multistory buildings: Steel, concrete and timber structures. *Journal of Industrial Ecology*, *25*(2), 403–418. https://doi.org/10.1111/jiec.13139

Hasan, S., Bouferguene, A., Al-Hussein, M., Gillis, P., & Telyas, A. (2013). Productivity and CO2 emission analysis for tower crane utilization on high-rise building projects. *Automation in Construction*, *31*, 255–264. https://doi.org/10.1016/j.autcon.2012.11.044

Herr, C. M., & Fischer, T. (2019). BIM adoption across the Chinese AEC industries: An extended BIM adoption model. *Journal of Computational Design and Engineering*, *6*(2), 173–178. https://doi.org/10.1016/j.jcde.2018.06.001

Hester, J., Gregory, J., Ulm, F. J., & Kirchain, R. (2018). Building design-space exploration through quasi-optimization of life cycle impacts and costs. *Building and Environment*, *144*(June), 34–44. https://doi.org/10.1016/j.buildenv.2018.08.003

Hollberg, A. (2016). LCA in architectural design — a parametric approach. *The International Journal of Life Cycle Assessment*, 943–960. https://doi.org/10.1007/s11367-016-1065-1

Hollberg, A., & Ruth, J. (2016). LCA in architectural design—a parametric approach. *International Journal of Life Cycle Assessment*, *21*(7), 943–960. https://doi.org/10.1007/s11367-016-1065-1

Hong, J., Shen, G. Q., Feng, Y., Lau, W. S., & Mao, C. (2015). Greenhouse gas emissions during the construction phase of a building: a case study in China. *Journal of Cleaner Production*, *103*(Carbon Emissions Reduction: Policies, Technologies, Monitoring, Assessment and Modeling), 249–259. http://10.0.3.248/j.jclepro.2014.11.023

Hong, J., Shen, G. Q., Li, Z., Zhang, B., & Zhang, W. (2018). Barriers to promoting prefabricated construction in China: A cost–benefit analysis. *Journal of Cleaner Production*, *172*, 649–660. https://doi.org/10.1016/j.jclepro.2017.10.171

Hong, J., Shen, G. Q., Mao, C., Li, Z., & Li, K. (2016). Life-cycle energy analysis of prefabricated building components: An input-output-based hybrid model. *Journal of Cleaner Production*, *112*(2016), 2198–2207. https://doi.org/10.1016/j.jclepro.2015.10.030

Hough, M. J., & Lawson, R. M. (2019). Design and construction of high-rise modular buildings based on recent projects. *Proceedings of the Institution of Civil Engineers: Civil Engineering*, *172*(6), 37–44. https://doi.org/10.1680/jcien.18.00058

Huang, G., Song, G., Yu, L., & Xu, Y. (2010). Overview of the Comprehensive Mobile Source Emissions Model: MOVES. *Computer and Communications*, *28*(4), 49–53.

Hyun, C., Jin, C., Shen, Z., & Kim, H. (2018). Automated optimization of formwork design through spatial analysis in building information modeling. *Automation in Construction*, *95*, 193–205. https://doi.org/10.1016/j.autcon.2018.07.023

Iacovidou, E., Purnell, P., Tsavdaridis, K. D., & Poologanathan, K. (2021). Digitally enabled modular construction for promoting modular components reuse: A UK view. I: *Journal of Building Engineering* (Bd. 42). Elsevier Ltd. https://doi.org/10.1016/j.jobe.2021.102820

Ibrahim, Y., Kershaw, T., Shepherd, P., & Elwy, I. (2021). A parametric optimisation study of urban geometry design to assess outdoor thermal comfort. *Sustainable Cities and Society*, *75*. https://doi.org/10.1016/j.scs.2021.103352

Ismail, M. A., & Mueller, C. T. (2021). Minimizing embodied energy of reinforced concrete floor systems in developing countries through shape optimization. *Engineering Structures*, *246*. https://doi.org/10.1016/j.engstruct.2021.112955

ISO 14040:2006: Environmental management - Life cycle assessment - Principles and framework, ISO. https://www.iso.org/standard/37456.html

ISO 14001:2015: Environmental management systems — Requirements with guidance for use, Pub. L. No. ISO 14001:2015, ISO. https://www.iso.org/standard/60857.html

ISO 19650: Organization and digitization of information about buildings and civil engineering works, including building information modelling (BIM) — Information management using building information modelling, Pub. L. No. ISO 19650-1:2018. https://www.iso.org/standard/68078.html

Jafary Nasab, T., Monavari, S. M., Jozi, S. A., & Majedi, H. (2020). Assessment of carbon footprint in the construction phase of high-rise constructions in Tehran. *International Journal of Environmental Science and Technology*, *17*(6), 3153–3164. https://doi.org/10.1007/s13762-019-02557-3

Jayasinghe, A., Orr, J., Ibell, T., & Boshoff, W. P. (2021). Minimising embodied carbon in reinforced concrete beams. *Engineering Structures*, *242*. https://doi.org/10.1016/j.engstruct.2021.112590

Jayasinghe, A., Orr, J., Ibell, T., & Boshoff, W. P. (2022). Minimising embodied carbon in reinforced concrete flat slabs through parametric design. *Journal of Building Engineering*, *50*. https://doi.org/10.1016/j.jobe.2022.104136

Ji, Y., Zhu, F., Li, H. X., & Al-Hussein, M. (2017). Construction industrialization in China: Current profile and the prediction. *Applied Sciences (Switzerland)*, *7*(2). https://doi.org/10.3390/app7020180

Jin, K., Zheng, M., Qu, Z., & Xie, H. (2022). Building Design Process and Prefabricated Building Scheme Design based on BIM Technology. *Construction Science and Technology*, *17*, 70–73.

Jusselme, T., Rey, E., & Andersen, M. (2020). Surveying the environmental life-cycle performance assessments: Practice and context at early building design stages. *Sustainable Cities and Society*, *52*(January 2019), 101879. https://doi.org/10.1016/j.scs.2019.101879

Kanafani, K., Kjaer Zimmermann, R., Nygaard Rasmussen, F., & Birgisdóttir, H. (2019). Early Design Stage Building LCA using the LCAbyg Tool: New Strategies for Bridging the

Data Gap. *IOP Conference Series: Earth and Environmental Science*, *323*(1). https://doi.org/10.1088/1755-1315/323/1/012117

Kanyilmaz, A., Tichell, P. R. N., & Loiacono, D. (2022). A genetic algorithm tool for conceptual structural design with cost and embodied carbon optimization. *Engineering Applications of Artificial Intelligence*, *112*. https://doi.org/10.1016/j.engappai.2022.104711

Karlsson, I., Rootzén, J., & Johnsson, F. (2020). Reaching net-zero carbon emissions in construction supply chains – Analysis of a Swedish road construction project. *Renewable and Sustainable Energy Reviews*, *120*. https://doi.org/10.1016/j.rser.2019.109651

Kreiner, H., Passer, A., & Wallbaum, H. (2015). A new systemic approach to improve the sustainability performance of office buildings in the early design stage. *Energy and Buildings*, *109*, 385–396. https://doi.org/10.1016/j.enbuild.2015.09.040

Kremer, P. D. (2018). Design for Mass Customised Manufacturing and Assembly (DfMCMA): A New Framework for Mass Timber Construction. *Mass Timber Construction Journal*, *1*(1). www.masstimberconstructionjournal.com

Kyngäs, H., & Kaakinen, P. (2020). Deductive Content Analysis. I: H. Kyngäs, K. Mikkonen, & M. Kääriäinen (Red.), *The Application of Content Analysis in Nursing Science Research* (s. 23–30). Springer International Publishing. https://doi.org/10.1007/978-3-030-30199-6_3

Leon, M., & Laing, R. (2022). A concept design stages protocol to support collaborative processes in architecture, engineering and construction projects. *Journal of Engineering, Design and Technology*, *20*(3), 777–799. https://doi.org/10.1108/JEDT-10-2020-0399

Li, C. Z., Lai, X., Xiao, B., Tam, V. W. Y., Guo, S., & Zhao, Y. (2020). A holistic review on life cycle energy of buildings: An analysis from 2009 to 2019. *Renewable and Sustainable Energy Reviews*, *134*(September), 110372. https://doi.org/10.1016/j.rser.2020.110372

Li, D., Cui, P., & Lu, Y. (2016). Development of an automated estimator of life-cycle carbon emissions for residential buildings: A case study in Nanjing, China. *Habitat International*, *57*, 154–163. https://doi.org/10.1016/j.habitatint.2016.07.003

Li, J., Afsari, K., Li, N., Peng, J., Wu, Z., & Cui, H. (2020). A review for presenting building information modeling education and research in China. I: *Journal of Cleaner Production* (Bd. 259). Elsevier Ltd. https://doi.org/10.1016/j.jclepro.2020.120885

Li, L., Li, Z., Li, X., Zhang, S., & Luo, X. (2020). A new framework of industrialized construction in China: Towards on-site industrialization. *Journal of Cleaner Production*, *244*, 118469. https://doi.org/10.1016/j.jclepro.2019.118469

Li, W., Yang, M., Long, R., He, Z., Zhang, L., & Chen, F. (2021). Assessment of greenhouse gasses and air pollutant emissions embodied in cross-province electricity trade in China. *Resources, Conservation and Recycling*, *171*. https://doi.org/10.1016/j.resconrec.2021.105623

Li, X. juan, Xie, W. jun, Xu, L., Li, L. lu, Jim, C. Y., & Wei, T. bing. (2022). Holistic life-cycle accounting of carbon emissions of prefabricated buildings using LCA and BIM. *Energy and Buildings*, *266*. https://doi.org/10.1016/j.enbuild.2022.112136

Li, Z., Shen, G. Q., & Xue, X. (2014). Critical review of the research on the management of prefabricated construction. *Habitat International*, *43*, 240–249. https://doi.org/10.1016/j.habitatint.2014.04.001

Liao, L., Teo, E. A. L., Li, L., Zhao, X., & Wu, G. (2021). Reducing Non-Value-Adding BIM Implementation Activities for Building Projects in Singapore: Leading Causes. *Journal of Management in Engineering*, *37*(3). https://doi.org/10.1061/(asce)me.1943-5479.0000900

Lidelöw, S., Engström, S., & Samuelson, O. (2023). The promise of BIM? Searching for realized benefits in the Nordic architecture, engineering, construction, and operation industries. *Journal of Building Engineering*, *76*. https://doi.org/10.1016/j.jobe.2023.107067

Lim, A., Rodrigues, B., & Yang, Y. (2005). 3-D container packing heuristics. *Applied Intelligence*, *22*(2), 125–134. https://doi.org/10.1007/s10489-005-5601-0

Lim, T. K., Gwak, H. S., Kim, B. S., & Lee, D. E. (2016). Integrated carbon emission estimation method for construction operation and project scheduling. *KSCE Journal of Civil Engineering*, *20*(4), 1211–1220. https://doi.org/10.1007/s12205-015-0360-x

Lin, J., Li, H., Huang, W., Xu, W., & Cheng, S. (2019). A Carbon Footprint of High-Speed Railways in China: A Case Study of the Beijing-Shanghai Line. *Journal of Industrial Ecology*, *23*(4), 869–878. https://doi.org/10.1111/jiec.12824

Liu, G., Chen, R., Xu, P., Fu, Y., Mao, C., & Hong, J. (2020). Real-time carbon emission monitoring in prefabricated construction. *Automation in Construction*, *110*(174), 102945. https://doi.org/10.1016/j.autcon.2019.102945

Liu, G., Gu, T., Xu, P., Hong, J., Shrestha, A., & Martek, I. (2019). A production line-based carbon emission assessment model for prefabricated components in China. *Journal of Cleaner Production*, *209*, 30–39. https://doi.org/10.1016/j.jclepro.2018.10.172

Liu, G., Yang, H., Fu, Y., Mao, C., Xu, P., Hong, J., & Li, R. (2020). Cyber-physical system-based real-time monitoring and visualization of greenhouse gas emissions of prefabricated construction. *Journal of Cleaner Production*, *246*, 119059. https://doi.org/10.1016/j.jclepro.2019.119059

Liu, H., Singh, G., Lu, M., Bouferguene, A., & Al-Hussein, M. (2018). BIM-based automated design and planning for boarding of light-frame residential buildings. *Automation in Construction*, *89*, 235–249. https://doi.org/10.1016/j.autcon.2018.02.001

Liu, Q., Cheng, H., Tian, T., Wang, Y., Leng, J., Zhao, R., Zhang, H., & Wei, L. (2021). Algorithms for the variable-sized bin packing problem with time windows. *Computers and Industrial Engineering*, *155*(May 2020), 107175. https://doi.org/10.1016/j.cie.2021.107175

Liu, Y., van Nederveen, S., & Hertogh, M. (2017). Understanding effects of BIM on collaborative design and constructionAn empirical study in China. *International Journal of Project Management*, *35*(4), 686–698. https://doi.org/10.1016/j.ijproman.2016.06.007

Lodi, A., Martello, S., & Monaci, M. (2002). Two-dimensional packing problems: A survey. *European Journal of Operational Research*, *141*(2), 241–252. https://doi.org/10.1016/S0377-2217(02)00123-6

Lodi, A., Martello, S., & Vigo, D. (2002). Heuristic algorithms for the three-dimensional bin packing problem. *European Journal of Operational Research*, *141*(2), 410–420. https://doi.org/10.1016/S0377-2217(02)00134-0

Lotteau, M., Loubet, P., & Sonnemann, G. (2017). An analysis to understand how the shape of a concrete residential building influences its embodied energy and embodied carbon. *Energy and Buildings*, *154*, 1–11. https://doi.org/10.1016/j.enbuild.2017.08.048

Lu, K., Jiang, X., Tam, V. W. Y., Li, M., Wang, H., Xia, B., & Chen, Q. (2019). Development of a carbon emissions analysis framework using building information modeling and life cycle assessment for the construction of hospital projects. *Sustainability (Switzerland)*, *11*(22), 1–18. https://doi.org/10.3390/su11226274

Luo, T., Xue, X., Wang, Y., Xue, W., & Tan, Y. (2021). A systematic overview of prefabricated construction policies in China. *Journal of Cleaner Production*, *280*. https://doi.org/10.1016/j.jclepro.2020.124371

LÜ, C., ZHANG, Z., CHEN, X., MA, D., & CAI, B. (2021). Study on CO2 emission factors of road transport in Chinese provinces. *China Environmental Science*, *41*(7), 3122–3130.

Ma, X., Darko, A., Chan, A. P. C., Wang, R., & Zhang, B. (2022). An empirical analysis of barriers to building information modelling (BIM) implementation in construction projects: evidence from the Chinese context. *International Journal of Construction Management*, *22*(16), 3119–3127. https://doi.org/10.1080/15623599.2020.1842961

Mao, C., Shen, Q., Shen, L., & Tang, L. (2013). Comparative study of greenhouse gas emissions between off-site prefabrication and conventional construction methods: Two case studies of residential projects. *Energy & Buildings*, *66*, 165–176. http://10.0.3.248/j.enbuild.2013.07.033

Marsh, E., Orr, J., & Ibell, T. (2021). Quantification of uncertainty in product stage embodied carbon calculations for buildings. *Energy and Buildings*, *251*. https://doi.org/10.1016/j.enbuild.2021.111340

Marsh, R. (2016). LCA profiles for building components: Strategies for the early design process. *Building Research and Information*, *44*(4), 358–375. https://doi.org/10.1080/09613218.2016.1102013

Mattern, H., & König, M. (2017). Concepts for Formal Modeling and Management of Building Design Options. *Computing in Civil Engineering 2017*.

Minunno, R., O'Grady, T., Morrison, G. M., & Gruner, R. L. (2021). Investigating the embodied energy and carbon of buildings: A systematic literature review and meta-analysis of life cycle assessments. *Renewable and Sustainable Energy Reviews*, *143*(March), 110935. https://doi.org/10.1016/j.rser.2021.110935

Calculation standard of building carbon emissions GB/T 51366-2019, 19. https://www.mohurd.gov.cn

Technical specification for precast concrete structures. http://www.mohurd.gov.cn/wjfb/202002/t20200221_244041.html

MOHURD. (2015). *Notice on the Issuance of Guidelines for Promoting the Application of Building Information Modeling by the Ministry of Housing and Urban-Rural Development*.

MOHURD. (2022). *Circular of the standard quota Department of the Ministry of housing and urban rural development on the development of prefabricated buildings in China in 2021*. https://www.mohurd.gov.cn

Notice from the Ministry of Housing and Urban-Rural Development on Promoting the Standardization, Normalization, and Facilitation of Engineering Construction Project Approvals. https://www.mohurd.gov.cn

Moncaster, A., Malmqvist, T., Forman, T., Pomponi, F., & Anderson, J. (2022). Embodied carbon of concrete in buildings, Part 2: are the messages accurate? *Buildings and Cities*, *3*(1), 334–355. https://doi.org/10.5334/bc.199

Monedero, J. (2000). Parametric design: a review and some experiences. *Automation in Construction*, *9*, 369–377. https://doi.org/https://doi.org/10.1016/S0926-5805(99)00020-5

Moon, I., & Nguyen, T. V. L. (2014). Container packing problem with balance constraints. *OR Spectrum*, *36*(4), 837–878. https://doi.org/10.1007/s00291-013-0356-1

Moynihan, M. C., & Allwood, J. M. (2014). Utilization of structural steel in buildings. I: *Proceedings of the Royal Society A: Mathematical, Physical and Engineering Sciences* (Bd. 470, Nummer 2168). Royal Society. https://doi.org/10.1098/rspa.2014.0170

Munien, C., & Ezugwu, A. E. (2021). Metaheuristic algorithms for one-dimensional bin-packing problems: A survey of recent advances and applications. *Journal of Intelligent Systems*, *30*(1), 636–663. https://doi.org/10.1515/jisys-2020-0117

Muresan, B., Capony, A., Goriaux, M., Pillot, D., Higelin, P., Proust, C., & Jullien, A. (2015). Key factors controlling the real exhaust emissions from earthwork machines. *Transportation Research Part D: Transport and Environment*, *41*, 271–287. https://doi.org/10.1016/j.trd.2015.10.002

Murti, C. K., & Muslim, F. (2023). Relationship between Functions, Drivers, Barriers, and Strategies of Building Information Modelling (BIM) and Sustainable Construction Criteria: Indonesia Construction Industry. *Sustainability*, *15*(6), 5526. https://doi.org/10.3390/su15065526

Muthumanickam, N. K., Duarte, J. P., & Simpson, T. W. (2023). Multidisciplinary concurrent optimization framework for multi-phase building design process. *Artificial Intelligence for Engineering Design, Analysis and Manufacturing: AIEDAM*, *37*. https://doi.org/10.1017/S0890060422000191

Nanjing Municipal Bureau of Planning and Natural Resources. (2021). *Notice on Accelerating the Promotion of Building Information Modeling (BIM) Technology Application in Nanjing*. https://ghj.nanjing.gov.cn

Nawarathna, A., Siriwardana, M., & Alwan, Z. (2021). Embodied carbon as a material selection criterion: Insights from sri lankan construction sector. *Sustainability (Switzerland)*, *13*(4), 1–20. https://doi.org/10.3390/su13042202

Nembrini, J., Samberger, S., & Labelle, G. (2014). Parametric scripting for early design performance simulation. *Energy and Buildings*, *68*(PART C), 786–798. https://doi.org/10.1016/j.enbuild.2013.09.044

Nidheesh, P. V., & Kumar, M. S. (2019). An overview of environmental sustainability in cement and steel production. I: *Journal of Cleaner Production* (Bd. 231, s. 856–871). Elsevier Ltd. https://doi.org/10.1016/j.jclepro.2019.05.251

O'driscoll, M. (2002). Design for manufacture. *Journal of Materials Processing Technology*, *122*(2–3), 318–321. https://doi.org/10.1016/S0924-0136(01)01132-3

Olanrewaju, O. I., Kineber, A. F., Chileshe, N., & Edwards, D. J. (2022). Modelling the relationship between Building Information Modelling (BIM) implementation barriers, usage and awareness on building project lifecycle. *Building and Environment*, *207*. https://doi.org/10.1016/j.buildenv.2021.108556

Orr, J., Drewniok, M. P., Walker, I., Ibell, T., Copping, A., & Emmitt, S. (2019). Minimising energy in construction: Practitioners' views on material efficiency. *Resources, Conservation and Recycling*, *140*, 125–136. https://doi.org/10.1016/j.resconrec.2018.09.015

Ozturk, G. B., Arditi, D., Yitmen, I., & Yalcinkaya, M. (2016). The Factors Affecting Collaborative Building Design. *Procedia Engineering*, *161*, 797–803. https://doi.org/10.1016/j.proeng.2016.08.712

Pan, W., Li, K., & Teng, Y. (2018). Rethinking system boundaries of the life cycle carbon emissions of buildings. I: *Renewable and Sustainable Energy Reviews* (Bd. 90, s. 379–390). Elsevier Ltd. https://doi.org/10.1016/j.rser.2018.03.057

Paulson, B. C. (1976). DESIGNING TO REDUCE CONSTRUCTION COSTS. *Journal of the Construction Division*, *102*(4). https://doi.org/https://doi.org/10.1061/JCCEAZ.0000639

Pauwels, P., Van Deursen, D., de Roo, J., Van Ackere, T., de Meyer, R., Van de Walle, R., & Van Campenhout, J. (2011). Three-dimensional information exchange over the semantic web for the domain of architecture, engineering, and construction. *Artificial Intelligence for Engineering Design, Analysis and Manufacturing: AIEDAM*, *25*(4), 317–332. https://doi.org/10.1017/S0890060411000199

Phillips, D. C., & Burbules, N. C. (2000). *Postpositivism and educational research* (1. udg., Bd. 1). Rowman & Littlefield.

Polat, G. (2008). Factors Affecting the Use of Precast Concrete Systems in the United States. *Journal of Construction Engineering and Management*, *134*(3), 169–178. https://doi.org/10.1061/ASCE0733-93642008134:3169

Ren, Z., Anumba, C. J., & Yang, F. (2013). Development of CDPM matrix for the measurement of collaborative design performance in construction. *Automation in Construction*, *32*, 14–23. https://doi.org/10.1016/j.autcon.2012.11.019

RIBA. (2020). *RIBA Plan of Work 2020*. www.ribaplanofwork.com

Richard, R. B. (2005). Industrialised building systems: Reproduction before automation and robotics. *Automation in Construction*, *14*(4), 442–451. https://doi.org/10.1016/j.autcon.2004.09.009

Roberts, M., Allen, S., & Coley, D. (2020). Life cycle assessment in the building design process – A systematic literature review. *Building and Environment*, *185*(June), 107274. https://doi.org/10.1016/j.buildenv.2020.107274

Rodrigues, C., Kirchain, R., Freire, F., & Gregory, J. (2018). Streamlined environmental and cost life-cycle approach for building thermal retro fi ts : A case of residential buildings in South European climates. *Journal of Cleaner Production*, *172*, 2625–2635. https://doi.org/10.1016/j.jclepro.2017.11.148

School of Transportation and Logistics of Southwest Jiaotong University. (2020). *Preliminary Report on the Freight Industry*. https://www.efchina.org

Sean Carroll. (2023). *Finite Element Analysis of 3D Structures using Python*. Degree Tutors. https://www.degreetutors.com/

Sebaibi, N., & Boutouil, M. (2020). Reducing energy consumption of prefabricated building elements and lowering the environmental impact of concrete. *Engineering Structures*, *213*(April), 110594. https://doi.org/10.1016/j.engstruct.2020.110594

Seo, J., Yun, B., Kim, J., Shin, M., & Park, S. (2022). Development of a cold-start emission model for diesel vehicles using an artificial neural network trained with real-world driving data. *Science of the Total Environment*, *806*, 151347. https://doi.org/10.1016/j.scitotenv.2021.151347

Shadram, F., Johansson, T. D., Lu, W., Schade, J., & Olofsson, T. (2016). An integrated BIM-based framework for minimizing embodied energy during building design. *Energy and Buildings*, *128*, 592–604. https://doi.org/10.1016/j.enbuild.2016.07.007

Shadram, F., & Mukkavaara, J. (2018). An integrated BIM-based framework for the optimization of the trade-off between embodied and operational energy. *Energy and Buildings*, *158*, 1189–1205. https://doi.org/10.1016/j.enbuild.2017.11.017

Shang, Z., Gu, J., & Huang, Q. (2020). *Algorithm and application of packing problem* (X. He, Red.; 1. udg.). China University of Mining and Technology Assets Management CO., LTD.

Shen, X., Lv, T., Zhang, X., Cao, X., Li, X., Wu, B., Yao, X., Shi, Y., Zhou, Q., Chen, X., & Yao, Z. (2021). Real-world emission characteristics of black carbon emitted by on-road China IV and China V diesel trucks. *Science of the Total Environment*, *799*, 149435. https://doi.org/10.1016/j.scitotenv.2021.149435

Shi, Y., Du, J., Asce, M., Qi Zhu, ;, & Liu, X. (2020). The Impact of Engineering Information Formats on Workers' Cognitive Load in Working Memory Development. *Construction Research Congress 2020*.

Shi, Y., Du, J., & Worthy, D. A. (2020). The impact of engineering information formats on learning and execution of construction operations: A virtual reality pipe maintenance experiment. *Automation in Construction*, *119*. https://doi.org/10.1016/j.autcon.2020.103367

Shiel, P., Tarantino, S., & Fischer, M. (2018). Parametric analysis of design stage building energy performance simulation models. *Energy and Buildings*, *172*, 78–93. https://doi.org/10.1016/j.enbuild.2018.04.045

Solomon, H., & Weiner, H. (1986). A review of the packing problem. *Communications in Statistics - Theory and Methods*, *15*(9), 2571–2607. https://doi.org/10.1080/03610928608829274

Stephan, A., & Stephan, L. (2016). Life cycle energy and cost analysis of embodied, operational and user-transport energy reduction measures for residential buildings. *Applied Energy*, *161*, 445–464. https://doi.org/10.1016/j.apenergy.2015.10.023

Stephen Emmitt, & Christopher A. Gorse. (2003). *Construction Communication* (1. udg.). Wiley-Blackwell.

Stocker, T. F., Qin, D., Plattner, G. K., Tignor, M. M. B., Allen, S. K., Boschung, J., Nauels, A., Xia, Y., Bex, V., & Midgley, P. M. (2014). *Climate Change 2013 – The Physical Science Basis* (Intergovernmental Panel on Climate Change, Red.). Cambridge University Press. https://doi.org/10.1017/CBO9781107415324

Sweany, J., Goodrum, P., & Miller, J. (2016). Analysis of empirical data on the effects of the format of engineering deliverables on craft performance. *Automation in Construction*, *69*, 59–67. https://doi.org/10.1016/j.autcon.2016.05.017

Tabadkani, A., Banihashemi, S., & Hosseini, M. R. (2018). Daylighting and visual comfort of oriental sun responsive skins: A parametric analysis. *Building Simulation*, *11*(4), 663–676. https://doi.org/10.1007/s12273-018-0433-0

Tan, T., Chen, K., Xue, F., & Lu, W. (2019). Barriers to Building Information Modeling (BIM) implementation in China's prefabricated construction: An interpretive structural modeling (ISM) approach. *Journal of Cleaner Production*, *219*, 949–959. https://doi.org/10.1016/j.jclepro.2019.02.141

Tan, T., Mills, G., Papadonikolaki, E., & Liu, Z. (2021). Combining multi-criteria decision making (MCDM) methods with building information modelling (BIM): A review. I: *Automation in Construction* (Bd. 121). Elsevier B.V. https://doi.org/10.1016/j.autcon.2020.103451

Teng, Y., Li, K., Pan, W., & Ng, T. (2018). Reducing building life cycle carbon emissions through prefabrication: Evidence from and gaps in empirical studies. *Building and Environment*, *132*(January), 125–136. https://doi.org/10.1016/j.buildenv.2018.01.026

Teng, Y., & Pan, W. (2020). Estimating and minimizing embodied carbon of prefabricated high-rise residential buildings considering parameter, scenario and model uncertainties. *Building and Environment*, *180*. https://doi.org/10.1016/j.buildenv.2020.106951

Teo, E. A. L., Ofori, G., Tjandra, I. K., & Kim, H. (2016). The Use of BIM in the Singapore Construction Industry: Opportunities and Challenges. *CIB World Building Congress*.

Specification for information management for the capital/delivery phase of construction projects using building information modelling: PAS 1192-2:2013, BSI Standards Publication.

Tian, Y., & Spatari, S. (2022). Environmental life cycle evaluation of prefabricated residential construction in China. *Journal of Building Engineering*, *57*. https://doi.org/10.1016/j.jobe.2022.104776

Togpographic-map.com. (2022). *Topographic map of China*. https://zh-cn.topographic-map.com

Tribelsky, E., & Sacks, R. (2010). Measuring information flow in the detailed design of construction projects. *Research in Engineering Design*, *21*(3), 189–206. https://doi.org/10.1007/s00163-009-0084-3

Trinh, H. T. M. K., Chowdhury, S., Nguyen, M. T., & Liu, T. (2021). Optimising flat plate buildings based on carbon footprint using Branch-and-Reduce deterministic algorithm. *Journal of Cleaner Production*, *320*. https://doi.org/10.1016/j.jclepro.2021.128780

Tu, R., Li, T., Meng, C., Chen, J., Sheng, Z., Xie, Y., Xie, F., Yang, F., Chen, H., Li, Y., Gao, J., & Liu, Y. (2021). Real-world emissions of construction mobile machines and comparison to a non-road emission model. *Science of the Total Environment*, *771*, 145365. https://doi.org/10.1016/j.scitotenv.2021.145365

UKBIMA. (2021). *State of the Nation Survey 2021*. https://ukbimalliance.co.uk/ukbima-state-of-the-nation-annual-survey-report-2021/

United Nations. (2021, 23. februar). *Climate Change 'Biggest Threat Modern Humans Have Ever Faced', World-Renowned Naturalist Tells Security Council, Calls for Greater Global Cooperation*. United Nations.

United Nations Environment Programme. (2022). *2022 Global Status Report for Buildings and Construction: Towards a Zero-emission, Efficient and Resilient Buildings and Construction Sector.* www.globalabc.org.

United Nations environment programme. (2024). *2023 Global Status Report for Buildings and Construction: Beyond foundations - Mainstreaming sustainable solutions to cut emissions from the buildings sector*. United Nations Environment Programme. https://doi.org/10.59117/20.500.11822/45095

Urbieta, M., Urbieta, M., Laborde, T., Villarreal, G., & Rossi, G. (2023). Generating BIM model from structural and architectural plans using Artificial Intelligence. *Journal of Building Engineering*, *78*, 107672. https://doi.org/10.1016/j.jobe.2023.107672

USGBC. (2024). *LEED rating system*. https://www.usgbc.org/leed

Vallamsundar, S., & Lin, J. (2011). MOVES Versus MOBILE: Comparison of greenhouse gas and criterion pollutant emissions. *Transportation Research Record*, *2233*, 27–35. https://doi.org/10.3141/2233-04

Victoria, M. F., & Perera, S. (2018). Managing embodied carbon in buildings: a Pareto approach. *Built Environment Project and Asset Management*, *8*(5), 504–514. https://doi.org/10.1108/BEPAM-10-2017-0095

Wallace, H. W., Jobson, B. T., Erickson, M. H., McCoskey, J. K., VanReken, T. M., Lamb, B. K., Vaughan, J. K., Hardy, R. J., Cole, J. L., Strachan, S. M., & Zhang, W. (2012). Comparison of wintertime CO to NO x ratios to MOVES and MOBILE6.2 on-road emissions inventories. *Atmospheric Environment*, *63*(x), 289–297. https://doi.org/10.1016/j.atmosenv.2012.08.062

Wang, A., Tu, R., Xu, J., Zhai, Z., & Hatzopoulou, M. (2022). A novel modal emission modelling approach and its application with on-road emission measurements. *Applied Energy*, *306*(PA), 117967. https://doi.org/10.1016/j.apenergy.2021.117967

Wang, H., Zhang, H., Hou, K., & Yao, G. (2021). Carbon emissions factor evaluation for assembled building during prefabricated component transportation phase. *Energy Exploration and Exploitation*, *39*(1), 385–408. https://doi.org/10.1177/0144598720973371

Wang, H., Zhao, L., Zhang, H., Qian, Y., Xiang, Y., Luo, Z., & Wang, Z. (2023). Carbon emission analysis of precast concrete building Construction: A study on component transportation phase using Artificial Neural Network. *Energy and Buildings*, *301*. https://doi.org/10.1016/j.enbuild.2023.113708

Wang, J., Gui, H., Yang, Z., Yu, T., Zhang, X., & Liu, J. (2022). Real-world gaseous emission characteristics of natural gas heavy-duty sanitation trucks. *Journal of Environmental Sciences (China)*, *115*, 319–329. https://doi.org/10.1016/j.jes.2021.06.023

Wang, W., Zmeureanu, R., & Rivard, H. (2005). Applying multi-objective genetic algorithms in green building design optimization. *Building and Environment*, *40*(11), 1512–1525. https://doi.org/10.1016/j.buildenv.2004.11.017

Wang, Yangyang, Yang, X., Hou, Q., Tao, J., & Dong, J. (2022). Quantitative Study on the Life-Cycle Carbon Emissions of a Nearly Zero Energy Building in the Severe Cold Zones of China. *Sustainability (Switzerland)*, *14*(3). https://doi.org/10.3390/su14031448

Wang, Yuna, Xue, X., Yu, T., & Wang, Y. (2020). Mapping the dynamics of China's prefabricated building policies from 1956 to 2019: a bibliometric analysis. *Building Research and Information*, 1–18. https://doi.org/10.1080/09613218.2020.1789444

Wei, H. M., & Hu, W. J. (2014). What are the resistances that hamper the application of BIM in China? *Applied Mechanics and Materials*, *525*, 681–684. https://doi.org/10.4028/www.scientific.net/AMM.525.681

Wen, X., Teng, Y., & Shen, G. Q. (2024). Extended end-of-life carbon assessment and savings: A case study of steel-framed modular buildings in Hong Kong. *Building and Environment*, *266*. https://doi.org/10.1016/j.buildenv.2024.112056

Wong, F., & Tang, Y. T. (2012). Comparative Embodied Carbon Analysis of the Prefabrication Elements compared with In-situ Elements in Residential Building Development of Hong Kong. *World Academy of Science, Engineering and Technology*, *62*(2), 161–166.

Wu, K., García de Soto, B., Adey, B. T., & Zhang, F. (2020). BIM-based estimation of vertical transportation demands during the construction of high-rise buildings. *Automation in Construction*, *110*. https://doi.org/10.1016/j.autcon.2019.102985

Wäscher, G., Haußner, H., & Schumann, H. (2007). An improved typology of cutting and packing problems. *European Journal of Operational Research*, *183*(3), 1109–1130. https://doi.org/10.1016/j.ejor.2005.12.047

Xiang, Y. (2020). *A Research on Component-based Site Record Framework: Cased on C-House and the Dogaba in Qixia Temple* [Master of Architecture, Southeast University]. https://doi.org/10.27014/d.cnki.gdnau.2020.003746

Xiang, Y., Ma, K., Mahamadu, A.-M., Florez-Perez, L., Zhu, K., & Wu, Y. (2022). Embodied Carbon Determination in the Transportation Stage of Prefabricated Constructions: A Micro-level Model Using the Bin-packing Algorithm and Modal Analysis Model. *Energy and Buildings*, *279*, 112640. https://doi.org/10.1016/j.enbuild.2022.112640

Xiang, Y., Mahamadu, A.-M., & Florez-Perez, L. (2024). Engineering Information Format Utilisation Across Building Design Stages: An Exploration of BIM Applicability in China. *Journal of Building Engineering*, 110030. https://doi.org/10.1016/j.jobe.2024.110030

Xiang, Y., Mahamadu, A.-M., Florez-Perez, L., & Wu, Y. (2024). Design optimisation towards lower embodied carbon of prefabricated buildings: Balancing standardisation and customisation. *Developments in the Built Environment*, *18*, 100413. https://doi.org/https://doi.org/10.1016/j.dibe.2024.100413

Xiang, Y., Opoku, A., & Florez-Perez, L. (2021). Carbon emissions optimisation in prefabrication construction: A review of current design integrated approaches. *Proceedings of the 37th Annual ARCOM Conference, ARCOM 2021*, *September*, 814–823.

Xu, J., Teng, Y., Pan, W., & Zhang, Y. (2022). BIM-integrated LCA to automate embodied carbon assessment of prefabricated buildings. *Journal of Cleaner Production*, *374*(April), 133894. https://doi.org/10.1016/j.jclepro.2022.133894

Yang, X., Zhang, S., & Wang, K. (2021). Quantitative study of life cycle carbon emissions from 7 timber buildings in China. *International Journal of Life Cycle Assessment*, *26*(9), 1721–1734. https://doi.org/10.1007/s11367-021-01960-8

Yang, Yingnan, Liu, X., Xie, H., & Zhang, Z. (2023). Towards an Integrated Framework for Information Exchange Network of Construction Projects. *Buildings*, *13*(3). https://doi.org/10.3390/buildings13030763

Yang, Yu, Shao, S., & Cao, D. (2024). Diffusion of BIM policies in China: an event history analysis. *Engineering, Construction and Architectural Management*. https://doi.org/10.1108/ECAM-08-2023-0826

Yuan, Z., Sun, C., & Wang, Y. (2018). Design for Manufacture and Assembly-oriented parametric design of prefabricated buildings. *Automation in Construction*, *88*, 13–22. https://doi.org/10.1016/j.autcon.2017.12.021

Yue, Y., Song, G., Huang, G., & Yu, L. (2013). Application of MOVES in the microscopic Evaluation of Traffic Emissions. *Journal of Transport Information and Safety*, *31*(6), 47–53.

Zhang, C., Hu, M., Yang, X., Amati, A., & Tukker, A. (2020). Life cycle greenhouse gas emission and cost analysis of prefabricated concrete building façade elements. *Journal of Industrial Ecology*, *24*(5), 1016–1030. https://doi.org/10.1111/jiec.12991

Zhang, J., Liu, N., & Wang, S. (2021). Generative design and performance optimization of residential buildings based on parametric algorithm. *Energy and Buildings*, *244*. https://doi.org/10.1016/j.enbuild.2021.111033

Zhang, L., Hu, X., & Qiu, R. (2017). A Review of Research on Emission Models of Vehicle Exhausts. *WORLD SCI-TECH R&D*, *39*(4), 355–362.

Zhang, X., & Wang, F. (2022). Influence of parameter uncertainty on the low-carbon design optimization of reinforced concrete continuous beams. *Structural Concrete*. https://doi.org/10.1002/suco.202100903

Zhang, X., & Zhang, X. (2021). Sustainable design of reinforced concrete structural members using embodied carbon emission and cost optimization. *Journal of Building Engineering*, *44*. https://doi.org/10.1016/j.jobe.2021.102940

Zhao, C., Liu, Y., Ren, S., & Quan, J. (2018). Study on carbon emission calculation method of concrete. *Key Engineering Materials*, *768 KEM*, 293–305. https://doi.org/10.4028/www.scientific.net/KEM.768.293

Zhou, G., Yuan, S., Lu, Q., & Xiao, X. (2018). A carbon emission quantitation model and experimental evaluation for machining process considering tool wear condition. *International Journal of Advanced Manufacturing Technology*, *98*(1–4), 565–577. https://doi.org/10.1007/s00170-018-2281-6

Zhou, Y., Tam, V. W., & Le, K. N. (2023). Sensitivity analysis of design variables in life-cycle environmental impacts of buildings. *Journal of Building Engineering*, *65*. https://doi.org/10.1016/j.jobe.2022.105749

Zhu, C., Li, X., Zhu, W., & Gong, W. (2022). Embodied carbon emissions and mitigation potential in China's building sector: An outlook to 2060. *Energy Policy*, *170*. https://doi.org/10.1016/j.enpol.2022.113222

Zhu, H., Hong, J., Shen, G. Q., Mao, C., Zhang, H., & Li, Z. (2018). The exploration of the life-cycle energy saving potential for using prefabrication in residential buildings in China. *Energy and Buildings*, *166*, 561–570. https://doi.org/10.1016/j.enbuild.2017.12.045